Imperial College of Science, Technology and Medicine
Department of Infectious Disease Epidemiology

Drivers underpinning heterogeneity in host-pathogen systems

Kieran Alexander Bates

A thesis submitted for the degree of Doctor of Philosophy
September 2018

Statement of originality

I declare that the contents of this thesis are original. Any contributions made by others are acknowledged appropriately.

Copyright declaration

The copyright of this thesis rests with the author and is made available under a Creative Commons Attribution Non-Commercial No Derivatives licence. Researchers are free to copy, distribute or transmit the thesis on the condition that they attribute it, that they do not use it for commercial purposes and that they do not alter, transform or build upon it. For any reuse or redistribution, researchers must make clear to others the licence terms of this work.

Abstract

The amphibian-infecting chytrid fungi, *Batrachochytrium dendrobatidis* (*Bd*) and *Batrachochytrium salamandrivorans* (*Bsal*) cause the disease chytridiomycosis and are major agents of global amphibian decline. Despite catastrophic species loss associated with outbreaks of these pathogens, there is within- and between-species heterogeneity in susceptibility to infection, of which our understanding is limited. In this thesis, I investigate the key factors underpinning disease outcome in amphibians. In particular, I focus on the importance of host microbial ecology and whether defensive or synergistic microbe-pathogen relationships shape the host response to infection. In my first data chapter, I show that in wild midwife toad (*Alytes obstetricans*) populations exhibiting enzootic or epizootic *Bd* disease dynamics, there is no association between pathogen genetics and epidemiological trends. Meanwhile, I demonstrate strong associations between the host microbiome and disease outcome, with reduced bacterial diversity and differences in community composition in epizootic versus enzootic populations. I further demonstrate that the host skin microbiome differs profoundly based on life stage with larvae and metamorphs exhibiting different bacterial community composition and sharing relatively few microbial taxa. In the following chapter, I begin to disentangle microbe-mediated protection from pathogen-induced disruption of the microbiome by showing that *Bsal*-induced mortality is associated with microbiome perturbation in two amphibian host species. I further show that transitioning from the wild to captivity results in changes in bacterial and fungal community composition and reduced diversity of the amphibian skin microbiome. In my final chapter, I reveal that skin microbial community structure is linked to mucosal metabolome composition in wild *A. obstetricans*. In addition, I uncover microbe-metabolite associations linked to population-level disease outcomes. Overall, this thesis exposes some of the key factors driving chytridiomycosis disease dynamics and demonstrates that amphibian skin-associated microbes play an important role in shaping the host response to infection.

Acknowledgements

I wish to first thank my supervisors, Matthew Fisher, Trenton Garner and Xavier Harrison, who have given me the ideal balance of freedom and guidance. They have also been unfaltering in keeping my passion for science burning. I thank Trent for taking me under his wing as a second year undergraduate; believing that I had potential and proving that academia could be fun beyond research. Secondly, I thank the Department of Infectious Disease Epidemiology at Imperial College London and in particular, the various members of my lab (past and present): Rhys Farrer, Pria Ghosh, Jennifer Shelton, Claudia Wierzbicki, Johanna Rhodes, Thomas Sewell, Simon O'Hanlon and Julia Halder. Thank you for putting up with my jokes, making the office a place of fun rather than work and above all being supportive throughout my PhD. I thank my colleagues at the Institute of Zoology: Kevin Hopkins, Lola Brookes and Chris Sergeant for their support. I also thank Frances Clare, Jaime Bosch, Dirk Schmeller and Adeline Loyau for their help in making fieldwork a success. Thanks to the community of Lescun for welcoming me to their wonderful village, a place for which I have great fondness and will surely visit again.

Thanks to Sam, Australian Nick, Dorian, English Nick, Stoffer, Hamish, Ed and Joe for being my closest friends and all that entails. Finally, I thank my family, without whom this PhD would not have been possible. In particular I thank my grandparents for all they have done and whom I hope I have done proud. I also thank my siblings, Oliver, Brendan and Sophie who have always shown encouragement, perspective and been absolute in supporting me. Finally, thanks to my parents from whom I could not wish for more.

Acronyms

AMP: Anti-microbial peptide

ANOVA: Analysis of variance

Bd: *Batrachochytrium dendrobatidis*

Bsal: *Batrachochytrium salamandrivorans*

BWA: Burrows-Wheeler aligner

DCA: Detrended correspondence analysis

DNA: Deoxyribonucleic acid

EID: Emerging infectious disease

FDR: False discovery rate

GE: Genomic equivalents

ITS: Internal transcribed spacer

KEGG: Kyoto Encyclopedia of Genes and Genomes

KO: Kegg orthology

LD: Linkage disequilibrium

LDA: Linear discriminant analysis

LEfSe: Linear discriminant analysis effect size

MHC: Major histcompatibility complex

MAMPs: Microbe-associated molecular patterns

NGS: Next generation sequencing

NMDS: Non-metric multidimensional scaling

OTU: Operational taxonomic unit

PAMPs: Pathogen-associated molecular patterns

PCA: Principal component analysis

(q)PCR: (quantitative) Polymerase chain reaction

PERMANOVA: Permutational multivariate analysis of variance

PLS-DA: Partial least squares - discriminant analysis

PQN: Probabilistic quotient normalisation

QC: Quality control

RNA: ribonucleic acid

rRNA: Ribosomal ribonucleic acid

SNP: Single nucleotide polymorphism

SPE: Solid phase extraction

ssu rRNA: Small subunit ribosomal ribonucleic acid

TLR: Toll-like receptor

TMRCA: Time to most recent common ancsestor

UHPLC-MS: Ultra high pressure liquid chromatography-mass spectrometry

VCF: Variant call format

VIP: Variable influence on the projection

Contents

Abstract **iii**

Acknowledgements **iv**

Acronyms **v**

1 Introduction **1**

1.0.1 Emerging fungal pathogens 1

1.0.2 *Batrachochytrium dendrobatidis* (*Bd*) 3

1.0.3 Origin and spread of *Bd* 4

1.0.4 *Bd* biology and life cycle 7

1.0.5 *Bd* pathology and pathogenesis 9

1.0.6 Host defences 11

1.0.7 Host-associated microbes 15

1.0.8 Focal study species: *Alytes obstetricans* 21

1.0.9 The Pyrenees study system 22

1.1 Aims and Objectives 24

1.2 Hypotheses 24

1.3 Funding 25

1.4 Publications 26

2 Amphibian chytridiomycosis outbreak dynamics are linked with host skin bacterial community structure 27

2.1 Abstract 28

2.2 Introduction 28

2.3 Material and Methods 31

2.3.1 Monitoring long-term infection dynamics of *Batrachochytrium dendrobatidis* (*Bd*) among Pyrenean populations of *Alytes obstetricans* 31

2.3.2 Sample collection 31

2.3.3 DNA extraction and sample processing 32

2.3.4 16S sequence analysis 33

2.3.5 Infection analysis 33

2.3.6 Bacterial communities across space and life history stage 34

2.3.7 Microbiota in epizootic and enzootic metamorph populations 35

2.3.8 *Bd* isolation and genome sequencing 36

2.3.9 Data availability 37

2.3.10 Ethics statement 37

2.4 Results 38

2.4.1 Host skin microbiota differs by life stage and population 38

2.4.2 Microbiota differ by metamorph population and disease state 41

2.4.3 Predicted function differs by population and disease state 48

2.4.4 *Bd* genomic analysis 48

2.5 Discussion 50

2.6 Acknowledgements 56

3 Captivity and experimental exposure to the emerging fungal pathogen *Batrachochytrium salamandrivorans* are linked to perturbation and dysbiosis of the amphibian skin microbiome 57

3.1 Abstract 59

3.2 Introduction 59

3.3 Material and Methods 63

3.3.1 Field sampling and captivity study 63

3.3.2 *Bsal* exposure experiment 63

3.3.3 Sample processing, DNA extraction and quantification of *Bsal* infection . 64

3.3.4 Bacterial microbiome sample processing 64

3.3.5 Fungal mycobiome sample processing 65

3.3.6 Bacterial microbiome analysis 66

3.3.7 Fungal mycobiome analysis 66

3.3.8 Statistical analysis 67

3.3.9 Ethics statement 68

3.4 Results 69

3.4.1 Captivity impacts cross-Kingdom microbial diversity and structure . . . 69

3.4.2 *Bsal* infection perturbs host microbiome structure 72

3.5 Discussion 75

3.6 Acknowledgements 79

4 Skin microbiome composition and metabolomic profiles of amphibian populations reflect enzootic and epizootic chytridiomycosis disease dynamics 81

4.1 Abstract 83

4.2 Introduction 83

4.3 Material and Methods 86

4.3.1 Field sampling 86

4.3.2 Sample processing, DNA extraction and quantification of *Bd* infection . . 87

4.3.3 Infection analysis 88

4.3.4 Bacterial microbiome bioinformatics 89

4.3.5 Fungal mycobiome bioinformatics 89

4.3.6 Bacterial and fungal community statistical analysis 90

4.3.7 Metabolite extraction protocol 91

4.3.8 UHPLC-MS metabolomics of skin mucus samples 91

4.3.9 UHPLC-MS spectral processing 92

4.3.10 Metabolome analysis 92

4.3.11 Integration of microbiome and metabolome data 93

4.4 Results 94

4.4.1 *Bd* infection analysis . . . 94

4.4.2 Cross-Kingdom microbiota profiles are associated with population and *Bd* disease dynamics . . . 94

4.4.3 Cutaneous metabolites are linked to population, disease state and host microbiota . . . 100

4.4.4 Microbiome-metabolome associations . . . 103

4.5 Discussion . . . 105

4.6 Acknowledgements . . . 112

5 General Discussion **113**

5.1 Future Directions . . . 118

Bibliography **121**

.1 Appendix 1: Bacterial indicator OTUs by disease dynamic 2015 . . . 156

.2 Appendix 2: Bacterial indicator OTUs by population 2015 . . . 158

.3 Appendix 3: KO terms with LDA score > 2.00 . . . 162

.4 Appendix 4: Summary of *Bd* isolates used for whole genome sequencing . . . 163

.5 Appendix 5: Wild versus captive bacterial indicator OTUs for *T. cristatus* . . . 165

.6 Appendix 6: Wild versus captive bacterial indicator OTUs for *L. vulgaris* . . . 170

.7 Appendix 7: Mean Bsal prevalence (95% CI) and proportion of animals with lesions (%) for *Lissotriton vulgaris* and *Triturus cristatus* . . . 174

.8 Appendix 8: Results of survival analysis . . . 175

.9 Appendix 9: Bacterial indicator OTUs at day 28 based on *Bsal* infection for *L. vulgaris* and *T. cristatus*. . . . 176

.10 Appendix 10: Bacterial indicator taxa for each *A. obstetricans* metamorph population, 2016 177

.11 Appendix 11: Bacterial indicator taxa based on chytrid disease dynamics 2016 . 179

.12 Appendix 12: Fungal indicator taxa for each *A. obstetricans* metamorph population, 2016 181

.13 Appendix 13: Fungal indicator taxa based on chytrid disease dynamics 2016 . . 182

.14 Appendix 14: Top metabolite biomarkers of enzootic and epizootic *A. obstetricans* populations 183

.15 Appendix 15: Table of bacterial-metabolite correlations 186

.16 Appendix 16: Articles published from chapters in this thesis 194

List of Tables

2.1 Sample summary of each population. N = 2 environmental samples each of water and sediment for each population. 39

2.2 Shared OTUs between larvae, metamorphs and environment for each population. 39

2.3 Results of PERMANOVA comparing beta diversity of larvae and metamorphs to environmental samples. 40

2.4 Visual estimates of larval abundance from 2010 to 2015. + less than 100; ++ 100-1000; +++ more than 1000. 42

2.5 Significance of pairwise differences in infection intensity (GE) between *A. obstetricans* populations. 43

4.1 Significance of pairwise differences in infection intensity (GE) between *A. obstetricans* populations. 94

5.1 Key microbial taxa associated with *Bd* or *Bsal* identified in this thesis. 121

List of Figures

1.1 Life cycle of *Bd* from motile zoospore to sessile zoosporangium. Taken from (Rosenblum et al., 2010) 8

1.2 Common midwife toad, *Alytes obstetricans*. (**a**) adult male with egg string, (**b**) over-wintered tadpole. 22

1.3 Pyrenean mountain lakes sampled in this thesis. The altitutude and total area of each lake is shown in parentheses. (**a**) Puits d'Arious (1859m, 0.2ha), (**b**) Lhurs (1691m, 1.5ha), (**c**) Ibon Acherito (1869m, 5.6ha), (**d**) Ansabere (1859m, 0.2ha), (**e**) Arlet (1986m, 2.7ha), (**f**) Map of study sites. 23

2.1 (**a**) OTUs common among life stages and environmental samples (**b**) Shannon diversity by sample type (boxes represent 25^{th} and 75^{th} percentile, the horizontal line is the median, whiskers are maximum and minimum values) (**c**) NMDS plot of bacterial communities based on life stage, environmental samples and population (**d**) Stacked bar chart of the 10 most abundant phyla for lake water, sediment, larvae and metamorphs. Sample sizes were: n=63 (larvae), n=51 (metamorphs), n=20 (environment). 41

2.2 (**a**) Boxplots of metamorph infection intensity (2010-2015) for each population. Boxes represent the 25th and 75th percentile, the horizontal black line is the median, whiskers represent the maximum and minimum values of infection intensity, open circles are outliers. (**b**) Metamorph *Bd* prevalence (2010-2015). Sample sizes were: n=169 (Arlet), n=37(Ansabere), n=104 (Acherito), n=166 (Lhurs), n=123 (Puits d'Arious). 44

2.3 (**a**) Boxplot of *Bd* infection intensity in metamorphs sampled in 2015 showing reduced infection intensity in enzootic populations (Chi-sq=59.855, p<0.0001). Boxes represent 25th and 75th percentile, the horizontal line is the median and whiskers are maximum and minimum values of infection intensity (**b**) bar chart of *Bd* infection prevalence in metamorphs. Enzootic populations are coloured in blue, epizootic populations are coloured in red. Sample sizes: n=32 (Enzootic: Acherito=14, Lhurs=11, Puits d'Arious=7), n=19 (Epizootic: Arlet=16, Ansabere=3). 45

2.4 (**a**) Shannon diversity of metamorph populations. Epizootic populations are in red and enzootic populations are blue. Boxes represent 25th and 75th percentile, the horizontal line is the median and whiskers are maximum and minimum values (**b**) NMDS plot based on Bray-Curtis distances displaying beta diversity of enzootic and epizootic populations (**c**) Stacked bar chart of abundant bacterial phyla for each metamorph population (**d**) Map showing location of enzootic and epizootic populations. Map generated using ArcGIS version 10.0 (http://www.esri.com/software/arcgis) with the World Imagery Basemap. Source: Esri, DigitalGlobe, GeoEye, Earthstar, Geographics, CNES/Airbus DS, USDA, USGS, AeroGRID, IGN, the GIS User Community. Sample sizes: n=32 (Enzootic: Acherito=14, Lhurs=11, Puits d'Arious=7), n=19 (Epizootic: Arlet=16, Ansabere=3). 46

2.5 Heatmap displaying the normalised relative abundance of the top 20 bacterial OTUs from enzootic and epizootic populations identified from indicator analysis. Sample sizes: n=32 (Enzootic: Acherito=14, Lhurs=11, Puits d'Arious=7), n=19 (Epizootic: Arlet=16, Ansabere=3). 47

2.6 NMDS plot based on Bray-Curtis distances displaying clustering of KO functional predictions from metamorph skin bacterial communities from each Pyrenean population. Sample sizes: n=32 (Enzootic: Acherito=14, Lhurs=11, Puits d'Arious=7), n=19 (Epizootic: Arlet=16, Ansabere=3). 48

2.7 (**a**) Phylogeny of *Bd* isolates collected from the Pyrenees and other European localities. Red stars indicate bootstrap values of 100 (**b**) PCA plot of identified SNPs from *Bd* isolates from all localities (**c**) PCA plot of identified *Bd* SNPs from Pyrenean lakes only. Sample sizes: n=6 (Ansabere), n=7 (Arlet), n=26 (Acherito), n=14 (Lhurs), n=6 (Puits d'Arious), n=22 (other European isolates). 49

2.8 PCA plot of identified *Bd* SNPs from Pyrenean lakes sampled between 2004 and 2015 shows no temporal structure in *Bd* genotypes. Sample sizes: n=6 (Ansabere), n=7 (Arlet), n=26 (Acherito), n=14 (Lhurs), n=6 (Puits d'Arious). 50

3.1 Microbiome of animals in the wild and after 14 days in captivity. Boxplots displaying Shannon diversity in wild and captive *Lissotriton vulgaris* and *Triturus cristatus* for **(a)** bacteria **(b)** fungi. Boxes represent 25th and 75th percentile, the horizontal line is the median, whiskers are maximum and minimum values. Detrended correspondence analysis (DCA) plots of beta diversity in wild and captive *L. vulgaris* and *T. cristatus* for **(c)** bacteria **(d)** fungi. Ellipses indicate 95% confidence intervals. Where ellipses are absent, insufficient samples were present. Stacked bar plots of **(e)** bacterial taxa with relative abundance > 1% and **(f)** fungal taxa with relative abundance > 0.5%. Sample sizes bacteria: n=15 (wild *L. vulgaris*), n=15 (wild *T. cristatus*), n=15 (captive *L. vulgaris*), n=15 (captive *T. cristatus*). Sample sizes fungi: n=10 (wild *L. vulgaris*), n=10 (wild *T. cristatus*), n=3 (captive *L. vulgaris*), n=8 (captive *T. cristatus*). 70

3.2 Heatmap of normalised relative abundance of bacterial indicator OTUs for animals in the wild and after 14 days in captivity labelled by Phylum and Class for **(a)** *T. cristatus* **(b)** *L. vulgaris*. Sample sizes: n=15 (wild *L. vulgaris*), n=15 (wild *T. cristatus*), n=15 (captive *L. vulgaris*), n=15 (captive *T. cristatus*). . . 71

3.3 Plot of infection intensity for *Bsal* exposed animals for **(a)** *T. cristatus* **(b)** *L. vulgaris*. **(c)** Lesions evident on *L. vulgaris*. Sample sizes: n=5 (control *L. vulgaris*), n=5 (control *T. cristatus*),n=10 (exposed *L. vulgaris*), n=10 (exposed *T. cristatus*). 73

3.4 Detrended correspondence analysis (DCA) plots displaying temporal variation in bacterial beta diversity in **(a)** *L. vulgaris* **(b)** *T. cristatus*. Ellipses indicate 95% confidence intervals. Scatterplot of relative abundance of OTU016 *Stenotrophomonas* identified as an indicator OTU for *Bsal* infection in both **(c)** *L. vulgaris* and **(d)** *T. cristatus*. Sample sizes: n=15 (Day 0 *L. vulgaris*), n=15 (Day 28 *L. vulgaris*), n=14 (Day 56 *L. vulgaris*), n=15 (Day 0 *T. cristatus*), n=15 (Day 28 *T. cristatus*), n=12 (Day 56 *T. cristatus*). 74

4.1 (**a**) Boxplot of *Bd* infection intensity for each *A. obstetricans* population. (**b**) *Bd* prevalence in each *A. obstetricans* population. Microbial Shannon diversity of *A. obstetricans* skin for each population for (**c**) bacteria and (**d**) fungi. Boxes represent 25^{th} and 75^{th} percentile, the horizontal line is the median, whiskers are maximum and minimum values. Scatterplots of (**e**) bacterial Shannon diversity versus log10 GE+1 and (**f**) fungal Shannon diversity versus log10 GE+1. Sample sizes for fungi were: n=11 (Acherito), n=6 (Lhurs), n=8 (Puits d'Arious), n=10 (Arlet). Sample sizes for bacteria were: n=14 (Acherito), n=14 (Lhurs), n=14 (Puits d'Arious), n=14 (Arlet). 96

4.2 Non-metric multidimensional scaling (NMDS) plots of beta diversity based on Bray-Curtis dissimilarity for each *A. obstetricans* population for (**a**) bacteria (**b**) fungi. Stacked bar plots displaying composition of microbial phyla for (**c**) bacteria (**d**) fungi. Sample sizes for fungi: n=11 (Acherito), n=6 (Lhurs), n=8 (Puits d'Arious), n=10 (Arlet). Sample sizes for bacteria: n=14 (Acherito), n=14 (Lhurs), n=14 (Puits d'Arious), n=14 (Arlet). 97

4.3 (**a**) Heatmap of bacterial indicator taxa based on disease dynamic (**b**) boxplots of key indicator OTUs with relative abundance (%) on Y axis and population on X axis. Sample sizes were: n=14 (Acherito), n=14 (Lhurs), n=14 (Puits d'Arious), n=14 (Arlet). 99

4.4 Boxplots of of fungal indicator taxa based on disease dynamic (**a**) *Batrachochytrium* sp. and (**b**) *Phoma* sp. Enzootic populations are coloured blue, epizootics are red. Sample sizes were: n=11 (Acherito), n=6 (Lhurs), n=8 (Puits d'Arious), n=10 (Arlet). 100

4.5 Population level differences in metabolome structure as indicated by (**a**) separation of populations in a non-metric multidimensional scaling (NMDS) plot and (**b**) Partial least squares discriminant analysis (PLS-DA) of skin mucosal metabolites. Ellipses indicate 95% confidence intervals. Sample sizes were: n=14 (Acherito), n=14 (Lhurs), n=14 (Puits d'Arious), n=14 (Arlet). 101

4.6 (**a**) Heatmap of metabolites driving differences in metabolome of populations based on VIP score > 2 and $q < 0.05$. (**b**) Boxplots of key metabolites. Sample sizes: n=14 (Acherito), n=14 (Lhurs), n=14 (Puits d'Arious), n=14 (Arlet). . . 102

4.7 Spearman correlations between bacterial OTUs and metabolites. Sub-networks display discriminating taxa for (**a**) enzootic (Acherito, Puits d'Arious, Lhurs) and (**b**) epizootic (Arlet) populations. Edges represent correlation co-efficients with thickness indicating strength of correlation. Node size is proportional to betweenness centrality. Nodes coloured by metabolite (orange) and bacterial family (or phylum where family-level taxonomic resolution is not possible). * and + denote bacteria identified as indicator taxa for enzootic and epizootic populations respectively. Sample sizes were: n=14 (Acherito), n=14 (Lhurs), n=14 (Puits d'Arious), n=14 (Arlet). 104

Chapter 1

Introduction

1.0.1 Emerging fungal pathogens

Pathogens that are increasing in their abundance, virulence, and geographic or host range are classified as emerging infectious diseases (EIDs) (Daszak et al., 2000; Jones et al., 2008). EIDs have played an integral part in the human story and can be intrinsically linked to our past. For example, during the Spanish conquest of the 15th and 16th century, diseases such as typhus, measles and smallpox were introduced to South America resulting in the deaths of 50 million Native Americans (Daszak et al., 2000). Similarly, during the 19th century in Ireland the oomycete *Phytophthora infestans* caused the potato blight that led to severe famine and subsequent migrations of the Irish people. The historic impacts of EIDs are not limited to humans; when rinderpest (a pathogenic *Morbillivirus* endemic to Asia) was introduced into Africa in 1889, the rapid spread of the virus led to the decline of 90% of the Kenyan buffalo population within 8 years (Daszak et al., 2000). Wildlife EIDs remain a significant threat today. Recent examples that have resulted in major population decline or local extinction include canine distemper virus in African wild dogs (Alexander and Appel, 1994), avian malaria (Woodworth et al., 2005), and the protozoan parasite *Stenhausia* which was a key driver in the global extinction of the land snail *Partula turgida* (Cunningham and Daszak, 1998). Classical disease theory predicts that a pathogen will co-evolve with its host rather than extirpate it

entirely (Van Valen, 1973; Paterson et al., 2010). This theory is supported by deterministic models of density dependent transmission which predict that a population will never be driven to extinction by disease alone since the pathogen will die out once the host population falls below a threshold density, a phenomenon termed pathogen fade out (Swinton et al., 1998; McCallum et al., 2001). There are three key theoretical mechanisms by which population level extinction may be brought about by a disease outbreak (De Castro and Bolker, 2005). These are (1) stochastic and Allee effects at low population density induced by disease, (2) spatial or frequency dependent disease transmission allowing for high incidence of infection even at low host population density (3) abiotic or biotic pathogen reservoirs facilitating the independent existence of the pathogen.

Fungal pathogens have until relatively recently been overlooked as major drivers of population decline in wildlife. Attitudes have since changed based on the emergence of several high profile fungal EIDs which have had profound effects on a multitude of species (Fisher et al., 2012). Fungal EIDs that have resulted in severe population decline include White nose syndrome in bats (Gargas et al., 2009; Lorch et al., 2011), *Batrachochytrium dendrobatidis* in amphibians (Stuart et al., 2004), and the recently discovered *Batrachochytrium salamandrivorans* that has decimated salamander populations in Europe (Martel et al., 2013, 2014). The ability of many fungal pathogens to extirpate entire populations is largely attributed to their life history. Fungi have high reproductive potential that can allow for an entire host population to become infected before mortality occurs and subsequently the limitations of density dependent transmission to take effect. Such dynamics have been observed in yellow legged frog populations of the Sierra Nevada mountain range (Briggs et al., 2010). Many fungi are also capable of existing independently from their primary host and can survive as saprotrophs or by forming durable spores. This facilitates the easy spread of pathogens in environmental inocula (Mitchell et al., 2008) and allows infection of host populations at extremely low density (Fisher et al., 2012). Finally, fungi exhibit the broadest host range of any group of pathogens with differential susceptibility often common among host species (Fisher et al., 2012). This effectively provides a biotic pathogen reservoir that can allow for sympatric transmission between host populations. Together, these general features of fungal biology fulfil the requirements for infection driven

extinction (De Castro and Bolker, 2005). It is therefore unsurprising that a meta-analysis identified fungal pathogens as an extinction threat to 72% of animal species and 64% of plant species where infection was known to be associated with extinction or extirpation (Fisher et al., 2012). It is likely that these estimates are conservative when one considers the poor diagnostics and reporting protocols for EIDs of wildlife (Ghosh et al., 2018). This potential loss to biodiversity will not only impact ecosystem function, but may have profound socio-economic impacts. For the year 2011 it was predicted that mitigation of low level persistent fungal EIDs infecting arable crops would have generated enough biomass to feed 8.5% of the worlds population (Fisher et al., 2012). Today this figure is likely to be much higher once the loss of ecosystem services brought about by declining biological pest controllers such as amphibians and bats are taken into account. There is consequently an urgent need to improve our understanding of the epidemiology of fungal EIDs and mitigate their impact and spread.

1.0.2 *Batrachochytrium dendrobatidis* (*Bd*)

Amphibians are the most threatened vertebrate class on the planet (Gascon, 2007; Gerwin, 2008) with up to 50% of all species at risk of extinction (Stuart et al., 2004; Fisher et al., 2009). A major driver of amphibian declines is the emerging fungal pathogen, *Batrachochytrium dendrobatidis* (*Bd*) that causes the disease chytridiomycosis (Berger et al., 1998). *Bd* was first discovered in 1997 but not formally taxonomically classified until 1999 (Longcore et al., 1999). Today *Bd* is known to infect at least 500 species of amphibian and has been implicated in the decline of over 200 species on all continents except Antarctica (Skerrat et al., 2007; Olson et al., 2013). This extremely broad host range and often fatal pathogenicity has resulted in chytridiomycosis being described as the worst infectious disease ever recorded among vertebrates (Gascon, 2007).

1.0.3 Origin and spread of *Bd*

Two main hypotheses postulate the spread of *Bd* and the resulting decline in amphibian populations globally. The novel pathogen hypothesis posits that *Bd* is a spreading pathogen that, when introduced into new regions, is capable of extirpating native host species (Rachowicz et al., 2005). Conversely, the endemic pathogen hypothesis proposes that *Bd* is a widespread amphibian commensal or symbiont that has become more virulent due to environmental shifts perturbing a benign microbe-host interaction (Rachowicz et al., 2005). Early research favoured the novel pathogen hypothesis. Specifically, *Bd* population genetics studies showed low genetic diversity of *Bd* across space and host species (Morehouse et al., 2003; Morgan et al., 2007; James et al., 2009). In addition, ecological data showed that *Bd* has a patchy global distribution, and is associated with wavelike patterns of amphibian decline as documented in Australia (Laurance et al., 1996), South and Central America (Berger et al., 1998; Lips et al., 2006, 2008), the United States Sierra Nevada mountain range (Vredenburg et al., 2010), and the French and Spanish Pyrenees (Bosch et al., 2001; Walker, 2008). Finally, the global spread of *Bd* in the amphibian trade is widely documented (Fisher and Garner, 2007) and has undoubtedly facilitated its introduction to naive hosts across wide geographic distributions. Analysis of museum samples has however shown that *Bd* has been present in several countries for at least 100 years which precedes the first documentation of severe amphibian declines (Weldon et al., 2004; Ouellet et al., 2005; Bai et al., 2012; Rodriguez et al., 2014; Talley et al., 2015). In addition there are quantifiable associations between the condition and health of amphibians (Reading, 2007), global warming, and the onset of chytridiomycosis (Pounds et al., 2006; Bosch et al., 2007) . All of these factors are compatible with *Bd* being an endemic pathogen, though by no means provide conclusive support for this theory.

In 2011, a pivotal discovery was made that identified the existence of multiple endemic *Bd* lineages in addition to a more recently emerged global panzootic lineage (*Bd*GPL) (Farrer et al., 2011). Importantly, the lineages from South Africa and Mallorca (*Bd*CAPE) and Switzerland (*Bd*CH) showed both reduced virulence and different morphological traits compared to *Bd*GPL. Detailed genetic analysis of *Bd*GPL revealed the hallmarks of genomic recombination

manifested as extensive linkage disequilibrium and patchily distributed heterozygosity. Based on this finding it was postulated that *Bd*GPL came into existence as a result of an ancestral recombination of previously reproductively isolated endemic *Bd* lineages and has since spread via the global amphibian trade (Farrer et al., 2011). This is further supported by the onset of major amphibian declines in the late 20$^{\text{th}}$ century which coincides with *Bd*GPL emergence estimated at 35 - 257 years before present (Farrer et al., 2011), though another study estimated a much earlier emergence at 26000 years before present (Rosenblum et al., 2013). Further studies identified two additional endemic lineages, *Bd*Asia (Goka et al., 2008) and *Bd*Brazil (Schloegel et al., 2012). These lineages have also been identified in museum specimens demonstrating their presence in wild amphibian populations for at least 100 years (Bai et al., 2012; Rodriguez et al., 2014). Of particular importance is the confirmation of recombination in *Bd* (Schloegel et al., 2012) and the finding that *Bd*Brazil and *Bd*GPL have coexisted for the past century.

For over a decade, studies have yielded conflicting conclusions as to the geographic origin of *Bd* with possible ancestral centres including Africa (Weldon et al., 2004), North America (Fisher and Garner, 2007), South America (Rodriguez et al., 2014), Japan (Goka et al., 2008; Bai et al., 2012) and East Asia (Bataille et al., 2013). A great many of hypotheses regarding the origin of *Bd* were founded upon identifying *Bd* preserved in historic museum specimens. The out of Africa hypothesis proposed the spread of *Bd* through the global trade in *Xenopus leavis* that was used in pregnancy testing and scientific research for decades (Weldon et al., 2004). Support for an African origin of *Bd* was further bolstered through the identification of *Bd* in a preserved specimen of *Xenopus fraseri* that was collected in 1933 in Cameroon. The origin of *Bd* in Africa was later refuted when higher genetic diversity was found in *Bd* isolated from North American bullfrogs (James et al., 2009) and *Bd* was detected in a southern leopard frog (*Rana sphenocephala*) specimen collected in 1888 in the Midwestern United States (Talley et al., 2015). Meanwhile, the Atlantic Forests of Brazil as the ancestral origin of *Bd* was suggested based on the presence of *Bd* in the region for over 100 years and a stable prevalence of approximately 20% throughout this period coinciding with high host species diversity, indicating endemic disease status (Rodriguez et al., 2014).

In recent years, the focus on the origin of *Bd* has looked east to Asia. As is similarly the

case for the other candidate origin centres of *Bd*, museum specimens of amphibians collected from Asia have identified *Bd* in the region from the early 1900s (in this case at least 1902) (Goka et al., 2008). Moreover, Asian amphibians appear to lack clinical signs of infection and low prevalence indicative of a history of coevolution between an endemic Asian *Bd* and native Asian amphibians (Bai et al., 2012). The most convincing and robust evidence for an Asian origin of *Bd* however came from a landmark 2018 study that interrogated whole genome sequences of 234 *Bd* isolates collected from every continent where the pathogen is known to exist (O'Hanlon et al., 2018). This study recovered the previously known *Bd* lineages (*Bd*CAPE, *Bd*GPL, *Bd*CH, *Bd*Brazil) in addition to two new lineages originating from the Korean peninsula (*Bd*ASIA-1 and *Bd*ASIA-2) (O'Hanlon et al., 2018). The discovery of these new *Bd* lineages resulted in the overall *Bd* phylogeny being redefined with *Bd*CH that was previously considered enzootic to Switzerland (Farrer et al., 2011) now being placed within the *Bd*ASIA-1 lineage. In addition, *Bd*BRAZIL was shown to be highly similar to *Bd*ASIA-2 resulting in the co-classification of these lineages as *Bd*ASIA-2/*Bd*Brazil. Further analysis demonstrated that *Bd*ASIA-1 is the most likely ancestral *Bd* lineage based on (i) a higher number of segregating sites and nucleotide diversity for *Bd*ASIA-1 than any other lineage (ii) a greater number of shared haplotypes within isolates of *Bd*ASIA-1 and between *Bd*ASIA-1 and all other lineages, demonstrating that *Bd*ASIA-1 shares more genetic diversity with the global panel of lineages than any other lineage does. A time to most recent common ancestor (TMRCA) that accounted for recombination and evolutionary rates more robustly than prior methods (Rosenblum et al., 2013) estimated emergence of *Bd*GPL as between 50 to 120 years ago (O'Hanlon et al., 2018). This date broadly coroborates a previous estimate (Farrer et al., 2011) and has biological plausibility in coinciding with the global expansion of the amphibian trade (Fisher and Garner, 2007). Pertinently, the closely related *Batrachochytrium salamandrivorans* is also thought to originate from Asia (Martel et al., 2014) suggesting that the continent may be a hot spot for chytrid diversity and evolutionary innovation. Overall these findings provide support for ancestral *Bd*GPL being spread to novel regions where it has subsequently wreaked havoc with naive, endemic amphibian fauna. Given the variation in virulence among *Bd* lineages, there remains the question of how these may interact in sympatry

and whether protection may be conferred against *Bd*GPL when hosts are instead infected by an endemic hypovirulent lineage.

1.0.4 *Bd* biology and life cycle

Chytrids are a basal fungal grouping separated by 1-1.5 billion years of branch length to the nearest fully sequenced fungal genome (Taylor and Berbee, 2006). A key defining feature of this phylum is the presence of a life stage with a motile zoospore, typically propelled by a single posterior flagellum. The production of a motile zoospore initially caused contention regarding the taxonomic placement of this phylum, with some arguing it should be placed as a transitional group between fungi and protists (Barr, 1980). However, the identification of specific traits such as the presence of chitin cell wall, the alpha-aminoadipic acid lysine synthetic pathway and storage of carbohydrates as glycogen has placed the Chytridiomycota in the fungal kingdom (James et al., 2006). This positioning has been further confirmed by phylogenetic analysis of ribosomal RNA genes (Forster et al., 1990). Members of the genus *Batrachochytrium* are unique to other members of the Chytridiomycota based on zoospore ultrastructure, small subunit ribosomal DNA (ssu-rDNA) sequence, and their ability to infect vertebrates (Berger et al., 1998; Longcore et al., 1999; James et al., 2000). The life cycle of *Bd* is divided into two key stages; the substrate independent and dependent stage. The substrate independent stage is characterised by un-walled, waterborne, motile, flagellated zoospores (Longcore et al., 1999; Berger et al., 2005). Zoospores measure 3 µm - 5 µm in diameter with a posterior flagellum measuring 19 µm - 20 µm in length (Longcore et al., 1999), travel short distances and exhibit a brief activity period (Piotrowski et al., 2004). The initiation of the substrate-dependent stage is marked by motile zoospores encysting within the stratum corneum and stratum granulosum epidermal layers of the host where the flagellum is resorbed and a cell wall forms (Berger et al., 2005). The developing germling then produces branching rhizoids and continues development as an immature sporangium. As the sporangium develops, its cytoplasm becomes more complex with subsequent mitotic divisions resulting in it becoming multinuclear. Discharge papillae form on the zoosporangium that at maturity (when the epidermal layer in which it is embedded is at its

most superficial) dissolve, facilitating the dispersal of zoospores into the external environment where subsequent infection of new hosts or the same host occurs (Fig. 1.1) (Berger et al., 2005). *Bd* development may be monocentric or colonial. In monocentric development a thallus (fungal vegetative body) forms a single sporangium. In colonial development, thin septa divide the thalli creating individual compartments each possessing discharge papillae (Longcore et al., 1999). Genomic studies have indicated that differential expression of *Bd* enzymes, specifically serine proteases and fungalysin metallopeptidases may aid in host colonisation by degrading host antimicrobial peptides and keratin respectively (Rosenblum et al., 2008). Interestingly zoospores exhibit chemotaxis towards soluble keratin (Moss et al., 2008), which presumably aids in the location of suitable host tissue in which to encyst. Zoospores are capable of surviving for up to 7 weeks in water (Johnson and Speare, 2003) and have an optimal growth temperature of between 17-25°C (Woodhams et al., 2008).

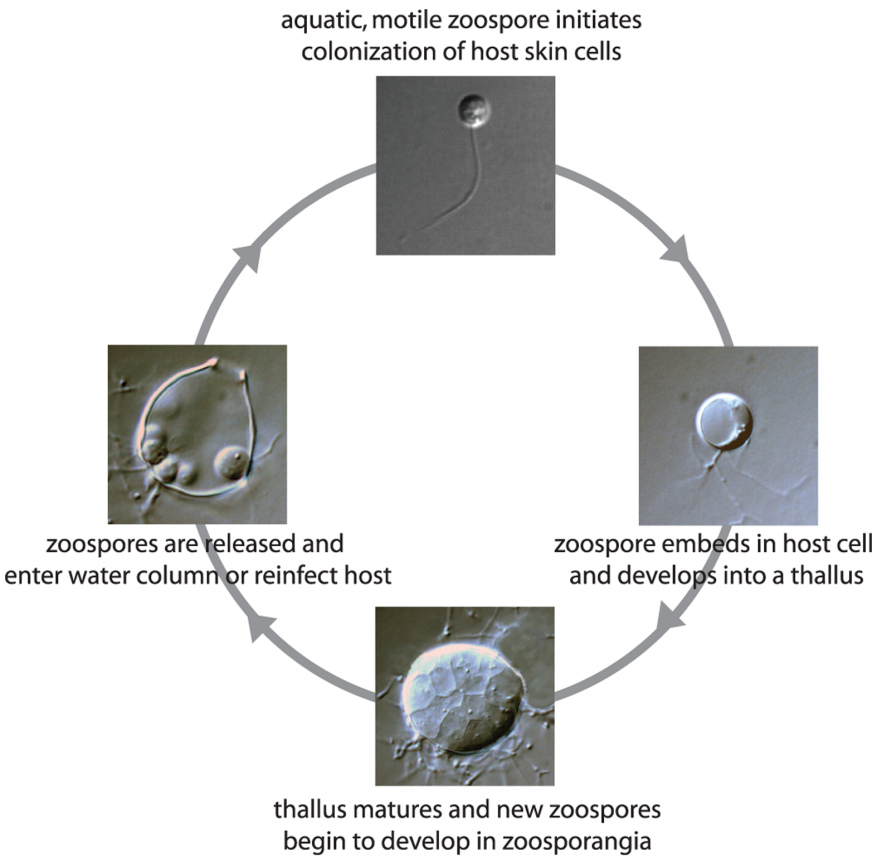


Figure 1.1: Life cycle of *Bd* from motile zoospore to sessile zoosporangium. Taken from (Rosenblum et al., 2010)

1.0.5 *Bd* pathology and pathogenesis

The pathology of chytridiomycosis differs based on amphibian life stage. In tadpoles, infection is restricted to the keratinised jaw sheaths and labial teeth (Berger et al., 1998) and normally does not cause mortality although exhibits some detrimental effects in certain species (Blaustein et al., 2005). Minor negative impacts of *Bd* infection on tadpole health include altered feeding kinematics reducing foraging efficiency (Venesky et al., 2010), and reduced growth and developmental rates (Parris and Cornelius, 2004).

In post-metamorphic animals chytridiomycosis causes pathophysiological changes (hyperplasia and hyperkeratosis) in the skin that disrupt cutaneous function (Berger et al., 2005; Voyles et al., 2009). This results in a reduction of sodium and potassium plasma concentration due to reduced absorption via ion channels. The subsequent electrolyte imbalance ultimately leads to cardiac contractile abnormalities, contractile failure, reduced blood flow and finally asystolic cardiac arrest and death (Voyles et al., 2009). The exact mechanism underlying this biochemical channel disruption is unknown but it has been suggested that release of fungal toxins or direct cellular damage could be implicated (Voyles et al., 2009). Gene expression profiling has corroborated that *Bd* disrupts the structural integrity of amphibian skin (Rosenblum et al., 2012). Specifically, *Bd* infection is associated with changes in expression of key genes involved in skin structural components such as collagen, fibrinogen, elastin and keratin (Rosenblum et al., 2012) which likely contribute to ion leakage leading to systemic ionic imbalance. There is also evidence for downstream effects of loss of skin integrity on other vital organs such as altered expression of genes involved in cellular stress and detoxification in the liver (Rosenblum et al., 2012). In addition to the direct effects of disrupted skin integrity, it is possible that changes in dermal histology could have additional knock-on effects that may lead to increased exposure to environmental toxins and increased susceptibility to infection by other pathogens.

Bd has also been shown to paralyse host immune defences by activating caspase signalling pathways that inhibit splenocyte function (Fites et al., 2013). It is likely that *Bd* releases a soluble factor that arrests proliferation of lymphocyte and other cell types rendering them incapable of normal function. Evidence suggests that these factors are cell wall components

since their production was absent in zoospores, and treatment with a chitin synthase inhibitor, Nikkomycin Z (which disrupts cell wall synthesis) reduced the incidence of inhibition (Fites et al., 2013). Other immunomodulatory candidates include methylthioadenosine (MTA) and kyneurenine (an oxidised product of tryptophan) which are metabolites produced by *Bd* that have been shown to inhibit amphibian lymphocyte survival and proliferation *in-vitro* (Rollins-Smith et al., 2015).

A wide range of candidate genes involved in host colonisation and subsequent pathogenesis have also been identified (Rosenblum et al., 2008; Joneson et al., 2011; Rosenblum et al., 2013; Farrer et al., 2017; Ellison et al., 2017). Specifically expression of adhesin genes and triglyceride lipases that are associated with binding to host cells were up-regulated during infection (Joneson et al., 2011; Rosenblum et al., 2013). Though triglyceride lipases have not been formally examined in *Bd*, in another fungal pathogen, (*Malassezia furfur*) that infects human skin, the expression of this gene group was associated with incorporation of host lipids into the cell wall of the fungus, potentially leading to enhanced adherence to the host and immune evasion (Brunke and Hube, 2006). Another key group of genes involved in *Bd* adhesion to host cells are the carbohydrate binding module (CBM) proteins (in particular CBM18 that binds chitin) that are expanded in *Bd* (Abramyan and Stajich, 2012). CBMs are also enriched in other pathogenic fungi (Soanes et al., 2008).

Additional putative virulence factors include the M36 metalloproteases, S41 serineproteases and the aspartylproteases that are expanded in the *Bd* genome relative to other non-pathogenic fungi (Rosenblum et al., 2008; Joneson et al., 2011; Rosenblum et al., 2013). Interestingly, transcriptome analysis of an anuran host demonstrated increased expression of protease inhibitors in *Bd* infected individuals compared to control animals (Ellison et al., 2014a). This may suggest that an arms race exists between pathogen virulence factors and host defences. *Bd* is also enriched for crinkler (CRN) like microbial effectors (Joneson et al., 2011) that act in the host cytoplasm where they disrupt host metabolism and defences (Kamoun, 2006; Haas et al., 2009). CRNs are rare in the fungal kingdom and are most commonly associated with oomycete plant pathogens belonging to the kingdom Chromista (Kamoun, 2006). More recent transcriptome studies have identified high expression of genes involved in membrane transport mechanisms

such as amino acid permeases being associated with successful *Bd* infection (Ellison et al., 2017). It is hypothesised that amino acid permeases aid in the acquisition of essential amino acids during *Bd* colonisation, as is the case for some plant pathogens (Solomon et al., 2003). In addition, putative major facilitator super family (MFS) transporters, which in other fungi play a role in the secretion of toxic compounds (Del Sorbo et al., 2000), were up-regulated during *in-vivo Bd* infection (Ellison et al., 2017). MFS transporters may be a particularly important component in the pathogen virulence mechanism given the link between secretory factors, *Bd* derived metabolites and inhibition of host lymphocytes (Fites et al., 2013; Rollins-Smith et al., 2015).

In summary, while larval amphibians experience little *Bd* induced pathology, there are significant negative health impacts in post-metamorphic animals. The overall pathology exhibited in susceptible hosts is a culmination of several virulence mechanisms. In particular, the negative systemic effects and immunopathology brought about by the secretion of *Bd* toxins and secondary metabolites weaken the host immune response allowing *Bd* proliferation and secondary infection. Meanwhile, disruption of dermal tissue integrity brought about by the action of secreted metalloproteases and the subsequent impairment of sodium/potassium pumps contributes to the plasma ionic imbalance that eventually causes cardiac arrest and death.

1.0.6 Host defences

Amphibians are similar to mammals, birds and reptiles both in terms of their immunogenetic architecture and cellular mechanisms of immunity (Du Pasquier et al., 1989; Ohta et al., 2006). As for other jawed vertebrates, the immune system of amphibians can be divided into two broad arms, the innate and the adaptive immune systems.

Innate Immunity

The first line of amphibian defence against pathogens is the skin, which contains granular and mucus glands (Rollins-Smith et al., 2011). Granular glands produce a range of bioac-

tive molecules including antimicrobial peptides that have been shown to be inhibitory to *Bd* (Rollins-Smith and Conlon, 2005; Woodhams et al., 2006), lysozymes (Zhao et al., 2006) and toxins (Colombo et al., 2015). Mucus glands produce secretions that are rich in mucopolysaccharides (Duellman and Treub, 1986) and glycosylated mucins (Schumacher et al., 1994). The primary purpose of these secretions is to keep the skin moist, however they may also serve as a nutritional substrate for commensal microbes that form complex communities on the skin. Amphibian antimicrobial peptides (AMPs) are a key component of innate defence that are usually cationic and hydrophobic and are made up of 15 to 20 amino acid residues. When bound to charged residues on target cell membranes, AMPs can form an amphipathic (containing both a hydrophobic and hydrophilic region) alpha helix. This structure is involved in target cell membrane disruption and subsequent cell death (Van Rooij et al., 2015; Rollins-Smith et al., 2011). AMP production is not evident among all amphibian species, and in species that do secrete AMPs there is intra- and interspecific variability in the efficacy of AMPs against *Bd* (Woodhams et al., 2007; Conlon et al., 2009; Tennessen et al., 2009). Although lysozyme has not been extensively studied in *Bd* exposed amphibians, it has fungicidal potential (Rollins-Smith et al., 2009). The primary substrate of lysozyme is peptidoglycan, which is the major component of the bacterial cell wall and consists of a polymer of N-acetylglucosamine and N-acetylmuramic acid (Van Rooij et al., 2015). By breaking the beta-1,4 bonds in peptidoglycan, lysozyme induces cell lysis resulting in cell death. Since fungal cells walls are composed largely of chitin, which is a polymer of successive N-acetylglucoasmine units joined by beta-1,4 bonds, it has been suggested that lysozyme may also be an effective antifungal against *Bd* (Van Rooij et al., 2015).

Once a pathogen such as *Bd* has bypassed the physical barrier of the skin, the first key component of the cellular immune response is pathogen recognition. Antigens present on invading pathogens often possess structural features called pathogen-associated molecular patterns (PAMPs) that may be common to a range of microbes and in some cases can be recognised by certain host immune cells. Pattern recognition receptors (PRRs) expressed in various host immune cells (e.g. dendritic Langherans cells, macrophages) bind to PAMPs eliciting a downstream inflammatory response (Grogan et al., 2018b). In mammals, which share many im-

munological similarities to amphibians, there are four classes of PRR. These are (1) C-type lectin receptors (CLRs) (2) Toll-like receptors (TLRs) (3) Retinoic acid-inducible gene (RIG)-I-like receptors (RLRs) and (4) NOD-like receptors (NLRs) (Takeuchi and Akira, 2010). While mammalian gene homologs of PRRs are found in amphibians (Grogan et al., 2018b), our understanding of their role in amphibian fungal infections remains limited. Prior studies have demonstrated increased expression of TLRs and NLRs but not CLRs in *Bd* infected animals (Ellison et al., 2014a,b; Grogan et al., 2018a).

Another key component to innate immunity in jawed vertebrates is the complement system, which consists of receptors, soluble plasma proteins and enzymes that when activated are involved in agglutinating extracellular pathogens followed by cell lysis or phagocytosis (Speth et al., 2008). Studies have demonstrated that increased expression of genes associated with the complement system during the early stages of *Bd* infection are linked to increased disease resistance (Grogan et al., 2018a). Cytokine pathways that mediated inflammation are also likely to be an active component of the host immune response against chytridiomycosis. Studies to date have found evidence of up-regulation of cytokine genes in *Bd* infected animals (Rosenblum et al., 2009; Grogan et al., 2018a) with expression being greatest in skin tissue of highly susceptible individuals at a late stage of infection (Ellison et al., 2014a,b; Grogan et al., 2018a). Thus, while it appears that cytokine expression is active during *Bd* infection, in some cases it is possible that extreme increases in expression of cytokine genes are a result of a dysregulated immune response indicative of immunopathology (Ellison et al., 2014a; Grogan et al., 2018b,a).

Adaptive immunity

The adaptive immune system provides a more targeted defence against invading pathogens than the innate immune system. In recent years there has been a growing body of evidence to suggest that some adaptive immunity to *Bd* may exist. A pivotal study demonstrated that repeated *Bd* exposure followed by forced clearance of infection resulted in acquired immunological resistance (McMahon et al., 2014). Specifically, the number of previous *Bd* exposures was a negative predictor of both infection burden and disease induced mortality, but a positive

predictor of lymphocyte abundance and proliferation (McMahon et al., 2014). Other studies have characterised the immune response at the cellular and genetic level. In one study, immunization against *Bd* resulted in elevated pathogen specific serum antibodies (IgM, IgY). In addition, the skin mucus of animals previously exposed to *Bd* showed significant amounts of IgM, IgY and IgX antibodies, all of which are capable of binding to *Bd* (Ramsey et al., 2010). Further evidence of a primed or acquired immune response is that chitinases (enzymes involved in fungal cell wall degradation) were up regulated more in anurans that had previously been exposed to *Bd* and re-infected than in animals that had been exposed once (Ellison et al., 2014a).

The major histocompatibility complex class II molecule (MHCII) presents antigens of extracellular pathogens (such as the pre-intracellular phase of *Bd* infection) to $CD4^+$ helper T cells resulting in the activation of other immune effector cells such as B cells. Studies of wild amphibian populations have shown that certain genotypes of MHCII are significant predictors of survival in *Bd* infected animals (Savage and Zamudio, 2011, 2016; Bataille et al., 2015). It has further been demonstrated that alleles encoding specific conformations of the P9 pocket within the antigen-binding groove of MHCII are markers for *Bd* resistance (Bataille et al., 2015). In addition to genetic association studies, transcriptome analyses have shown an increase in expression of MHC genes coinciding with *Bd* infection (Ellison et al., 2014a). Studies of the MHC class I molecule, which is expressed on nucleated cells and presents antigens from intracellular pathogens (i.e. fully encysted *Bd*) to $CD8^+$ helper T cells that differentiate into cytotoxic T cells that recognise and kill infected host cells have also been identified as under selection in *Bd* infected amphibians (Ellison et al., 2014a; Kosch et al., 2017; Lau et al., 2016); though this molecule class is less well studied than MHCII.

Host immunity and *Bd*/*Bsal* susceptibility

An important mechanism underlying differences in host susceptibility to *Bd* appears to be *Bd*-induced immunosuppression in some species but not others. Evidence in support of this hypothesis comes from studies that have shown that *Bd* infection is associated with either a lack

of robust immune response (Rosenblum et al., 2009, 2012) or that in more susceptible species there is down-regulation of key immune genes when exposed to *Bd* (Ellison et al., 2014a,b; Poorten and Rosenblum, 2016). In addition, prior studies have demonstrated that species susceptible to *Bd* are not able to mount an effective initial immune response as evident by early down regulation of complement system genes (Rosenblum et al., 2012). This hypothesis is further reinforced by *in-vitro* studies demonstrating that *Bd* inhibits host lymphyocytes (Fites et al., 2013; Rollins-Smith et al., 2015). Based on knowledge of other fungal pathogens that evade or suppress the host immune system, *Bd* may be circumventing host defences in several different ways (Ellison et al., 2014b). These include (i) disruption of normal host immune signalling (Brandhorst et al., 2004) (ii) pathogen sequestration within host cells to avoid recognition by host immune receptors (Woods, 2003) (iii) the pathogen digesting its own antigens with metalloproteases to avoid host recognition (Hung et al., 2005). Future studies that characterise the fine-scale dynamics of *Bd* within its amphibian host will therefore yield important findings in our understanding of infection outcome and differential host susceptibility.

1.0.7 Host-associated microbes

In recent years the advent of high throughput sequencing technologies have enabled the constituents of microbial communities to be characterised at unparalleled resolution. Next generation sequencing (NGS) has unshackled microbiologists from often laborious and unsuccessful attempts at isolating fastidious microbes in the laboratory, to identifying them based on their genomic content. As a result, biologists are beginning to shed light on Earth's enormous diversity of unknown microbial 'dark matter'.

Whilst microbes have long been known for their impact on health and disease, their importance to the function of multicellular organisms has arguably been underestimated. Studies of host associated microbiota (the collection of microbes that inhabit a host) and the host microbiome (the collection of DNA from microbes) have shown that microbes are intrinsically linked to the physiology of their hosts (Ottman et al., 2012; Dorrestein et al., 2014). The contribution of the microbiota to host function in many instances is underscored by the ratio of host to microbial

cells. For example, in humans for which the microbiome has been extensively studied, estimates suggest that for each host cell, there are 1.3 bacterial cells (Sender et al., 2016) and as many as 100 times bacterial genes as human genes (Turnbaugh et al., 2007). What's more, these figures are conservative in their estimate of microbial functional contribution to the host since they do not take into account fungi, archaea, viruses and protists. Given the diversity of host-associated microbes and their connection with host physiology, there has been a paradigm shift in how we consider multicellular organisms, from individuals to complex assemblages of microbe and host cells that function together as a dynamic ecosystem (Rynkiewicz et al., 2015).

Host-associated microbes make important functional contributions to their multicellular hosts. Prior studies involving a broad spectrum of host species have demonstrated strong associations between the microbiota and host development (Fraune and Bosch, 2010), inflammation (Honda and Littman, 2012), brain function/behaviour (Rogers et al., 2016) and metabolism (Smith et al., 2007). While many studies have identified microbial function in localised host compartments such as the skin or gut, in many cases the microbiota is linked to systemic effects (Dorrestein et al., 2014). One such example is the microbial breakdown of dietary fibre into short chain fatty acids (SCFAs) in the gut. SCFAs not only provide an energy source for intestinal epithelial cells but also impact the host immune system (Maslowski et al., 2009; Vinolo et al., 2011). Specifically, microbial derived SCFAs can modulate development and function of anti-inflammatory regulatory T (Treg) cells that stem uncontrolled inflammation and as such play a role in suppressing conditions such as ulcerative colitis (Smith et al., 2013). A key component of the innate immune system is pattern-recognition receptors (PRRs) that recognise and bind to microbe-associated molecules called microbe-associated molecular patterns (MAMPs) (Dorrestein et al., 2014). While MAMPs are often associated with microbial pathogenesis through host inflammation, in some instances they confer benefits to the host in terms of immune system development and function (Chu and Mazmanian, 2013). For example, one study demonstrated that differentiation of innate immune cells was disrupted in germ free animals making them susceptible to bacterial infection, however when microbe derived ligands were orally administered normal immune cell differentiation was restored (Khosravi et al., 2014). In addition to MAMPs interacting with the host immune system, microbes may

also produce metabolites that modulate host physiology (Dorrestein et al., 2014). For example indole-3-aldehyde is a product of microbial tryptophan metabolism produced by taxa such as *Lactobacillus* and is known to up-regulate host interleukin-22 (IL-22) making the gut mucosa more resistant to colonisation by the fungal pathogen *Candida albicans* (Zelante et al., 2013). Perturbations of host microbial communities can consequently impact beneficial host-microbe relationships as well as disrupt microbial community function with negative effects to host health in a process termed dysbiosis. In addition to the health consequences brought about dysbiosis, unstable host microbial communities may also be more susceptible to infection by invading pathogens (Croswell et al., 2009; Khosravi and Mazmanian, 2013).

Successfully identifying a dysbiotic state remains methodologically challenging. In healthy animals, the defensive activities of the host and its microbiota are predicted to limit the membership of the microbiota to taxa that are beneficial or at least benign to host health, limiting the number of possible "healthy' microbiome configurations. A key hypothesis defining the mechanism of dysbiosis is that a departure from the normal regulation of host microbiome membership caused by a stressor results in stochastic changes to the microbiome and a wider range of possible microbiome configurations compared to the similar, stable microbiome's of healthy individuals (Zaneveld et al., 2017). This hypothesis has been termed the Anna Karenina Principle (AKP) inspired from a phrase in Leo Tolstoy's famous book: "all happy families are all alike; each unhappy family is unhappy in its own way". This hypothesis has held true across a range of animal systems. For example, the obese human gut microbiome is associated with a more eclectic range of microbiome profiles than in lean individuals (Holmes et al., 2012). Similarly, a controlled laboratory experiment in which an amphibian host was infected with *Bd* resulted in greater dispersion of microbiome structure in infected compared to control animals (Walke et al., 2015a).As with many rules, there are notable exceptions to AKP, described as anti-AKP effects in the literature (Zaneveld et al., 2017). For example, in some instances a stressor such as infection may reduce microbiome diversity due to a small number of specific microbes dominating the microbiome. For example, eczematous dermatitis was associated with changes in the normal skin microbiota with proliferation of *Corynebacterium mastitidis*, *Staphylococcus aureus* and *Corynebacterium bovis* (Kobayashi et al., 2015). The causal association

between these microbes and eczematous dermatitis was demonstrated when symptoms (specifically dermal inflammation) were reversed using targeted antibiotic therapy. A key challenge in microbiome research is accurately disentangling true dysbiotic effects from other factors that may shape the microbiome but not be linked to any negative health impacts. Such issues may arise due to poor experimental design, biases in sequencing and not taking into account other key factors such as host body mass or the environment. Development of more sophisticated analyses will no doubt improve diagnosis of dysbiotic states in animals. In light of the importance of the microbiota and the negative health effects brought about by dysbiosis, there has been interest in studies investigating the microbiome in diseased and healthy organisms. Such studies may be of particular value in providing a mechanistic insight into the drivers of disease outcome, in addition to identifying biomarkers and formulating future clinical interventions (Gilbert et al., 2018).

The skin of amphibians is rich in mucosal secretions containing molecules such as mucopolysaccharides that are of nutritional value to microbes enabling it to harbour a complex microbiota. Microbial colonisation of the skin begins at hatching with changes in community composition on going throughout development (Kueneman et al., 2014, 2016b; Longo et al., 2015; Knutie et al., 2017). Skin microbes may be acquired from environmental sources (Muletz et al., 2012; Walke et al., 2014; Loudon et al., 2016), through horizontal transfer between different hosts (Rebollar et al., 2016a), or vertically from parent to offspring (Walke et al., 2011). In addition to environmental and host-host acquisition of microbes, the microbial composition of the skin has been shown to be affected by a multitude of factors including diet (Antwis et al., 2014), abiotic factors such as climate (Longo et al., 2015), host physiology/genetics (Griffiths et al., 2018) and age (Kueneman et al., 2014).

The amphibian skin microbiome has increasingly been studied for its importance in pathogen defence. Microbes typically have short generation times, high rates of mutation and large within-host population sizes that facilitates faster adaptation of defensive traits against pathogens than is possible in a long-lived host such as an amphibian (May and Nelson, 2014). Consequently, some constituents of the host microbiota may provide effective, real time defence against pathogens that would not be possible from the host alone. Microbe-mediated protec-

tion against pathogens such as *Bd* may occur through resource competition (Collado et al., 2008), modulation of the host immune system (Grice and Segre, 2011) or by production of metabolites that are inhibitory to pathogen growth (Brucker et al., 2008b). In the case of chytridiomycosis, *in-vitro* assays have demonstrated that certain skin associated bacteria and fungi can inhibit pathogen growth (Harris et al., 2006; Lauer et al., 2007; Woodhams et al., 007b; Muletz-Wolz et al., 2017; Kearns et al., 2017) and that microbial diversity is often negatively correlated with *Bd* infection load (Piovia-Scott et al., 2017). Compelling evidence has also come from *in-vivo* lab and field studies that have shown that differences in amphibian skin microbial diversity, community structure and function are linked to chytridiomycosis disease outcome through microbe mediated protection or perturbations to community structure with negative host effects (Harris et al., 2009; Jani and Briggs, 2014; Jani et al., 2017; Rebollar et al., 2016b; Woodhams et al., 2014; Kueneman et al., 2016b; Becker et al., 2015; Walke et al., 2015b). Amphibian skin bacteria have also been shown to produce specific anti-*Bd* metabolites such as violacein, indole-3-carboxaldehyde, 2,4-diacetylphloroglucinol (2,4-DAPG) and tryptophol (Brucker et al., 2008b; Loudon et al., 2014a; Woodhams et al., 2017). Interestingly, the production of certain *Bd* inhibitory metabolites is dependent on microbial community structure. For example tryptophol was produced only when *Bacillus sp.* and *Chitinophaga arvensicola* were grown in co-culture but not when either was grown singly (Loudon et al., 2014a). Amphibian skin microbes may also produce volatile organic compounds and antimicrobial peptides such as bacteriocins that may inhibit *Bd* or augment the host microbial community (Woodhams et al., 2016). These molecular classes however remain largely unexplored.

As a result of the strong associations between the host microbiota and *Bd* infection outcome in field and lab systems, there has been an effort to identify probiotics and microbiome augmentations that may provide prophylactic benefits to host species at particular risk of chytridiomycosis (Bletz et al., 2013). While studies have demonstrated that probiotics have prevented *Bd* induced mortality and reduced the severity of chytridiomycosis outcome in *in-vivo* laboratory experiments (Harris et al., 2009, 009b; Kueneman et al., 2016a), probiotics are unlikely to be a silver bullet in chytridiomycosis mitigation. In particular, *in-vitro* studies have demonstrated that the same bacterial strain can have polarising effects on *Bd* growth ranging from inhibition

to promotion depending on *Bd* genotype and the wider microbial community structure (Antwis et al., 2015; Antwis and Harrison, 2018). Given the broad diversity of *Bd* genotypes and high within-species microbial diversity, a 'one size fits all' probiotic that can establish in different complex microbial communities, maintain *Bd* inhibition, and not negatively impact host health seems unlikely. There may however be merit in utilising a personalised medicine based approach to treat severely at-risk single species populations. To maximise theoretical success, such populations should be infected by a low diversity of *Bd* genotypes and have similar host microbiome composition. Overall, determining the importance of the amphibian microbiome in chytrid infection and how it relates to broad ecological patterns in nature may be of significant value to our understanding of wild disease outbreaks and their future mitigation.

1.0.8 Focal study species: *Alytes obstetricans*

The common midwife toad, *Alytes obstetricans* has a broad species distribution from northern Portugal and Spain through to France, southern Belgium, southeastern Netherlands, Luxembourg, western and north-central Germany, and western and northern Switzerland. Introduced populations also exist in the UK (Bosch et al., 2009). While the overall conservation status of *A. obstetricans* is listed as least concern (Bosch et al., 2009), local population decline and extinction in parts of its range have led to it being given protected status in some countries. Post-metamorphic *A. obstetricans* live in terrestrial habitats with breeding occurring in ponds or slow moving rivers. *A. obstetricans* feeds predominantly on invertebrates and is nocturnal, spending much of the day under rocks or buried in gravel near water sources. Both adult males and females can typically reach a snout to vent length of approximately 55 mm and possess small parotid glands with a visible tympanum. Additional glands are found on the ankles and underarms. The dorsal colouration can vary but is generally a greyish-brown with a grey spotted ventral side (Fig. 1.2a). There is often a row of red-pigmented warts that extend from the loin area to the tympanum (Bosch, 2009). Tadpoles typically have a pale brown dorsum and light golden ventral side with a distinct silver stripe. Many larvae overwinter and may typically reach 8cm in length (Bosch, 2009) (Fig. 1.2b). *A. obstetricans* exhibits reciprocal calling in which both male and females produce vocalisations during courtship. Mating is a lengthy process in which a female is clasped in inguinal amplexus by a male with release of eggs occurring from fifteen minutes to two hours later (Bosch, 2009). Females lay a string of approximately forty eggs (Marquez, 1993) which are then intertwined around the males ankles. Males then carry eggs and locate hideouts with optimal conditions for embryogenesis to occur (Bosch, 2009). From fifteen to forty five days post-amplexus the larvae have developed within the eggs, at which point the male deposits the eggs in a body of water where the eggs subsequently hatch (Bosch, 2009). In addition to the fascinating life-history of *A. obstetricans*, studies of its chemical secretions have identified a range of antimicrobial peptides with possible clinical relevance. Specifically, *A. obstetricans* secretes antimicrobial peptides belonging to a family of molecules called the alyteserins that have been demonstrated to inhibit both gram negative and gram positive bacteria in culture (Conlon et al., 009b).

A. obstetricans is considered highly susceptible to *Bd* with population declines widely noted across the Pyrenees (Bosch et al., 2001; Walker, 2008; Clare, 2014; Clare et al., 2016) and other parts of its range (Tobler and Schmidt, 2010). Over-wintering can have important effects on disease dynamics in the wild with over-wintered larvae, whilst not being susceptible to *Bd* acting as a pathogen reservoirs facilitating transmission to more susceptible post-metamorphic conspecifics (Clare et al., 2016). Despite significant population decline in the Pyrenees, variation in susceptibility of *A. obstetricans* to *Bd* can exist, with some populations demonstrating signs of tolerance to infection (Tobler and Schmidt, 2010; Bates et al., 2018).

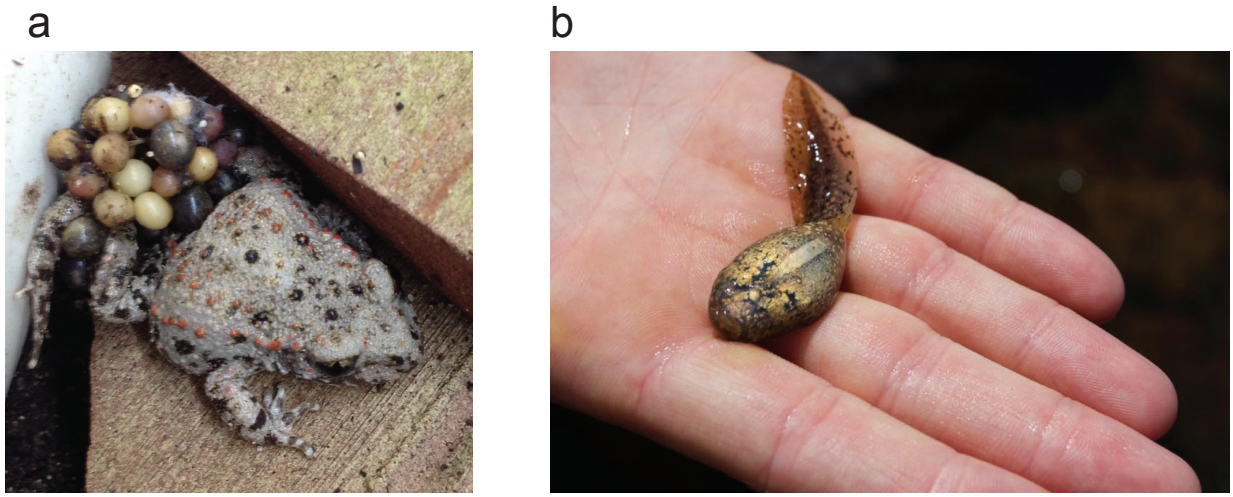


Figure 1.2: Common midwife toad, *Alytes obstetricans*. (**a**) adult male with egg string, (**b**) over-wintered tadpole.

1.0.9 The Pyrenees study system

The majority of fieldwork for this thesis (Chapters Two and Four) has been conducted at high altitude montane lakes in the district of Aragon in Spain and the Valle de Aspe in the Western Pyrenees of France (Fig 1.3). Sampling of *Bd* from wild amphibians in the Pyrenees has been carried out since 2004 when the pathogen was first detected from a single population (Ibon Acherito) where it subsequently spread to all five study sites. I carried out fieldwork from June to August from 2014-2016, in addition to analysing a long-term data set of samples that were collected from 2010 onward in some instances.

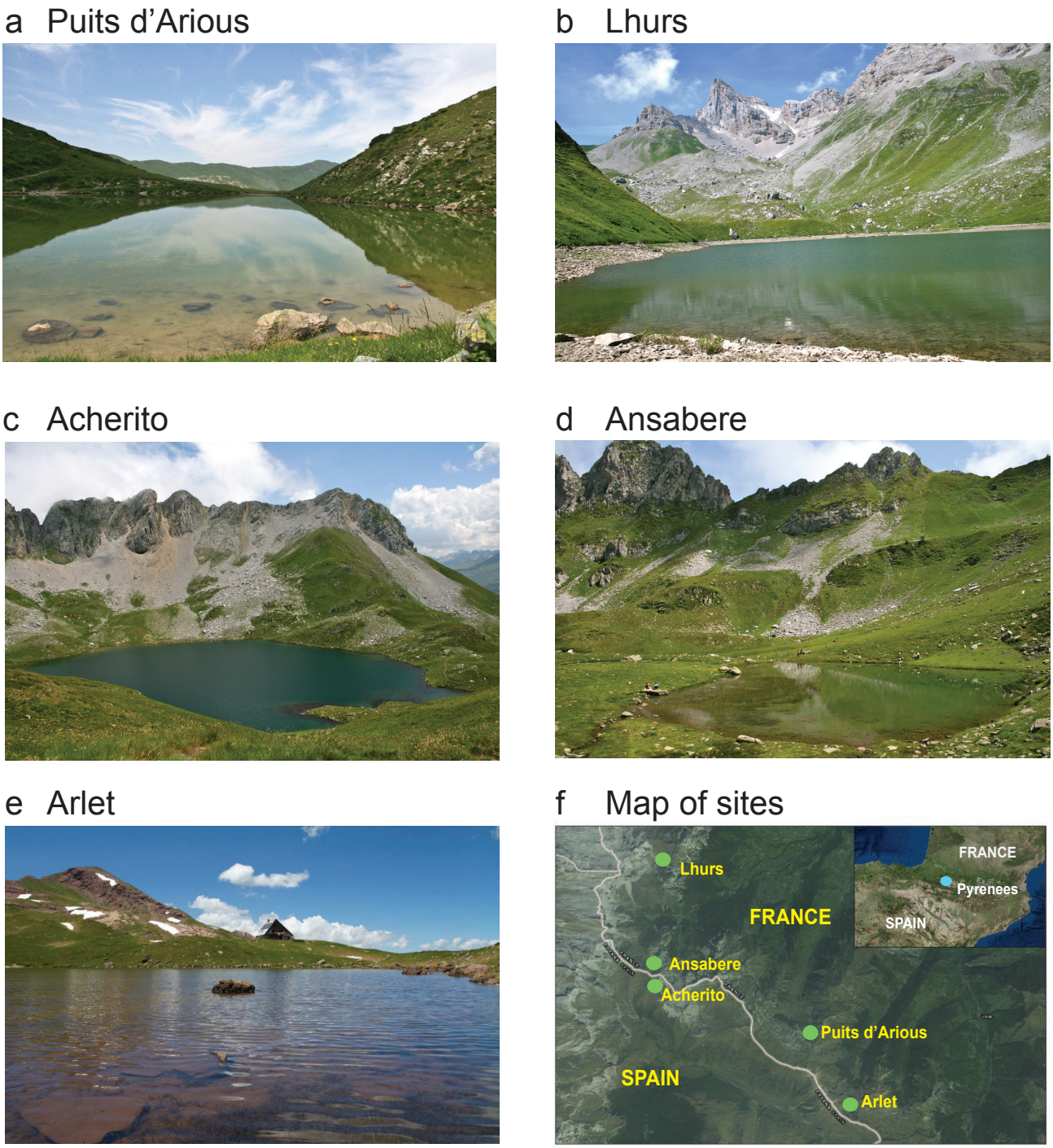


Figure 1.3: Pyrenean mountain lakes sampled in this thesis. The altitutude and total area of each lake is shown in parentheses. (**a**) Puits d'Arious (1859m, 0.2ha), (**b**) Lhurs (1691m, 1.5ha), (**c**) Ibon Acherito (1869m, 5.6ha), (**d**) Ansabere (1859m, 0.2ha), (**e**) Arlet (1986m, 2.7ha), (**f**) Map of study sites.

1.1 Aims and Objectives

This thesis focuses on the key drivers underpinning heterogeneity in host response to emerging fungal pathogens. In particular I sought to answer the following key questions relating to the overall aim of the thesis:

1. How important are pathogen genetics and the host skin microbiome in shaping the outcome of infection in a wild chytridiomycosis outbreak?

2. Does the amphibian skin microbiome differ across life-stages and to what extent does host environment shape dermal bacterial communities?

3. Does captivity and exposure to an emerging chytrid pathogen impact the skin microbiome of different amphibian host species and how does this relate to disease susceptibility?

4. Are differences in host skin microbiome across wild amphibian populations and chytridiomycosis disease states functionally important?

1.2 Hypotheses

I hypothesised the following:

1. Differences in chytridiomycosis disease outcome in a wild outbreak system will be driven by population-level differences in both pathogen genetics and host skin microbiome structure.

2. The amphibian skin microbiome will differ between larval and metamorph life stages and will be shaped by the host environmnent.

3. The skin microbiome of captive amphibians will differ to those in the wild, with captivity potentially impacting the hosts response to infection.

4. Infection by the emerging fungal pathogen *Batrachochytrium salamandrivorans* will negatively impact host health and affect the skin microbiome of two different caudate species.

5. Differences in skin microbiome composition across different disease states will be associated with skin metabolic function.

To study these questions, I utilised both laboratory and field based amphibian-chytrid systems in addition to molecular biology and chemical analyses. In my first data chapter, **Chapter Two**, I examined the relative importance of *Bd* genotype and host skin microbial communities in the epidemiology of a wild chytridiomycosis outbreak system. This study focussed on midwife toad (*Alytes obsetricans*) populations in my primary field sites in the Pyrenees mountains of France and Spain. In addition, I investigated how the *A. obstetricans* bacterial microbiome differed across ontogeny in larval compared to recently metamorphosed animals, and the relative importance of environmental microbial reservoirs in shaping the host microbiome. This chapter has been published in *Nature Communications*.

In **Chapter Three**, I investigated whether infection outcome of a recently discovered pathogenic chytrid fungus, *Batrachochytrium salamandrivorans* (*Bsal*) was linked to the skin microbiome of two amphibian host species. I also examined the effect of captivity on host fungal and bacterial communities and the potential implications this may have for host disease resistance. This Chapter has been submitted for publication.

In **Chapter Four**, I examined whether taxonomic differences in microbiome composition of *A. obstetricans* from Pyrenean populations exhibiting enzootic or epizootic chytridiomycosis disease dynamics were linked to functional differences in the skin mucosal metabolome. This chapter is in preparation for submission for publication.

1.3 Funding

The UK Natural Environment Research Council (NERC) and the Leverhulme Trust have provided funding for this research.

1.4 Publications

Chapter 2 of this thesis was published as:

Bates, K.A., Clare, F.C., O'Hanlon, S., Bosch, J., Brookes, L., Hopkins, K., McLaughlin, E., Daniel, O., Garner, T.W.J., Fisher, M.C., Harrison, X.A. (2018). Amphibian chytridiomycosis outbreak dynamics are linked with host skin bacterial community structure. *Nature Communications*, 9, 693. doi:10.1038/s41467-018-02967-w.

Chapters 3 and 4 are in preparation for publication. During my PhD I also contributed to the following publications:

Ghosh, P.N., Fisher, M.C., **Bates, K.A.** (2018). Diagnosing emerging fungal threats: a one health perspective. *Frontiers in Genetics*. 9, 376. doi:10.3389/fgene.2018.00376.

O'Hanlon, S...(56 authors)..**Bates, K.A.**...Fisher, M.C. (2018). Recent Asian origin of chytrid fungi causing global amphibian declines. *Science*, 360(6389), 621-627. doi:10.1126/science.aar1965.

Fisher, M.C., Ghosh, P., Shelton, J.M.G., **Bates, K.A.** *et al.* (2018). Development and worldwide use of a non-lethal and minimal population-level impact protocols for the isolation of chytrids from amphibians. *Scientific Reports*, 8, 7772. doi:10.1038/s41598-018-24472-2.

Dillon, M.J., Bowkett, A.E., Bungard, M.J., Beckman, K., O'Brien, M., **Bates, K.A.**, Fisher, M.C., Stevens, J.R. Thornton, C.R. (2017). Tracking the amphibian pathogens *Batrachochytrium dendrobatidis* and *Batrachochytrium salamandrivorans* by using a highly specific monoclonal antibody and lateral-flow technology. *Microbial Biotechnology*, 10(2), 381-394. doi:10.1111/1751-7915.12464.

Chapter 2

Amphibian chytridiomycosis outbreak dynamics are linked with host skin bacterial community structure

Kieran A. Bates[1,2], Frances C. Clare[2], Simon O'Hanlon[1], Jaime Bosch[3], Kevin P. Hopkins[2], Emilia J. McLaughlin[2], Olivia Daniel[1], Trenton W.J. Garner[2], Matthew C. Fisher[1], Xavier A. Harrison[2]

[1]Department of Infectious Disease Epidemiology and MRC Centre for Global Infectious Disease Analysis, School of Public Health, Imperial College London, London W2 1PG, UK; [2]Institute of Zoology, Zoological Society of London, Regents Park, London, NW1 4RY, UK; [3]Museo Nacional de Ciencias Naturales, CSIC, Jose Gutierrez Abascal, 2 28006, Madrid, Spain

Author contributions: K.A.B., F.C.C., O.D., J.B., T.W.J.G. and M.C.F. conducted field surveys. K.A.B., F.C.C., K.H., E.J.M. and S.O. performed data processing. K.B. and S.O. performed data analysis. K.A.B prepared the figures.

2.1 Abstract

Host-associated microbes are vital for combating infections and maintaining health. In amphibians, certain skin-associated bacteria inhibit the fungal pathogen *Batrachochytrium dendrobatidis* (*Bd*), yet our understanding of host microbial ecology and its role in disease outbreaks is limited. I sampled skin-associated bacteria and *Bd* from Pyrenean midwife toad populations exhibiting enzootic or epizootic disease dynamics. I demonstrate that bacterial communities differ between life stages with few shared taxa, indicative of restructuring at metamorphosis. A significant effect of infection history on metamorph skin microbiota was detected, with reduced bacterial diversity in epizootic populations and differences in community structure and predicted function. Genome sequencing of *Bd* isolates supports a single introduction to the Pyrenees and reveals no association between pathogen genetics and epidemiological trends. My findings provide an ecologically relevant insight into the microbial ecology of amphibian skin and highlight the relative importance of host microbiota and pathogen genetics in predicting disease outcome.

2.2 Introduction

The communities of bacteria resident on multicellular organisms are of significant importance to host health (Ottman et al., 2012). In addition to their involvement in essential host physiological processes (Smith et al., 2007; Fraune and Bosch, 2010; Honda and Littman, 2012; Rogers et al., 2016), bacterial interactions with invading pathogens are key in defining disease outcome (Hooper et al., 2012). Commensal bacteria may confer protection against pathogens through limiting pathogen adhesion to host cells (Buffie and Pamer, 2013), resource competition (Kamada et al., 2012), interacting with the host immune system (Gensollen et al., 2016), or production of antimicrobial compounds (Brucker et al., 2008b). Conversely, some commensal bacteria interact synergistically with pathogens exacerbating infection (Stacy et al., 2016). At a community level, disruption of the microbiome (a process termed dysbiosis) can negatively impact host health bringing about pathophysiological changes and in some instances facilitating

infection by opportunistic pathogens (Croswell et al., 2009).

The emerging infectious disease, chytridiomycosis caused by the fungal pathogen *Batrachochytrium dendrobatidis* (*Bd*) is known to affect over 500 amphibian species worldwide (Olson et al., 2013). *Bd* infects keratinized skin of post-metamorphic anurans where it disrupts osmoregulation leading to cardiac abnormalities and in some cases death (Voyles et al., 2009). Larval anurans exhibit little *Bd* induced pathology since the skin is deficient of keratin and infection is restricted to the mouthparts (Berger et al., 1998). Prior studies have gained insight into the drivers of *Bd* infection dynamics by examining host and pathogen biology in addition to environmental effects on disease outcome (Savage and Zamudio, 2011; Farrer et al., 2011; Clare et al., 2016). Recently attention has shifted to include the role of skin-associated bacteria in infection based on findings that certain taxa inhibit *Bd* (Woodhams et al., 007b; Kueneman et al., 2016b). Other studies have shown associations between bacterial communities and infection in the field (Jani and Briggs, 2014; Kueneman et al., 2016a; Rebollar et al., 2016b; Jani et al., 2017), however research has largely focused on within-population infection dynamics and on species solely from the Americas. With the exception of an amphibian study system in the Western United States (Jani and Briggs, 2014; Jani et al., 2017), most studies to date are based on short-term surveillance programs and therefore lack vital information such as time of initial *Bd* emergence. In addition, while previous studies have demonstrated that pathogen genetics can underpin *Bd* virulence (Farrer et al., 2011) and disease dynamics in the field (Piovia-Scott et al., 2015), the relative importance of the microbiome and pathogen genetics have not been simultaneously investigated in the wild. Therefore, it remains to be established whether pathogen genetics and microbiome covary and the extent to which they are associated with disease dynamics. Consequently prior studies have been limited in their ability to examine the relationships between host bacterial communities and disease dynamics in complex ecosystems.

In this chapter, we used 16S metabarcoding to disentangle the relationship between skin bacterial community structure, life stage and *Bd* infection in wild common midwife toads (*Alytes obstetricans*). We also used whole genome sequencing to investigate the spatial and temporal genetic structure of *Bd* isolates from host populations exhibiting distinct disease dynamics. Our work focuses on a long-term study system in the Pyrenees of France and Spain in which

infection has been monitored continuously for over 10 years (Walker, 2008; Clare, 2014). While *A. obstetricans* is native throughout Europe, it has shown catastrophic declines in the Pyrenees with several populations undergoing mass mortality events (Walker, 2008; Clare, 2014; Bosch et al., 2001). In recent years however, certain populations have shown signs of resistance to infection based on a reduction in infection intensity and an associated resurgence in population abundance consistent with the establishment of enzootic disease dynamics. Importantly, resistance is defined here as as the host's ability to reduce pathogen burden, which may be differentiated from tolerance in which a host can withstand the damage caused by a pathogen or the host immune response. In a field system, tolerance would be evident by an increase in population abundance but not a decline in infection intensity. In contrast to the establishment of enzootic disease dynamics in some populations, other populations infected at approximately the same time remain in decline, exhibit high infection intensity and show high susceptibility to *Bd* indicative of epizootic dynamics.

Our results demonstrate that *Bd* in the Pyrenees arose from a single introduction and isolates from enzootic and epizootic populations are not genetically distinct. Significant differences were however found in the skin microbiome of amphibians, with life stage, population and *Bd* infection dynamics exhibiting a strong association with bacterial community structure. We further show that the predicted function of metamorph skin bacterial communities differs based on disease dynamics. We identify a conserved set of bacterial taxa associated with different disease states that may represent a dysbiosis contributing to epizootic dynamics, or selection of protective symbionts leading to an enzootic disease state. Our findings show that among populations with little spatial separation, bacterial community structure but not pathogen genetics is associated with divergent disease outcomes.

2.3 Material and Methods

2.3.1 Monitoring long-term infection dynamics of *Batrachochytrium dendrobatidis* (*Bd*) among Pyrenean populations of *Alytes obstetricans*

Bd has been monitored in each *A. obstetricans* population since its initial emergence in Acherito in 2004. Prior studies conducting temporal surveys incorporating catch-mark-recapture (CMR) and visual encounter surveys of larvae from each population have shown different trajectories of disease outcome (Clare, 2014). Population abundance estimates were made based on larvae rather than metamorphs due to the elusiveness of metamorphs. Larvae are also considered a good proxy for metamorph abundance given that larval numbers are a function of adult breeding success and are therefore proportional to the abundance of surviving metamorphs. To determine *A. obstetricans* over-wintered larval population abundance at each lake, a 2m area of water from the lakes edge was scanned and approximate counts (less than 100; 100-1000; more than 1000) were made following the methods of a prior study (Clare et al., 2016). To elucidate the general trends in infection dynamics over time for each host population, we collected data from each population in the summer of 2015 in addition to analysing a historical data set of *A. obstetricans* metamorph infection intensities spanning the years 2010 to 2014.

2.3.2 Sample collection

Recently metamorphosed and larval *A. obstetricans* were captured and rinsed with sterile water to remove transient bacteria on the skin (Culp et al., 2007). Using single sterile swabs, we sampled the skin microbiome by swabbing the body of tadpoles and metamorphs 10 times, additionally swabbing the fore- and hindlimbs of metamorphs 5 times. To sample for *Bd* in metamorphs, we swabbed the pelvic patch and ventral surface of the hind limbs 10 times. A fresh pair of sterile latex gloves was worn for each animal to avoid cross contamination of *Bd* or bacteria. Environmental water samples were collected following previously published methods

(Kueneman et al., 2014). For water samples a sterile swab was moved through lake water for 30s at a depth of approximately 30cm. Sediment samples were collected at the same location as water samples by embedding the swab into sediment for 30s. All swabs were immediately stored on ice before being transferred to a freezer. MW100 rayon tipped dry swabs (MWE Medical Wire, Corsham, UK) were used for *Bd* and bacterial sampling.

2.3.3 DNA extraction and sample processing

Genomic DNA was extracted from microbiome swabs using the DNeasy Blood and Tissue kit (Qiagen, Venlo, Netherlands) according to the manufacturers instructions. A pre-treatment with mutanolysin was included to enhance recovery of bacterial DNA (Yuan et al., 2012). DNA extracted from swabs was used to amplify the V4 region of the 16S rRNA gene using custom barcoded primers and PCR conditions adapted from a prior study (Kozich et al., 2013). PCR conditions consisted of a denaturing step of 95°C for 15 min, followed by 28 cycles of 95°C for 20s, 50°C for 60s, 72°C for 60s and a final extension step of 72°C for 10 min. Each PCR including a negative water control was performed in triplicate. Amplicons were visualized on a 2% agarose gel and pooled yielding a final per sample volume of 24 µl. Pooled amplicon DNA was purified using an Ampure XP PCR purification kit (Beckman Coulter, California, USA). Following purification, 1 µl of each combined sample was pooled into a preliminary library and the concentration was determined using Qubit fluorometric quantification (Life Technologies, California, USA). Amplicon quality and incidence of primer dimer was assessed using an Agilent 2200 TapeStation system (Agilent Technologies, California, USA). A titration run of 300 sequencing cycles was performed on a MiSeq instrument (Illumina, California, USA) to quantify the number of reads yielded per sample from the preliminary library. An equimolar concentration of each sample was then pooled into a final composite library based on the index representation from the titration run and subsequently sequenced on a 500 cycle MiSeq run with a 250 bp paired-end strategy. Genomic DNA from *Bd* swabs was extracted using a bead-beating protocol (Boyle et al., 2004). DNA extractions were diluted 1/10 before undergoing qPCR amplification with each sample run in duplicate (Boyle et al., 2004) and with *Bd* standards of

100, 10, 1 and 0.1 zoospore genomic equivalents (GE). Samples with greater than 0.1 GE were considered positive for *Bd*.

2.3.4 16S sequence analysis

Sequences were processed using MOTHUR (Schloss et al., 2009) following a previously described method (Kozich et al., 2013). Paired-end reads were split by sample and assembled into contigs. Sequences were quality filtered by removing ambiguous base calls, removing homopolymer regions longer than 8 bp, and trimming reads longer than 275 bp. Duplicate sequences were merged and aligned with 16S reference sequences from the SILVA small-subunit rRNA sequence database (Pruesse et al., 2007). A pre-clustering step grouped sequences differing by a maximum of 2 bp. Chimeric sequences were removed using UCHIME (Edgar et al., 2011) as implemented in MOTHUR. 16S rRNA gene sequences were clustered into groups according to their taxonomy at the level of order and assigned operational taxonomic units (OTUs) at a 3% dissimilarity level. Sequences were taxonomically classified with an 80% bootstrap confidence threshold using a nave Bayesian classifier with a training set (version 9) made available through the Ribosomal Database Project (http://rdp.cme.msu.edu) (Wang et al., 2007). Sequences derived from chloroplasts, mitochondria, archaea, eukaryotes or unknown reads were eliminated. The number of sequences per sample ranged from 3345 to 252910. To mitigate the effects of uneven sampling (Schloss et al., 2011), all samples were rarefied to 3345 sequences corresponding to the size of the lowest read sample. Rarefying at a higher threshold of 10000 sequences led to some samples being discarded but had minimal impact on results for alpha and beta diversity. Downstream analysis of OTUs was carried out using the package Phyloseq (McMurdie and Holmes, 2013) in R (R Core Team, 2017) version 3.4.1.

2.3.5 Infection analysis

All statistical analyses were carried out using R (R Core Team, 2017) version 3.4.1. Analysis of infection intensity followed previously published methods (Clare et al., 2016). Genomic

equivalents were rounded to whole numbers and treated as count data. A Negative binomial regression model (function glm.nb, package MASS (Venables and Ripley, 2002)) was used to establish if infection intensity differed between populations. A likelihood ratio test was used to assess significance of population in the model. Tukey post-hoc testing (function glht, package multcomp (Hothorn et al., 2008)) was performed to identify populations that had significantly different infection intensities. Genomic equivalents data were visualised using boxplots and log+1 transformed for presentation purposes. Prevalence data was displayed using barplots.

2.3.6 Bacterial communities across space and life history stage

To determine the relationship between life stage, environmental bacteria and host bacterial communities, we calculated the proportion of shared and unique OTUs between host and environmental samples and between developmental stages. Water and sediment samples were combined into a single factor called 'Environment' for computing shared OTUs since we were interested in how the environment regardless of specific sample type shaped the host associated bacterial community. Shared OTUs between groups of interest were visualised using venn diagrams generated using the program Venny (Oliveros, 2007).

Shannon diversity was calculated for each life stage and environmental samples. We used ANOVA to compare Shannon diversity of different samples and Tukeys test to identify which groups differed significantly. A Bray-Curtis distance matrix was used to calculate beta diversity of samples and visualised using a non-metric multidimensional scaling (NMDS) plot. The relative contribution of life stage and population in structuring the microbiome was assessed using permutational multivariate analysis of variance (PERMANOVA) (Anderson, 2001) using the adonis function in the Vegan package (Oksanen et al., 2016) in R. PERMANOVA was also carried out to compare community structure of larvae and metamorphs with environmental samples. Analysis was performed for combined populations to isolate the effect of site as well as for individual populations to compare between site effects.

2.3.7 Microbiota in epizootic and enzootic metamorph populations

To determine the extent to which metamorph skin bacterial communities differed between populations, Shannon diversity was calculated and ANOVA was used to determine significant differences between groups. A post hoc Tukeys test was carried out to identify populations that differed significantly. Beta diversity of populations was calculated using a Bray-Curtis distance matrix and visualised using NMDS plots. PERMANOVA was carried out to determine the relative effects of disease dynamic and population in shaping bacterial communities. Indicator analysis (Dufrene and Legendre, 1997) was performed using the labdsv package (Roberts, 2016) in R to identify OTUs that best explained differences between populations and disease states. Indicator analysis calculates the product of an OTUs frequency and relative abundance in predefined groups. An indicator value of 1 represents the presence of an OTU in one group but not others, while an indicator value of zero is indicative of an OTU evenly distributed across all groups. Multiple comparisons were taken into account using the false discovery rate procedure (Benjamini and Hochberg, 1995). OTUs with an indicator value >0.5 and q-value <0.05 were considered informative. A heatmap displaying the relative abundance of the top 20 OTUs for enzootic and epizootic populations was generated using the function heatmap.2 in the gplots (Warnes et al., 2009) package in R.

To examine whether function of bacterial communities from enzootic and epizootic metamorph populations differed, gene prediction was performed using Piphillin (Iwai et al., 2016). A sequence identity cut-off of 97% was used and sequences were assigned putative function using the KEGG reference database (May 2017 release). Beta diversity of KEGG orthology (KO) abundances was calculated using the Bray-Curtis metric. Comparison of functional profiles of each population was performed using NMDS ordination and PERMANOVA in the R packages Phyloseq (McMurdie and Holmes, 2013) and Vegan (Oksanen et al., 2016) . Differentially abundant features between enzootic and epizootic populations were determined using linear discriminant analysis (LDA) effect size (LEfSe) (Segata et al., 2011). Classes were defined as enzootic or epizootic with population as a subclass and an LDA score of > 2.0 was used as a cut-off.

2.3.8 *Bd* isolation and genome sequencing

Bd was isolated from *Alytes obstetricans* toe clips taken from each population between 2004 and 2015. Isolates were grown in 50ml Nalgene Nunc^{TM} tissue culture-treated flasks (Thermo Fisher Scientific, Massachusetts, USA) for 10-14 days at 18-20 °C. DNA extraction was performed using the MasterPure Yeast DNA Purification Kit (Epicentre, Wisconsin, USA) or Qiagen Genomic Tips 20/G and DNeasy Blood and Tissue Kits (Qiagen, Venlo, Netherlands). DNA extractions were quantified using a Tapestation 2200 (Agilent Technologies, California, United States) and Quibt 2.0 fluorometer (Thermo Fisher Scientific, Massachusetts, USA). DNA samples for sequencing were prepared on an Illumina HiSeq 2000 (Illumina, California, USA).

Raw sequencing reads were first cleaned of adapter sequences and quality trimmed using cutadapt v1.10 (Martin, 2011). Reads were mapped to the JEL423 reference genome (GenBank assembly accecssion: GCA_000149865.1) using Burrows-Wheeler Aligner (BWA-mem) v0.7.8 (Li and Durbin, 2009). Resulting sequence alignment/map (SAM) files were processed using SAMtools v1.3.1 (Li et al., 2009) using the fixmate and sort programs to ready the files for variant discovery. Variant discovery was done using freebayes version dbb6160 (Garrison, 2012). In the first step, sorted BAM files for each of the isolates in the study were independently called to find variant positions. The set of all variable positions identified across all samples were merged into a single variant call format (VCF) file. In the second step, genotype calls were independently made for each isolate, at each of the positions identified in the first step to produce a squared-off call set (each sample VCF has genotype calls at the same loci, including homozygous reference calls, and explicitly identifying positions without sequencing read coverage). The sample VCF files were processed by vcflib (Garrison and Marth, 2012) to break complex variants into allelic primitives and then to normalize short insertion and deletion sequences (indels). VCFs were then quality filtered with bcftools version 1.3.1 (Li et al., 2009). Sites with homozygous reference genotypes covered by 4 reads, or sites not covered by any reads were set to missing. Subsequently, putative non-reference genotype calls were set to homozygous reference if they failed any of the following filters: there was not enough evidence to support a variant genotype call; an alternate allele is in the called genotype without support-

ing reads ('AC > 0 && NUMALT == 0); The phred-scaled quality score is less than 5 when there are any reads covering the position (%QUAL < 5 && DP > 0); any called allele is not supported by at least two reads (AF[*] <= 0.5 && DP < 4); alternate alleles are supported by only low quality reads (AF[*] <= 0.5 && DP < 13 && %QUAL < 10)| (AF[*] > 0.5 && DP < 4 && %QUAL < 50); the quality, scaled by depth of supporting reads is less than a threshold (%QUAL / AO < 10); a called allele does not appear on both forward and reverse strands (SAF == 0 | SAR == 0); alleles are only supported by reads entirely placed right or left of the query variant (RPR = 0 | RPL = 0). The individual filtered VCF files were merged into a single multi-sample VCF using vcfstreamsort (Garrison and Marth, 2012) to ensure sorting of out of order variants resulting from breaking complex variants in individual files into their simplest allelic representation. A phylogeny of the *Bd* isolates used in this study was visualised using ggtree (Yu et al., 2017).

Principal component analysis (PCA) was carried out using bi-allelic SNP positions using the package SNPrelate v1.10.2 (Zheng et al., 2012) in R version 3.4.1. SNPs in high linkage disequilibrium (LD) were pruned using a threshold of approximately half the maximum value of LD in *Bd*GPL (an LD50 of 0.125). A subset of 771 from 50,561 SNPs were used in the PCA analysis. PCA data was plotted using ggplot2 (Wickham, 2009).

2.3.9 Data availability

Sequence data have been deposited on the BioProject database under accession codes PRJNA421328 and PRJNA413876. All other data are available upon request from the authors.

2.3.10 Ethics statement

Research was performed under licence from the Parc National des Pyrenees and the Instituto Aragons de Gestin Ambiental.

2.4 Results

2.4.1 Host skin microbiota differs by life stage and population

We collected midwife toad larvae and metamorphs in August 2015 from five populations in the Pyrenees mountains of France and Spain (Table 2.1). We quantified the bacterial communities of amphibian skin and environmental samples by sequencing the V4 region of the 16S rRNA gene. To determine the importance of life stage and the environment in shaping the amphibian microbiome, we first calculated the proportion of bacterial operational taxonomic units (OTUs) common to different samples. We detected a total of 11112 OTUs, of which 17.3% were shared by larvae and metamorphs, 10.8% were shared by larvae and the environment, 10.1% were shared by metamorphs and the environment, and 7.8% were common to all sample types (Fig. 2.1a). Similar results were obtained when analysing populations on an individual basis (Table 2.2). In larvae and metamorphs, over 98% of OTUs had a relative abundance of less than 1% in the environment.

To assess differences in bacterial community structure between amphibian life stages and the environment, we calculated alpha and beta diversity metrics. Shannon diversity differed only among samples from Acherito (ANOVA $F_{(3,30)} = 6.462$, p=0.002) in which sediment had a significantly lower value relative to larvae, metamorphs and lake water (Tukeys test: sediment-larva p=0.001; sediment-metamorph p=0.002; sediment-water p=0.04, Fig.2.1b) . Both life stage and population were associated with variation in beta diversity of amphibian skin (Life Stage: PERMANOVA Pseudo-$F_{(1,112)}$ = 19.821, p=0.001; Population: PERMANOVA Pseudo-$F_{(4,109)}$ = 6.6086, p=0.001; Fig. 2.1c). There was a significant difference in beta diversity of environmental samples compared to larvae and metamorphs (Larva-Environment: PERMANOVA $F_{(1,81)}$=12.372, p=0.001; Metamorph-Environment: PERMANOVA $F_{(1,69)}$=6.0735, p=0.001; Table 2.3).

The composition of bacterial communities also differed between amphibian life stages and the environment. Larvae had a higher relative abundance of Firmicutes and Spirochaetes compared to metamorphs, while metamorphs were enriched for Actinobacteria and Acidobacteria. Of the

environmental samples, water had a higher relative abundance of Verrucomicrobia compared to sediment and amphibian skin, while sediment exhibited the highest relative abundance of Firmicutes and Bacteroidetes of any sample type (Fig. 2.1d).

Population	**Larvae**	**Metamorphs**	**Environmental samples**	**Elevation (m)**	***Bd* detected**	***Bd* status**
Acherito	16	14	Water sediment	1869	2004	Enzootic
Lhurs	15	11	Water sediment	1691	2009	Enzootic
Puits	17	7	Water sediment	1867	2006	Enzootic
Ansabere	15	3	Water sediment	1859	2005	Epizootic
Arlet	0	16	Water sediment	1986	2005	Epizootic

Table 2.1: Sample summary of each population. N = 2 environmental samples each of water and sediment for each population.

Category	**Combined**	**Acherito**	**Puits**	**Lhurs**	**Ansabere**	**Arlet**
Unique to larvae	3561	1855	1562	1716	1617	NA
Unique to metamorphs	4115	2418	1301	1623	265	1154
Unique to environment	920	313	257	213	278	602
Shared by larvae and metamorphs	1923	631	469	791	180	NA
Shared by larvae and environment	1206	385	255	361	366	NA
Shared by metamorphs and environment	1127	326	177	371	108	228
Shared across samples	870	242	142	295	92	NA

Table 2.2: Shared OTUs between larvae, metamorphs and environment for each population.

Population	**Comparison**	$\mathbf{R^2}$	**F**	***p* value**
Combined	Larva-Environment	0.1325	$F_{(1,81)}$=12.372	0.000999
Combined	Metamorph-Environment	0.0809	$F_{(1,69)}$=6.0735	0.000999
Acherito	Larva-Environment	0.17552	$F_{(1,18)}$=3.8319	0.000999
Acherito	Metamorph-Environment	0.15426	$F_{(1,16)}$=2.9184	0.002997
Puits	Larva-Environment	0.25355	$F_{(1,19)}$=6.4538	0.000999
Puits	Metamorph-Environment	0.22667	$F_{(1,9)}$=2.6380	0.004995
Lhurs	Larva-Environment	0.28544	$F_{(1,17)}$=6.7908	0.000999
Lhurs	Metamorph-Environment	0.1624	$F_{(1,13)}$=2.5205	0.002997
Ansabere	Larva-Environment	0.23975	$F_{(1,17)}$=5.3611	0.000999
Ansabere	Metamorph-Environment	0.25365	$F_{(1,5)}$=1.6993	0.2637
Arlet	Metamorph-Environment	0.11166	$F_{(1,18)}$=2.2624	0.008991

Table 2.3: Results of PERMANOVA comparing beta diversity of larvae and metamorphs to environmental samples.

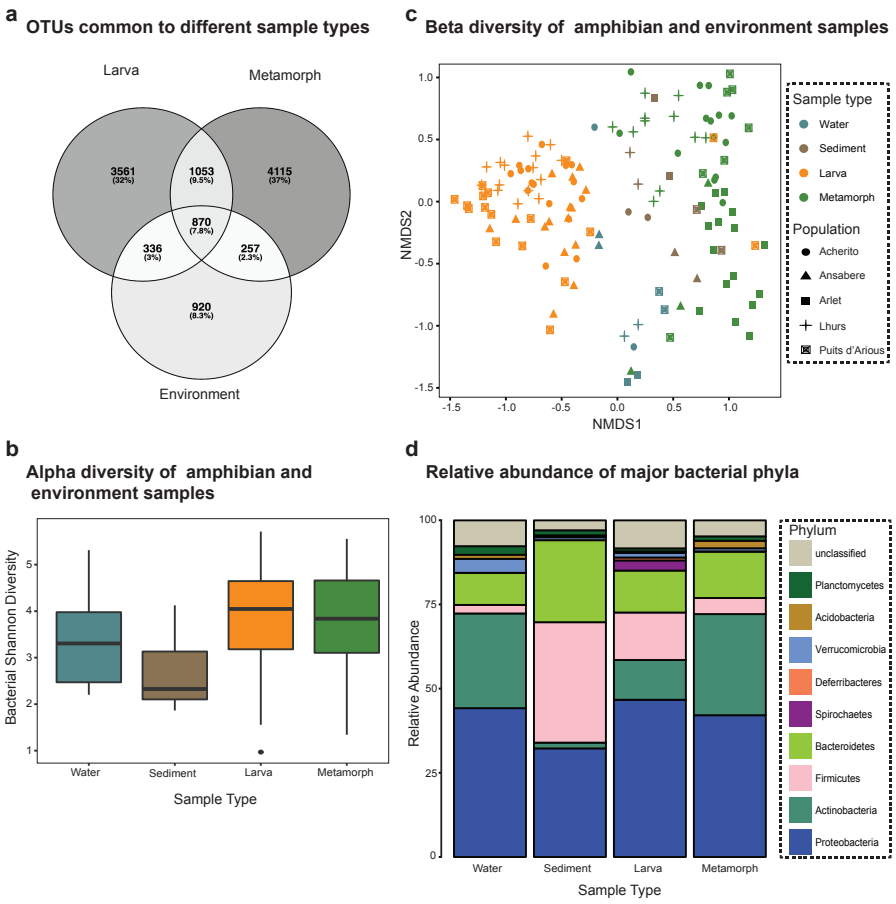


Figure 2.1: (**a**) OTUs common among life stages and environmental samples (**b**) Shannon diversity by sample type (boxes represent 25$^{\text{th}}$ and 75$^{\text{th}}$ percentile, the horizontal line is the median, whiskers are maximum and minimum values) (**c**) NMDS plot of bacterial communities based on life stage, environmental samples and population (**d**) Stacked bar chart of the 10 most abundant phyla for lake water, sediment, larvae and metamorphs. Sample sizes were: n=63 (larvae), n=51 (metamorphs), n=20 (environment).

2.4.2 Microbiota differ by metamorph population and disease state

The infection history of each Pyrenean population is well documented with estimates of *Bd* emergence for each locality. Analysis of infection history data for each Pyrenean *A. obstetricans* population has revealed different responses to infection over time with Arlet and Ansabere exhibiting epizootic disease dynamics based on continued declining larval population abundance

coinciding with *Bd* infection. Meanwhile, though Lhurs, Acherito and Puits d'Arious displayed *Bd* associated decline in the initial years from when *Bd* was first detected, all have recently shown the hallmarks of enzootic infection characterised by stable larval population abundance in the presence of sustained *Bd* infection (Fig. 2.2, Table 2.4). Analysis of the relationship between *Bd* infection dynamics and bacterial community structure was performed for metamorphs only since we were not able to collect larvae from one epizootic population (Arlet). *Bd* associated mortality occurs during or after metamorphosis so we consider the bacterial communities of metamorph skin to be most informative in terms of response to infection.

Year	**Acherito**	**Puits d'Arious**	**Lhurs**	**Ansabere**	**Arlet**
2010	+++	+	+++	+++	+++
2011	+++	+	+++	++	+++
2012	+++	++	+++	++	++
2013	+++	++	+++	+	+
2014	+++	++	+++	+	+
2015	+++	++	+++	+	0

Table 2.4: Visual estimates of larval abundance from 2010 to 2015. + less than 100; ++ 100-1000; +++ more than 1000.

Enzootic populations exhibited lower *Bd* prevalence and significantly reduced infection intensity compared to epizootic populations (Chi-sq=59.855, df=4, $p<0.0001$, Fig. 2.3, Table 2.5). Bacterial Shannon diversity was reduced in epizootic populations compared to enzootic populations (ANOVA $F_{(4,46)}= 6.837$, $p=0.0002$; Tukey's tests: Ansabere-Acherito, $p=0.008$; Ansabere-Lhurs , $p=0.05$; Ansabere-Puits d'Arious $p=0.06$; Arlet-Acherito, $p=0.001$; Arlet-Lhurs, $p=0.04$; Arlet-Puits d'Arious, $p=0.08$; Fig. 2.4a). Beta diversity of host skin bacterial communities based on Bray-Curtis distances differed according to both population (PERMANOVA Pseudo-$F_{(4,46)}=3.175$, $p=0.001$) and infection dynamic (PERMANOVA Pseudo-$F_{(1,49)}=4.5125$, $p=0.001$, Fig. 2.4b).

Bacterial community composition differed in enzootic and epizootic populations (Fig. 2.4c). Enzootic populations had a higher relative abundance of OTUs from the phyla Acidobacteria, Verrucomicrobia and Planctomycetes, while epizootic populations had higher relative abundance of Bacteroidetes. In addition, Arlet, which has shown the highest mortality rate of any lake, featured an increased relative abundance of Chlamydiae, a phylum whose members are

obligate intracellular pathogens (Wyrick, 2000). The differences in bacterial community structure and composition between enzootic and epizootic populations is not an artefact of spatial non-independence given the lack of clustering of sites displaying similar disease dynamics (Fig. 2.4d).

Comparison	***P* value**
Ansabere-Acherito	<0.0001
Ansabere-Lhurs	<0.0001
Ansabere-Puits	<0.0001
Arlet-Acherito	<0.0001
Arlet-Lhurs	<0.0001
Arlet-Puits	<0.0001
Acherito-Puits	0.997
Acherito-Lhurs	0.756
Puits-Lhurs	0.959
Ansabere-Arlet	0.995

Table 2.5: Significance of pairwise differences in infection intensity (GE) between *A. obstetricans* populations.

We performed indicator analysis to identify bacterial taxa driving the differences in beta diversity based on both disease dynamic and population. We identified 61 indicator OTUs that were associated with enzootic dynamics and 25 OTUs associated with epizootic dynamics (Fig. 2.5, Appendix 1). Indicator OTUs from enzootic sites spanned nine phyla and 16 classes with the orders Actinomycetales and Rhizobiales accounting for the majority of taxa. Conversely OTUs from epizootic populations represented a less diverse array of lineages with six phyla and nine classes of which Pseudomonadales and Flavobacteriales were the most abundant orders. A range of OTUs contributed to differences in bacterial community structure between individual populations (Appendix 2). Lhurs, Acherito and Puits d'Arious were characterised by 73, 51 and 29 OTUs respectively, while Arlet and Ansabere had a total of 11 and four indicator OTUs.

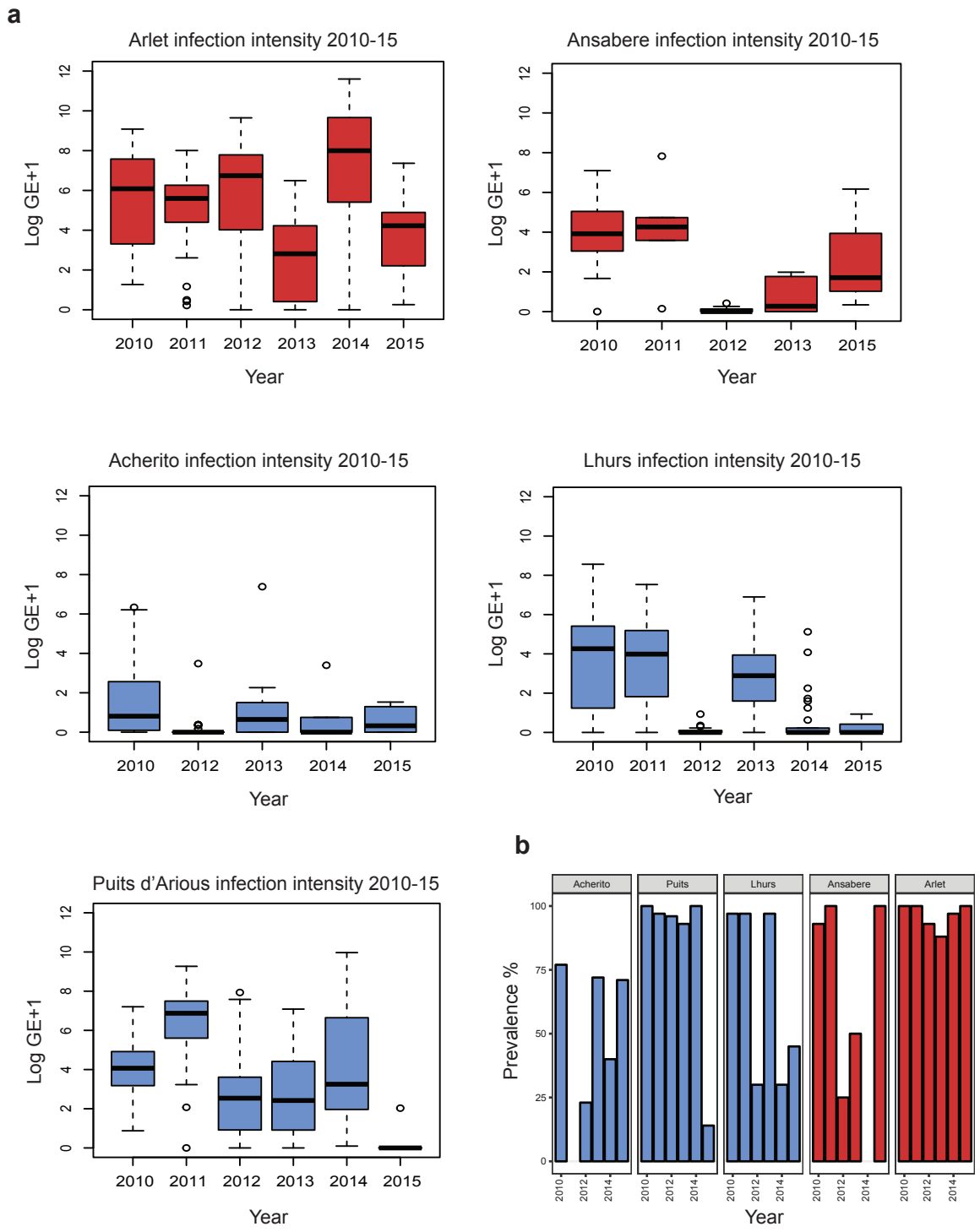


Figure 2.2: (**a**) Boxplots of metamorph infection intensity (2010-2015) for each population. Boxes represent the 25th and 75th percentile, the horizontal black line is the median, whiskers represent the maximum and minimum values of infection intensity, open circles are outliers. (**b**) Metamorph *Bd* prevalence (2010-2015). Sample sizes were: n=169 (Arlet), n=37(Ansabere), n=104 (Acherito), n=166 (Lhurs), n=123 (Puits d'Arious).

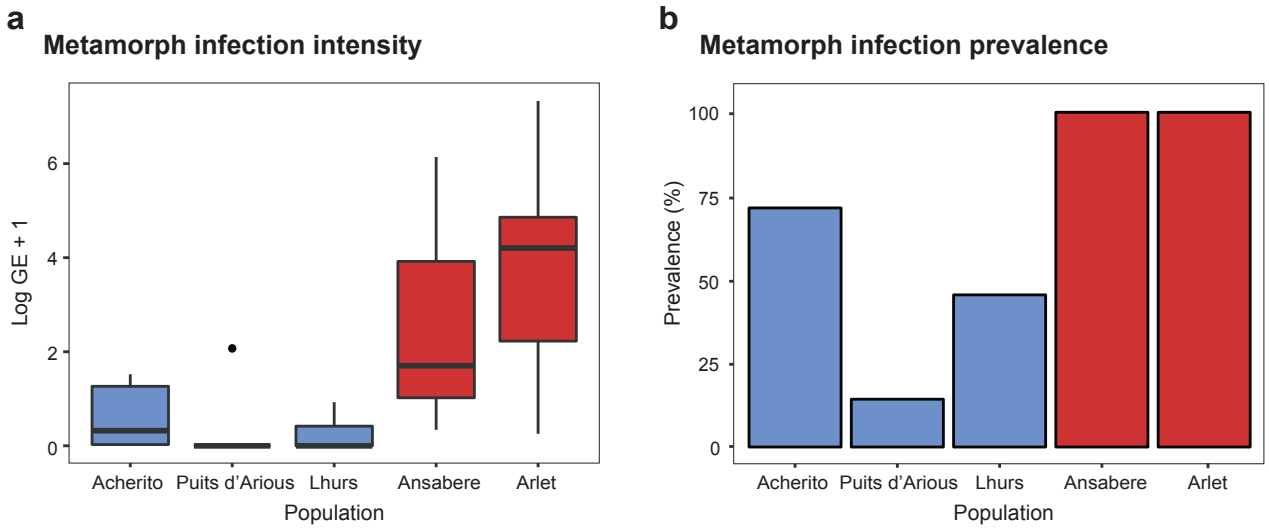


Figure 2.3: (**a**) Boxplot of *Bd* infection intensity in metamorphs sampled in 2015 showing reduced infection intensity in enzootic populations (Chi-sq=59.855, p<0.0001). Boxes represent 25th and 75th percentile, the horizontal line is the median and whiskers are maximum and minimum values of infection intensity (**b**) bar chart of *Bd* infection prevalence in metamorphs. Enzootic populations are coloured in blue, epizootic populations are coloured in red. Sample sizes: n=32 (Enzootic: Acherito=14, Lhurs=11, Puits d'Arious=7), n=19 (Epizootic: Arlet=16, Ansabere=3).

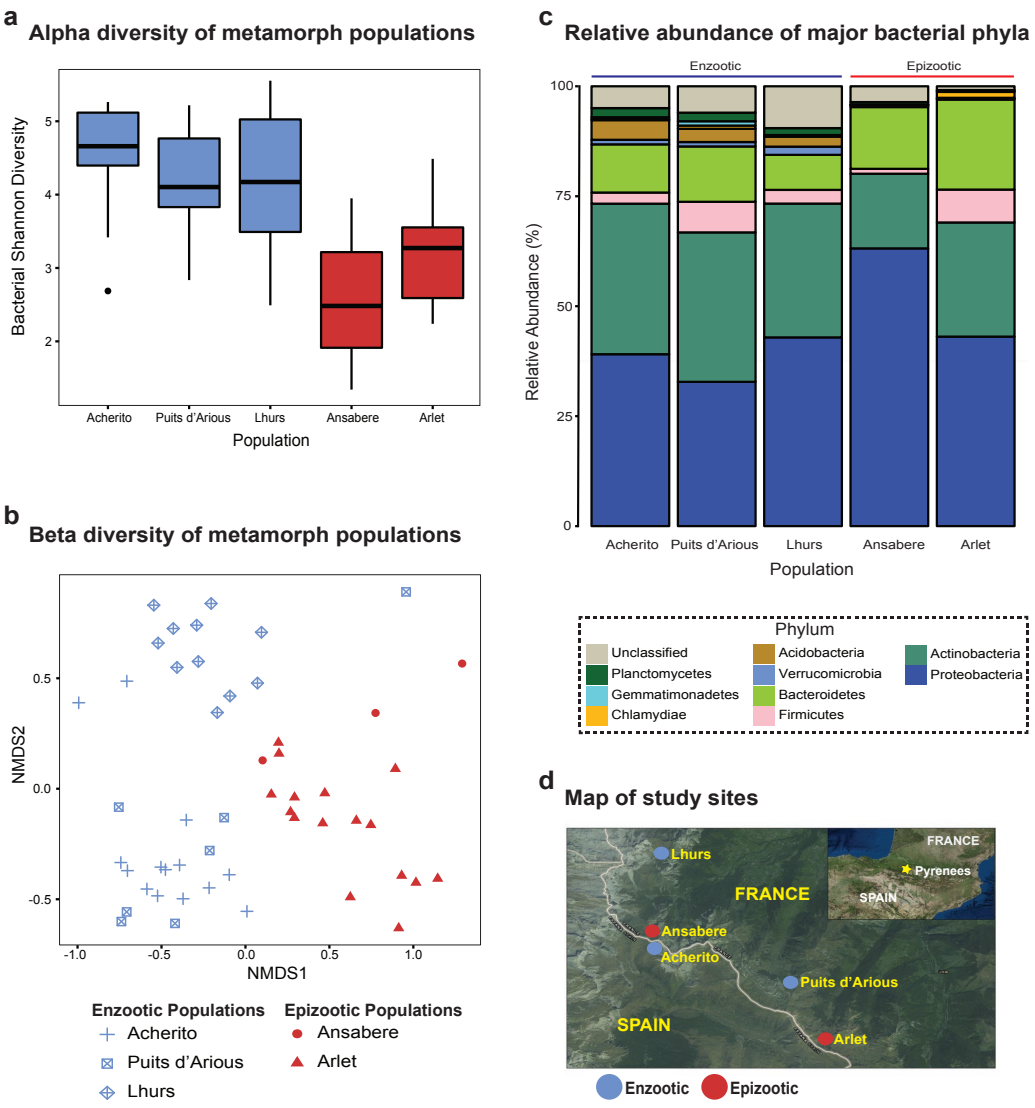


Figure 2.4: (**a**) Shannon diversity of metamorph populations. Epizootic populations are in red and enzootic populations are blue. Boxes represent 25th and 75th percentile, the horizontal line is the median and whiskers are maximum and minimum values (**b**) NMDS plot based on Bray-Curtis distances displaying beta diversity of enzootic and epizootic populations (**c**) Stacked bar chart of abundant bacterial phyla for each metamorph population (**d**) Map showing location of enzootic and epizootic populations. Map generated using ArcGIS version 10.0 (http://www.esri.com/software/arcgis) with the World Imagery Basemap. Source: Esri, DigitalGlobe, GeoEye, Earthstar, Geographics, CNES/Airbus DS, USDA, USGS, AeroGRID, IGN, the GIS User Community. Sample sizes: n=32 (Enzootic: Acherito=14, Lhurs=11, Puits d'Arious=7), n=19 (Epizootic: Arlet=16, Ansabere=3).

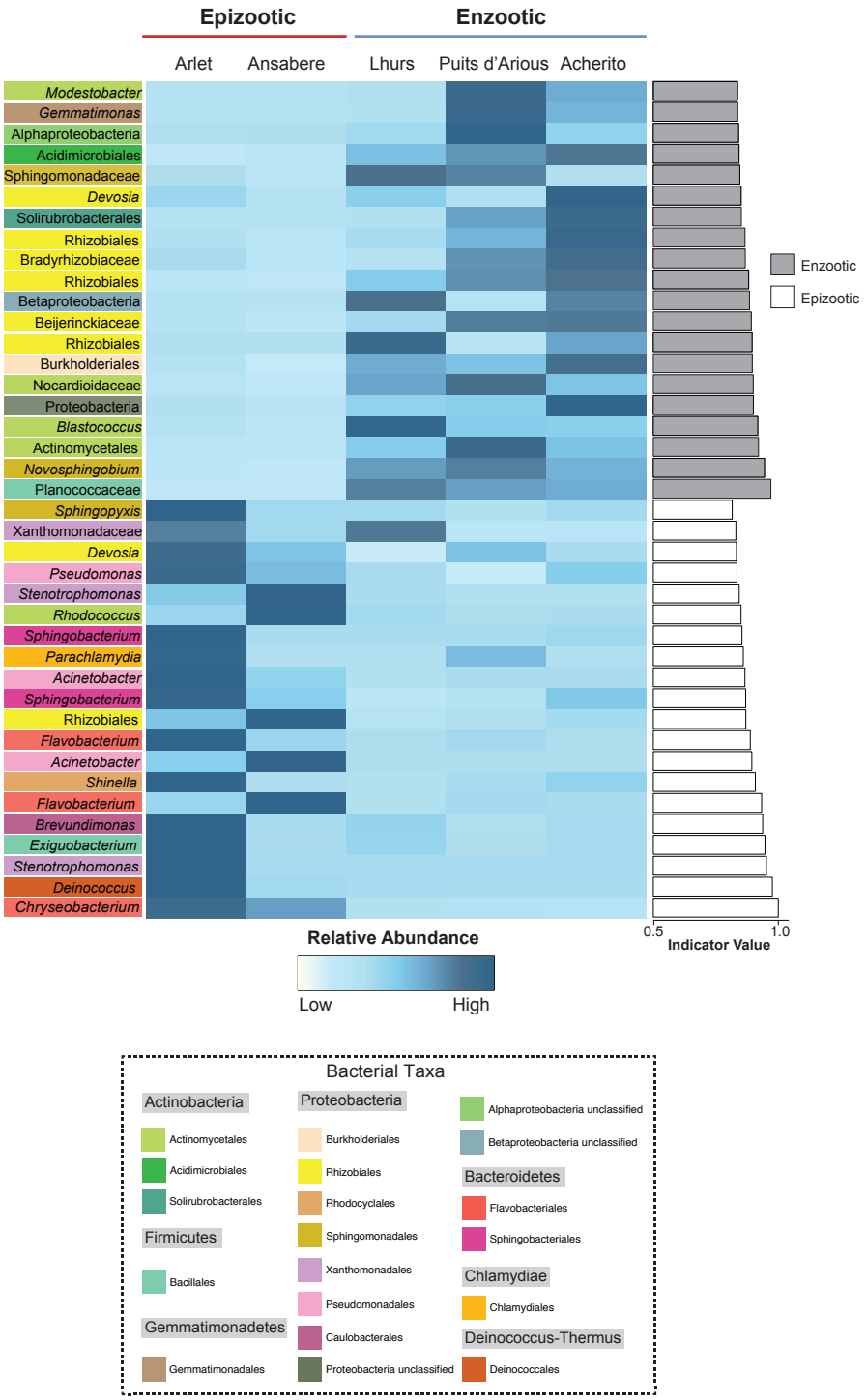


Figure 2.5: Heatmap displaying the normalised relative abundance of the top 20 bacterial OTUs from enzootic and epizootic populations identified from indicator analysis. Sample sizes: n=32 (Enzootic: Acherito=14, Lhurs=11, Puits d'Arious=7), n=19 (Epizootic: Arlet=16, Ansabere=3).

2.4.3 Predicted function differs by population and disease state

The predicted function of bacterial communities supported the patterns shown by bacterial taxonomic composition with significant differences based on both disease dynamic (PERMANOVA Pseudo-$F_{(1,49)}$=7.1993, p=0.001) and population (PERMANOVA Pseudo-$F_{(4,46)}$=2.9201, p=0.005, Fig. 2.6). In addition, 11 functional features were found to be significantly differentially abundant between enzootic and epizootic populations (LEfSe LDA >2). Nine functional features were more abundant in enzootic populations and two were more abundant in epizootic populations (Appendix 3). Differential functional features in both enzootic and epizootic populations were largely associated with mineral and ion transport (Appendix 3).

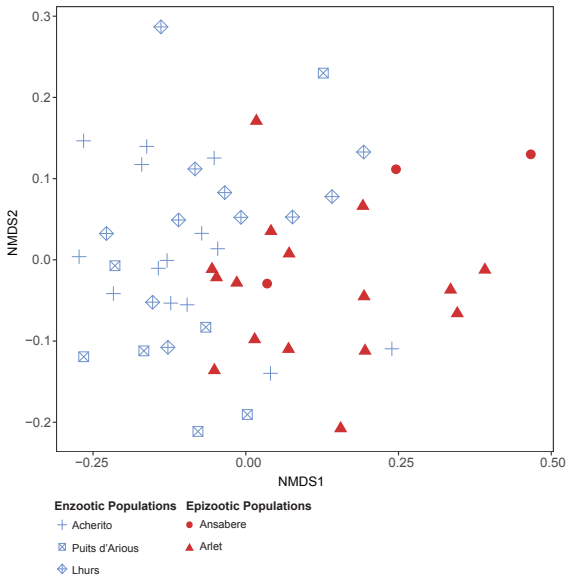


Figure 2.6: NMDS plot based on Bray-Curtis distances displaying clustering of KO functional predictions from metamorph skin bacterial communities from each Pyrenean population. Sample sizes: n=32 (Enzootic: Acherito=14, Lhurs=11, Puits d'Arious=7), n=19 (Epizootic: Arlet=16, Ansabere=3).

2.4.4 *Bd* genomic analysis

Whole genome sequencing was performed on 81 *Bd* isolates collected between 2004 and 2015 (Appendix 4). Phylogenetic analysis with the inclusion of *Bd* isolates collected from other Eu-

ropean localities gave 100% bootstrap support for a single introduction of *Bd* into the Pyrenees (Fig. 2.7a). A principle component analysis (PCA) of identified single nucleotide polymorphisms (SNPs) revealed little spatial (Fig 2.7b,c) or temporal (Fig 2.8) genetic structure among populations in the pathogen.

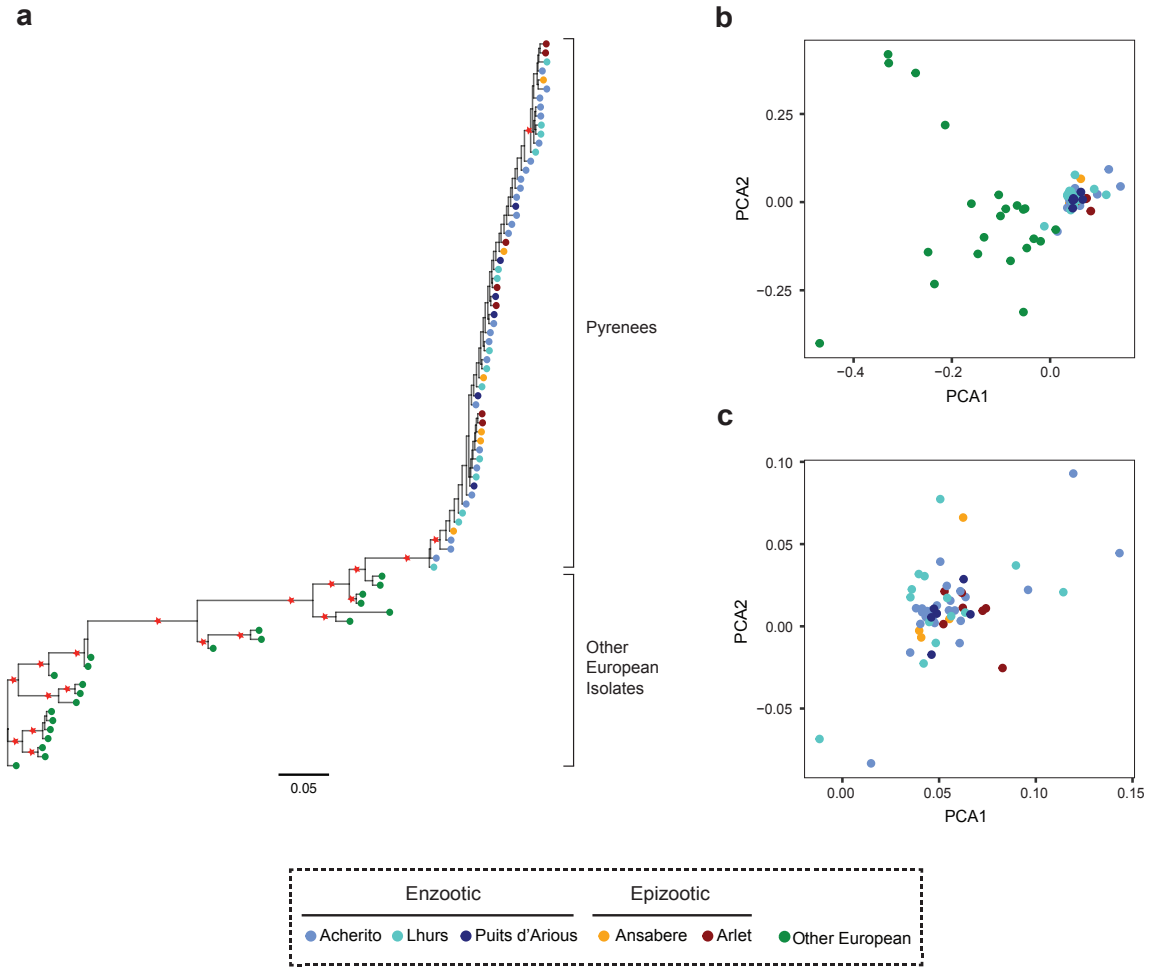


Figure 2.7: (**a**) Phylogeny of *Bd* isolates collected from the Pyrenees and other European localities. Red stars indicate bootstrap values of 100 (**b**) PCA plot of identified SNPs from *Bd* isolates from all localities (**c**) PCA plot of identified *Bd* SNPs from Pyrenean lakes only. Sample sizes: n=6 (Ansabere), n=7 (Arlet), n=26 (Acherito), n=14 (Lhurs), n=6 (Puits d'Arious), n=22 (other European isolates).

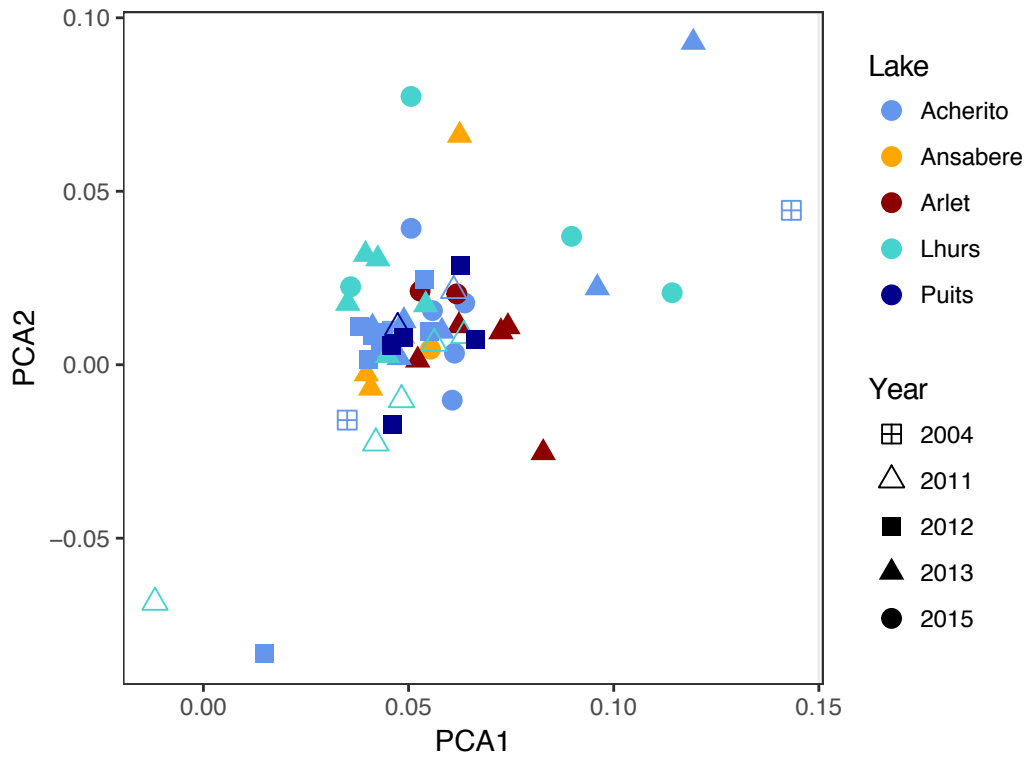


Figure 2.8: PCA plot of identified *Bd* SNPs from Pyrenean lakes sampled between 2004 and 2015 shows no temporal structure in *Bd* genotypes. Sample sizes: n=6 (Ansabere), n=7 (Arlet), n=26 (Acherito), n=14 (Lhurs), n=6 (Puits d'Arious).

2.5 Discussion

Our understanding of the microbial ecology of amphibian skin is rapidly increasing (Jani and Briggs, 2014; Walke et al., 2014; Kueneman et al., 2014, 2016b; Rebollar et al., 2016b). However, examining the dynamics of bacterial communities across wild populations exhibiting enzootic and epizootic disease states remains an important and understudied area (Jani and Briggs, 2014; Jani et al., 2017). In addition, our knowledge of how bacterial communities of amphibian skin differ between developmental stages is based on a limited number of studies (Kueneman et al., 2014, 2016b; Knutie et al., 2017). In this study we address these gaps in our knowledge by characterising the skin associated bacterial communities of amphibians from different life stages and metamorph populations displaying enzootic or epizootic disease dynamics. In addition, for the first time we investigate the relationship between *Bd* genetics and the microbiome in

disease outcome by sequencing *Bd* isolates from each population. We demonstrate that host population, infection dynamics and life stage are all significant factors in shaping amphibian skin bacterial communities, with population accounting for the greatest amount of variation. While there was a clear microbiome signature corresponding to disease outcome, an association between disease state and pathogen genetics was not evident.

The bacterial community structure of amphibian skin differed significantly based on both life stage and population, accounting for 15% and 20% of variation respectively. Despite the strong effect of population, few OTUs were shared between amphibian skin and the environment, and those that were had a low relative abundance in the environment. The small proportion of OTUs shared between the host and its surrounding environment, coupled with the low abundance of environmental OTUs has been found in similar studies (Walke et al., 2014) and may be indicative of selection occurring on the skin for rare environmental bacterial species (Loudon et al., 2016). This finding is surprising given the strong effect that host population was found to have on bacterial community structure, and existing evidence from other studies suggesting environmental reservoirs are important in shaping the vertebrate microbiome (Kueneman et al., 2016b; Lax et al., 2014; Hyde et al., 2016). Our results may therefore reflect that host OTUs also present in the environment may be at sub-detectable levels.

Larvae and metamorphs were dominated by the phylum Proteobacteria of which an OTU belonging to the family Comamonadaceae was most abundant. Comamonadaceae have also been identified as the most common taxonomic group in other studies of North American amphibian species (Kueneman et al., 2016b; McKenzie et al., 2012), suggesting some members of the core skin microbiota may be conserved across continents as has previously been shown for constituents of the tadpole gut microbiome (Vences et al., 2016). Unlike prior studies (Kueneman et al., 2014, 2016b), we found no significant difference in alpha diversity of metamorph and larval amphibians. There was however clear evidence for restructuring of skin associated bacterial communities during metamorphosis. Specifically, there was a significant difference in beta diversity of metamorphs and larvae and only a small proportion (17.3%) of OTUs were shared between life stages. This restructuring of the skin bacterial community is probably due to a combination of factors including the shift from a wholly aquatic to terrestrial environment

and the extensive physiological changes that the skin undergoes during metamorphosis. Of particular importance is likely to be the heavily expanded repertoire of skin secretions produced post-metamorphosis that transforms the skin into a very different niche for bacteria (Rollins-Smith et al., 2011).

Our findings show that while there was no distinction in pathogen genetic structure across enzootic and epizootic populations, there were clear differences in community structure and predicted function of bacteria on metamorph skin based on population and disease dynamic. Importantly, differences in bacterial community structure also reflect variation in bacterial predicted function. This finding is not indicative of functional redundancy among disparate bacterial communities and supports an active role of bacteria in host defence. Alpha diversity was significantly lower in epizootic populations compared to those presenting enzootic dynamics. This finding corroborates that of other studies (Longo et al., 2015) and may indicate that high alpha diversity offers enhanced protection, for example through production of a larger arsenal of antifungal metabolites or by competing for resources more effectively than the invading *Bd*. High *Bd* infection intensity in epizootic populations also results in increased skin sloughing which has been shown to decrease resident bacterial community diversity (Meyer et al., 2012). Further, epizootic populations may experience a more severe inflammatory response to *Bd* and impaired immune function (Fites et al., 2013) that promotes dysbiosis. This in turn can lead to enrichment of bacteria that exploit weakened host defences and consequently outcompete beneficial symbionts leading to dominance of a small number of opportunistic pathogenic bacterial species (Pham and Lawley, 2014).

Indicator analysis based on population identified key taxa driving differences in beta diversity and revealed OTUs of potential importance to population specific disease dynamics. Of particular interest is the indicator OTU profile of Lhurs, where metamorphs carried a high abundance of an OTU belonging to the *Lysobacter* genus. *Lysobacter* is inhibitory to several fungal pathogens including *Bd* (Woodhams et al., 2015) and anti-*Bd* functional traits have been identified for this genus. Genomic studies reveal that *Lysobacter* possesses strong chitinase functionality (de Bruijn et al., 2015) that may make it efficient at breaking down the chitin rich cell wall of *Bd* zoosporangia. Further, one study showed that *Lysobacter gummosus* pro-

duced the metabolite 2,4-diacetylphloroglucinol (2,4-DAPG) which is strongly inhibitory to *Bd* (Brucker et al., 2008b). Since Lhurs was the most recently infected population, it is unlikely to have fixed host-associated genes for resistance faster than previously infected populations that remain susceptible. Therefore, one possibility is that resistance to *Bd* may have arisen through selection of beneficial bacteria such as *Lysobacter*. This biotic shift has the potential to occur over a relatively short temporal scale given the rapid generation time of bacteria, which can subsequently become established members of the skin bacterial community and confer protective benefits to the host.

Arlet also revealed an interesting indicator OTU profile with high abundance of an OTU belonging to the *Parachlamydia* genus. The Chlamydiae comprise obligate intracellular pathogens that infect mucosal epithelial cells (Wyrick, 2000). Prior studies show that co-infection with Chlamydiae and *Bd* can result in mortality and epizootic dynamics (Reed et al., 2000). Arlet experienced a severe population decline coinciding with *Bd* emergence (Clare, 2014; Clare et al., 2016) and despite being infected longer than two enzootic populations (Lhurs and Puits d'Arious) has shown no signs of recovery. Analysis of Chlamydiae across all populations shows a higher relative abundance in metamorphs than either larvae or environmental samples indicating either colonisation or proliferation at metamorphosis. If Chlamydiae are found to induce pathology in Arlet metamorphs, then identifying whether this phylum is potentially associated with secondary infection or acting synergistically to promote *Bd* growth will be of paramount importance.

Indicator analysis based on infection dynamic identified a wide range of bacterial groups. The OTU with the highest indicator value for enzootic populations belonged to the family Planococcaceae of which several taxa are known to possess strong inhibitory capabilities against multiple pathogenic fungi including *Bd* (Woodhams et al., 2015; Chen et al., 2009). Members of the Actinomycetales and Rhizobiales represented the most abundant indicator OTUs in enzootic populations. These orders are common constituents of soil (Janssen, 2006) and have previously been documented for their anti-*Bd* activity *in-vitro* (Woodhams et al., 2015). Actinomycetales in particular are likely to be important candidates contributing to *Bd* resistance with prior studies identifying associations between members of this order and *Bd* resistance in the wild

(Jani and Briggs, 2014; Rebollar et al., 2016b). The Actinomycetales are also functionally important producing an estimated 53% of bioactive microbial metabolites of known antibiotic capability (Berdy, 2005). Among epizootic populations, members of the Moraxellaceae, and Flavobacteriaceae were highly represented indicator OTUs that have all been associated with high *Bd* loads in prior studies (Jani and Briggs, 2014; Woodhams et al., 2015; Becker et al., 2015; Rebollar et al., 2016b). All indicator OTUs assigned to the family Moraxellaceae belonged to the *Acinetobacter* genus. Isolates of *Acinetobacter* taken from multiple amphibian species (including *A. obstetricans*) have shown a great deal of functional diversity, including both *Bd* enhancement and inhibition (Woodhams et al., 2015). These results extend to *in-vivo* studies of which one field study found *Acinetobacter* to be enriched in non-susceptible populations (Rebollar et al., 2016b), while a controlled experiment showed members of the Moraxellaceae to be strongly associated with *Bd* induced mortality (Becker et al., 2015). Flavobacteriaceae are also often positively correlated with *Bd* load in wild amphibian populations (Jani and Briggs, 2014) and in some cases enhance *Bd* growth in co-culture (Woodhams et al., 2015).

Overall, our findings reveal that while individual populations may be characterised by unique OTUs that likely reflect the ecology of each habitat, there exists a subset of bacterial taxa that are conserved across populations depending on disease state. This may indicate the existence of common selection pressures linked with disease dynamics across sites that are associated with enhanced success of certain taxa. Such selection pressures are likely to be complex and mediated by the host, microbe-microbe interactions and the environment (Foster et al., 2017).

One possibility is that the pathogen itself may contribute to shaping the skin bacterial community of amphibians from each population. While *Bd* from epizootic and enzootic populations lacked marked differences in genetic structure, it remains possible that there is among-population heterogeneity in the way that bacterial taxa could respond to *Bd* genotypes (Antwis et al., 2015; Antwis and Harrison, 2018). Differences in bacterial communities amongst populations exhibiting contrasting infection dynamics may also be mediated by host factors such as the composition and volume of skin secretions that may be linked to proliferation of certain bacteria (Grice and Segre, 2011). If co-evolution of the host with protective symbionts has occurred, this may not only lead to resistance of infection through direct inhibition of *Bd* but

may also culminate in reduced pathogen virulence (Ford et al., 2016). Such a scenario may provide an elegant explanation for the dynamics of the Pyrenees system whereby *Bd* persists in enzootic populations without causing pathology to the host. Ultimately, identifying the selection pressures acting on amphibian associated bacteria, whether mediated by the host, pathogen or environment will be insightful in furthering our knowledge of microbial ecology of disease dynamics in nature. While a great body of work has focussed on *in-vitro* studies identifying single bacterial isolates that are inhibitory to *Bd*, our findings highlight that differences in epizootic and enzootic populations are likely driven by communities of bacteria. This may be particularly important since many constituents of a bacterial community may not directly inhibit or promote *Bd* growth, but instead may produce metabolic by-products that interact with *Bd* (Loudon et al., 2014a). In addition, our current knowledge of bacterial phenotypic plasticity, which can be affected by factors such as community structure and other biotic and abiotic conditions (Gray et al., 2006) reinforces the necessity to shift attention from single bacterial studies to those that take into account entire communities.

Amphibians globally are facing an extinction crisis and emerging infectious diseases are a major contributor to their decline. Understanding the role of host-associated bacteria in infection will greatly enhance our knowledge of the drivers underpinning heterogeneity in disease dynamics across space and time. By demonstrating significant associations between host skin bacterial communities, life stage and infection dynamics, this study develops an insight into the microbial ecology of amphibian skin in its natural setting. In addition, the lack of association between pathogen genetics and disease outcome suggests that the microbiome may play a more important role in infection than previously expected. In this Pyrenean montane system, we identify a conserved assemblage of bacterial taxa associated with disease state, many of which have previously been identified for their positive or negative impact on *Bd*. Despite the convincing patterns in bacterial community structure and predicted function based on disease state, our findings lack direct functional evidence to support the hypothesis that putatively beneficial or detrimental bacteria are associated with clinically relevant effects on disease outcome. In addition, other potentially important microbial groups such as fungi were not examined in this study. Future studies should therefore seek to survey a broader range of microbial king-

doms. There is a need to move beyond functional prediction based on 16S marker genes and instead capture direct functional information, for example through metabolomics to uncover associations between microbial community structure and function in disease ecology.

2.6 Acknowledgements

Dirk Schmeller and Adeline Loyau were invaluable in their support and organisation of permits. Jennifer Shelton, Nick Grassly and Maryam Grassly provided dedicated field support. I thank the community of Lescun and Parc National de Pyrenees for continued support.

Chapter 3

Captivity and experimental exposure to the emerging fungal pathogen *Batrachochytrium salamandrivorans* are linked to perturbation and dysbiosis of the amphibian skin microbiome

Kieran A. Bates[1,2], Jennifer M.G. Shelton[1], Victoria L. Mercier[1], Kevin P. Hopkins[2], Xavier A. Harrison[2], Silviu O. Petrovan[3,4], Matthew C. Fisher[1]

[1]Department of Infectious Disease Epidemiology and MRC Centre for Global Infectious Disease Analysis, School of Public Health, Imperial College London, London W2 1PG, UK; [2]Institute of Zoology, Zoological Society of London, Regents Park, London, NW1 4RY, UK; [3]Department of Zoology, University of Cambridge, Cambridge, CB2 3QZ, UK; [4]Froglife, Peterborough, PE4 5BW, UK

Author contributions: K.A.B. and V.L.M. conducted field surveys and animal experiments. K.A.B., V.L.M., K.H., X.A.H., and J.M.G.S. performed data processing and analysis. K.A.B prepared the figures.

3.1 Abstract

The emerging fungal pathogen, *Batrachochytrium salamandrivorans* (*Bsal*) is responsible for the catastrophic decline of European salamanders and poses a threat to amphibians globally. The amphibian skin microbiome is strongly associated with disease outcome for several host-pathogen systems, yet its role in *Bsal* infection remains unresolved. In addition, many *in-vivo Bsal* studies to date have relied on specimens that have been kept in captivity for long periods without considering the influence of environment on the microbiome and how this may impact the host response to pathogen exposure. We characterised the impact of captivity and exposure to *Bsal* on the skin bacterial and fungal communities of two co-occurring European newt species, the smooth newt (*Lissotriton vulgaris*) and the great-crested newt (*Triturus cristatus*). *Bsal* infection and subsequent mortality in both newt species was associated with perturbation of the skin microbiome and possible dysbiosis. In addition, reduced microbial diversity and changes in microbiome structure accompanied the transition of newts from the wild to captivity, suggesting a possible decline in microbe-associated protection and increased risk of infection by opportunistic pathogens. Our findings advance current understanding of the role of host-associated microbiota in *Bsal* infection and highlight important considerations for *ex-situ* amphibian conservation programmes.

3.2 Introduction

Microbial communities associated with amphibian skin are increasingly recognised for their ecological complexity and importance in pathogen defence (Bletz et al., 2013; Walke and Belden, 2016). In particular, studies have demonstrated that skin-associated bacteria are linked to disease outcome in amphibians infected by the chytrid fungus *Batrachochytrium dendrobatidis* (*Bd*) (Lauer et al., 2007; Harris et al., 2009; Jani and Briggs, 2014; Kueneman et al., 2016b; Bates et al., 2018). In recent years, the recognition of the microbiome's often beneficial role in ameliorating disease outcome has led to a search for pathogen-inhibiting probiotics and microbial manipulations that could mitigate host infection and subsequently be utilised as a

tool in wildlife conservation (Bletz et al., 2013; Kueneman et al., 2016a).

In 2013 a novel pathogenic chytrid fungus, *Batrachochytrium salamandrivorans* (*Bsal*), was discovered that was attributed to a 96% decline in the number of fire salamanders (*Salamandra salamandra*) in the Netherlands over the space of just three years (Spitzen-van der Sluijs et al., 2013). *Bsal* has since spread to other countries in Europe (Martel et al., 2013, 2014) and threatens amphibians worldwide (Yap et al., 2015). While *Bd* and *Bsal* are closely related phylogenetically and occupy similar niches as the only known species within the Chytridiomycota capable of infecting vertebrates (Berger et al., 1998; Martel et al., 2013), they show marked differences in their biology. *Bd* infects over 500 amphibian species (Stuart et al., 2004; Fisher et al., 2009) that span all amphibian orders, whereas *Bsal* is thought to have a narrower host range limited mostly to caudates (Martel et al., 2014). *Bd* and *Bsal* also differ in their pathogenesis with *Bd* causing hyperkeratosis and hyperplasia of the amphibian epidermis, compared to lesions and focal necrosis in *Bsal* (Martel et al., 2013). Prior studies have shown variability in *Bsal* susceptibility between caudate species (Martel et al., 2014), however little is known of the determinants of disease outcome. Given its importance in *Bd* infection, the amphibian skin microbiome is a candidate driver of within- and between-species variability in response to *Bsal* exposure. Although studies have shown that the host skin microbiota is important in *Bd* infection outcome (Jani and Briggs, 2014; Bates et al., 2018), little is known of the *in-vivo* host microbiome response to *Bsal* infection (Bletz et al., 2018). One prior study showed that the host microbiota may be important in *Bsal* infection outcome by showing that inoculation of the skin of fire salamanders with *Bsal* inhibiting bacteria slowed the rate of disease progression (Bletz et al., 2018). In this prior study only six salamanders were experimentally exposed to *Bsal* and therefore the conclusions that may be drawn are limited due to a small sample size. Importantly, it is not possible to predict the impact of *Bsal* on amphibian microbiota based on prior *Bd* studies, or to presume a microbiome response similar to that of *Bd*. This is due to a range of factors including intrinsic biological differences between *Bd* and *Bsal* (Farrer et al., 2017), and the variable responses that single bacterial strains can have with different pathogen isolates. For example, it is well established that the same bacterial strain can be either inhibitory or growth-promoting depending on what genotype of *Bd* it is in co-culture

with and inhibition can vary based on the make-up of the microbial community (Antwis et al., 2015; Antwis and Harrison, 2018). In addition, more recent studies have shown that certain bacteria isolated from amphibian skin inhibit *Bsal*, but not always *Bd in-vitro* (Muletz-Wolz et al., 2017). Further, *Bd* and *Bsal* metabolites can modulate growth of bacteria in different ways (Woodhams et al., 2017). Taken together, these findings suggest that differences exist in the way *Bsal* and *Bd* interact with the microbiome of amphibians, reinforcing the importance of investigating the *in-vivo* host microbiota response to *Bsal* exposure.

A great deal of our understanding of wildlife diseases comes from laboratory challenge experiments, while a major conservation strategy for highly threatened species is the establishment of assurance populations or disease treatment in captivity (Mendelson et al., 2006; Gascon, 2007). Despite recognition of the importance of the microbiome in host health and pathogen defence and the potential for captivity based microbiome bioaugmentation (Bletz et al., 2013), few studies have investigated the impact of captivity on the amphibian skin microbiome (Becker et al., 2014; Loudon et al., 2014b; Bataille et al., 2016; Kueneman et al., 2016a; Sabino-Pinto et al., 2016) and none have investigated this with respect to *Bsal* mitigation. Prior studies have yielded mixed results with reductions in bacterial alpha diversity and depletion of chytrid-inhibiting bacteria in captive compared to wild individuals for some host species (Loudon et al., 2014b; Bataille et al., 2016; Kueneman et al., 2016b; Sabino-Pinto et al., 2016) while increased alpha diversity was seen in other species (Becker et al., 2014). In addition, studies investigating the impact of captivity on the amphibian skin microbiome have neglected to examine microbial kingdoms other than bacteria, despite recent advances demonstrating that fungi may be equally important to host health and chytrid disease resistance (Kearns et al., 2017). In other systems the host fungal community (also known as the mycobiome) has been shown to be integral to host health, for example humans with enteric *Clostridium difficile* infection also often present dysbiosis of the gut mycobiome with proliferation of *Candida albicans* and reduced fungal diversity (Zuo et al., 2018). Importantly, cross-kingdom responses to captivity may not be uniform making it essential that a more holistic outlook of the skin microbiome is taken. Understanding the effect of captivity on the host microbiome is especially important with regard to *Bsal* exposure since models suggest that field based interventions are unlikely

to be successful owing to disease outbreaks being capable of occurring at lower population densities than host populations exist at in the wild, thus making pathogen fade out unlikely (Schmidt et al., 2017). In addition, currently the only effective *Bsal* treatments are captivity based (Blooi et al., 2015b,a). Gaining insights into how both *Bsal* exposure and the transition from the wild to captivity affect the caudate skin microbiome is therefore an important advancement in our understanding of infection as well as being valuable in informing future captivity-based conservation interventions.

In this study, we combine field and laboratory studies to investigate how the amphibian skin microbiome changes with the transition from the wild to captivity followed by subsequent exposure to *Bsal*. We focus on two UK caudate species, the smooth newt (*Lissotriton vulgaris*) and the great crested newt (*Triturus cristatus*). While *L. vulgaris* is ubiquitous in the UK, *T. cristatus* is rarer, more localised and declining in many parts of its natural range (Edgar et al., 2005). *T. cristatus* is also listed as a protected species in Annexes II and IV of the European Commission Habitats Directive and under the UK Wildlife and Countryside Act 1981. Consequently, the long-term population viability of *T. cristatus* is particularly vulnerable to local disease outbreaks. The susceptibility of captive-raised *T. cristatus* to *Bsal* has been tested in a prior study (Martel et al., 2014) which showed mortality in all infected animals. Meanwhile, no study to date has investigated the lethality of *Bsal* in *L. vulgaris*. Testing the effect of *Bsal* on endemic UK species and the possible risk it poses to wild populations is vital given the recent emergence of *Bsal* in private collections (Cunningham et al., 2015) and the continued spread of pathogenic chytrids through the global trade (O'Hanlon et al., 2018) suggesting a wild outbreak is possible. Understanding the effects of *Bsal* exposure and the influence of captivity on the amphibian skin microbiome could therefore not only improve the capacity for developing adequate national response protocols to disease outbreaks, but also inform effective captivity based measures that seek to maximise natural pathogen protection.

3.3 Material and Methods

3.3.1 Field sampling and captivity study

A total of 15 adult *Triturus cristatus* and 15 adult *Lissotriton vulgaris* were collected from a reserve in Cambridgeshire, UK. Individual newts were generally found under rocks at night and represented less than 0.1% of the total estimated site population. Using a single sterile MW100 rayon tipped dry swab (MWE Medical Wire, Corsham, UK), the skin microbiome was sampled by swabbing the ventral and dorsal surfaces 10 times, and the fore- and hindlimbs five times. Swabs were stored at -80°C until processed. Animals were transferred to individual 1.6L plastic boxes containing moss collected from the field site and transported to the Central Biomedical Services (CBS) Unit at Imperial College London. In captivity animals were housed individually in plastic boxes containing a damp paper towel substrate and a cover object. Enclosures were cleaned with Rely+On Virkon (Antect International Ltd., Suffolk, UK) and animals were fed mealworms (*Tenebrio molitor*) or crickets (*Acheta domesticus*) *ad libitum* twice weekly. The animal room was kept on a 12 hour light/dark cycle and was maintained at 16°C. At two weeks post capture animals were swabbed again to measure the effects of captivity on the skin bacterial and fungal community.

3.3.2 *Bsal* exposure experiment

In order to compare species response to *Bsal*, experiments were designed to be as similar as possible to those described in a previous study (Martel et al., 2014). *Batrachochytrium salamandrivorans* (isolated from a *Salamandra salamandra* outbreak in the Netherlands, isolate AMFP13/1) was grown in 25cm^3 Nunc^{TM} tissue culture flasks (Thermo Fisher Scientific, Massachusetts, USA) containing mTGhL liquid media (8g tryptone, 2g gelatin hydrosylate, 4g lactose, 950ml distilled water) and incubated at 15°C. At fourteen days post-capture, ten individuals from each caudate species were randomly assigned to a treatment group and exposed to 500 µl of mTGhL media containing 50 x 10^4 *Bsal* zoospores. The remaining five individuals

from each species were assigned to a control group and exposed to 500 µl of mTGhL liquid media. The inoculum was pipetted directly onto the dorsum of the animal. During exposure, *T. cristatus* were placed individually in 0.7L plastic boxes and *L. vulgaris* were placed in sterile petri dishes for 22 hours. Animals were weighed and swabbed prior to *Bsal* infection on day 0 of the experiment and then every 7 days post infection for a period of 58 days. On day 58 of the experiment surviving animals were euthanized by an overdose of tricaine methanesulfonate (MS222) and subsequent destruction of the brain following UK Home Office animal procedure guidelines. In agreement with ethical protocols, any animals exhibiting pre-defined endpoint criteria (lack of righting reflex within five seconds of being inverted, persistent skin lesions covering over 20% of the body or that became septic, greater than 20% loss in body weight) were euthanized prior to day 58.

3.3.3 Sample processing, DNA extraction and quantification of *Bsal* infection

Genomic DNA was extracted from swabs using a bead beating protocol (Boyle et al., 2004) and diluted 1/10 before undergoing subsequent PCR based analyses. Quantification of *Bsal* infection load was done using qPCR amplification following a modified published method (Boyle et al., 2004) that included a *Bsal* specific probe (STerCVIC), forward primer (STerFC) and reverse primer (STerT). Each sample was run in duplicate and with *Bsal* standards of 100, 10 and 1 genomic equivalents (GE). A distilled water negative control was also included. Samples were considered positive if both wells gave a GE of greater than 0.1.

3.3.4 Bacterial microbiome sample processing

DNA extracted from swabs was used to amplify the V4 region of the 16S rRNA gene using custom barcoded primers and PCR conditions adapted from a prior study (Kozich et al., 2013). PCR conditions consisted of a denaturing step of 95°C for 15 min, followed by 28 cycles of 95°C for 20s, 50°C for 60s, 72°C for 60s and a final extension step of 72°C for 10 min. Each PCR

including a negative water control was performed in triplicate. Amplicons were visualized on a 2% agarose gel and pooled yielding a final per sample volume of 24 µl. Pooled amplicon DNA was purified using an Ampure XP PCR purification kit (Beckman Coulter, California, USA). Following purification, 1 µl of each combined sample was pooled into a preliminary library and the concentration was determined using Qubit fluorometric quantification (Life Technologies, California, USA). Amplicon quality and incidence of primer dimer was assessed using an Agilent 2200 TapeStation system (Agilent Technologies, California, USA). A titration run of 300 sequencing cycles was performed on a MiSeq instrument (Illumina, California, USA) to quantify the number of reads yielded per sample from the preliminary library. An equimolar concentration of each sample was then pooled into a final composite library based on the index representation from the titration run and subsequently sequenced on a 500 cycle MiSeq run with a 250 bp paired-end strategy.

3.3.5 Fungal mycobiome sample processing

DNA extracted from swabs was used to amplify the ITS2 region of the fungal internal transcribed spacer (ITS) using custom barcoded primers (Kozich et al., 2013) and the following PCR conditions: denaturing step of 95°C for 2 min, followed by 35 cycles of 95°C for 20s, 50°C for 20s, 72°C for 5 min and a final extension step of 72°C for 5 min. Each PCR plate included a negative control and was performed in duplicate. Amplicons were visualized on a 1.5% agarose gel and pooled yielding a final per sample volume of 50 µl. Pooled amplicon DNA was purified using AMPure XP bead clean-up (Beckman Coulter, California, USA). Qubit fluorometric quantification (Life Technologies, California, USA) was used to determine the concentration of each purified sample, which were equimolar pooled to create the final library sample. This pooled sample was run on an Agilent 2200 TapeStation system (Agilent Technologies, California, USA) to assess amplicon distribution and presence of primer dimer. The sample underwent 300bp paired-end sequencing using V3 chemistry on an Illumina MiSeq platform.

3.3.6 Bacterial microbiome analysis

Sequences were processed using MOTHUR (Schloss et al., 2009) following a previously described method (Kozich et al., 2013). Paired-end reads were split by sample and assembled into contigs. Sequences were quality filtered by removing ambiguous base calls, removing homopolymer regions longer than 8 bp, and trimming reads longer than 275 bp. Duplicate sequences were merged and aligned with 16S reference sequences from the SILVA small-subunit rRNA sequence database (Pruesse et al., 2007). A pre-clustering step grouped sequences differing by a maximum of 2 bp. Chimeric sequences were removed using UCHIME (Edgar et al., 2011) as implemented in MOTHUR. 16S rRNA gene sequences were clustered into groups according to their taxonomy at the level of order and assigned operational taxonomic units (OTUs) at a 3% dissimilarity level. Sequences were taxonomically classified with an 80% bootstrap confidence threshold using a naive Bayesian classifier with a training set (version 9) made available through the Ribosomal Database Project (http://rdp.cme.msu.edu) (Wang et al., 2007). Sequences derived from chloroplasts, mitochondria, archaea, eukaryotes or unknown reads were eliminated. The number of sequences per sample ranged from 17804 to 63367. To mitigate the effects of uneven sampling (Schloss et al., 2011) all samples were rarefied to 17804 sequences corresponding to the size of the lowest read sample. OTUs making up less than 0.01% of the total reads were removed (Bokulich et al., 2013). Downstream analysis of OTUs was carried out using the package Phyloseq (McMurdie and Holmes, 2013) in R version 3.4.1 (R Core Team, 2017).

3.3.7 Fungal mycobiome analysis

Analysis of fungal communities was performed for the captivity study only. Following sequencing, forward and reverse reads were assigned to samples according to dual index combinations and were paired using Paired-End reAd mergeR (PEAR) (Zhang et al., 2014). Paired-end reads were trimmed by per-base quality score using MOTHUR (Schloss et al., 2009) and reads shorter than 50bp or containing ambiguous base calls were removed. UCHIME (Edgar et al., 2011) was used to identify and remove chimeric sequences, and remaining sequences were clustered into Operational Taxonomic Units (OTUs) based on 97% similarity using Cd-hit (Li and

Godzik, 2006). The most abundant sequence in each OTU was used for BLASTn searches against the User-friendly Nordic ITS Ectomycorrhiza (UNITE) database (Koljalg et al., 2005). Unidentified sequences or those belonging to kingdoms other than fungi were removed, as were fungal sequences with BLASTn search result e-values >e20 or identity <85%. The number of sequences per sample ranged from 579 to 38919. To mitigate the effects of uneven sampling (Schloss et al., 2011) all samples were rarefied to 1000 sequences resulting in some samples being discarded. OTUs making up less than 0.01% of the total reads were removed (Bokulich et al., 2013). Downstream analysis of OTUs was carried out using the package Phyloseq (McMurdie and Holmes, 2013) in R version 3.4.1.

3.3.8 Statistical analysis

To determine the effect of captivity and *Bsal* exposure on the microbiome, we calculated both alpha and beta diversity metrics using the phyloseq package (McMurdie and Holmes, 2013) in R version 3.4.1 (R Core Team, 2017). Shannon diversity was calculated for all samples and a mixed linear model (package lme4 (Bates et al., 2015)) was used to investigate changes in diversity in the captivity study with Shannon diversity as the response variable, day of sampling as a fixed effect and newt ID as a random effect to take into account repeated sampling. For the exposure experiment, mixed linear models were used for each newt species with Shannon diversity as the response variable, mass, day of sampling and Bsal exposure group as fixed effects and newt ID as a random effect. *P*-values were calculated using the Kenward-Roger approximation of degrees of freedom in the afex package (Singmann et al., 2017). A Bray-Curtis distance matrix was used to calculate beta diversity for both the captivity study and *Bsal* challenge experiment. Beta diversity for both the captivity study and *Bsal* challenge experiment was visualised using detrended correspondence analysis (DCA) plots. For the captivity study, the effects of captivity, host species and their interaction on skin microbial community structure was assessed using permutational multivariate analysis of variance (PERMANOVA) (Anderson, 2001) using the adonis function in the vegan package (Oksanen et al., 2016). For the *Bsal* challenge experiment differences in beta diversity based on *Bsal* exposure, *Bsal* infection

status and survival were investigated using PERMANOVA for each day of the experiment. To assess bacterial OTUs that differed in abundance in the wild versus captivity for each species, we used indicator analysis (Dufrene and Legendre, 1997) using the labdsv package (Roberts, 2016). An indicator score of > 0.7 and q-value <0.05 was used as a cut-off to define potentially informative OTUs (Becker et al., 2015; Longo and Zamudio, 2017). For the infection experiment, beta diversity differed only on day 28, we therefore performed indicator analysis on the top 1% of OTUs for this time point only to determine what specific core OTUs were driving differences in beta diversity. Indicator analysis for the infection experiment was performed for each host species with *Bsal* infection status (control, exposed negative, exposed positive) used a predictor variables. Differences in survival among animals in the *Bsal* exposure experiment was investigated using a cox proportional-hazard regression model in the survival package (Therneau, 2015) with mass at the beginning of the experiment, species, and GE at time of death or at the end of the experiment included as covariates.

3.3.9 Ethics statement

Animal work was conducted under UK Home Office Project Licence PPL 70/8402 held by Matthew Fisher and was reviewed by the Imperial College London Animal Welfare Ethical Review Board for approval. The experiment was carried out in accordance with The Animals (Scientific Procedures) Act of 1986 Directive 2010/63/EU and followed all of the Codes of Practice which reinforce this law, including all elements of housing, care and euthanasia. Animals were collected in the wild under Natural England Licence 2015-15771-SCI-SCI and following ethical review by the board of Froglife.

3.4 Results

3.4.1 Captivity impacts cross-Kingdom microbial diversity and structure

We show rapid reductions in bacterial and fungal Shannon diversity associated with the transition from the wild to captivity for both host species (bacteria: $p<0.0001$,fungi: $p=0.03$, Fig. 3.1a, b). Bacterial and fungal beta diversity differed in wild versus captive conditions (PERMANOVA, bacteria wild-captive: Pseudo-$F_{(1,56)}=66.84$, $R^2=0.505$, $p=0.001$, fungal wild-captive: Pseudo-$F_{(1,26)}=11.35$, $R^2=0.285$, $p=0.001$) and a host species effect was present for bacterial communities (PERMANOVA, host species: Pseudo-$F_{(1,56)}= 5.46$, $R^2=0.041$, $p=0.007$, host species*wild-captive: Pseudo-$F_{(1,56)}=4.02$, $R^2=0.030$, $p=0.016$, Fig. 3.1c-d). Interestingly, changes in alpha and beta diversity associated with captivity were mirrored for bacteria and fungi demonstrating a common response across microbial kingdoms. Captivity was associated with compositional changes in the core microbiome of both species with reductions in taxa such as *Cladosporium* and *Pseudomonas* (Fig. 3.1.e,f). Indicator analysis of wild versus captive specimens identified 176 and 167 differentially abundant bacterial OTUs in *T. cristatus* and *L. vulgaris* respectively (Fig. 3.2a,b; Appendix 5, 6). No significant differences in fungal OTU abundance associated with captivity for *T. cristatus* or *L. vulgaris*. Interestingly both host species demonstrated similar indicator OTU profiles of major bacterial groups (Fig. 3.2a,b) with changes in abundance of potentially important taxa such as the Actinomycetales that are a major source of antimicrobial compounds (Berdy, 2005) and *Lysobacter* that was previously identified as inhibitory against the closely related *Batrachochytrium dendrobatidis* (Brucker et al., 2008b). In addition to the reduction in putatively protective microbes, in captive *T. cristatus* there was an increase (though not statistically significant) in pathogenic fungi such as *Basidiobolus ranarum* which has previously been shown to cause disease in amphibians (Taylor et al., 1999).

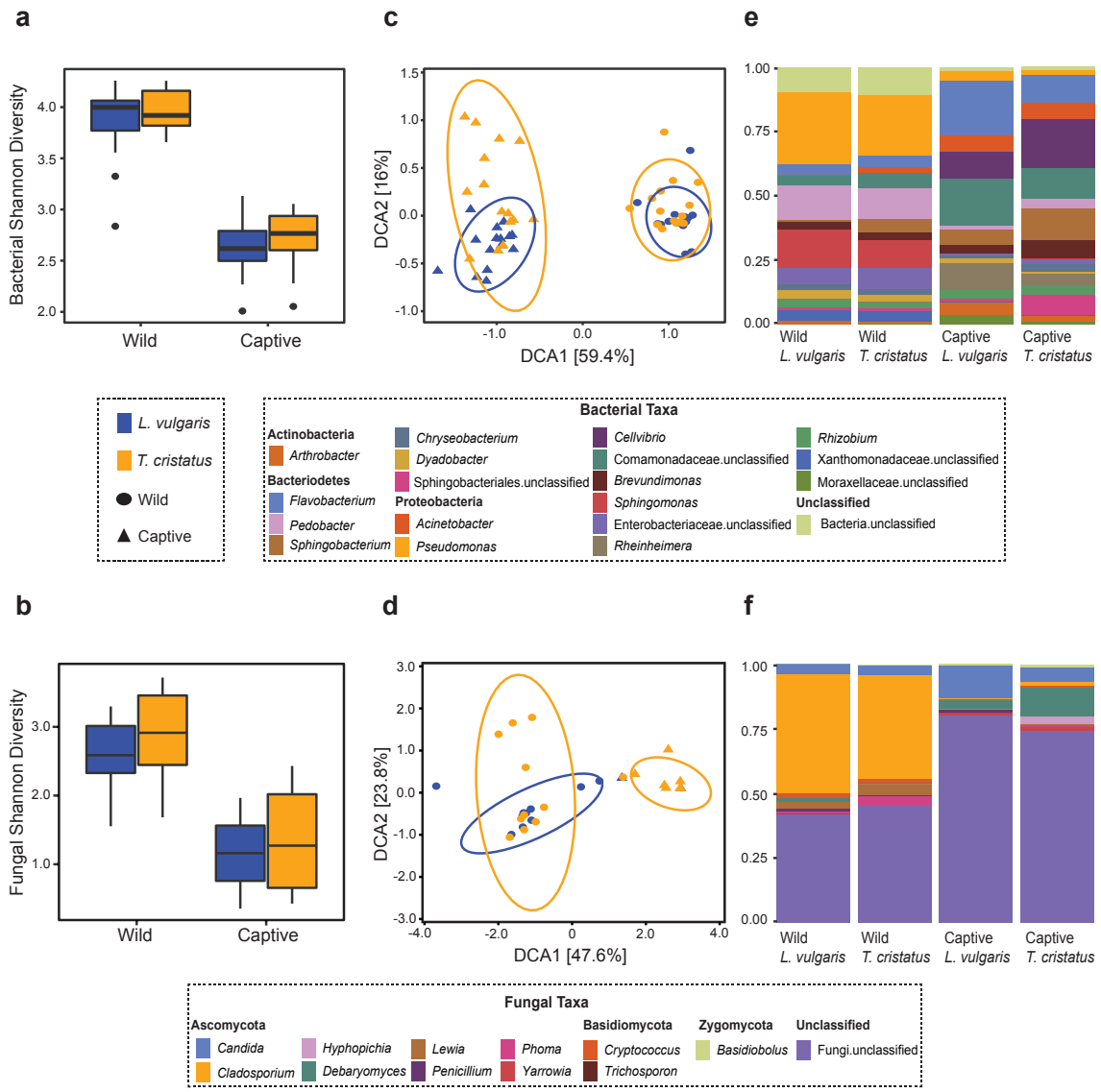


Figure 3.1: Microbiome of animals in the wild and after 14 days in captivity. Boxplots displaying Shannon diversity in wild and captive *Lissotriton vulgaris* and *Triturus cristatus* for **(a)** bacteria **(b)** fungi. Boxes represent 25$^{\text{th}}$ and 75$^{\text{th}}$ percentile, the horizontal line is the median, whiskers are maximum and minimum values. Detrended correspondence analysis (DCA) plots of beta diversity in wild and captive *L. vulgaris* and *T. cristatus* for **(c)** bacteria **(d)** fungi. Ellipses indicate 95% confidence intervals. Where ellipses are absent, insufficient samples were present. Stacked bar plots of **(e)** bacterial taxa with relative abundance $> 1\%$ and **(f)** fungal taxa with relative abundance $> 0.5\%$. Sample sizes bacteria: n=15 (wild *L. vulgaris*), n=15 (wild *T. cristatus*), n=15 (captive *L. vulgaris*), n=15 (captive *T. cristatus*). Sample sizes fungi: n=10 (wild *L. vulgaris*), n=10 (wild *T. cristatus*), n=3 (captive *L. vulgaris*), n=8 (captive *T. cristatus*).

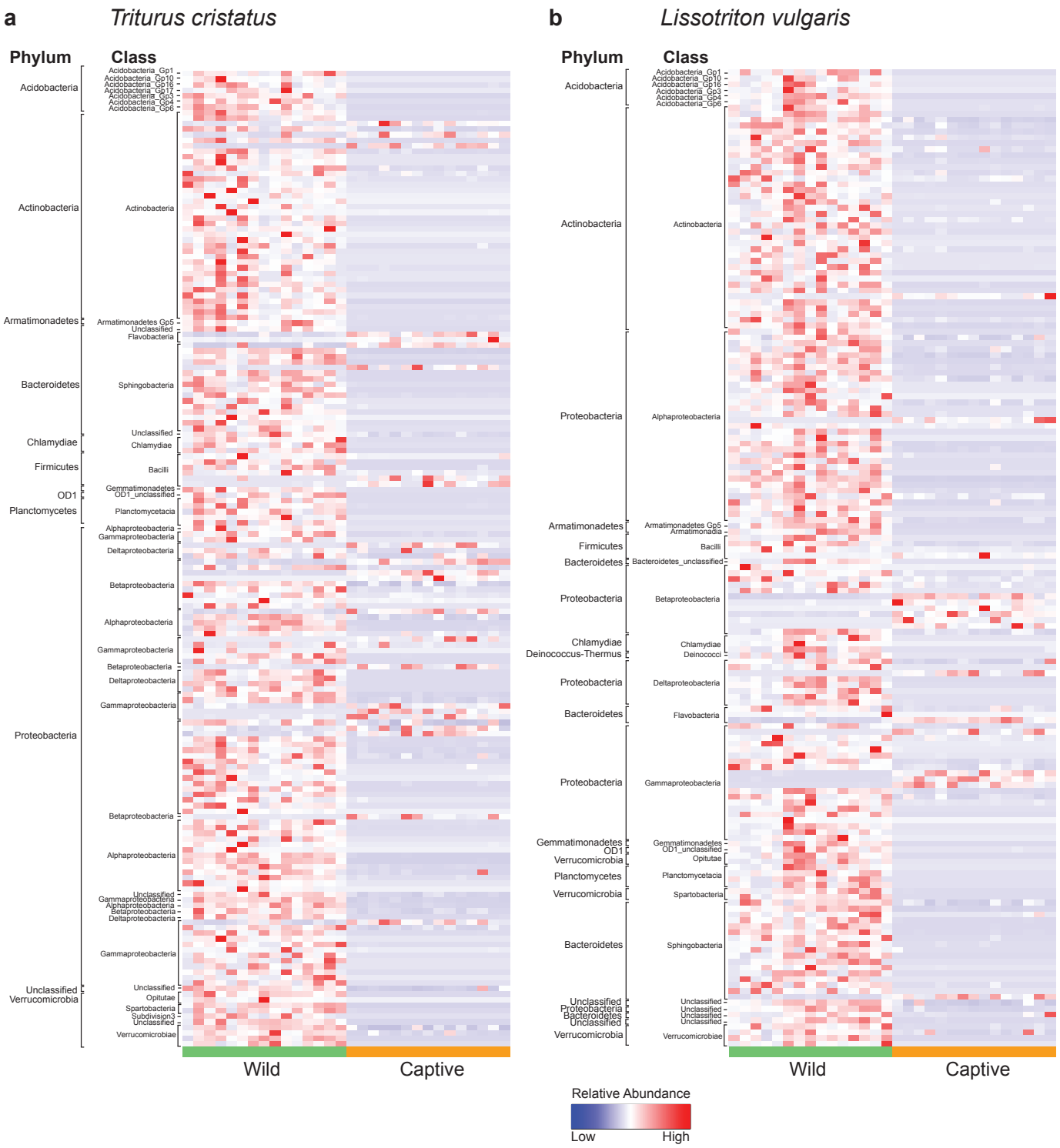


Figure 3.2: Heatmap of normalised relative abundance of bacterial indicator OTUs for animals in the wild and after 14 days in captivity labelled by Phylum and Class for **(a)** *T. cristatus* **(b)** *L. vulgaris*. Sample sizes: n=15 (wild *L. vulgaris*), n=15 (wild *T. cristatus*), n=15 (captive *L. vulgaris*), n=15 (captive *T. cristatus*).

3.4.2 *Bsal* infection perturbs host microbiome structure

Bsal exposure resulted in infection in 40% (four out of ten animals) of *L. vulgaris* and 60% (six out of ten animals) of *T. cristatus*. Prevalence and infection intensity fluctuated throughout the experiment for both species (Appendix 7, Fig. 3a,b) with *T. cristatus* exhibiting consistently higher infection intensity and prevalence than *L. vulgaris*. Lesions were evident in 50% of *T. cristatus* and 75% of *L. vulgaris* that tested *Bsal* positive (Appendix 7, Fig. 3c). Of the animals that tested positive for *Bsal*, 50% of *T. cristatus* died, while 25% of *L. vulgaris* died over the 58 days of the experiment. Of the four *L. vulgaris* that became infected with *Bsal*, three animals cleared infection, while for *T. cristatus* only one of six *Bsal* positive animals cleared infection. Survival analysis showed that infection intensity but not species or mass were significantly associated with mortality (hazard-ratio=1.07, p=0.022, Appendix 8).

Bacterial Shannon diversity differed based on day of sampling and mass but not *Bsal* exposure for *T. cristatus* (day: $F_{(2,30.5)}$=14.35, p<0.0001, mass: $F_{(1,15.26)}$=4.71, p=0.05, *Bsal* exposure: $F_{(1,12.3)}$=12.3, p=0.60), but did not significantly alter over the course of the experiment in *L. vulgaris* (day: p=0.17, mass: p=0.47, *Bsal* exposure: p=0.75). Beta diversity differed only on day 28 based on treatment for *T. cristatus* (PERMANOVA Pseudo-$F_{(1,11)}$=2.34, R^2=0.108, p=0.045) and for both host species based on disease status (PERMANOVA *T. cristatus* Pseudo-$F_{(1,11)}$=4.48, R^2=0.199, p=0.002, *L. vulgaris* Pseudo-$F_{(1,11)}$=4.95, R^2=0.247, p=0.001, Fig. 3.4a,b) and survival (PERMANOVA *T. cristatus* Pseudo-$F_{(1,11)}$=4.59, R^2=0.204, p=0.006, *L. vulgaris* Pseudo-$F_{(1,11)}$=2.44, R^2=0.122, p=0.048). In *L. vulgaris*, on day 28 two individuals demonstrated microbiome perturbation, but cleared infection and returned to a microbiome state that did not differ significantly from control animals by day 56 (Fig. 3.4a). Indicator analysis of microbiome samples based on control, exposed *Bsal* negative and exposed *Bsal* positive animals from day 28 identified two and one differentially abundant bacterial operational taxonomic units (OTUs) in *L. vulgaris* and *T. cristatus* respectively (Appendix 9). Both *L. vulgaris* and *T. cristatus* exhibited an indicator taxa identified as *Stenotrophomonas* (Fig. 3.4c,d), which was strongly associated with *Bsal* infection in both species (indval > 0.8, q < 0.05).

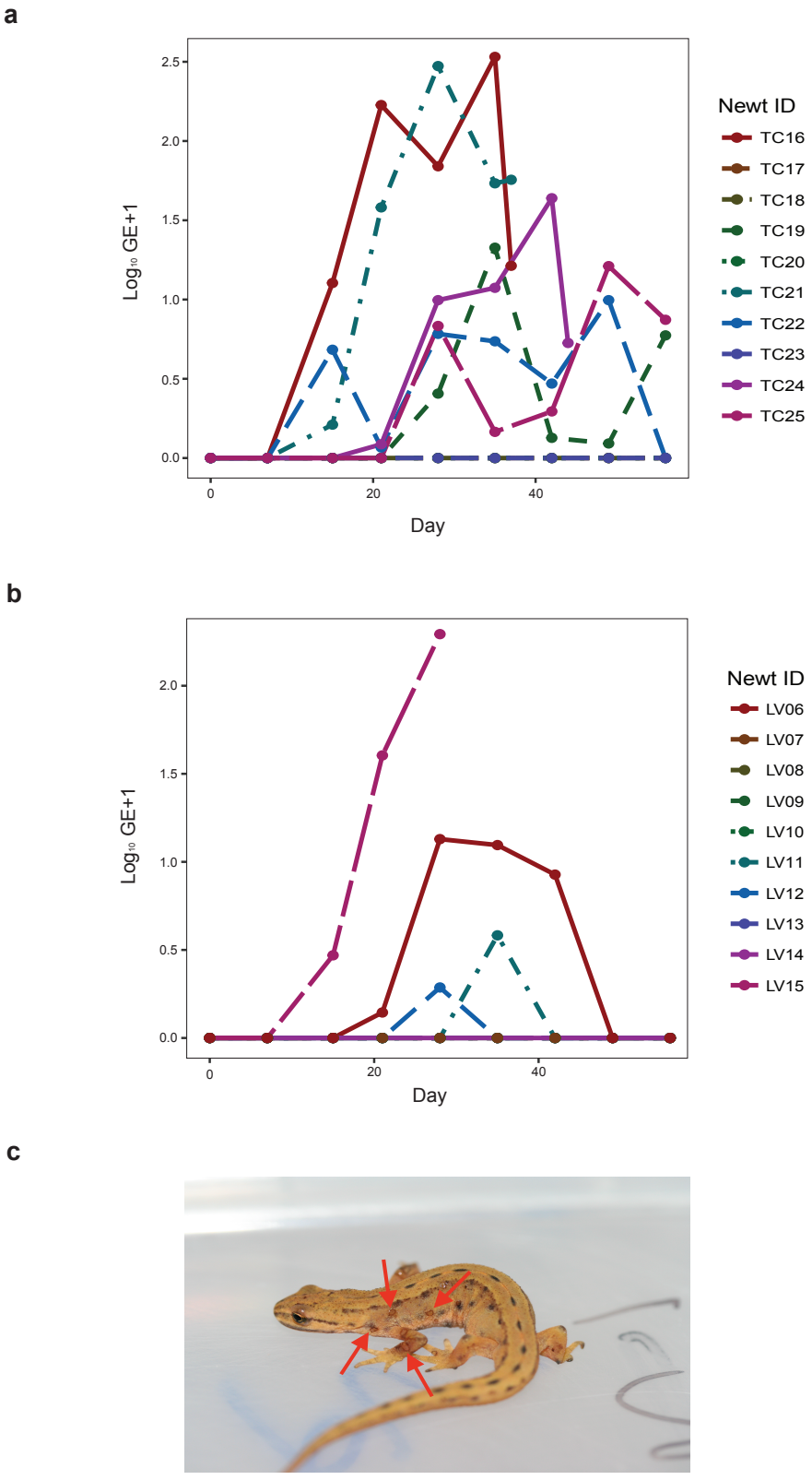


Figure 3.3: Plot of infection intensity for *Bsal* exposed animals for **(a)** *T. cristatus* **(b)** *L. vulgaris*. **(c)** Lesions evident on *L. vulgaris*. Sample sizes: n=5 (control *L. vulgaris*), n=5 (control *T. cristatus*),n=10 (exposed *L. vulgaris*), n=10 (exposed *T. cristatus*).

Fig. 4

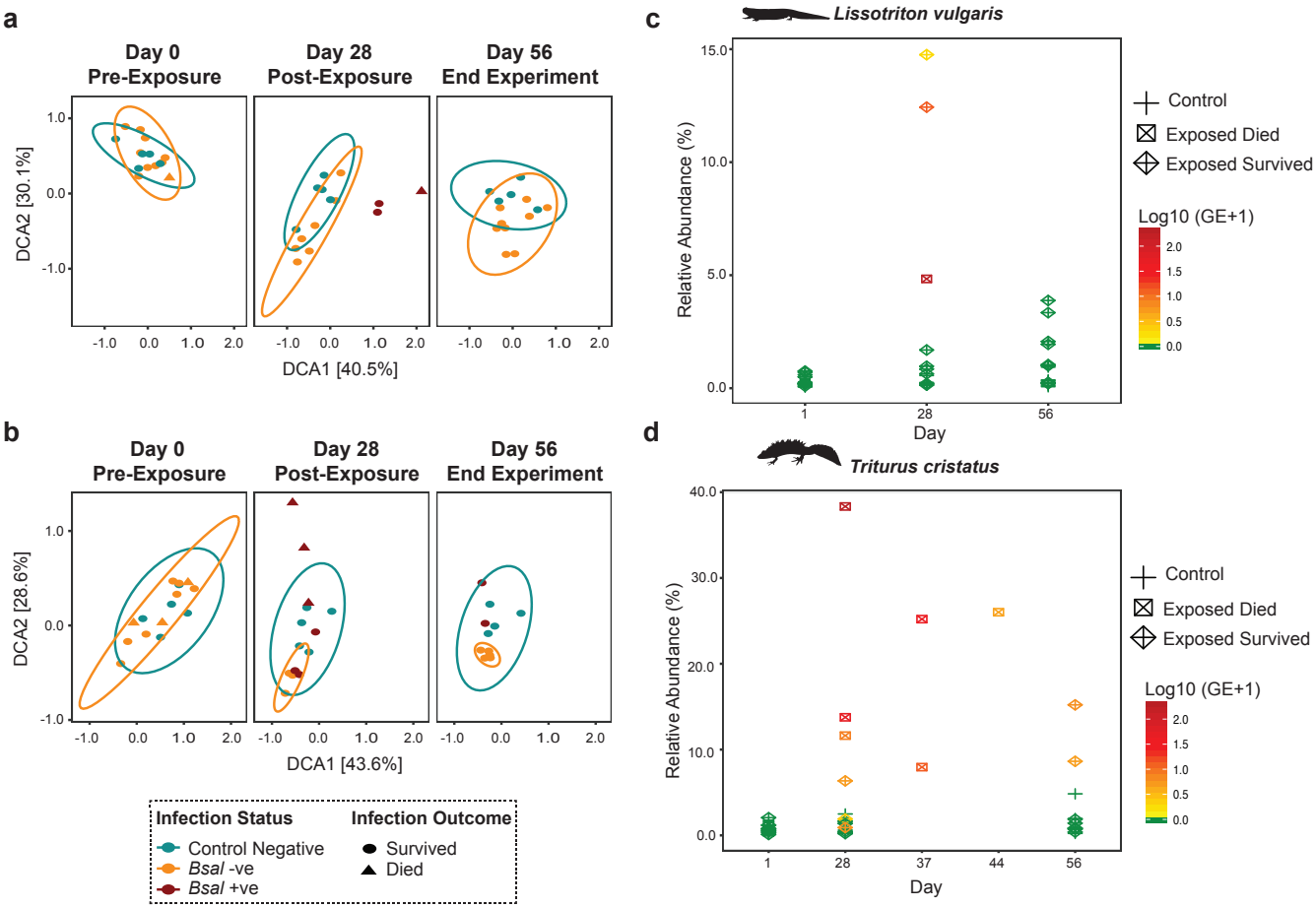


Figure 3.4: Detrended correspondence analysis (DCA) plots displaying temporal variation in bacterial beta diversity in **(a)** *L. vulgaris* **(b)** *T. cristatus*. Ellipses indicate 95% confidence intervals. Scatterplot of relative abundance of OTU016 *Stenotrophomonas* identified as an indicator OTU for *Bsal* infection in both **(c)** *L. vulgaris* and **(d)** *T. cristatus*. Sample sizes: n=15 (Day 0 *L. vulgaris*), n=15 (Day 28 *L. vulgaris*), n=14 (Day 56 *L. vulgaris*), n=15 (Day 0 *T. cristatus*), n=15 (Day 28 *T. cristatus*), n=12 (Day 56 *T. cristatus*).

3.5 Discussion

We demonstrate that both captivity and exposure to *Bsal* impact the amphibian skin microbiome. The decrease in microbial Shannon diversity and changes in beta diversity associated with captivity supports findings of previous studies (Becker et al., 2014; Kueneman et al., 2016a) and is likely correlated with a reduction in environmental microbes and changes to the host environment (Harrison et al., 2017). Importantly, both fungi and bacteria exhibited similar changes in alpha and beta diversity suggesting that both microbial kingdoms may respond in broadly similar ways to the selection pressures associated with the amphibian skin environment.

The perturbation in microbial diversity that occurs due to the transition from the wild to captivity may also change the ecological dynamics and functional capacity of the skin by altering host-microbe and microbe-microbe interactions (Foster et al., 2017). For example, when animals are brought into a captive environment where microbial reservoirs are likely to be less complex than in the wild, the subsequent reduced propagule pressure from environmental microbes may result in greater host or microbe-mediated control in shaping the skin microbiome. For example, in a prior study of red backed salamanders (*Plethodon cinereus*), a small subset of bacterial taxa were maintained in the host microbiome both in the wild and in captivity suggesting that these taxa had a close relationship with the host and were less susceptible to fluctuations in the environment (Loudon et al., 2014b). There is similar evidence to suggest intimate host-microbe associations in this study, whereby the most abundant bacterial and fungal taxa of both host species changed in their relative abundance when animals were brought into captivity, but were not lost entirely from the host. In addition, captivity was also associated with decline of some putatively pathogenic taxa as signified by the reduction in OTUs belonging to the Chlamydiales (Fig. 3.2a,b) which have previously been associated with amphibian epizootics (Reed et al., 2000). The loss of opportunisitc pathogens such as Chlamydiales may be more easily achieved by a host in captivity whereby microbes that may initially be destroyed by antimicrobial peptides are not able to re-invade the host from environmental sources.

An alternative hypothesis to captivity favouring host-microbe interactions that are beneficial to the host is that the decline in microbial alpha diversity that coincides with the transition

to captivity may reduce the ecological resistance of the host microbiota (Piovia-Scott et al., 2017) rendering the host more susceptible to pathogen invasion (Piovia-Scott et al., 2017). This hypothesis is supported by an increase in captivity in the relative abundance of the amphibian fungal pathogen *Basidiobolus ranarum* in both host species (though not statistically significant). Further evidence for a decline in microbe-mediated protection of the host comes from the reduction of putatively beneficial bacterial groups in captivity such as the Actinomycetales (Fig. 2a,b), which are well known for producing antimicrobial compounds (Berdy, 2005). Taxa belonging to the genus *Lysobacter* that have previously been associated with inhibition of other pathogenic chytrids (Brucker et al., 2008b; Bates et al., 2018) also showed a reduction in abundance in captivity. Ultimately, determining whether captivity is linked to changes in microbe-mediated protection will require functional assays of the host skin microbiota in the wild and captivity to determine if changes in diversity and taxonomic composition are related to altered pathogen resistance.

While the overall reduction in microbial diversity associated with captivity may impact host resistance to disease, the additional perturbation of microbial community structure may lead to dysbiotic effects (Zaneveld et al., 2017). These findings suggest that captivity induced changes in the microbiome may reduce host capability to evade pathogens and potentially predispose such individuals towards adverse health outcomes. Importantly, this is the first study of its kind to measure the effect of captivity on fungal communities, which despite being overlooked relative to bacteria, have been shown in some cases to confer higher rates of chytrid inhibition (Kearns et al., 2017). In light of the major perturbation of fungal communities, it is imperative that future studies utilise a more holistic view of the microbiome to include kingdoms other than bacteria. Overall, our results highlight that host microbial ecology should carefully be considered when transferring animals from the wild to captivity to reduce possible microbiome disturbance, prevent proliferation of opportunistic pathogens and preserve microbes that are beneficial to host health. For *ex-situ* conservation programmes that aim to rescue or re-establish wild amphibian populations using captive-bred stock, the implications are complex and suggest that maintenance or rewilding of the skin microbiome would be an essential aspect before reintroduction.

Exposure to *Bsal* resulted in mortality in both *L. vulgaris* and *T. cristatus*. While mortality was higher in *T. cristatus*, this was not statistically significant when compared to *L. vulgaris*. The intensity of infection was found to be higher in *T. cristatus*, which had a maximum GE of 338 compared to a maximum GE of 195 for *L. vulgaris*. These data suggest that *T. cristatus* may be more susceptible to Bsal infection than *L. vulgaris*. Interestingly, our findings counter those of a previous study that found 100% mortality in *T. cristatus* and a species effect on survival (Martel et al., 2014). The increased survival of *T. cristatus* here compared to the prior study (Martel et al., 2014) may be explained by a range of factors. In particular, the studies used animals collected from different countries (the UK versus the Netherlands) and there will likely be differences in host genetics and immunity. The higher mortality in the prior study may also be a function of a smaller sample size (only five *T. cristatus* were exposed to *Bsal* compared to ten animals in this study). In addition, the initial microbiome of the animals will almost certainly differ which may have an impact on the subsequent host microbial response to infection. These findings highlight the importance of investigating a geographically diverse range of hosts from the same species when conducting species level risks assessments of emerging pathogens. While this additional confirmation of *Bsal* induced death in *T. cristatus* warrants serious concern, the higher survivorship shown here may suggest a more optimistic outlook in the event of a wild *Bsal* outbreak for this species than previously predicted. Additional *Bsal* exposure experiments with larger host sample sizes, although challenging to perform given the protected status of *T. cristatus*, are however needed to make more robust conclusions regarding species level susceptibility.

Bacterial community structure of individuals in the *Bsal* exposure experiment differed significantly for both species based on infection status and survival. These findings are consistent with results of prior studies on *Bd* (Jani and Briggs, 2014), suggesting that infection by *Bsal* and *Bd* are both associated with microbiome disruption. Two *L. vulgaris* individuals tested positive for *Bsal* and demonstrated significant microbiome perturbation that may be indicative of dysbiosis on day 28 of the experiment, but subsequently cleared infection by day 56. In both cases *Bsal* clearance was associated with a change in microbiome profile with the subsequent community structure being similar to that of control animals. Determining what underpins this recovery in

L. vulgaris, whether driven by host factors such as secretion of antimicrobial peptides or *Bsal* inhibition by microbes, will be vital in determining the key parameters underpinning infection outcome.

Indicator analysis revealed that the bacterial taxa associated with disease state were different based on host species with the exception of one OTU classified as *Stenotrophomonas*. Interestingly, a prior study demonstrated *Stenotrophomonas* as inhibitory to *Bsal* and several *Bd* genotypes (Muletz-Wolz et al., 2017). Meanwhile, another study identified an isolate of *Stenotrophomonas* as inhibitory to *Bd in-vitro*, however when applied as a probiotic on an amphibian host exposed to *Bd in-vivo*, mortality was higher than in animals that were exposed to only *Bd* (Becker et al., 2015). More recently an *in-vivo* experiment, in which fire salamanders *Salamandra salamandra* were exposed to *Bsal*, identified an OTU belonging to the *Stenotrophomonas* genus as significantly increased in exposed compared to control animals (Bletz et al., 2018). Taken together these findings suggest that *Stenotrophomonas* abundance may be synergistic to *Bsal* growth, or opportunistically infect moribund animals. Interestingly, coinfection may be a plausible possibility given that *Stenotrophomonas* has been associated with opportunistic infection in other host systems (Adegoke et al., 2017). Ultimately, determining whether *Stenotrophomonas* is associated with microbe-mediated defence or synergistic growth/secondary infection with *Bsal* and whether or not this has pathological impacts to host health will require further experiments taking into account microbial function. While both newt species shared few taxa that were associated with disease outcome, the common perturbation in beta diversity associated with death in both *L. vulgaris* and *T. cristatus* may suggest that *Bsal* survival is not linked to specific taxa, but rather perturbation of a stable host microbiome resulting in an overall negative impact on health (Zaneveld et al., 2017). Further support to this hypothesis is given by the return to a stable microbiome state in animals that cleared infection.

While this study represents an important step in our understanding of how host environment and exposure to a recently discovered pathogen impacts the skin microbiome, there were several limitations which should be addressed in future studies. In particular, we show clear changes in the microbiome of both host species with the transition from the wild to captivity, yet quan-

titatively we do not know how much of this difference is due to changes in the environmental microbiome. Future studies should therefore seek to sample the host environment to more accurately determine how much environmental reservoirs in the wild and captivity differ and their effect on the host skin microbiome. Another key limitation was the relatively small sample size of animals used in this study (restricted due to the protected status of *T. cristatus*), combined with not all animals exposed to *Bsal* becoming infected meant that the statistical power in determining the effect of infection on the microbiome was limited. Future studies would therefore benefit from a larger sample size of animals exposed to *Bsal* (though may require use of a non-protected host species). Finally, although we have identified some convincing microbial associations with *Bsal* infection, in particular the positive association between an OTU belonging to the *Stenotrophomonas* genus and *Bsal*, we cannot reliably comment on what functional impact this is having on the the host and its microbiota. Culturing this bacterium and performing *in-vitro* co-culture experiments in addition to further animal experiments exposing newts to both *Stenotrophomonas* and *Bsal* will yield valuable information regarding the protective or detrimental nature of this bacterium to its host

Ultimately, our results build on the work of prior studies by demonstrating significant and potentially negative effects of captivity on the amphibian skin microbiome. In addition, we provide vital insight into the disease process of *Bsal* by demonstrating a close link between infection outcome and microbiome structure. Overall, our findings demonstrate that it is vital for host microbial ecology to be considered in future *Bsal* studies and captive based conservation programmes.

3.6 Acknowledgements

We thank A. Martel and F. Pasmans for providing the pathogen isolate used in the infection experiment. We are also grateful to Froglife for assistance with permits and field surveys. We thank P. Ghosh for help with experimental procedures and T. Garner for advice on experimental design. Finally, we wish to thank the Tedersoo group at the University of Tartu and the National

Heart and Lung Institute for assistance with mycobiome sequencing. This research was funded by the Leverhulme Trust grant RPG-2014-273.

Chapter 4

Skin microbiome composition and metabolomic profiles of amphibian populations reflect enzootic and epizootic chytridiomycosis disease dynamics

Kieran A. Bates[1,2], Ulf Sommer[3], Jennifer M.G. Shelton[1], Claudia Wierzbicki[1], Kevin P. Hopkins[2], Benjamin Tapley[2], Christopher Michaels[2], Mark Viant[3], Xavier A. Harrison[2],Trenton W.J. Garner[2], Matthew C. Fisher[1]

[1]Department of Infectious Disease Epidemiology and MRC Centre for Global Infectious Disease Analysis, School of Public Health, Imperial College London, London W2 1PG, UK; [2]Institute of Zoology, Zoological Society of London, Regents Park, London, NW1 4RY, UK; [3]NERC Biomolecular Analysis Facility - Metabolomics Node (NBAF-B), School of Biosciences, University of Birmingham, Edgbaston, Birmingham B15 2TT, UK

Author contributions: K.A.B., M.V., U.S., X.A.H., T.W.J.G. and M.C.F conceived study design. K.A.B. conducted field surveys. K.A.B., U.S., K.P.H., C.W., and J.M.G.S. performed data processing. K.A.B. performed data analysis, prepared figures and wrote the manuscript.

4.1 Abstract

The metabolic activities of host-associated microbes can have an important influence on host physiology. In amphibians, skin-associated bacteria and fungi have been shown to inhibit the fungal pathogen *Batrachochytrium denodrobatidis* (*Bd*), while the composition of microbial communities in the wild have been linked to *Bd* disease outbreak dynamics. Despite this, our understanding of whether differences in amphibian skin microbial community structure are linked to function and the importance of this in disease outcome is limited. To investigate the functional importance of the amphibian skin microbiota in infection, we characterised the skin microbiome and mucosal metabolome of wild Pyrenean midwife toad populations exhibiting enzootic or epizootic *Bd* disease dynamics. We show a significant effect of infection history on the host skin microbiome with differences in bacterial and fungal communities and reduced bacterial diversity associated with epizootic dynamics. Microbial community structure was also linked to metabolome composition with clear microbe-metabolite associations that discriminated between enzootic and epizootic host populations. Our results demonstrate that differences in host microbial ecology based on population and disease state are functionally relevant and likely play an important role in host susceptibility to pathogens.

4.2 Introduction

In amphibians the skin is the first line of defence against cutaneous fungal pathogens such as *Batrachochytrium dendrobatidis* (*Bd*). In addition to providing a physical barrier to entry of invading pathogens, the amphibian skin is coated in a mixture of mucosal and granular secretions such as mucin glycoproteins, biogenic amines, steroids, lysozymes, alkaloids, peptides and proteins (Daly et al., 1987; Clarke, 1997; Zhao et al., 2006). Collectively the complex collection of amphibian derived mucosal molecules may provide a source of nutrients for a diverse array of microbes, while antimicrobial compounds simultaneously police unwanted invaders (Rollins-Smith and Conlon, 2005; Rollins-Smith et al., 2009; Mina et al., 2015). In addition to occupying the host skin and utilising host-derived secretions as a source of nutrients, the

microbiome contributes to the chemical characteristics of the skin mucosa through secretion of metabolic by-products (Nicholson et al., 2010), signalling molecules (Waters and Bassler, 2005) and compounds (many of which are antimicrobial) that mediate microbe-microbe and host-microbe interactions (Hibbing et al., 2010). The microbiome of multicellular organisms is also important in maintaining homeostasis of host metabolism, for example in the human gut co-metabolic pathways between the host and its microbiota produce metabolites that are essential to host health and impact multiple organ systems (Nicholson et al., 2010). Disruption of normal host-microbe relationships and co-metabolic pathways can consequently lead to the onset of disease (Ley et al., 2006; Pedersen et al., 2016). In addition to the effects that can be brought about as a result of perturbation of the host microbiome, in the case of pathogens certain metabolites may have direct, negative impacts on host health. For example, *Bd* produces metabolites such as methylthioadenosine (MTA), tryptophan and kyneurenine that inhibit a robust host immune response to infection (Rollins-Smith et al., 2015). Investigating the host microbiome and metabolome in infection therefore not only provides insight into the mechanistic basis of pathology, but also has potential to yield clinically relavent biomarkers associated with different infection outcomes.

While studies of the amphibian skin microbiome have yielded convincing associations with *Bd* outcome in the lab and in wild outbreaks (Harris et al., 2009; Jani and Briggs, 2014; Jani et al., 2017; Bates et al., 2018), few have investigated whether differences in microbial taxonomic composition are associated with function. *In-vitro* studies have identified anti-*Bd* metabolites produced by amphibian skin associated bacteria (Brucker et al., 2008b,a; Loudon et al., 2014a; Woodhams et al., 2017), however *in-vivo* studies demonstrating a link between such metabolites and survival in *Bd* infected animals are limited (Brucker et al., 2008a). In addition, few studies have investigated the holistic metabolomic composition of the amphibian skin mucosa and its relationship with the microbiome and infection. Of these studies, the consensus as to whether *Bd* is associated with microbiome/metabolome structure has been mixed. In a laboratory challenge experiment the microbiome and metabolome differed in harlequin frogs (*Atelopus zeteki*) that cleared *Bd* infection or died (Becker et al., 2015) indicating that infection outcome is associated with perturbation of skin microbial composition and function. These findings

were subsequently corroborated in a different host species, the American bullfrog (*Lithobates catesbeiana*) that demonstrated different skin microbiome and metabolomic profiles in *Bd*-exposed and un-exposed animals (Walke et al., 2015b). Conversely, in another study of wild Panamanian amphibians, the host microbiome and metabolome were not associated with *Bd* infection dynamics (Belden et al., 2015), nor were any significant correlations uncovered between bacterial community structure and metabolome profile. The findings of this study suggest that in a wild disease system, the skin microbiome is not a key factor in mediating infection, while the lack of correlation between the microbiome and metabolome may indicate functional redundancy whereby different taxa perform similar functional roles within a community. Given the complexity of microbial interactions occurring on the amphibian skin (Antwis et al., 2015; Antwis and Harrison, 2018; Loudon et al., 2014a; Myers et al., 2012) and the scarcity of prior studies on this subject, there is a critical need to develop a holistic understanding of how amphibian microbiome structure relates to function within a disease framework.

Here, we investigate the relationship between the amphibian skin bacterial and fungal communities, skin metabolome profiles and *Bd* infection dynamics in a wild chytridiomycosis outbreak system. This work is a continuation of a long-term study in which *Bd* infection in midwife toad (*Alytes obstetricans*) populations has been identified as exhibiting enzootic or epizootic disease dynamics based on resistance (low or zero infection intensity and stable population abundance) versus high susceptibility to infection and population decline (Bates et al., 2018). In addition, prior work in this system has shown a strong association between skin bacterial communities and *Bd* disease dynamics, while no link was found between pathogen genetics and infection outcome (Bates et al., 2018) indicating that the host microbiota is influential in shaping response to infection. In this study we extend our analyses of the skin microbiome to include both bacteria and fungi in addition to characterising the metabolite profile of *A. obstetricans* skin. We coupled 16S and ITS metabarcoding of bacterial and fungal communities with metabolome analyses of the amphibian skin mucosa from four *A. obstetricans* populations exhibiting enzootic or epizootic disease dynamics (Bates et al., 2018). Our metabolome analysis of the skin mucosa captures both host and microbial derived metabolites and therefore provides a holistic metabolic profile of the skin from each host population. Specifically our goals were to:

1) investigate if both skin bacterial and fungal communities were associated with population level *Bd* disease dynamics in the year succeeding the study in Chapter Two; 2) identify if the *A. obstetricans* skin metabolome profile was shaped by host population and/or disease dynamics; 3) determine whether differences in host skin bacterial and fungal communities in enzootic and epizootic populations were correlated with skin mucosal metabolome profiles. Our findings provide an important step in our understanding of wild chytridiomycosis outbreak dynamics by elucidating the link between microbial community structure and metabolic function across different host populations and disease outcomes.

4.3 Material and Methods

4.3.1 Field sampling

This study was conducted on four *A. obstetricans* populations in the Pyrenees mountains of France and Spain. Each population has been part of a long-term *Bd* surveillance project in the Pyrenees and previously been identified as exhibiting either enzootic disease dynamics (Ibon Acherito, Puits d'Arious, Lhurs) or epizootic dynamics (Arlet) (Walker, 2008; Clare, 2014; Bates et al., 2018). We sampled fourteen *A. obstetricans* metamorphs for *Bd*, skin microbial communities and skin metabolome from each of the four populations (n=56) in August 2016. New nitrile gloves were worn for each animal sampled. Prior to sampling animals were washed with sterile water to remove any transient microbes or substrate debris that may be contaminants in downstream sample processing. Microbial communities and *Bd* were each sampled using a single sterile MW100 cotton dry tipped swabbed (MWE Medical Wire, Corsham, UK) that was rolled over the ventral and dorsal surfaces of the skin ten times, and the hindlimbs five times. To collect skin mucosal metabolome each animal was placed in a falcon tube containing 12ml of sterile water for twenty minutes to allow skin metabolites to diffuse into solution. A pilot study of metabolome collection showed that a combination of both bathing and swabbing was optimal for maximal metabolite recovery so after twenty minutes each animal was swabbed again following the same protocol as the microbiome collection. To collect metabolites from

solution, 10ml of the bath solution was passed through a combination of two solid phase extraction (SPE) cartridges - a 500mg 3ml Discovery DSC-18 cartridge (Sigma Aldrich, Missouri, USA) and a 100mg 1ml ISOLUTE ENV+ cartridge (Biotage, Uppsala, Sweden) connected by an SPE tube adaptor. SPE cartridges were pre-conditioned with 5ml of methanol (MeOH) and rinsed with 5ml of sterile water immediately prior to sample collection. The liquid sample was applied at consistent flow rate of one to two drops per second to ensure optimal metabolite retention. After sample application, the SPE cartridges were rinsed with 1ml of sterile water to aid in contaminant removal. Both metabolome and microbiome swabs and SPE cartridges were placed immediately on dry ice before being transferred to a -80°C freezer.

4.3.2 Sample processing, DNA extraction and quantification of *Bd* infection

For microbiome and mycobiome analysis genomic DNA was extracted from swabs using the DNeasy Blood and Tissue kit (Qiagen, Venlo, Netherlands) according to the manufacturers instructions. A pre-treatment with mutanolysin was included to enhance recovery of bacterial DNA (Yuan et al., 2012). For microbiome analysis DNA extracted from swabs was used to amplify the V4 region of the 16S rRNA gene using custom barcoded primers and PCR conditions adapted from a prior study (Kozich et al., 2013). PCR conditions consisted of a denaturing step of 95°C for 15 min, followed by 28 cycles of 95°C for 20s, 50°C for 60s, 72°C for 60s and a final extension step of 72°C for 10 min. Each PCR including a negative water control was performed in triplicate. Amplicons were visualized on a 2% agarose gel and pooled yielding a final per sample volume of 24 µl. Pooled amplicon DNA was purified using an Ampure XP PCR purification kit (Beckman Coulter, California, USA). Following purification, 1 µl of each combined sample was pooled into a preliminary library and the concentration was determined using Qubit fluorometric quantification (Life Technologies, California, USA). Amplicon quality and incidence of primer dimer was assessed using an Agilent 2200 TapeStation system (Agilent Technologies, California, USA). A titration run of 300 sequencing cycles was performed on a MiSeq instrument (Illumina, California, USA) to quantify the number of reads yielded per

sample from the preliminary library. An equimolar concentration of each sample was then pooled into a final composite library based on the index representation from the titration run and subsequently sequenced on a 500 cycle MiSeq run with a 250 bp paired-end strategy.

For fungal mycobiome analysis DNA extracted from swabs was used to amplify the ITS2 region of the fungal internal transcribed spacer (ITS) using custom barcoded primers (Kozich et al., 2013) and the following PCR conditions: denaturing step of 95°C for 2 min, followed by 35 cycles of 95°C for 20s, 50°C for 20s, 72°C for 5 min and a final extension step of 72°C for 5 min. Each PCR plate included a negative swab control and negative water control, and was performed in duplicate. Amplicons were visualized on a 1.5% agarose gel and pooled yielding a final per sample volume of 50 µl. Pooled amplicon DNA was purified using AMPure XP bead clean-up (Beckman Coulter, California, USA). Qubit fluorometric quantification (Life Technologies, California, USA) was used to determine the concentration of each purified sample, which were equimolar pooled to create the final library sample. This pooled sample was run on an Agilent 2200 TapeStation system (Agilent Technologies, California, USA) to assess amplicon distribution and presence of primer dimer. The sample underwent 300bp paired-end sequencing using V3 chemistry on an Illumina MiSeq platform.

To assess infection burden genomic DNA from *Bd* swabs was extracted using a bead-beating protocol (Boyle et al., 2004). DNA extractions were diluted 1/10 before undergoing qPCR amplification with each sample run in duplicate (Boyle et al., 2004) and with *Bd* standards of 100, 10, 1 and 0.1 zoospore genomic equivalents (GE). Samples with greater than 0.1 GE were considered positive for *Bd*.

4.3.3 Infection analysis

Analysis of infection intensity followed the methods outlined in Chapter 2 and in prior studies (Clare et al., 2016; Bates et al., 2018). Briefly, genomic equivalents were rounded to whole numbers and treated as counts. A negative binomial regression model (function glm.nb, package MASS) was used to test differences in infection intensity between *A. obstetricans* populations. A likelihood ratio test was used to assess significance of population in the model and Tukey

post-hoc test (function glht, package multcomp (Hothorn et al., 2008)) tested for pairwise differences between each population. Genomic equivalence data was log+1 transformed and visualised using boxplots.

4.3.4 Bacterial microbiome bioinformatics

Sequences were processed using MOTHUR (Schloss et al., 2009) following a previously described method (Kozich et al., 2013). Paired-end reads were split by sample and assembled into contigs. Sequences were quality filtered by removing ambiguous base calls, removing homopolymer regions longer than 8 bp, and trimming reads longer than 275 bp. Duplicate sequences were merged and aligned with 16S reference sequences from the SILVA small-subunit rRNA sequence database (Pruesse et al., 2007). A pre-clustering step grouped sequences differing by a maximum of 2 bp. Chimeric sequences were removed using UCHIME (Edgar et al., 2011) as implemented in MOTHUR. 16S rRNA gene sequences were clustered into groups according to their taxonomy at the level of order and assigned operational taxonomic units (OTUs) at a 3% dissimilarity level. Sequences were taxonomically classified with an 80% bootstrap confidence threshold using a naive Bayesian classifier with a training set (version 9) made available through the Ribosomal Database Project (http://rdp.cme.msu.edu) (Wang et al., 2007). Sequences derived from chloroplasts, mitochondria, archaea, eukaryotes or unknown reads were eliminated. Downstream analysis of OTUs was carried out using the package Phyloseq (McMurdie and Holmes, 2013) in R version 3.4.1 (R Core Team, 2017).

4.3.5 Fungal mycobiome bioinformatics

Forward and reverse reads were assigned to samples according to dual index combinations and were paired using Paired-End reAd mergeR (PEAR) (Zhang et al., 2014). Paired-end reads were trimmed by per-base quality score using MOTHUR (Schloss et al., 2009) and reads shorter than 50bp or containing ambiguous base calls were removed. UCHIME (Edgar et al., 2011) was used to identify and remove chimeric sequences, and remaining sequences were clustered into

Operational Taxonomic Units (OTUs) based on 97% similarity using Cd-hit (Li and Godzik, 2006). The most abundant sequence in each OTU was used for BLASTn searches against the User-friendly Nordic ITS Ectomycorrhiza (UNITE) database (Koljalg et al., 2005). Unidentified sequences or those belonging to kingdoms other than fungi were removed, as were fungal sequences with BLASTn search result e-values >e-20 or identity <85%. Downstream analysis of OTUs was carried out using the package Phyloseq (McMurdie and Holmes, 2013) in R version 3.4.1.

4.3.6 Bacterial and fungal community statistical analysis

The number of bacterial sequences per sample ranged from 1096 to 36971. Mycobiome sequences per sample range from 7 to 7309. To mitigate the effects of uneven sampling (Schloss et al., 2011) microbiome and mycobiome samples were rarefied. Microbiome samples were rarefied to 1096 sequences corresponding to the size of the lowest read sample. Mycobiome samples were rarefied to 233 reads per sample resulting in 35 samples out of 56 remaining for downstream analysis. To determine differences in bacterial and fungal diversity between populations, Shannon diversity was calculated for each population. Analysis of variance (ANOVA) was used to determine significant differences in Shannon diversity between populations and a post-hoc Tukey's test identified pairwise differences of populations. To deteremine if bacterial and fungal Shannon diversity were correlated with *Bd* infection intensity, Spearman's correlation was performed. For *Bd* and Shannon diversity correlation analyses, log10(GE+1) was used for *Bd* infection data.

Bacterial and fungal beta diversity of populations was calculated using a Bray-Curtis dissimilarity matrix and visualised using non-metric multidimensional scaling (NMDS) plots. Permutational multivariate analysis of variance (PERMANOVA) (Anderson, 2001) was carried out to determine the relative contribution of disease dynamic and population in shaping bacterial and fungal community structure. Correlations between *Bd* infection intensity (log GE +1) and both bacterial and fungal communities was determined using Mantel tests. *Bd* infection data was converted to a distance matrix prior to performing mantel tests. Indicator analysis (Dufrene

and Legendre, 1997) was performed on the top 0.1% of OTUs for both bacteria and fungi to determine OTUs that best explained differences based on either population or disease state. OTUs with indicator values >0.5 and a false discovery rate adjusted p value<0.05 were considered informative for both bacteria and fungi. Heatmaps displaying the relative abundance of the most informative indicator OTUs for enzootic and epizootic populations were generated using the function heatmap.2 in the gplots package in R (Warnes et al., 2009).

4.3.7 Metabolite extraction protocol

The SPE columns were eluted with 800 µl MeOH through the ENV+ column onto the C18 column, which was then eluted with and additional 400 µl MeOH. The combined eluate was then dried under nitrogen and stored at -80°C until mass spectrometry (MS) analysis.

4.3.8 UHPLC-MS metabolomics of skin mucus samples

For MS analysis, the samples were each taken up in 25 µl of 10% methanol and 7 µl was taken off from each sample to create a pooled QC sample. The samples were analysed in a controlled randomised order by ultra high pressure liquid chromatography-mass spectrometry (UHPLC-MS) on a Thermo Scientific Q Exactive mass spectrometer attached to a Thermo Dionex Ultimate 3000 RS system, equipped with a Thermo Hypersil Gold AQ column (100 x 1 mm, 1.9 µl particles). Solvents were (A) 0.1% formic acid in water and (B) 0.1% formic acid in methanol. Liquid chromatography was performed at 40°C over 19 min at a flow rate of 80 µl per minute, with 4 µl injections per sample, and MS start at 0.01 min, with the post-column flow between 0.4 and 0.7 min directed towards waste. The gradient was started at 100% A, ramped to 25% B from 0.4 min to 1.5 min, then over 6 min to 100% B, held for 5 min, then ramped back down to 100% A over 0.1 min for re-equilibration. The main data were acquired in negative ion mode, at m/z 100-900 Da, 70,000 resolution and AGC at 3E6 ions. Four additional runs of the pooled QC sample were performed at higher resolution (140,000), and again in data dependent MS/MS runs on the highest 5 signals per MS scan.

4.3.9 UHPLC-MS spectral processing

The main dataset was converted into mzML using MS Convert (ProteoWizard), and an in-house XCMS/CAMERA R-script used to create an initial raw intensity data matrix, which was imported into MatLab and processed using the Birmingham SimStitch pipeline (version 3.1). Peak signal filtering was applied using a filter requiring sample signal over blank > 2, and an 80% sample filter (i.e. signals have to be found in at least 80 % of samples), applied per group to generate a sample filtered matrix. The dataset was normalised using the probabilistic quotient normalisation (PQN), missing values were imputed using a K Nearest Neighbour algorithm (knn, k=5) and for multivariate statistics, the data were then transformed using a generalised logarithm (g-log) (Parsons et al., 2007; Di Guida et al., 2016). Putative metabolite annotations were created using the in-house software MIPack (Weber and Viant, 2010), matching m/z values against the KEGG database (www.genome.jp/kegg/pathway.html). The majority of metabolites were annotated to level 2 classification (putatively annotated compounds e.g. without chemical reference standards, based upon physicochemical properties and/or spectral similarity with public/commercial spectral libraries) as defined by the metabolomics standards initiative (Sumner et al., 2007).

4.3.10 Metabolome analysis

To determine if metabolome differed based on population and disease state, metabolome data was converted to a Bray-Curtis dissimilarity matrix and visualised using a non-metric multidimensional scaling (NMDS) plot using the vegan package in R (Oksanen et al., 2016). PERMANOVA was applied on the Bray-Curtis distance matrix of the metabolome data using the vegan package (Oksanen et al., 2016) to determine the proportion of variance attributed to population and disease dynamic and the statistical significance. Correlations between *Bd* infection intensity (log GE +1) and the metabolome were determined using a Mantel test. In addition, partial least squares discriminant analysis (PLS-DA) was performed using the R package mixomics (Rohart et al., 2017). PLS-DA Model significance was tested using a permutation analysis (999) implemented using MVA.test in the RVAideMemoire package (Herv,

2016). Metabolites driving differences in metabolome variation across populations were identified based on the variable influence on the projection (VIP) parameter using the PLSDA.VIP command from the RVAideMemoire package. Univariate ANOVA was also performed to determine metabolites with different abundance between populations. *P*-values were adjusted using the false discovery rate procedure using the p.adjust function in R. Metabolites were considered informative if they had a VIP score >2 and also showed a statistically significant profile at $q<0.05$ from the univariate analysis. Fold change was calculated for discriminatory metabolites.

4.3.11 Integration of microbiome and metabolome data

To determine the degree of association between bacterial or fungal communities and metabolome, procustes analysis was performed on Bray-Curtis dissimilarity matrices using the vegan package in R (Oksanen et al., 2016). Spearman correlation was used to identify associations between individual metabolites and OTUs using the associate function in the microbiome package in R (Lahti et al., 2017). Correlations that had a Spearmans rho of >0.6 with an adjusted p value of <0.05 were considered informative. Networks were generated using a force-directed algorithm and visualised using Cytoscape (Shannon et al., 2003).

4.4 Results

4.4.1 *Bd* infection analysis

A negative binomial regression analysis supported previous results of infection dynamics in the Pyrenees (Bates et al., 2018), with a significant difference in *Bd* infection intensity between the epizootic population (Arlet) and all enzootic populations (Chi-sq = 69.44958, df = 3, $p < 0.001$, Table 4.1, Fig 4.1a). All populations had 100% prevalence of *Bd* with exception of Acherito which had lower prevalence of 78.6% (Fig.4.1b).

Comparison	***P*-value**
Arlet-Acherito	<0.001
Lhurs-Acherito	0.755
Puits-Acherito	0.994
Lhurs-Arlet	<0.001
Puits-Arlet	<0.001
Puits-Lhurs	0.884

Table 4.1: Significance of pairwise differences in infection intensity (GE) between *A. obstetricans* populations.

4.4.2 Cross-Kingdom microbiota profiles are associated with population and *Bd* disease dynamics

Bacterial Shannon diversity was generally lower in the epizootic population compared to enzootic populations with significant differences in Lhurs and Acherito compared to Arlet (ANOVA $F_{(3,52)} = 6.576$, $p = 0.0008$, Tukeys tests: Arlet-Acherito, $p = 0.0005$; Arlet-Lhurs, $p = 0.017$, Arlet-Puits d'Arious $p = 0.1923$, Fig 4.1c). Fungal Shannon diversity did not differ between populations (ANOVA $F_{(3,31)} = 1.569$, p=0.217, Fig 4.1d). *Bd* infection intensity was significantly negatively correlated to bacterial Shannon diversity (Spearman rho = -0.33, $p = 0.01$, Fig.4.1e), while there was no significant correlation between fungal Shannon diversity and *Bd* infection intensity (Spearman rho = 0.05, $p = 0.768$, Fig.4.1e).

Beta diversity of host skin bacterial communities based on Bray-Curtis dissimilarity differed according to population and disease dynamic (PERMANOVA Population: Pseudo-$F_{(3,52)}$ =

7.1754, R^2 = 0.29277, p = 0.001, Dynamic: Psuedo-$F_{(1,54)}$=11.277, R^2=0.17276, p=0.001, Fig. 4.2a). Fungal beta diversity based on Bray-Curtis dissimilarity also differed between populations (PERMANOVA Pseudo-$F_{(3,31)}$=2.598, R^2 = 0.20091, p = 0.001) and based on disease dynamic (PERMANOVA Psuedo-$F_{(1,33)}$ = 2.7477, R^2 = 0.07686, p = 0.001, Fig. 4.2b). While bacterial community composition was significantly correlated with *Bd* infection intensity (Mantel test, r=0.11, p=0.04), fungal community composition was not (Mantel test, r=0.12, p=0.06). level compositional differences between populations were also evident for both bacterial and fungal communities (Fig. 4.2c,d). In particular epizootic populations were enriched for bacterial taxa belonging to the phyla Bacteroidetes and Chlamydiae, but exhibited reduced abundance of Firmicutes relative to enzootic populations (Fig. 4.2c). Fungal phyla demonstrated less pronounced compositional differences among enzootic and epizootic populations with the fungal communities of all animals being dominated by members of the Ascomycota. The epizootic population (Arlet) however did show higher relative abundance of members of the Chytridiomycota and the Rozellomycota compared to enzootic populations (Fig. 4.2d).

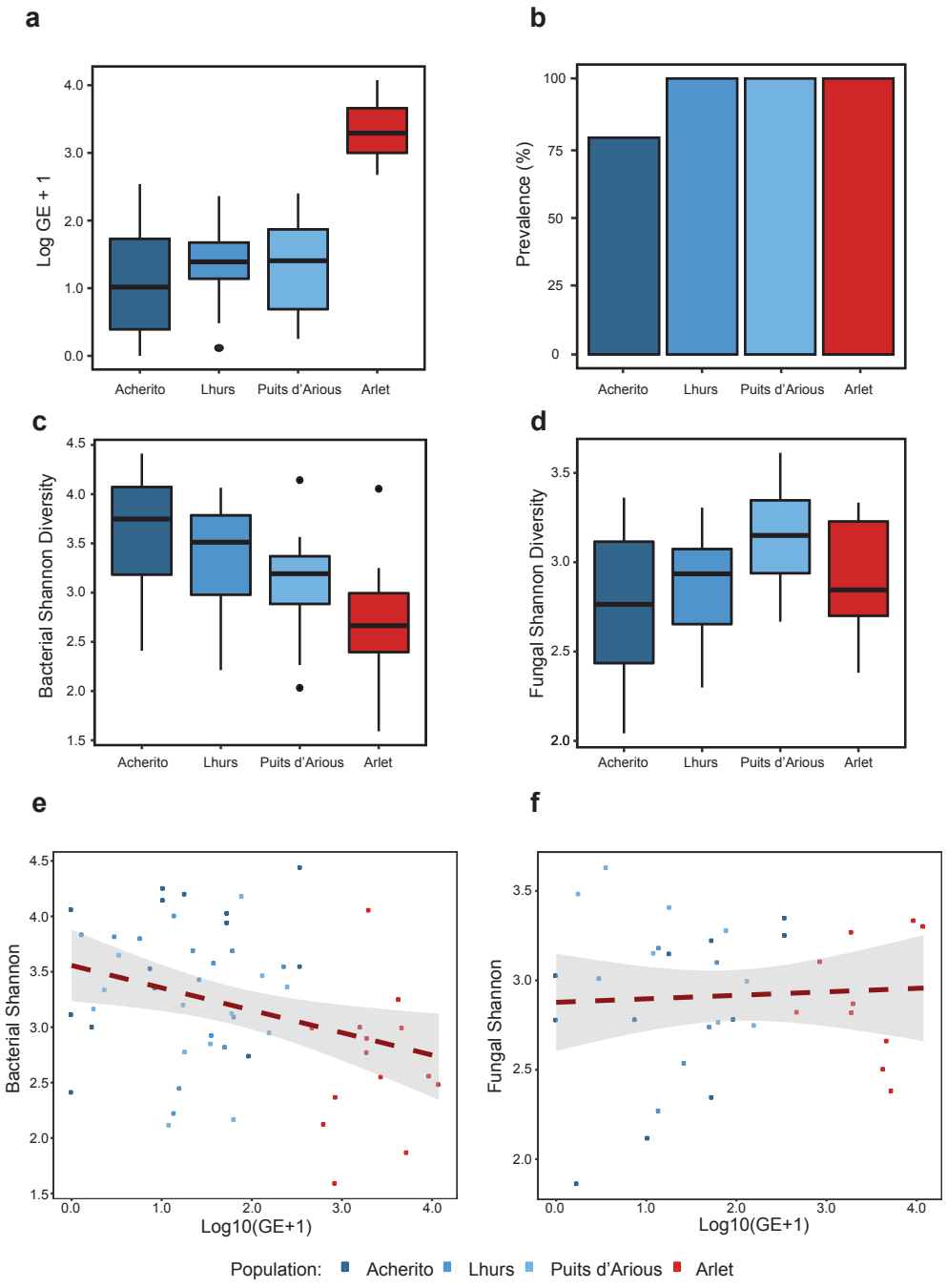


Figure 4.1: (**a**) Boxplot of *Bd* infection intensity for each *A. obstetricans* population. (**b**) *Bd* prevalence in each *A. obstetricans* population. Microbial Shannon diversity of *A. obstetricans* skin for each population for (**c**) bacteria and (**d**) fungi. Boxes represent 25$^{\text{th}}$ and 75$^{\text{th}}$ percentile, the horizontal line is the median, whiskers are maximum and minimum values. Scatterplots of (**e**) bacterial Shannon diversity versus log10 GE+1 and (**f**) fungal Shannon diversity versus log10 GE+1. Sample sizes for fungi were: n=11 (Acherito), n=6 (Lhurs), n=8 (Puits d'Arious), n=10 (Arlet). Sample sizes for bacteria were: n=14 (Acherito), n=14 (Lhurs), n=14 (Puits d'Arious), n=14 (Arlet).

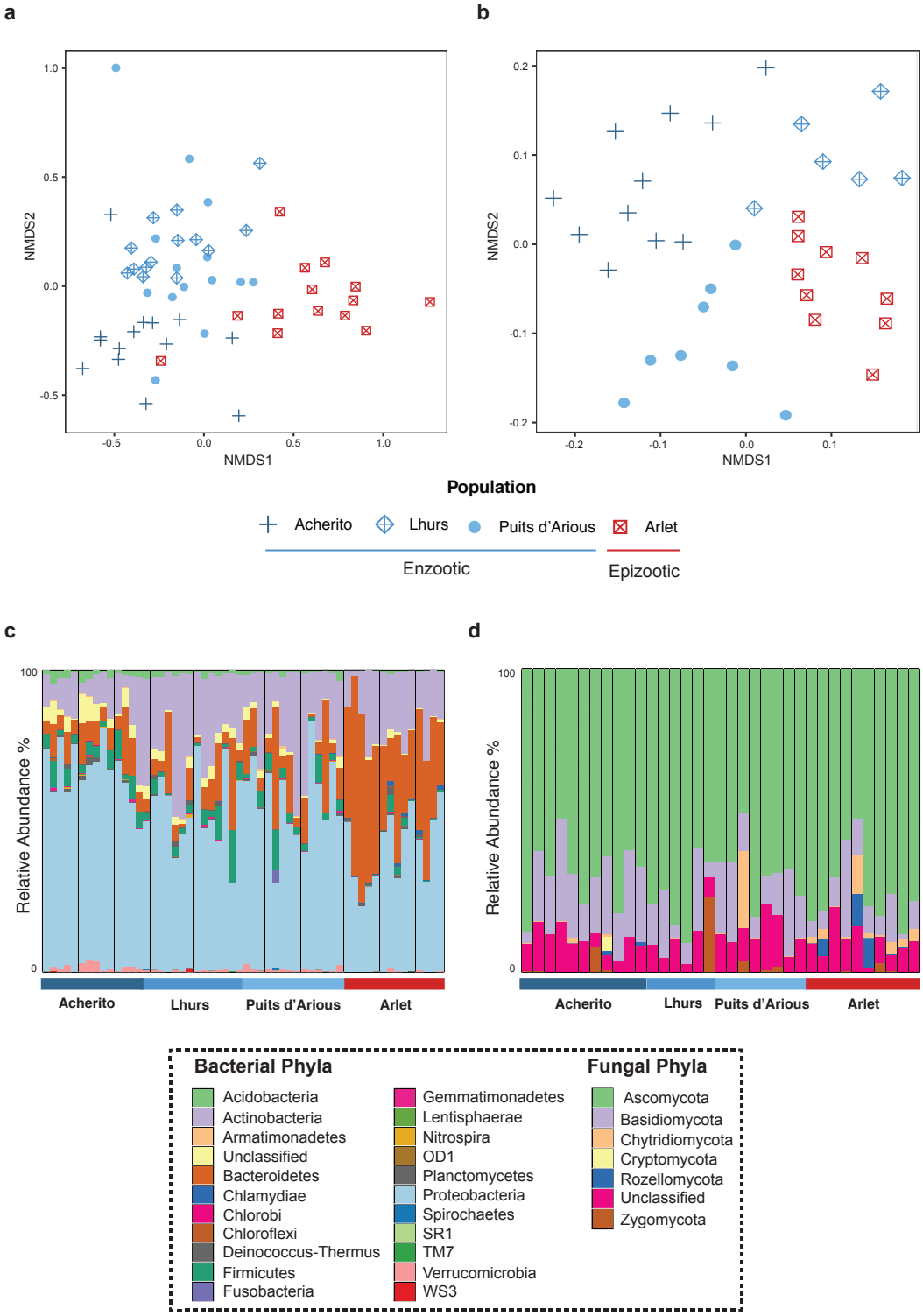


Figure 4.2: Non-metric multidimensional scaling (NMDS) plots of beta diversity based on Bray-Curtis dissimilarity for each *A. obstetricans* population for (**a**) bacteria (**b**) fungi. Stacked bar plots displaying composition of microbial phyla for (**c**) bacteria (**d**) fungi. Sample sizes for fungi: n=11 (Acherito), n=6 (Lhurs), n=8 (Puits d'Arious), n=10 (Arlet). Sample sizes for bacteria: n=14 (Acherito), n=14 (Lhurs), n=14 (Puits d'Arious), n=14 (Arlet).

We identified a total of 40 bacterial indicator OTUs based on population and 58 based on disease dynamic. A total of 16, 4, 16, and 13 bacterial indicator OTUs were identified for Ibon Acherito, Puits d'Arious, Lhurs and Arlet respectively (Appendix 10). In total, 42 bacterial indicator OTUs were associated with enzootic disease dynamics and 16 were associated with epizootic dynamics (Fig 4.3a,b, Appendix 11). Indicator OTUs associated with enzootic populations spanned 8 phyla and 17 classes of which the Actinomycetales were the most common. The epizootic population (Arlet) was associated with a less diverse range of bacterial taxa with indicator OTUs spanning 4 phyla and 6 classes of which the Rhizobiales was the most abundant order.

Indicator analysis of fungal taxa revealed a total of 6 indicator OTUs associated with individual populations of which 1, 3 and 2 OTUs were associated with Ibon Acherito, Puits d'Arious and Arlet respectively (Appendix 12). A total of 2 fungal indicator OTUs were identified based on disease dynamic (Fig. 4.4a,b, Appendix 13), both of which were associated with the epizootic population. The epizootic fungal indicator OTUs belonged to the genus *Batrachochytrium* and the genus *Phoma*.

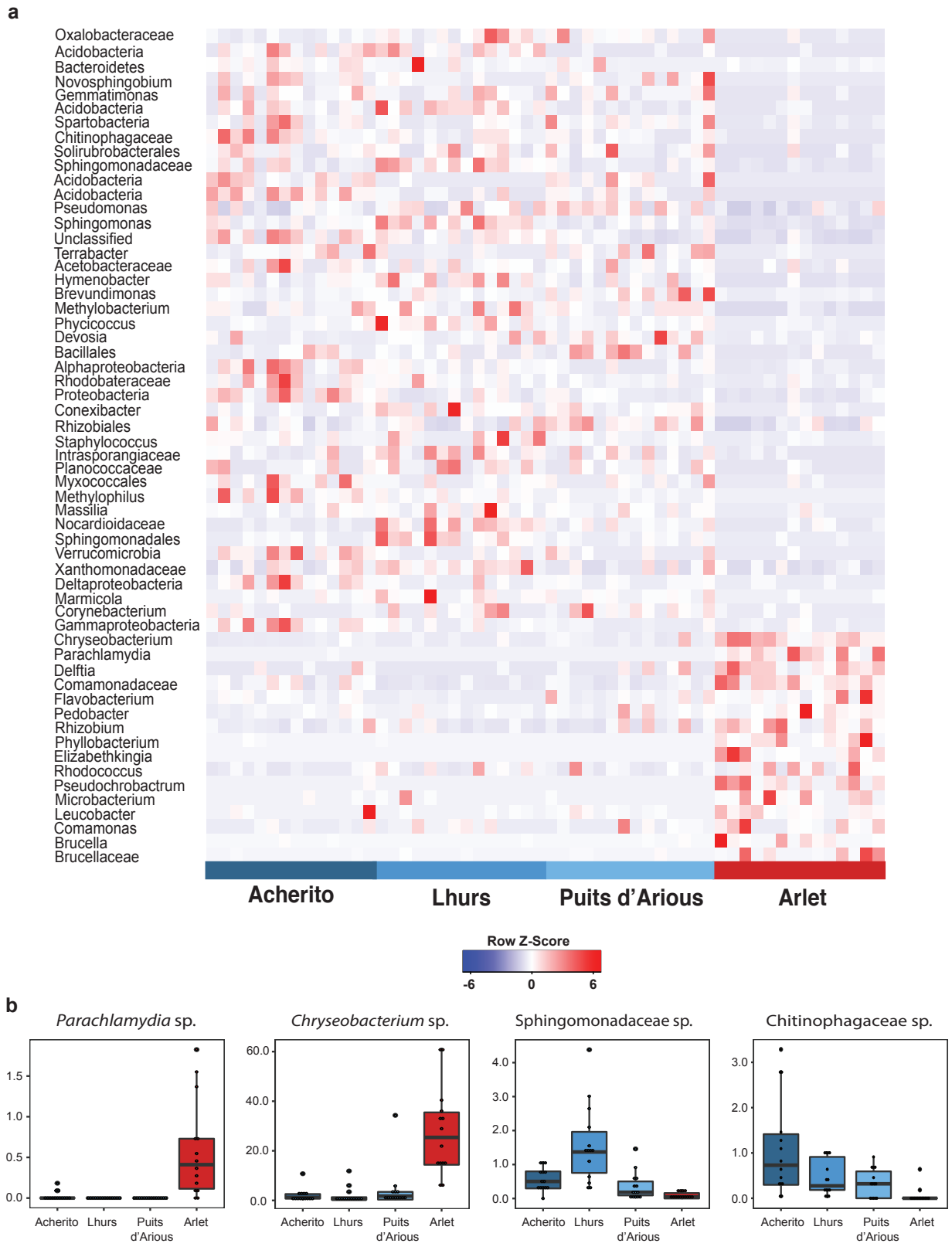


Figure 4.3: (**a**) Heatmap of bacterial indicator taxa based on disease dynamic (**b**) boxplots of key indicator OTUs with relative abundance (%) on Y axis and population on X axis. Sample sizes were: n=14 (Acherito), n=14 (Lhurs), n=14 (Puits d'Arious), n=14 (Arlet).

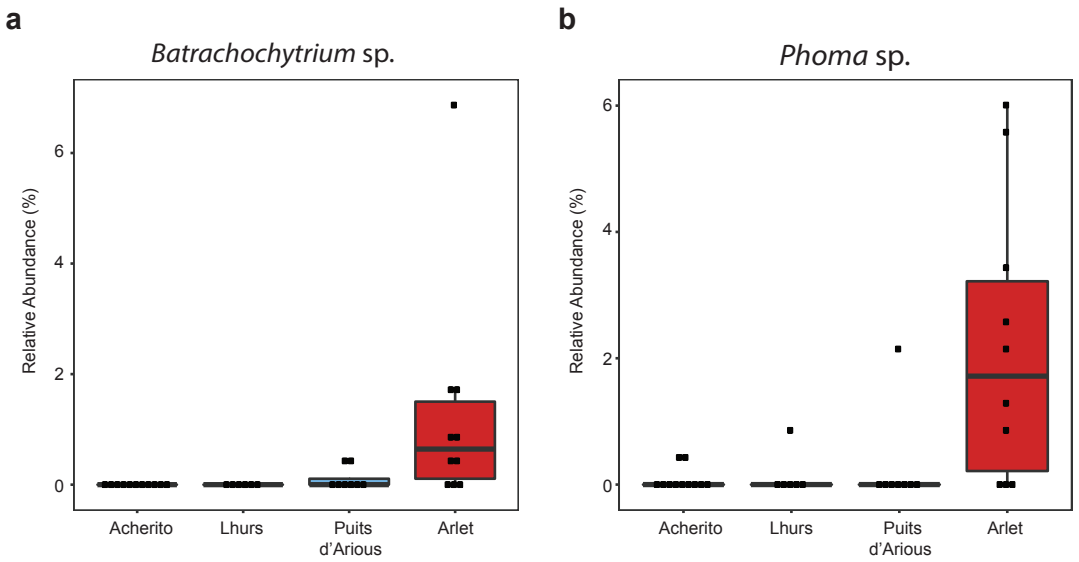


Figure 4.4: Boxplots of of fungal indicator taxa based on disease dynamic (**a**) *Batrachochytrium* sp. and (**b**) *Phoma* sp. Enzootic populations are coloured blue, epizootics are red. Sample sizes were: n=11 (Acherito), n=6 (Lhurs), n=8 (Puits d'Arious), n=10 (Arlet).

4.4.3 Cutaneous metabolites are linked to population, disease state and host microbiota

Processing of the UHPLC-MS data resulted in a peak list and data matrix of 2014 signals for negative ion mode. Both NMDS and PLS-DA analysis produced separation based on population (Fig. 4.5a,b). Results of PERMANOVA demonstrate significant differences in metabolome profile based on population and disease dynamic with population accounting for the greatest amount of variation (population: Pseudo-$F_{(3,52)}$=16.002, R^2=0.48003, p=0.001; disease dynamic: Pseudo-$F_{(1,54)}$=7.828, R^2=0.12661, p=0.001). Results of a mantel test als revealed a correlation between the metabolome and *Bd* infection intensity (r=0.36, p=0.001). The PLS-DA model was assessed using 5-fold cross-validation repeated 10 times. Analysis of the overall error rate and permutation analysis demonstrated that three components were optimal for the population analysis (error rate 0.00179, NMC=0.035714, p=0.001). The PLS-DA model based on population yielded 87 metabolite features with a VIP score >2, all of which were statistically significant at q<0.05. Of the 87 influential metabolites, 52 were putatively annotated

(Appendix 14). A Heatmap was generated to visualise the top metabolites and highlights clear differences in the chemical profile of *A. obstetricans* skin between different populations (Fig. 4.6a,b).

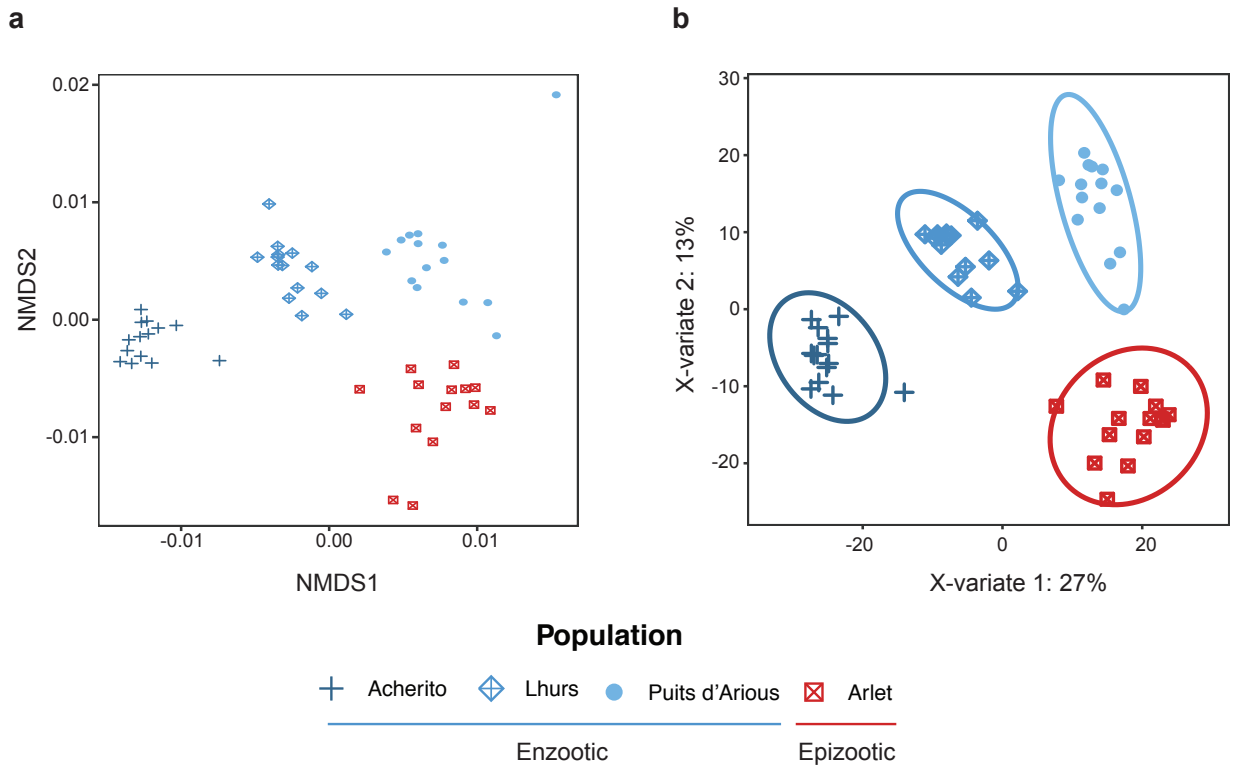


Figure 4.5: Population level differences in metabolome structure as indicated by (**a**) separation of populations in a non-metric multidimensional scaling (NMDS) plot and (**b**) Partial least squares discriminant analysis (PLS-DA) of skin mucosal metabolites. Ellipses indicate 95% confidence intervals. Sample sizes were: n=14 (Acherito), n=14 (Lhurs), n=14 (Puits d'Arious), n=14 (Arlet).

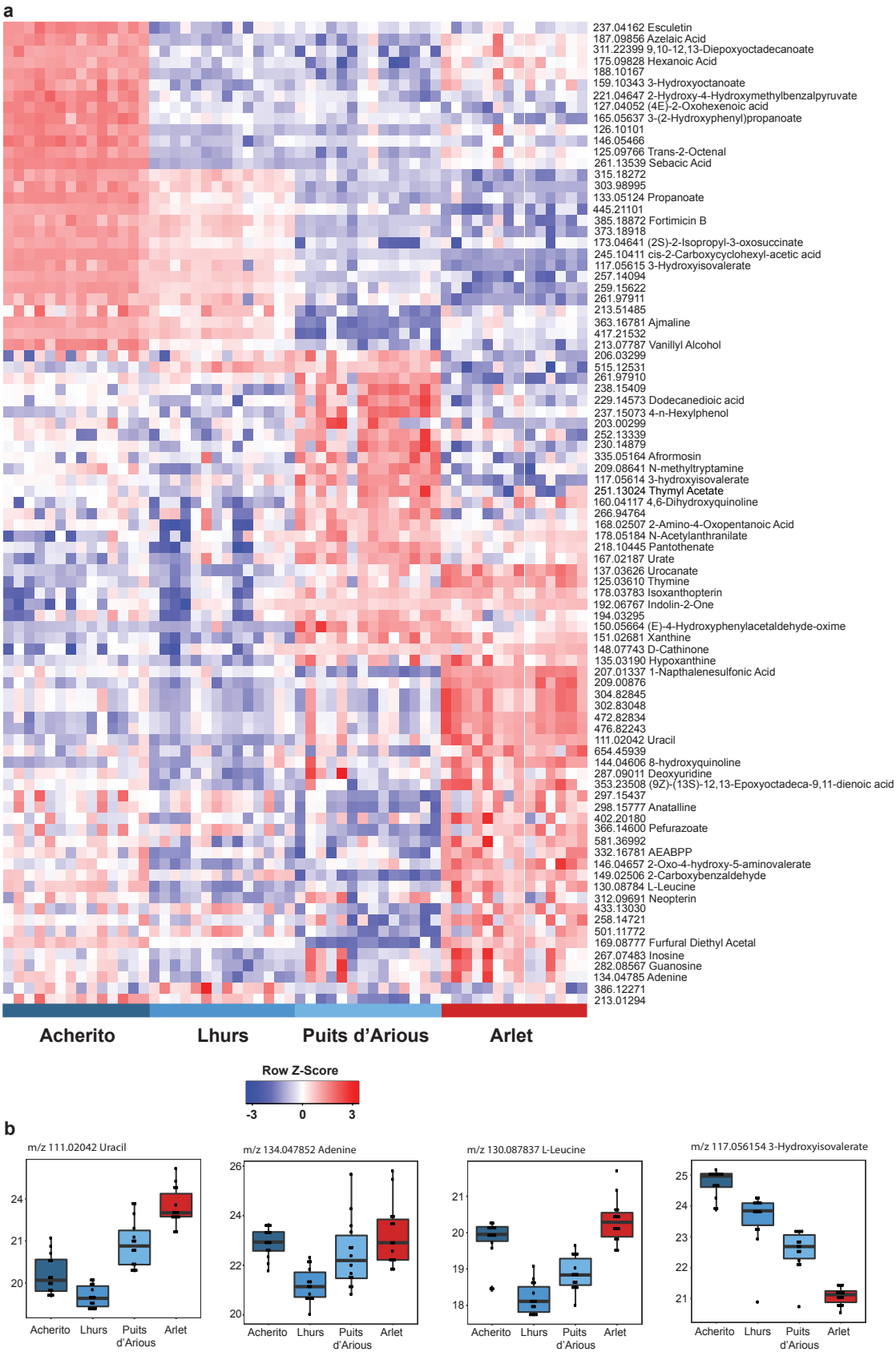


Figure 4.6: (**a**) Heatmap of metabolites driving differences in metabolome of populations based on VIP score > 2 and $q < 0.05$. (**b**) Boxplots of key metabolites. Sample sizes: n=14 (Acherito), n=14 (Lhurs), n=14 (Puits d'Arious), n=14 (Arlet).

4.4.4 Microbiome-metabolome associations

Procrustes analysis of Bray-Curtis dissimilarity between the metabolome and microbiome reveals significant associations between bacterial taxonomy and metabolic profiles across all sampled individuals (m12 square = 0.6359, correlation value = 0.6034, $p = 0.001$, PROTEST). Analysis of the mycobiome and metabolome data set also demonstrated a significant association between fungal taxonomy and the amphibian skin metabolome (m12 square = 0.5189, correlation value = 0.6936, $p = 0.001$, PROTEST).

Analysis of bacterial-metabolite associations identified 275 significant correlations (Spearman rho > 0.6, $q = 0.05$, Appendix 15). Meanwhile no significant fungal-metabolite associations were recovered. Network analysis of bacteria-metabolite correlations identified two major sub-networks representing the enzootic populations (Fig. 4.7a) and the epizootic population (Fig. 4.7b) based on discriminant microbial and metabolite biomarkers (previously identified from indicator analysis and PLS-DA respectively) for disease dynamic being present in each respective sub-network. In the epizootic sub-network, *Parachlamydia* and *Delftia* were the nodes with the highest betweenness centrality - a measure of functional relevance of a node and its ability to hold together other communicating nodes. An unclassified bacterial OTU and two OTUs belonging to the Nocardioidaceae and Sphingomonadaceae respectively were nodes with the greatest betweenness centrality in the enzootic sub-network. The high connectivity of enzootic and epizootic indicator OTUs with specific metabolites in their respective sub-networks suggests that indicator taxa of populations with differing disease dynamics are functionally different and may be keystone taxa in terms of their interactions within their microbial ecosystems. Consequently, such taxa may be especially important in their association with disease outcome.

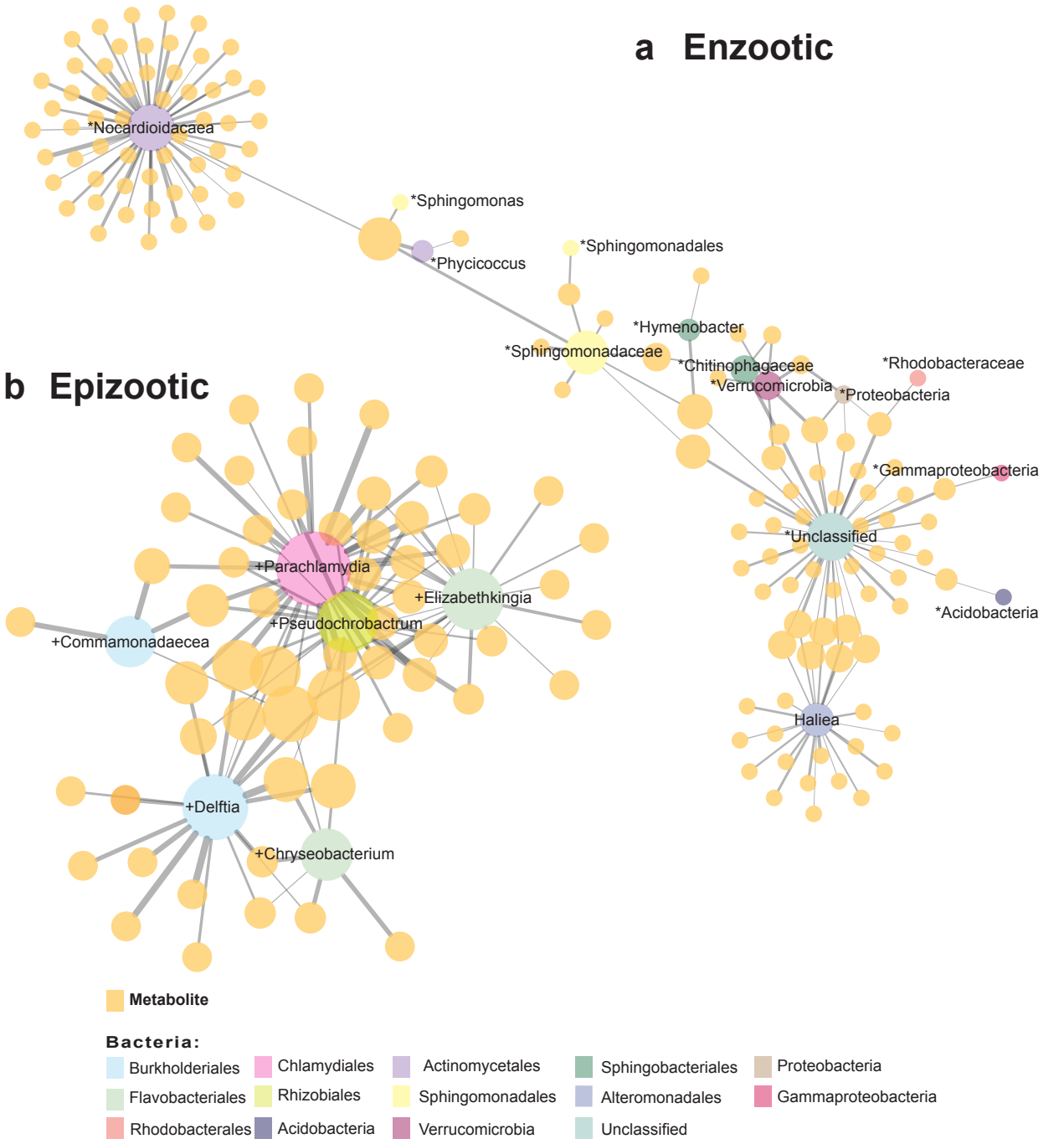


Figure 4.7: Spearman correlations between bacterial OTUs and metabolites. Sub-networks display discriminating taxa for (**a**) enzootic (Acherito, Puits d'Arious, Lhurs) and (**b**) epizootic (Arlet) populations. Edges represent correlation co-efficients with thickness indicating strength of correlation. Node size is proportional to betweenness centrality. Nodes coloured by metabolite (orange) and bacterial family (or phylum where family-level taxonomic resolution is not possible). * and + denote bacteria identified as indicator taxa for enzootic and epizootic populations respectively. Sample sizes were: n=14 (Acherito), n=14 (Lhurs), n=14 (Puits d'Arious), n=14 (Arlet).

4.5 Discussion

The amphibian skin microbiome has been the subject of great interest due to its association with wild *Bd* infection dynamics (Jani and Briggs, 2014; Jani et al., 2017; Rebollar et al., 2016b; Bates et al., 2018). The majority of studies to date have however drawn conclusions from associations between bacterial taxa and disease with few taking into account the impact of other microbial kingdoms (Kueneman et al., 2016b; Kearns et al., 2017), or whether differences in microbiome structure are functionally relevant (Becker et al., 2015; Walke et al., 2015b; Belden et al., 2015). In this study we address these gaps in our knowledge by sampling a broader cross-section of the host skin microbiome to include both bacteria and fungi in addition to functionally characterising the host skin mucosa using a metabolomics approach. We demonstrate that both host population and disease dynamics are significant factors shaping host skin bacterial and fungal communities in addition to the skin mucosal metabolome. We further show significant associations between microbial community composition and the metabolome profile of the amphibian skin mucosa. Overall our findings strongly support the hypothesis that the amphibian skin microbiota plays an important role in shaping the skin mucosal metabolome and consequently impacts the outcome of infection by *Bd*.

Analysis of microbial communities revealed that while bacterial alpha diversity was significantly lower in the epizootic populationn and was negatively correlated with *Bd* infection intensity, there were no differences in fungal alpha diversity based on population or disease dynamics. These findings may suggest that bacterial communities on the skin of animals from the epizootic population are more susceptible to perturbation by *Bd* invasion, or that naturally higher microbial diversity in enzootic populations confers greater invasion resistance as has been demonstrated in laboratory experiments (Piovia-Scott et al., 2017). Both bacterial and fungal beta diversity and composition differed based on population and disease dynamics with greater variation occurring in bacterial communities than in fungal communities. Taken together, the greater disease-associated differences in alpha and beta diversity of bacteria compared to fungi suggest that bacterial communities may be more important in shaping the overall host microbiome response to *Bd* infection and consequently are more intricately linked to disease

outcome.

The findings for bacterial alpha and beta diversity show similarities with patterns identified from the same populations that were sampled in the previous year (Bates et al., 2018). This suggests that bacterial communities of *A. obstetricans* skin exhibit a degree of temporal stability and that population level disease dynamics may be associated with predictable effects on the host microbiome. This hypothesis is supported by our indicator analyses based on population and disease dynamic, for which several bacterial genera were identified as biomarkers both here and in the previous study (Bates et al., 2018). In particular, both studies show a high proportion of indicator taxa associated with enzootic disease dynamics belonging to the Actinomycetales - an order of bacteria that is well characterised for producing antimicrobial compounds (Berdy, 2005) and therefore a strong candidate for providing microbe-mediated protection to a host. Similar patterns in indicator taxa were observed for the epizootic population (Arlet) which, as in the previous study (Bates et al., 2018) was characterised by a high abundance of Flavobacteriales. Interestingly, members of the Flavobacteriales have previously been associated with epizootic *Bd* infection in another wild amphibian host system (Jani and Briggs, 2014) suggesting that this group may commonly be linked with high *Bd* infection loads in the wild. Further, in both the current and prior Pyrenean microbiome study (Bates et al., 2018), *Parachlamydia*, a genus belonging to the widely pathogenic Chlamydiae phylum (Wyrick, 2000) of which certain taxa have been shown to cause epizootic outbreaks when co-occurring with *Bd* (Reed et al., 2000) was identified as an indicator taxa for epizootic disease dynamics. This finding provides compelling evidence that co-infection may be an important factor in *Bd*-linked amphibian decline and development of epizootic disease dynamics. The identification of bacterial indicator taxa in enzootic and epizootic populations that have previously been identified as both inhibitory or synergistic to *Bd* growth underscores that microbial function varies based on characteristics of the wider biotic community (Antwis and Harrison, 2018) and suggests that in many instances single microbial species may lie on a pathogen-mutualist continuum (King et al., 2016). As such, assigning microbial taxa binary characteristics with regard to microbe-derived protection or pathogen enhancement may often be uninformative or even damaging.

Fewer indicator taxa were identified based on population and disease dynamic for fungi than

bacteria. Interestingly, all fungal indicator OTUs identified based on disease dynamic were associated with an increased relative abundance in the epizootic population. The small number of fungal indicator OTUs identified relative to bacteria may be linked to the more minimal differences in fungal community beta diversity compared to bacteria. Alternatively, the few fungal indicator taxa identified may be a product of the lower overall fungal species diversity recovered in our study. Of the two fungal indicator OTUs identified based on disease dynamic, one was classified as a member of the *Batrachochytrium* genus. This findings indicates that differences in fungal beta diversity based on disease dynamics are linked to enrichment of a small number of taxa in the epizootic population (including *Bd*) that coincide with the high burden of chytrid.

Using an untargeted metabolomics approach, we show that the amphibian skin mucosal metabolome differed significantly based on population and disease dynamic, which accounted for 48% and 13% of variation respectively. Putative annotation of metabolites identified as important drivers underpinning differences in metabolome composition yielded a diverse range of metabolites of both host and microbial origin including lipids, alkaloids, amino acids, nucleic acids and heterocyclic organic compounds. The significant association between bacterial and fungal community composition and the metabolome demonstrates that taxonomic differences in microbial communities are not associated with functional redundancy, but rather confer complex functional differences. Interestingly, while several significant associations were found between individual bacterial taxa and metabolites, this was not the case for fungi. The lack of significant associations between individual fungal taxa and metabolites may suggest that while differences in fungal communities between host populations correlate with population differences in metabolome structure, within a population fungal communities collectively may be producing broadly similar metabolite classes that do not co-vary to a great enough extent with abundance of individual fungal taxa to yield significant associations. Network analysis demonstrated that bacterial-metabolite associations formed two major sub-networks. Inspection of the bacterial classifications revealed that each sub-network was highly representative of different disease dynamics with bacterial biomarkers of enzootic and epizootic disease dynamics being correctly co-assigned to each sub-network without *a priori* selection. Our network analysis also demon-

strates that multiple bacterial taxa are correlated with a individual metabolites. This could be taken to resemble some level of functional redundancy within a population with multiple bacterial taxa utilising or metabolising the same chemical feature, or alternatively could be an indication that production of specific metabolites is dependent on the interaction of metabolic pathways from multiple bacterial taxa. This phenomenon has been demonstrated for the production of emergent anti-*Bd* metabolites when bacterial taxa are in co-culture but not in monoculture (Loudon et al., 2014a).

While each population had a characteristic metabolome profile, key differences were evident in the epizootic population (Arlet) compared to the three enzootic populations. In particular, Arlet exhibited a higher abundance of discriminatory metabolites associated with nucleotide metabolism compared to enzootic populations. This finding is consistent with those of a prior study that demonstrated a link between *Bd* infection and nucleotide accumulation on the skin of another amphibian species (Grogan et al., 2018c). In particular, a key biomarker for disease may be adenine (m/z 134.04785), which was significantly elevated in the epizootic population and also linked to *Bd*-induced mortality in a prior study (Grogan et al., 2018c). The accumulation of nucleotides in the epizootic population may be due to the increased skin sloughing of heavily *Bd* infected animals, which results in the release of cellular debris including nucleotides onto the skin surface. An increase in nucleotide bioavailability may also facilitate enhanced microbial growth. For instance, while many microbes synthesise nucleotides *de-novo*, the utilisation of nucleotide salvage pathways to facilitate growth is also common and often more energy efficient (Chitty and Fraser, 2017). In addition, salvage of nucleotides in some cases may be essential for production of virulence factors and host adhesion, as is the case for the pathogen *Candida albicans* (Vylkova and Lorenz, 2017). The *Bd* genome contains purine salvage pathway genes such as hypoxine phosphoribosyltransferase (UniProt Accession: A0A177WVH8) that transfers a 5-phosphoribosyl group to a purine creating a nucleotide. It is therefore possible that the acquisition of exogenous nucleotides is a component of *Bd* colonisation and proliferation that may underlie enhanced invasion success in the epizootic population. In addition to *Bd*, other microbes such as bacteria may also be associated with the accumulation of nucleotides. For example, increased metabolism of purines and pyrimidines (nucleotide precursors) was found

in mouse epithelia infected with *Mycobacterium tuberculosis* (Shin et al., 2011). Interestingly, *Parachlamydia* which was identified as an epizootic indicator taxa belongs to the Chlamydiae phylum of which many constituents are unable to synthesise nucleotides *de-novo* (Saka and Valdiva, 2010). This may indicate that higher abundance of skin nucleotides in the epizootic population may also facilitate the proliferation of bacterial pathogens such as *Parachlamydia* that in turn cause host pathology and contribute to increased mortality. Network analysis also identified positive associations between epizootic indicator taxa and several nucleotides (Appendix 15) providing further evidence that patterns in metabolite and bacterial biomarkers may be functionally linked.

A key nucleotide biomarker that had significantly higher relative abundance in Arlet compared to all enzootic populations was uracil (m/z 207.01337). In addition to being an important requirement in microbial nutrition, uracil can be secreted by some bacteria and has been shown to induce homeostatic inflammation of gut mucosal epithelia required for pathogen clearance in mice (Lee et al., 2013). In some pathogens however, uracil is secreted in abundance causing chronic inflammation with negative consequences to host health (Lee et al., 2013). Further evidence for the link between uracil and chronic inflammation comes from studies that have identified it as a major biomarker for systemic inflammatory diseases such as rheumatoid arthritis (Weljie et al., 2007). A possible explanation for the existence of epizootic dynamics in Arlet but not the other populations may therefore be that *Bd*-bacteria co-infection results in chronic inflammation mediated through secretion of microbial metabolites such as uracil. The resulting weakened host immune defences may subsequently create a positive feedback loop enabling *Bd* and other microbial opportunists to proliferate to a high enough abundance to cause host mortality. Network analysis identified significant bacterial associations between uracil and three epizootic bacterial indicator taxa (*Pseudochrobactrum*, *Chryseobacterium* and *Delftia*). Interestingly, both *Chryseobacterium* and *Delftia* have been associated with infection or tissue damage in amphibians (Green et al., 1999; Nickerson et al., 2011) suggesting that these taxa may be linked to perturbations in host homeostasis. In addition, *Chryseobacterium* strains have been associated with synergistic growth of *Bd* (Antwis and Harrison, 2018), demonstrating that the relationship between these two microbes may have important functional effects

on disease outcome. Ultimately, identifying the link between candidate microbial biomarkers, nucleotide accumulation and *Bd* infection outcome may yield vital mechanistic insight to host susceptibility and possible co-infection dynamics.

Amino acids and associated metabolite biomarkers were also found to differ across populations and showed similarities with a prior study of the skin metabolome of alpine tree frogs (*Litoria verreauxii alpine*) (Grogan et al., 2018c). Specifically, we identified leucine as a biomarker for epizootic disease dynamics, which in a previous study was demonstrated to be positively correlated with animals that experienced *Bd* induced mortality (Grogan et al., 2018c). Branched chain amino acids (BCAAs) such as leucine require breakdown and elimination by terminal oxidation in the tricarobxylic acid cycle (TCA) cycle (Owen et al., 2002), however in cases of metabolic dysregulation this may not take place leading to their accumulation. The accumulation of BCAAs such as leucine have been associated with toxic host effects in other vertebrates (Manoli and Venditti, 2016) and are associated with various pathologies in mammals (Villani et al., 2017). Consequently, a high abundance of BCAAs may be an important hallmark of poorer host health in the epizootic population. In contrast, the enzootic populations but not Arlet presented a high relative abundance of 3-hydroxyisovalerate, a metabolic product of leucine degradation. Taken together, these findings may indicate a state of metabolic disruption on the skin of heavily *Bd* infected *A. obstetricans*. Microbial associations with leucine metabolism identified three enzootic indicator OTUs correlated with 3-hydroxyisovalerate. This may suggest that microbes in enzootic populations are metabolising and reducing build-up of toxic BCAAs with a subsequent reduction in the negative impacts to host health that may be occurring in the epizootic population. In addition to possible differences in leucine metabolism, we demonstrate population-level variation in pantothenate (also known as vitamin B5), which in a previous study exhibited the greatest difference in relative concentration between animals from different source populations (Grogan et al., 2018c). Pantothenate is a precursor of coenzyme-A (CoA), which is involved in fatty acid metabolism and the TCA cycle. While pantothenate is known to be important for the growth of pathogenic bacteria and fungi (Spry et al., 2008), the population level differences in the relative abundance of this metabolite did to not map to disease dynamics.

Alkaloids were widely represented in our analysis of differentially abundant metabolites. Two alkaloids with clear associations with different *Bd* disease states were putatively annotated as ajmaline (*m/z* 363.16781) and N-methyltryptamine (*m/z* 209.0864135), both of which showed increased relative abundance in the enzootic populations compared to Arlet. Ajmaline and N-methyltryptamine have previously been isolated from plants (Siddiqui and Siddiqui, 1931; Servillo et al., 2015) and it is likely that as for many alkaloids of amphibians (Daly et al., 1994), they have been sequestered in *A. obstetricans* skin via ingestion of herbivorous arthropod prey rather than synthesised *de-novo*. While alkaloids can be subject to microbial modifications (Rathbone and Bruce, 2002), a lack of association with bacterial taxa suggests that alkaloids are sequestered from prey items and secreted onto the skin with little or no change to molecular structure. The positive association between alkaloid biomarkers and enzootic populations may be an effect of habitat differences between populations (Clarke et al., 2006; Daly et al., 2008). Specifically differences in botanical species that are consumed by arthropods between sites may alter the bioavailability of certain beneficial compounds to *A. obstetricans*. This in turn may suggest that dietary differences of *A. obstetricans* populations and possible preference for prey items rich in alkaloids may influence host disease resistance given the anti-microbial properties of many alkaloids (Mina et al., 2015).

Deciphering the functional role of host-microbe interactions in the framework of wild disease dynamics is of fundamental importance to a range of disciplines including microbial ecology, epidemiology and conservation. Here we demonstrate that the bacterial and fungal communities of amphibian skin differ based on both population and disease state. Further, we reveal that differences in taxonomic composition of the microbiome are closely linked to the skin mucosal metabolome providing evidence of a strong microbiome structure-function relationship. Whilst this study yields a more detailed insight into our understanding of the role of host-associated microbes in wild amphibian chytridiomycosis outbreak dynamics, further work is necessary to elucidate specific mechanisms that impact disease outcome. In particular, determining how microbial community structure impacts metabolite production through antagonistic and synergistic mechanisms will aid in our understanding of microbe-microbe interactions and community function. Future studies should also seek to conclusively identify host versus microbe-derived

metabolites and confirm their functional importance in disease outcome using *in-vivo* experimental manipulation.

4.6 Acknowledgements

I thank Brendan Bates, Findley Mostyn, Nick Grassly and Maryam Grassly for field assistance. I also thank Dirk Schmeller and Adeline Loyau for help organising dry ice in the field. I thank Jaime Bosch for assistance with permits. I thank the community of Lescun and Parc National de Pyrenees for continued support.

Chapter 5

General Discussion

Emerging fungal pathogens represent a constant threat to global biodiversity, food security, health and the economy (Fisher et al., 2012). The emergence of pathogens that have been exacerbated by anthropogenic activities such as *Batrachochytrium dendrobatidis* (*Bd*) and *Batrachochytrium salamandrivorans* (*Bsal*) has left an irreparable scar on global biodiversity (Fisher et al., 2012; O'Hanlon et al., 2018). Determining the drivers underpinning the proliferation of such pathogens, both within- and among- species, represents a vital component to our understanding of outbreak dynamics and future disease mitigation.

In recent years, research focussing on the microbial ecology of multicellular organisms has drastically changed our outlook on health and disease (Gilbert et al., 2018). There is however much that remains to be discovered in terms of our understanding of how host-associated microbes are linked to spatial epidemiological trends, host disease susceptibility and the biotic and abiotic factors shaping the host microbiome. Collectively, these themes have important implications in our understanding of the ecology and evolution of host-pathogen interactions and how we approach disease mitigation. In this thesis I aimed to answer four primary questions surrounding what drives differences in host response to chytridiomycosis infection, with a particular focus on the importance of host microbial ecology.

1. *How important are pathogen genetics and the host skin microbiome in shaping the outcome of infection in a wild chytridiomycosis outbreak? (Chapter Two)*

Chytridiomycosis outbreak dynamics may be linked to a range of factors including climate (Clare et al., 2016), host biology (Savage and Zamudio, 2011), pathogen genetics (Farrer et al., 2011; Piovia-Scott et al., 2015), and the host microbiota (Jani and Briggs, 2014; Jani et al., 2017). In this chapter, I examined the relative importance of *Bd* genetics and the host bacterial microbiome in shaping epizootic and enzootic disease dynamics across midwife toad (*Alytes obstetricans*) metamorph populations in the French and Spanish Pyrenees.

I found that while whole genome sequencing of *Bd* isolates from enzootic and epizootic populations revealed no associations between pathogen genetics and epidemiological trends over space or time, there were clear associations between microbiome diversity, composition and predicted function. In particular, host bacterial alpha diversity was reduced in epizootic populations compared to enzootic populations and beta diversity mapped to both host population and disease dynamics. Patterns of bacterial beta diversity were mirrored in the beta diversity of predicted bacterial gene function, indicating that differences in host bacterial composition between populations are linked to functional differences that may be important in host responses to infection. Certain bacterial taxa were also associated with disease dynamics. Specifically, I found evidence of bacteria-*Bd* co-infection occurring in epizootic but not enzootic populations. Enzootic populations also exhibited a higher abundance of putatively protective bacteria such as taxa belonging to the Actinomycetales. These findings provide a degree of support for enzootic disease dynamics being driven by enhanced microbe-mediated protection, while epizootic populations may be associated with microbiome perturbation and secondary infection that in turn may contribute to high host mortality.

2. *Does the amphibian skin microbiome differ across life-stages and to what extent does host environment shape dermal bacterial communities? (Chapter Two)*

Understanding the factors that shape the microbiome of vertebrates is an important area of research in microbial ecology. By examining the microbiota present in the environment and on the host skin, we can better understand the extent to which the environment influences host microbial community structure relative to factors such as pathogen infection. Determining

differences in microbiome structure across amphibian life stages also represents a key area of microbial ecology that has seldom been addressed (Kueneman et al., 2014, 2016b; Knutie et al., 2017; Longo et al., 2015). In particular, metamorphosis in amphibians is characterised by significant changes in host physiology and a shift from an aquatic to predominantly terrestrial lifestyle, both of which have potential to alter host-microbe interactions and subsequent disease susceptibility.

In Chapter two, I demonstrated that the amphibian microbiome differs significantly to that of the environment with few shared taxa. Environmental bacteria also found on amphibian skin were of low relative abundance in the environment pointing to possible evidence of selection for rare environmental bacterial taxa rather than passive acquisition of environmental microbes (Walke et al., 2014; Loudon et al., 2016). Restructuring of the skin microbiome at metamorphosis was also evident with marked differences in bacterial community structure and composition in larvae and metamorphs. Together, these findings indicate that the amphibian skin is a specialised niche for bacteria that differs greatly to that of the environment. Further, host physiological changes coinciding with metamorphosis also have a substantial impact in structuring the microbiome.

3. *Does captivity and exposure to an emerging chytrid pathogen impact the skin microbiome of different amphibian host species and how does this relate to disease susceptibility? (Chapter Three)*

A growing area of interest in chytrid mitigation comes from probiotic therapies and host microbiome augmentation that have been suggested as prophylactic treatments against chytridiomycosis (Bletz et al., 2013). These treatments use the pathogen inhibiting properties of some microbes or microbial communities to prevent or limit infection to a level that does not cause significant host pathology. Such interventions are usually carried out *ex-situ*, however little is known regarding what effects captivity may have on the amphibian microbiome (Becker et al., 2014; Loudon et al., 2014b; Kueneman et al., 2016a; Sabino-Pinto et al., 2016). In addition, quantifying the impact of captivity on amphibian microbial communities and the extent to which captive conditions cause a departure from the wild microbiome is valuable in assessing

the ecological relevance of infection experiments, most of which occur in animal laboratories.

In 2013, amphibian biodiversity once again came under attack when a novel amphibian-infecting chytrid fungus called *Batrachochytrium salamandrivorans* (*Bsal*) was discovered (Martel et al., 2013). As for *Bd*, *Bsal* has been attributed to mass die offs of amphibians and as such represents a global threat to amphibian populations (Martel et al., 2014; Yap et al., 2015). Despite the growing literature related to *Bd* infection and its interaction with the host microbiome, little is known for *Bsal*.

In this chapter I investigated the effect of captivity on the skin bacterial and fungal communities of two newt species, the great crested newt (*Triturus cristatus*) and the smooth newt (*Lissotriton vulgaris*). I demonstrated that the microbiome underwent significant changes when animals of both species were brought into captivity with reductions in bacterial and fungal alpha diversity and changes in beta diversity. These findings suggest that captive conditions alter the host microbiome in such a way that it is likely to be no longer reflective of the wild. This suggests that caution should be exercised when drawing conclusions about ecological patterns from laboratory challenge experiments. This further raises questions on the effectiveness of testing probiotics in captivity if the host microbiome will subsequently alter when animals are reintroduced into the wild, potentially altering microbe-microbe interactions (Antwis and Harrison, 2018) and the chytrid inhibiting properties of the desired probiotic.

By performing a subsequent *in-vivo Bsal* exposure experiment, I further determined that both host species were susceptible to *Bsal* infection, though there were no significant species differences in response to infection. Importantly, both newt species used in this study are native to the UK where *Bsal* represents a significant predemic threat (Cunningham et al., 2015). Therefore defining the susceptibility of these host species and their response to infection is paramount in predicting the severity of a possible UK *Bsal* outbreak. I also showed that *Bsal* induced mortality was linked to microbiome perturbation and proliferation of a small number of bacterial taxa, in particular a bacterium belonging to the *Stenotrophomonas* genus. Animals that were infected with *Bsal* but survived infection did not demonstrate a pronounced departure in bacterial community structure relative to uninfected conspecifics, suggesting that microbiome

stability may be linked to tolerance to infection.

Taken together, these findings demonstrate that changes in host environment and pathogen exposure can modulate host skin microbial communities with potentially negative effects to host health. These findings have important implications in terms of the management of captive species and in our understanding of *Bsal* infection and approach to mitigating it.

4. *Are differences in host skin microbiome across wild amphibian populations and chytridiomycosis disease states functionally important? (Chapter Four)*

The majority of studies that have shown associations between the amphibian microbome and chytridiomycosis infection outcome have focussed exclusively on bacterial communities and ignored whether taxonomic differences are functionally redundant or important. In this chapter, I built on the discoveries of Chapter two by extending the characterisation of the *A. obstetricans* metamorph skin microbiome to include both bacteria and fungi. I further investigated whether differences in microbiome structure in enzootic and epizootic populations were related to function by sampling the skin mucosal metabolome and measuring microbe-metabolite associations.

My analysis of the composition of fungal and bacterial communities on the skin of *A. obstetricans* in the Pyrenees shows that the community structure of both microbial kingdoms is shaped by *Bd* disease dynamics and host population. These findings suggest that both bacterial and fungal communities on frog skin respond in similar ways to common selective pressures, for example host antimicrobial peptides or infection. While bacterial alpha diversity was significantly different between populations with the epizootic population (Arlet) exhibiting a reduction in diversity compared to enzootic populations, there were no significant differences in the alpha diversity of fungal communities. The significant differences in bacterial alpha between enzootic and epizootic populations may therefore indicate that bacterial diversity is more closely associated to infection outcome than fungal diversity. The amphibian skin metabolome, which represents a holistic measure of skin functional capacity including both host and microbial derived metabolites also differed between populations and disease states. Putative biomarkers associated with enzootic and epizootic populations were also identified. Both fungal and bac-

terial community structure correlated with metabolome structure indicating that differences in host skin microbial ecology of enzootic and epizootic populations were associated with functional differences that may be of importance in epidemiological outcomes. I further identified a subset of bacteria and metabolites that were strongly positively correlated. Interestingly, network analysis of bacteria-metabolite correlations revealed two clear sub-networks that were composed almost exclusively of either enzootic or epizootic bacterial biomarkers. This finding suggests that microbial indicator taxa of enzootic and epizootic populations are associated with different functional profiles that may be important in modulating response to *Bd* infection. Overall my results provide evidence that host microbial taxa across multiple kingdoms are functionally important and may shape chytridiomycosis outbreak dynamics in the wild. Bacteria and metabolites that are highly discriminatory of enzootic and epizootic populations may not only aid in our understanding of the mechanistic basis of differential host responses to infection, but may also be valuable as diagnostic biomarkers of disease outcome.

5.1 Future Directions

In this thesis, I have unravelled some of the key factors impacting amphibian chytridiomycosis disease outcome. However, questions remain that are pertinent in our understanding of how the host, pathogen, microbiome and environment interact in nature to shape infection.

While the findings from my first data chapter revealed no association between *Bd* genetics and the epidemiology of the Pyrenean system, it is unwise to rule out the potential importance of the pathogen in disease outcome. In particular, there remains the possibility of within-population heterogeneity in *Bd* genotype virulence. This subsequently begs the question as to whether selection of *Bd* genotypes of differing virulence is an ecologically important phenomenon and how the host, the host microbiota and the environment mediate this process. Pertinently, selection of *Bd* genotypes with reduced virulence could explain the persistence of *Bd* in enzootic *A. obstetricans* populations in the Pyrenees. One possible mechanism as to how reduced *Bd* virulence could occur is through co-evolution with host defensive microbes (Ford et al., 2016).

For example, studies have shown that when a microbe with host-protective properties (*Enterococcus faecalis*) was co-evolved with a pathogen (*Staphylococcus aureus*), the virulence of the pathogen decreased over time as a result of down-regulation of iron-scavenging siderophores (Ford et al., 2016). Although not examined as of yet, the differences in microbiome profile and microbial indicator taxa in enzootic and epizootic populations may be indicative of selection for microbes with host defensive properties in enzootic populations. Additional research utilising microbe-*Bd* inhibition assays, as well as *in-vivo* experimental manipulations of the host microbiome are required to investigate this question. Alternatively, within- and between -population heterogeneity in virulence could arise due to individual hosts posing different selective environments on pathogens that would not necessarily be evident through pathogen genetic analysis (Schmid-Hempel and Koella, 1994; Pfennig, 2001). Some evidence in support of this hypothesis comes from prior studies that have detected differences in growth rates of Pyrenean *Bd* isolates (Farrer et al., 2011). Therefore, in addition to more targeted host-pathogen studies, the Pyrenean system would also benefit from phenotyping of *Bd* isolates and identifying if phenotypic variants differ in their virulence *in-vivo*.

Investigating possible differences in *A. obstetricans* biology in enzootic and epizootic populations, while out of the scope of this thesis is an area of research that requires addressing in the future. In particular, examining host immunity, which is also known to interact with the microbiome in other host systems (Honda and Littman, 2012), may yield an integrative mechanism into the differential disease outcomes of Pyrenean *A. obstetricans* populations. Further, while selection for genetically resistant host populations is unlikely given the recent introduction of *Bd* and the long generation time of the host, investigating the genetics of *A. obstetricans* populations pre- and post-*Bd* emergence should be addressed (Savage and Zamudio, 2011), at the very least to rule out evolution of host tolerance to *Bd*. *In-vivo* experiments investigating how host physiology and the microbiome change through development and what impact this has on disease susceptibility may also be insightful (Knutie et al., 2017).

The importance of the abiotic environment and its interaction with the host, the host microbiota and pathogens also represents an area that has thus far been understudied. In Chapter Three of this thesis, I demonstrated that changes in the host environment had significant impacts on the

microbiome of two newt species. In addition, a previous study demonstrated that seasonality was a strong predictor of the severity of chytridiomycosis in the Pyrenees (Clare et al., 2016). Future studies should therefore seek to investigate how the abiotic environment impacts disease outcome whilst concurrently measuring the effects on the biology of the host, microbiome and the pathogen. Collectively, the findings of such studies could be highly informative in developing models that predict regions that are of high risk of disease outbreaks. This would not only inform our understanding of systems such as the Pyrenees, but could also be useful in predicting at-risk predemic areas for outbreaks of more recently emerging pathogens such as *Bsal*.

A key conclusion drawn from this thesis was that severe chytridiomycosis was associated with the proliferation of other potential pathogens. For example, in Chapters Two and Four, members of the Chlamydiae had increased relative abundance in *Bd* epizootic compared to enzootic populations. Moreover, in Chapter Three both host species infected with *Bsal* that succumbed to mortality had an increased abundance of *Stenotrophomonas*, which in other species has been noted as a commensal turned opportunistic pathogen (Adegoke et al., 2017). Table 5.1 (overleaf) lists microbial taxa that were identified for exhibiting strong associations with *Bd* or *Bsal* in this thesis and may therefore represent key taxa on which to focus in future studies. Ultimately, future studies should step away from reviewing chytridiomycosis outcome from the standpoint of a single pathogen infection, to a more holistic view of host microbial ecology taking into account both opportunistic pathogens, defensive mutualists and their interactions.

Given the findings from this thesis, in particular the associations between the host microbiome and disease outcome, there is a wealth of questions that should be addressed. In general terms, future studies should move beyond patterns to mechanisms. In chapter four, I demonstrated correlations between the skin microbiome and metabolome of midwife toads, indicating that the host microbiota is functionally important and may mediate the host response to infection. The methods used in this chapter however did not discriminate between host- and microbe-derived metabolites and therefore limit the mechanistic conclusions that can be drawn. Future studies should thus utilise targeted metabolomics in parallel with genomics and transcriptomics to more conclusively identify disease biomarkers or pathways and their biological origin. Such

studies should be run in combination with *in-vitro* experiments of microbes and pathogenic chytrids to identify and isolate metabolites that are relevant to disease outcome and unambiguously determine their microbial origin. Moreover, since my findings show associations between multiple microbes and single metabolite features, such studies would benefit from the use of microbial consortia rather than investigating bipartite microbe-pathogen interactions. Ultimately, disentangling the interactions between the host, its microbiota and the environment will not only advance our understanding of disease ecology, but may provide solutions to conserving biodiversity and controlling one of the worst infectious diseases the planet has seen.

Microbial taxa	**Association with *Bd* or *Bsal* (thesis chapter(s))**	**Possible interaction(s)**	**Supporting literature**
Lysobacter	Indicator taxa for enzootic population (Lhurs) (2).	*Bd* inhibition through production of antifungal compounds (2,4-diacetylphloroglucinol).	(Brucker et al., 2008b)
Chlamydiae	Indicator taxa for epizootic disease dynamics. Potentially functionally important based on associations with metabolite disease biomarkers (2,4).	Co-infection - prior studies show epizootic dynamics in amphibians co-infected with *Bd* and members of the Chlamydiae.	(Reed et al., 2000)
Chryseobacterium	Epizootic indicator taxa. Positive correlation with high uracil abundance known to cause inflammation of mucosal epithelia (2,4).	Synergistic growth with *Bd*.	(Antwis and Harrison, 2018)
Actinomycetales	Indicator taxa for enzootic disease dynamics (2,4).	Production of antifungal compounds, *Bd* inhibition.	(Woodhams et al., 2015; Jani and Briggs, 2014; Berdy, 2005)
Flavobacterials	Indicator taxa for epizootic disease dynamics (2,4).	Synergistic growth with *Bd*. Associated with epizootic dynamics in other *Bd* systems.	(Jani and Briggs, 2014)
Stenotrophomonas	Co-occurence with *Bsal* (3).	Not clear. Can inhibit *Bsal in-vitro* suggesting antagonistic relationship but positive correlation with *Bsal* abundance *in-vivo* suggests synergy.	(Muletz-Wolz et al., 2017; Bletz et al., 2018)

Table 5.1: Key microbial taxa associated with *Bd* or *Bsal* identified in this thesis.

Bibliography

Abramyan, J. and Stajich, J. (2012). Species-specific chitin-binding module 18 expansion in the amphibian pathogen *Batrachochytrium dendrobatidis*. *mBio*, 3:e00150–12.

Adegoke, A., Stenstrom, T., and Okoh, A. I. (2017). *Stenotrophomonas maltophila* as an emerging ubiquitous pathogen: looking beyond contemporary antibiotic therapy. *Frontiers in Microbiology*, 8:2276.

Alexander, K. and Appel, M. (1994). African wild dogs (*Lycaon rictus*) endangered by a canine distemper epizootic among domestic dogs near the masai mara national reserve. *Journal of Wildlife Diseases*, 30:481–485.

Anderson, M. J. (2001). A new method for non-parametric multivariate analysis of variance. *Austral Ecology*, 26:32–46.

Antwis, R., Haworth, R., Engelmoer, D., Ogilvy, V., Fidgett, A., and Preziosi, R. (2014). *Ex situ* diet inluences the bacterial community associated with the skin of red-eyed tree frogs (*Agalychnis callidryas*). *PLoS ONE*, 9:e85563.

Antwis, R. E. and Harrison, X. A. (2018). Probiotic consortia are not uniformly effective against different amphibian chytrid pathogen isolates. *Molecular Ecology*, 27:577–589.

Antwis, R. E., Preziosi, R. F., Harrison, X. A., and Garner, T. W. (2015). Amphibian symbiotic bacteria do not show a universal ability to inhibit growth of the global panzootic lineage of *Batrachochytrium dendrobatidis*. *Applied and Environmental Microbiology*, 81:3706–11.

Bai, C., Liu, X., Fisher, M., and Garner, T. (2012). Global and endemic asian lineages of

the emerging pathogenic fungus *Batrachochytrium dendrobatidis* widely infect amphibians in china. *Diversity and Distributions*, 18:307–318.

Barr, D. (1980). An outline for the reclassification of the chytridiales, and for a new order, the spizellomycetales. *Canadian Journal of Botany*, 58:2380–2394.

Bataille, A., Cashins, S., Grogan, L., Skerrat, L., Hunter, D., McFadden, M., Scheel, B., Brannely, L., Macris, A., Harlow, P., Bell, S., Berger, L., and Waldman, B. (2015). Susceptibility of amphibians to chytridiomycosis is associated with mhc class ii conformation. *Proceedings of the Royal Society Biological Sciences*, 282:20143127.

Bataille, A., Fong, J., Cha, M., Wogan, G., Baek, H., Lee, H., Min, M., and Waldman, B. (2013). Genetic evidence for a high diversity and wide distribution of endemic strains of the pathogenic chytrid fungus *Batrachochytrium dendrobatidis* in wild asian amphibians. *Molecular Ecology*, 16:4196–4309.

Bataille, A., Lee-Cruz, L., Tripathi, B., Kim, H., and Waldman, B. (2016). Microbiome variation across amphibian skin regions: implications for chytridiomycosis mitigation efforts. *Microbial Ecology*, 71:221–232.

Bates, D., Machler, M., Bolker, B. M., and Walker, S. C. (2015). Fitting linear mixed-effects models using lme4. *Journal of Statistical Software*, 67:1–48.

Bates, K. A., Clare, F. C., O'Hanlon, S., Bosch, J., Brookes, L., Hopkins, K., McLaughlin, E. J., Daniel, O., Garner, T. W. J., Fisher, M. C., and Harrison, X. A. (2018). Amphibian chytridiomycosis outbreak dynamics are linked with host skin bacterial community structure. *Nature Communications*, 9:693.

Becker, M. H., Richards-Zawacki, C. L., Gratwicke, B., and Belden, L. K. (2014). The effect of captivity on the cutaneous bacterial community of the critically endangered panamanian golden frog (*Atelopus zeteki*). *Biological Conservation*, 176:199–206.

Becker, M. H., Walke, J. B., Cikanek, S., Savage, A. E., Mattheus, N., Santiago, C. N., Minbiole, K. P., Harris, R. N., Belden, L. K., and Gratwicke, B. (2015). Composition of symbiotic bac-

teria predicts survival in panamanian golden frogs infected with a lethal fungus. *Proceedings of the Royal Society Biological Sciences*, 282:20142881.

Belden, L. K., Hughey, M. C., Rebollar, E. A., Umile, T. P., Loftus, S. C., Burzynski, E. A., Minbiole, K. P., House, L. L., Jensen, R. V., Becker, M. H., Walke, J. B., Medina, D., Ibanez, R., and Harris, R. N. (2015). Panamanian frog species host unique skin bacterial communities. *Frontiers in Microbiology*, 6:1171.

Benjamini, Y. and Hochberg, Y. (1995). Controlling the false discovery rate: A practical and powerful approach to multiple testing. *Journal of the Royal Statistical Society. Series B*, 57:289–300.

Berdy, J. (2005). Bioactive microbial metabolites - a personal view. *Journal of Antibiotics*, 58:1–26.

Berger, L., Hyatt, A., Speare, R., and Longcore, J. (2005). Life cycle stages of the amphibian chytrid *Batrachochytrium dendrobatidis*. *Diseases of Aquatic Organisms*, 68:51–63.

Berger, L., Speare, R., Daszak, P., Green, D. E., Cunningham, A. A., Goggin, C. L., Slocombe, R., Ragan, M. A., Hyatt, A. D., McDonald, K. R., Hines, H. B., Lips, K. R., Marantelli, G., and Parkes, H. (1998). Chytridiomycosis causes amphibian mortality associated with population declines in the rain forests of australia and central america. *Proceedings of the National Academy of Sciences of the United States of America*, 95:9031–9036.

Blaustein, A., Romansic, J., Scheesseele, E., Han, B., Pessier, A., and Longcore, J. (2005). Interspecific variation in susceptibility of frog tadpoles to the pathogenic fungus *Batrachochytrium dendrobatidis*. *Conservation Biology*, 19:1460–1468.

Bletz, M., Kelly, M., Sabino-Pinto, J., Bales, E., Van Praet, S., Bert, W., Boyen, F., Vences, M., Steinfartz, S., Pasmans, F., and Martel, A. (2018). Disruption of skin microbiota contributes to salamander disease. *Proceedings of the Royal Society Biological Sciences*, 285:20180758.

Bletz, M. C., Loudon, A. H., Becker, M. H., Bell, S. C., Woodhams, D. C., Minbiole, K. P. C., and Harris, R. N. (2013). Mitigating amphibian chytridiomycosis with bioaugmentation:

characteristics of effective probiotics and strategies for their selection and use. *Ecology Letters*, 16:807–820.

Blooi, M., Martel, A., Haesebrouck, F., Vercammen, F., Bonte, D., and Pasmans, F. (2015a). Treatment of urodelans based on temperature dependent infection dynamics of *Batrachochytrium salamandrivorans*. *Scientific Reports*, 5:8037.

Blooi, M., Pasmans, F., Rouffaer, L., Haesebrouck, F., Vercammen, F., and Martel, A. (2015b). Successful treatment of *Batrachochytrium salamandrivorans* infections in salamanders requires synergy between voriconazole, polymyxin e and temperature. *Scientific Reports*, 5:11788.

Bokulich, N. A., Subramanian, S., Faith, J. J., Gevers, D., Gordon, J. I., Knight, R., Mills, D. A., and Caporaso, J. G. (2013). Quality-filtering vastly improves diversity estimates from illumina amplicon sequencing. *Nature Methods*, 10:57–59.

Bosch, J. (2009). Sapo partero comn - *Alytes obstetricans*. in: Enciclopedia virtual de los vertebrados espaoles. salvador, a. (ed.). museo nacional de ciencias naturales, madrid.

Bosch, J., Beebee, T., Schmidt, B., Tejedo, M., Martinez-Solano, I., Salvador, A., Garcia Paris, M., Recuero-Gil, M., Arntzen, J., Diaz-Paniagua, C., and Marquez, L. (2009). The iucn red list of threatened species 2009, e.t55268a87541047.

Bosch, J., Carrascal, L., Duran, L., Walker, S., and Fisher, M. (2007). Climate change and outbreaks of amphibian chytridiomycosis in a montane area of central spain; is there a link? *Proceedings of the Royal Society Biological Sciences*, 274:253–260.

Bosch, J., Martinez-Solano, I., and Garcia-Paris, M. (2001). Evidence of a chytrid fungus infection involved in the decline of the common midwife toad (*Alytes obstetricans*) in protected areas of central spain. *Biological Conservation*, 97:331–337.

Boyle, D. G., Boyle, D. B., Olsen, V., Morgan, J. A. T., and Hyatt, A. D. (2004). Rapid quantitative detection of chytridiomycosis (*Batrachochytrium dendrobatidis*) in amphibian samples using real-time taqman pcr assay. *Diseases of Aquatic Organisms*, 60:141–148.

Brandhorst, T., Wuthrich, M., Finkel-Jimenez, B., Warner, T., and Klein, B. (2004). Exploiting type 3 complement receptor for tnf-α suppression, immune evasion, and progressive pulmonary fungal infection. *Journal of Immunology*, 173:7444–7453.

Briggs, C., Knapp, R., and Vredenburg, V. (2010). Enzootic and epizootic dynamics of the chytrid fungal pathogen of amphibians. *Proceedings of the National Academy of Sciences of the United States of America*, 107:96959700.

Brucker, R., Harris, R., Schwantes, C., Gallaher, T., Flaherty, D., Lam, B., and Minbiole, K. (2008a). Amphibian chemical defence: antifungal metabolites of the microsymbiont *Janthinobacterium lividium* on the salamander *Plethodon cinereus*. *Journal of Chemical Ecology*, 34:1422–1429.

Brucker, R. M., Baylor, C. M., Walters, R. L., Lauer, A., Harris, R. N., and Minbiole, K. P. (2008b). The identification of 2,4-diacetylphloroglucinol as an antifungal metabolite produced by cutaneous bacteria of the salamander *Plethodon cinereus*. *Journal of Chemical Ecology*, 34:39–43.

Brunke, S. and Hube, B. (2006). Mflip1, a gene encoding an extracellular lipase of the lipid dependent fungus, *Malassezia furfur*. *Microbiology*, 152:547–554.

Buffie, C. G. and Pamer, E. G. (2013). Microbiota-mediated colonization resistance against intestinal pathogens. *Nature Reviews Immunology*, 13:790–801.

Chen, L., Wang, G., Bu, T., Zhang, Y., Wang, Y., Liu, M., and Lin, X. (2009). Phylogenetic analysis and screening of antimicrobial and cytotoxic activities of moderately halophilic bacteria isolated from the weihai solar saltern (china). *World Journal of Microbiology and Biotechnology*, 26:879–888.

Chitty, J. and Fraser, J. (2017). Purine acquisition and synthesis by human fungal pathogens. *Microorganisms*, 5:33.

Chu, H. and Mazmanian, S. (2013). Innate immune recognition of the microbiota promotes host-microbial symbiosis. *Nature Immunology*, 14:668–675.

Clare, F. (2014). *Quantifying the impact of infection by Batrachochytrium dendrobatidis on montane populations of Alytes obstetricans*. Phd thesis.

Clare, F. C., Halder, J. B., Daniel, O., Bielby, J., Semenov, M. A., Jombart, T., Loyau, A., Schmeller, D. S., Cunningham, A. A., Rowcliffe, M., Garner, T. W. J., Bosch, J., and Fisher, M. C. (2016). Climate forcing of an emerging pathogenic fungus across a montane multi-host community. *Philosophical Transactions of the Royal Society Biological Sciences*, 371:20150454.

Clarke, B. (1997). The natural history of amphibian skin secretions, their normal functioning and potential medical applications. *Biological Reviews of the Cambridge Philosophical Society*, 72:365–379.

Clarke, V., Rakotomalala, V., Ramilijaona, O., Abrell, L., and Fisher, B. (2006). Individual variation in alkaloid content of poison frogs of madagascar (*Mantella*; mantellidate). *Journal of Chemical Ecology*, 32:2219–2233.

Collado, M., Isolauri, E., and Salminen, S. (2008). Specific probiotic strains and their contributions counteract adhesion of *Enterobacter sazakii* to intestinal mucus. *FEMS Microbiology Letters*, 285:58–64.

Colombo, B. M., Scalvenzi, T., Benlamara, S., and Pollet, N. (2015). Microbiota and mucosal immunity in amphibians. *Frontiers in Immunology*, 6:111.

Conlon, M., Demandt, A., Nielsen, P., Leprince, J., Vaudry, H., and Woodhams, D. (2009b). The alyteserins: Two families of antimicrobial peptides from the skin secretions of the midwife toad *Alytes obstetricans* (alytidae). *Peptides*, 30:1069–1073.

Conlon, M., Iwamuro, S., and King, J. (2009). Dermal cytolytic peptides and the system of innate immunity in anurans. *Annals of the New York Academy of Sciences*, 1163:75–82.

Croswell, A., Amir, E., Teggatz, P., Barman, M., and Salzman, N. H. (2009). Prolonged impact of antibiotics on intestinal microbial ecology and susceptibility to enteric *Salmonella* infection. *Infection and Immunity*, 77:2741–53.

Culp, C. E., Falkinham, J. O., and Belden, L. K. (2007). Identification of the natural bacterial microflora on the skin of eastern newts, bullfrog tadpoles and redback salamanders. *Herpetologica*, 63:66–71.

Cunningham, A. A., Beckmann, K., Perkins, M., Fitzpatrick, L., Cromie, R., Redbond, J., O'Brien, M. F., Ghosh, P., Shelton, J., and Fisher, M. C. (2015). Emerging disease in uk amphibians. *The Veterinary Record*, 176:468.

Cunningham, A. A. and Daszak, P. (1998). Extinction of a species of land snail due to infection with a microsporidian parasite. *Conservation Biology*, 12:1139–1141.

Daly, J. W., Garraffo, H., Spande, T., Giddings, L., Saporito, R., Vieites, D., and Vences, M. (2008). Individual and geographic variation of skin alkaloids in three species of madagascan poison frogs (*Mantella*). *Journal of Chemical Ecology*, 34:252–279.

Daly, J. W., Garraffo, H. M., Spande, T. F., Jamarillo, C., and Rand, A. (1994). Dietary source for skin alkaloids of poison frogs (dendrobatidae)? *Journal of Chemical Ecology*, 20:943–955.

Daly, J. W., Myers, C., and Whittaker, N. (1987). Further classification of skin alkaloids from neotropical poison frogs (dendrobatidae), with a general survey of toxic/noxious substances in the amphibia. *Toxicon*, 25:1023–1095.

Daszak, P., Cunningham, A., and Hyatt, A. (2000). Emerging infectious diseases of wildlife - threats to biodiversrity and human health. *Science*, 287:443–449.

de Bruijn, I., Cheng, X., de Jager, V., Exposito, R. G., Watrous, J., Patel, N., Postma, J., Dorrestein, P. C., Kobayashi, D., and Raaijmakers, J. M. (2015). Comparative genomics and metabolic profiling of the genus *Lysobacter*. *BMC Genomics*, 16:991.

De Castro, F. and Bolker, B. (2005). Mechanisms of disease-induced extinction. *Ecology Letters*, 8:117–126.

Del Sorbo, G., Schoonbeek, H., and De Waard, M. (2000). Fungal transporters involved in efflux of natural toxic compounds and fungicides. *Fungal Genetics and Biology*, 30:1–15.

Di Guida, R., Engel, J., Allwood, J., Weber, R., M.R., J., Sommer, U., Viant, M., and Dunn, W. (2016). Non-targeted uhplc-ms metabolomic data processing methods: a comparative investigation of normalisation, missing value imputation, transformation and scaling. *Metabolomics*, 12:93.

Dorrestein, P., Mazmanian, S., and Knight, R. (2014). Finding the missing links among metabolites, microbes and the host. *Immunity*, 40:824–832.

Du Pasquier, L., Schwager, J., and Flajnik, M. (1989). The immune system of *Xenopus*. *Annual Review of Immunology*, 7:251–275.

Duellman, W. and Treub, L. (1986). *Biology of Amphibians*. New York, NY: McGraw-Hill.

Dufrene, M. and Legendre, P. (1997). Species assemblages and indicator species: The need for a flexible asymmetrical approach. *Ecological Monographs*, 67:345–366.

Edgar, P., Griffiths, R., and Foster, J. (2005). Evaluation of translocation as a tool for mitigating development threats to great crested newts (*Triturus cristatus*) in england, 1990-2001. *Biological Conservation*, 122:45–52.

Edgar, R. C., Haas, B. J., Clemente, J. C., Quince, C., and Knight, R. (2011). Uchime improves sensitivity and speed of chimera detection. *Bioinformatics*, 27:2194–200.

Ellison, A., DiRenzo, G., McDonald, C., Lips, K., and Zamudio, K. (2017). First *in vivo* *Batrachochytrium dendrobatidis* transcriptomes reveal mechanisms of host exploitation, host-specific gene expression, and expressed genotype shifts. *G3:Genes. Genomes. Genetics*, 7:269–278.

Ellison, A., Savage, A., DiRenzo, G., Langhammer, P., Lips, K., and Zamudio, K. (2014a). Fighting a losing battle: vigorous immune response countered by pathogen suppression of host defences in the chytridiomycosis susceptible frog *Atelopus zeteki*. *G3:Genes. Genomes. Genetics*, 4:1275–1289.

Ellison, A., Tunstall, T., DiRenzo, G., Hughey, M., Rebollar, E., Belden, L., Harris, R., Ibanez,

R., Lips, K., and Zamudio, K. (2014b). More than skin deep: functional genomic basis for resistance to amphibian chytridiomycosis. *Genome Biology and Evolution*, 7:286–298.

Farrer, R. A., Martel, A., Verbrugghe, E., Abouelleil, A., Ducatelle, R., Longcore, J. E., James, T. Y., Pasmans, F., Fisher, M. C., and Cuomo, C. A. (2017). Genomic innovations linked to infection strategies across emerging pathogenic chytrid fungi. *Nature communications*, 8:14742.

Farrer, R. A., Weinert, L. A., Bielby, J., Garner, T. W. J., Balloux, F., Clare, F., Bosch, J., Cunningham, A. A., Weldon, C., du Preez, L. H., Anderson, L., Pond, S. L. K., Shahar-Golan, R., Henk, D. A., and Fisher, M. C. (2011). Multiple emergences of genetically diverse amphibian-infecting chytrids include a globalized hypervirulent recombinant lineage. *Proceedings of the National Academy of Sciences of the United States of America*, 108:18732–18736.

Fisher, M. and Garner, T. (2007). The relationship between the emergence of *Batrachochytrium dendrobatidis*, the international trade in amphibians and introduced amphibian species. *Fungal Biology Review*, 21:2–9.

Fisher, M., Henk, D., Briggs, C., Brownstein, J., Madoff, L., S.L., M., and Gurr, S. (2012). Emerging fungal threats to animal, plant and ecosystem health. *Nature*, 484:186–194.

Fisher, M. C., Garner, T. W., and Walker, S. F. (2009). Global emergence of *Batrachochytrium dendrobatidis* and amphibian chytridiomycosis in space, time, and host. *Annual Review of Microbiology*, 63:291–310.

Fites, J. S., Ramsey, J. P., Holden, W. M., Collier, S. P., Sutherland, D. M., Reinert, L. K., Gayek, A. S., Dermody, T. S., Aune, T. M., Oswald-Richter, K., and Rollins-Smith, L. A. (2013). The invasive chytrid fungus of amphibians paralyzes lymphocyte responses. *Science*, 342:366–369.

Ford, S. A., Kao, D., Williams, D., and King, K. C. (2016). Microbe-mediated host defence drives the evolution of reduced pathogen virulence. *Nature Communications*, 7:13430.

Forster, H., Coffey, M., Elwood, H., and Sogin, M. (1990). Sequence analysis of the small subunit

ribosomal rnas of three zoosporic fungi and implications for fungal evolution. *Mycologia*, 82:306–312.

Foster, K., Schluter, J., Coyte, K., and Rakoff-Nahoum, S. (2017). The evolution of the host microbiome as an ecosystem on a leash. *Nature*, 548:43–51.

Fraune, S. and Bosch, T. (2010). Why bacteria matter in animal development and evolution. *BioEssays*, 32:571–580.

Gargas, A., Trest, M., Christensen, M., Volk, T., and Blehert, D. (2009). *Geomyces destructans sp. nov.* associated with bat white-nose syndrome. *Mycotaxon*, 108:147–154.

Garrison, E. (2012). vcflib: A c++ library for parsing and manipulating vcf files. *https://github.com/vcflib/vcflib (accessed July 21, 2015).*

Garrison, E. and Marth, G. (2012). Haplotype-based variant detection from short-read sequencing. *arXiv*, page 1207.3907.

Gascon, C. (2007). *Amphibian conservation action plan : proceedings IUCN/SSC Amphibian Conservation Summit 2005*. World Conservation Union (IUCN).

Gensollen, T., Iyer, S. S., Kasper, D. L., and Blumberg, R. S. (2016). How colonization by microbiota in early life shapes the immune system. *Science*, 352:539–544.

Gerwin, V. (2008). Riders of a modern-day ark. *PLoS Biology*, 6:e24.

Ghosh, P., Fisher, M., and Bates, K. (2018). Diagnosing emerging fungal threats: a one health perspective. *Frontiers in Genetics*, 9:376.

Gilbert, J., Blaser, M., Caporaso, J., Jansson, J., Lynch, S., and Knight, R. (2018). Current understanding of the human microbiome. *Nature Medicine*, 24:392–399.

Goka, K., Yokoyama, J., Une, Y., Kuroki, T., Suzuki, K., Nakahara, M., Kobaayashi, A., Inaba, S., Mizutani, T., and Hyatt, A. (2008). Amphibian chytridiomycosis in japan: distribution, haplotypes and possible route of entry into japan. *Molecular Ecology*, 18:4757–4774.

Gray, M. J., Freitag, N. E., and Boor, K. J. (2006). How the bacterial pathogen *Listeria monocytogenes* mediates the switch from environmental dr. jekyll to pathogenic mr. hyde. *Infection and Immunity*, 74:2505–12.

Green, S., Bouley, D., Tolwani, R., Waggie, K., Lifland, B., Otto, G., and Ferrell, J. (1999). Identification and management of an outbreak of *Flavobacterium meningosepticum* infection in a colony of south african clawed frogs (*Xenopus laevis*). *Journal of the American Veterinary Medical Association*, 214:1833–8, 1792–3.

Grice, E. A. and Segre, J. A. (2011). The skin microbiome. *Nature Reviews Microbiology*, 9:244–53.

Griffiths, S., Harrison, X., Weldon, C., Wood, M., Pretorius, A., Hopkins, K., Fox, G., Preziosi, R., and Antwis, R. (2018). Genetic variability and ontogeny predict microbiome structure in a disease-challenged montane amphibian. *The ISME Journal*.

Grogan, L., Cashins, S., Skerratt, L., Berger, L., McFadden, M., Harlow, P., Hunter, D., Scheele, B., and Mulvenna, J. (2018a). Evolution of resistance to chytridiomycosis is associated with a robust early immune response. *Molecular Ecology*, 27:919–934.

Grogan, L., Robert, J., Berger, J., Skerratt, L., Scheele, B., Castley, J., Newell, D., and McCallum, H. (2018b). Review of the amphibian immune response to chytridiomycosis, and future directions. *Frontiers in Immunology*, 9:2536.

Grogan, L., Skerratt, L., Berger, L., Cashins, S., Trengove, R., and Gummer, J. (2018c). Chytridiomycosis causes catastrophic organism-wide metabolic dysregulation including profound failure of cellular energy pathways. *Scientific Reports*, 8:8188.

Haas, B., Kamoun, S., Zody, M., Jiang, R., and Handsaker, R. e. a. (2009). Genome sequence and analysis of the irish potato famine pathogen *Phytophora infestans*. *Nature*, 461:393–398.

Harris, R. N., Brucker, R. M., Walke, J. B., Becker, M. H., Schwantes, C. R., Flaherty, D. C., Lam, B. A., Woodhams, D. C., Briggs, C. J., Vredenburg, V. T., and Minbiole, K. P. (2009). Skin microbes on frogs prevent morbidity and mortality caused by a lethal skin fungus. *The ISME Journal*, 3:818–24.

Harris, R. N., James, T., Lauer, A., Simon, M., and Patel, A. (2006). Amphibian pathogen *Batrachochytrium dendrobatidis* is inhibited by the cutaneous bacteria of amphibian species. *Ecohealth*, 3:53–56.

Harris, R. N., Lauer, A., Simon, M., Banning, J., and Alford, R. (2009b). Addition of antifungal skin bacteria to salamanders ameliorates the effects of chytridiomycosis. *Diseases of Aquatic Organisms*, 83:11–16.

Harrison, X., Price, S., Hopkins, K., Leung, W. M., Sergeant, C., and Garner, T. (2017). Host microbiome richness predicts resistance to disturbance by pathogenic infection in a vertebrate host. *bioRxiv*, page 158428.

Herv, M. (2016). Rvaidememoire: diverse basic statistical and graphical functions. *R package version 0.9-68*.

Hibbing, M., Fuqua, C., Parsek, M., and Paterson, S. (2010). Bacterial competition: surviving and thriving in the microbial jungle. *Nature Reviews Microbiology*, 8:15–25.

Holmes, I., Harris, K., and Quince, C. (2012). Dirichlet multinomial mixtures: generative models for microbial metagenomics. *PLoS ONE*, 7:e30126.

Honda, K. and Littman, D. R. (2012). The microbiome in infectious disease and inflammation. *Annual Review of Immunology*, 30:759–95.

Hooper, L. V., Littman, D. R., and Macpherson, A. J. (2012). Interactions between the microbiota and the immune system. *Science*, 336:1268–1273.

Hothorn, T., Bretz, F., and Westfall, P. (2008). Simultaneous inference in general parametric models. *Biometrical Journal*, 50:346–363.

Hung, C., Seshan, J., Schaller, R., Xue, J., Basrur, V., Gardner, M., and Cole, G. (2005). A metalloprotease of *Coccidioides posadassi* contributes to evasion of host detection. *Infection and Immunity*, 73:6689–6703.

Hyde, E., Navas-Molina, J., Song, S., Kueneman, J., Ackermann, G., Cardona, C., Humphrey, G., Boyer, D., Weaver, T., Mendelson, J., McKenzie, V., Gilbert, J., and Knight, R. (2016).

The oral and skin microbiomes of captive komodo dragons are significantly shared with their habitat. *mSystems*, 1:e00046–16.

Iwai, S., Weinmaier, T., Schmidt, B. L., Albertson, D. G., Poloso, N. J., Dabbagh, K., and DeSantis, T. Z. (2016). Piphillin: improved prediction of metagenomic content by direct inference from human microbiomes. *PLoS ONE*, 11:e0166104.

James, T. Y., Letcher, P. M., Longcore, J. E., Mozley-Standridge, S. E., Porter, D., Powell, M. J., Griffith, G. W., and Vilgalys, R. (2006). A molecular phylogeny of the flagellated fungi (chytridiomycota) and description of a new phylum (blastocladiomycota). *Mycologia*, 98:860–871.

James, T. Y., Litvintseva, A., Vilgalys, R., Morgan, J., Taylor, J., Fisher, M., Berger, L., Weldon, C., du Preez, L., and Longcore, J. (2009). Rapid global expansion of the fungal disease chytridiomycosis into declining and healthy amphibian populations. *PLoS Pathogens*, 5:e1000458.

James, T. Y., Porter, D., Leander, C. A., Vilgalys, R., and Longcore, J. E. (2000). Molecular phylogenetics of the chytridiomycota supports the utility of ultrastructural data in chytrid systematics. *Canadian Journal of Botany*, 78:336–350.

Jani, A. J. and Briggs, C. J. (2014). The pathogen *Batrachochytrium dendrobatidis* disturbs the frog skin microbiome during a natural epidemic and experimental infection. *Proceedings of the National Academy of Sciences of the United States of America*, 111:E5049–58.

Jani, A. J., Knapp, R. A., and Briggs, C. J. (2017). Epidemic and endemic pathogen dynamics correspond to distinct host population microbiomes at a landscape scale. *Proceedings of the Royal Society Biological Sciences*, 284:20170944.

Janssen, P. H. (2006). Identifying the dominant soil bacterial taxa in libraries of 16s rrna and 16s rrna genes. *Applied and Environmental Microbiology*, 72:1719–28.

Johnson, M. L. and Speare, R. (2003). Survival of *Batrachochytrium dendrobatidis* in water: Quarantine and disease control implications. *Emerging Infectious Diseases*, 9:922–925.

Jones, K., Patel, N., Levy, M., Storeygard, A., Balk, D., Gittleman, J., and Daszak, P. (2008). Global trends in emerging infectious diseases. *Nature*, 451:990–993.

Joneson, S., Stajich, J., Shiu, S., and Rosenblum, E. (2011). Genomic transition to pathogenicity in chytrid fungi. *PLoS Pathogens*, 7:e1002338.

Kamada, N., Kim, Y. G., Sham, H. P., Vallance, B. A., Puente, J. L., Martens, E. C., and Nunez, G. (2012). Regulated virulence controls the ability of a pathogen to compete with the gut microbiota. *Science*, 336:1325–9.

Kamoun, S. (2006). A catalogue of the effector secretome of plant pathogenic oomycetes. *Annual Review of Phytopathology*, 44:41–60.

Kearns, P. J., Fischer, S., Fernandez-Beaskoetxea, S., Gabor, C. R., Bosch, J., Bowen, J. L., Tlusty, M. F., and Woodhams, D. C. (2017). Fight fungi with fungi: antifungal properties of the amphibian mycobiome. *Frontiers in Microbiology*, 8:2494.

Khosravi, A. and Mazmanian, S. K. (2013). Disruption of the gut microbiome as a risk factor for microbial infections. *Current Opinion in Microbiology*, 16:221–7.

Khosravi, A., Yanez, A., Price, J., Chow, A., Merad, M., Goodridge, H., and Mazmanian, S. (2014). Gut microbiota promote hematopoiesis to control bacterial infection. *Cell Host Microbe*, 15:374–381.

King, K. C., Brockhurst, M. A., Vasieva, O., Paterson, S., Betts, A., Ford, S. A., Frost, C. L., Horsburgh, M. J., Haldenby, S., and Hurst, G. D. (2016). Rapid evolution of microbe-mediated protection against pathogens in a worm host. *The ISME Journal*, 10:1915–24.

Knutie, S. A., Wilkinson, C. L., Kohl, K. D., and Rohr, J. R. (2017). Early-life disruption of amphibian microbiota decreases later-life resistance to parasites. *Nature Communications*, 8:86.

Kobayashi, T., Glatz, M., Horiuchi, K., Kawasaki, H., Akiyama, H., Kaplan, D., Kong, H., Amagai, M., and Nagao, K. (2015). Dysbiosis and *Staphylococcus aureus* colonization drives inflammation in atopic dermatitis. *Immunity*, 42:756–766.

Koljalg, U., Larsson, K. H., Abarenkov, K., Nilsson, R. H., Alexander, I. J., Eberhardt, U., Erland, S., Hoiland, K., Kjoller, R., Larsson, E., Pennanen, T., Sen, R., Taylor, A. F. S., Tedersoo, L., Vralstad, T., and Ursing, B. M. (2005). Unite: a database providing web-based methods for the molecular identification of ectomycorrhizal fungi. *New Phytologist*, 166:1063–1068.

Kosch, T., Eimes, J., Didinger, C., Brannely, L., Waldman, B., Berger, L., and Skerrat, L. (2017). Characterization of mhc class ia in the endangered southern corroboree frog. *Immunogenetics*, 69:167–174.

Kozich, J. J., Westcott, S. L., Baxter, N. T., Highlander, S. K., and Schloss, P. D. (2013). Development of a dual-index sequencing strategy and curation pipeline for analyzing amplicon sequence data on the miseq illumina sequencing platform. *Applied and Environmental Microbiology*, 79:5112–5120.

Kueneman, J. G., Parfrey, L. W., Woodhams, D. C., Archer, H. M., Knight, R., and McKenzie, V. J. (2014). The amphibian skin-associated microbiome across species, space and life history stages. *Molecular Ecology*, 23:1238–50.

Kueneman, J. G., Woodhams, D. C., Harris, R., Archer, H. M., Knight, R., and McKenzie, V. J. (2016a). Probiotic treatment restores protection against lethal fungal infection lost during amphibian captivity. *Proceedings of the Royal Society Biological Sciences*, 283:20161553.

Kueneman, J. G., Woodhams, D. C., Van Treuren, W., Archer, H. M., Knight, R., and McKenzie, V. J. (2016b). Inhibitory bacteria reduce fungi on early life stages of endangered colorado boreal toads (*Anaxyrus boreas*). *The ISME Journal*, 10:934–44.

Lahti, L., Shetty, S., Blake, T., and Salojarvi, J. (2017). Tools for microbiome analysis in r. *Microbiome package version 1.1.10013*.

Lau, Q., Igawa, T., Komaki, S., and Satta, Y. (2016). Characterisation of major histocompatibility complex class i genes in japanese ranidae frogs. *Immunogenetics*, 68:797–806.

Lauer, A., Simon, M. A., Banning, J. L., Andre, E., Duncan, K., and Harris, R. N. (2007).

Common cutaneous bacteria from the eastern red-backed salamander can inhibit pathogenic fungi. *Copeia*, 2007:630–640.

Laurance, W. F., McDonald, K. R., and Speare, R. (1996). Epidemic disease and the catastrophic decline of australian rain forest frogs. *Conservation Biology*, 10:406–413.

Lax, S., Smith, D. P., Hampton-Marcell, J., Owens, S. M., Handley, K. M., Scott, N. M., Gibbons, S. M., Larsen, P., Shogan, B. D., Weiss, S., Metcalf, J. L., Ursell, L. K., Vazquez-Baeza, Y., Van Treuren, W., Hasan, N. A., Gibson, M. K., Colwell, R., Dantas, G., Knight, R., and Gilbert, J. A. (2014). Longitudinal analysis of microbial interaction between humans and the indoor environment. *Science*, 345:1048–1052.

Lee, K., Kim, S., Kim, E., Ha, E., You, H., Kim, B., Kim, M., Kwon, Y., Ryu, J., and Lee, W. (2013). Bacterial-derived uracil as a modulator of mucosal immunity and gut-microbe homeostasis in *Drosophila*. *Cell*, 153:797–811.

Ley, R., Turnbaugh, P., Klein, S., and Gordon, J. (2006). Microbial ecology: Human gut microbes associated with obesity. *Nature*, 444:1022–1023.

Li, H. and Durbin, R. (2009). Fast and accurate short read alignment with burrows-wheeler transform. *Bioinformatics*, 25:1754–60.

Li, H., Handsaker, B., Wysoker, A., Fennell, T., Ruan, J., Homer, N., Marth, G., Abecasis, G., Durbin, R., and Genome Project Data Processing, S. (2009). The sequence alignment/map format and samtools. *Bioinformatics*, 25:2078–2079.

Li, W. Z. and Godzik, A. (2006). Cd-hit: a fast program for clustering and comparing large sets of protein or nucleotide sequences. *Bioinformatics*, 22:1658–1659.

Lips, K. R., Brem, F., Brenes, R., Reeve, J., Alford, R., Voyles, J., Carey, C., Livo, L., Pessier, A., and Collins, J. (2006). Emerging infectious disease and the loss of biodiversity in a neotropical amphibian community. *Proceedings of the National Academy of Sciences of the United States of America*, 104:3165–3170.

Lips, K. R., Diffendorfer, J., Mendelson, J. R., and Sears, M. W. (2008). Riding the wave: Reconciling the roles of disease and climate change in amphibian declines. *PLoS Biology*, 6:441–454.

Longcore, J. E., Pessier, A. P., and Nichols, D. K. (1999). *Batrachochytrium dendrobatidis* gen et sp nov, a chytrid pathogenic to amphibians. *Mycologia*, 91:219–227.

Longo, A. V., Savage, A. E., Hewson, I., and Zamudio, K. R. (2015). Seasonal and ontogenetic variation of skin microbial communities and relationships to natural disease dynamics in declining amphibians. *Royal Society Open Science*, 2:140377.

Longo, A. V. and Zamudio, K. R. (2017). Temperature variation, bacterial diversity and fungal infection dynamics in the amphibian skin. *Molecular Ecology*, 26:4787–4797.

Lorch, J. M., Meteyer, C. U., Behr, M. J., Boyles, J. G., Cryan, P. M., Hicks, A. C., Ballmann, A. E., Coleman, J. T. H., Redell, D. N., Reeder, D. M., and Blehert, D. S. (2011). Experimental infection of bats with *Geomyces destructans* causes white-nose syndrome. *Nature*, 480:376–378.

Loudon, A. H., Holland, J. A., Umile, T. P., Burzynski, E. A., Minbiole, K. P. C., and Harris, R. N. (2014a). Interactions between amphibians' symbiotic bacteria cause the production of emergent anti-fungal metabolites. *Frontiers in Microbiology*, 5:441.

Loudon, A. H., Venkataraman, A., Van Treuren, W., Woodhams, D. C., Parfrey, L. W., McKenzie, V. J., Knight, R., Schmidt, T. M., and Harris, R. N. (2016). Vertebrate hosts as islands: dynamics of selection, immigration, loss, persistence, and potential function of bacteria on salamander skin. *Frontiers in Microbiology*, page 333.

Loudon, A. H., Woodhams, D. C., Parfrey, L. W., Archer, H., Knight, R., McKenzie, V., and Harris, R. N. (2014b). Microbial community dynamics and effect of environmental microbial reservoirs on red-backed salamanders (*Plethodon cinereus*). *The ISME Journal*, (4):830–40.

Manoli, I. and Venditti, C. (2016). Disorders of branched chain amino acid metabolism. *Translational Science of Rare Diseases*, 1:91–110.

Marquez, R. (1993). Male reproductive success in two midwife toads, *Alytes obstetricans* and *A. cisternasii*. *Behavioral Ecology and Sociobiology*, 32:283–291.

Martel, A., Blooi, M., Adriaensen, C., Van Rooij, P., Beukema, W., Fisher, M. C., Farrer, R. A., Schmidt, B. R., Tobler, U., Goka, K., Lips, K. R., Muletz, C., Zamudio, K. R., Bosch, J., Lotters, S., Wombwell, E., Garner, T. W. J., Cunningham, A. A., Spitzen-van der Sluijs, A., Salvidio, S., Ducatelle, R., Nishikawa, K., Nguyen, T. T., Kolby, J. E., Van Bocxlaer, I., Bossuyt, F., and Pasmans, F. (2014). Recent introduction of a chytrid fungus endangers western palearctic salamanders. *Science*, 346:630–631.

Martel, A., Spitzen-van der Sluijs, A., Blooi, M., Bert, W., Ducatelle, R., Fisher, M. C., Woeltjes, A., Bosman, W., Chiers, K., Bossuyt, F., and Pasmans, F. (2013). *Batrachochytrium salamandrivorans* sp nov causes lethal chytridiomycosis in amphibians. *Proceedings of the National Academy of Sciences of the United States of America*, 110:15325–15329.

Martin, M. (2011). Cutadapt removes adapter sequences from high-throughput sequencing reads. *EMBnet Journal*, 17:10–12.

Maslowski, K., Vieira, A., Ng, A., Kranich, J., Sierro, F., Yu, D., Schilter, H., Rolph, M., Mackay, F., Artis, D., Xavier, R., Teixeira, M., and Mackay, C. (2009). Regulation of inflammatory responses by gut microbiota and chemoattractant receptor gpr43. *Nature*, 461:1282–1286.

May, G. and Nelson, P. (2014). Defensive mutualisms: do microbial interactions within hosts drive the evolution of defensive traits? *Functional Ecology*, 28:356–363.

McCallum, H., Barlow, N., and Hone, J. (2001). How should pathogen transmission be modelled? *Trends in Ecology and Evolution*, 16:295–300.

McKenzie, V. J., Bowers, R. M., Fierer, N., Knight, R., and Lauber, C. L. (2012). Co-habiting amphibian species harbor unique skin bacterial communities in wild populations. *The ISME Journal*, 6:588–596.

McMahon, T. A., Sears, B. F., Venesky, M. D., Bessler, S. M., Brown, J. M., Deutsch, K., Halstead, N. T., Lentz, G., Tenouri, N., Young, S., Civitello, D. J., Ortega, N., Fites, J. S.,

Reinert, L. K., Rollins-Smith, L. A., Raffel, T. R., and Rohr, J. R. (2014). Amphibians acquire resistance to live and dead fungus overcoming fungal immunosuppression. *Nature*, 511:224–227.

McMurdie, P. J. and Holmes, S. (2013). phyloseq: an r package for reproducible interactive analysis and graphics of microbiome census data. *PLoS ONE*, 8:e61217.

Mendelson, J. R., Lips, K. R., Gagliardo, R. W., Rabb, G. B., Collins, J. P., Diffendorfer, J. E., Daszak, P., Ibanez, R., Zippel, K. C., Lawson, D. P., Wright, K. M., Stuart, S. N., Gascon, C., da Silva, H. R., Burrowes, P. A., Joglar, R. L., La Marca, E., Lotters, S., du Preez, L. H., Weldon, C., Hyatt, A., Rodriguez-Mahecha, J. V., Hunt, S., Robertson, H., Lock, B., Raxworthy, C. J., Frost, D. R., Lacy, R. C., Alford, R. A., Campbell, J. A., Parra-Olea, G., Bolanos, F., Domingo, J. J. C., Halliday, T., Murphy, J. B., Wake, M. H., Coloma, L. A., Kuzmin, S. L., Price, M. S., Howell, K. M., Lau, M., Pethiyagoda, R., Boone, M., Lannoo, M. J., Blaustein, A. R., Dobson, A., Griffiths, R. A., Crump, M. L., Wake, D. B., and Brodie, E. D. (2006). Biodiversity - confronting amphibian declines and extinctions. *Science*, 313:48–48.

Meyer, E. A., Cramp, R. L., Bernal, M. H., and Franklin, C. E. (2012). Changes in cutaneous microbial abundance with sloughing: possible implications for infection and disease in amphibians. *Diseases of Aquatic Organisms*, 101:235–42.

Mina, A., Ponti, A., Woodcraft, N., Johnson, E., and Saporito, R. (2015). Variation in alkaloid-based microbial defences of the dendrobatid poison frog *Oophaga pumilio*. *Chemoecology*, 25:169–178.

Mitchell, K. M., Churcher, T. S., Garner, T. W. J., and Fisher, M. C. (2008). Persistence of the emerging pathogen *Batrachochytrium dendrobatidis* outside the amphibian host greatly increases the probability of host extinction. *Proceedings of the Royal Society Biological Sciences*, 275:329–334.

Morehouse, E. A., James, T. Y., Ganley, A. R. D., Vilgalys, R., Berger, L., Murphy, P. J.,

and Longcore, J. E. (2003). Multilocus sequence typing suggests the chytrid pathogen of amphibians is a recently emerged clone. *Molecular Ecology*, 12:395–403.

Morgan, J. A. T., Vredenburg, V. T., Rachowicz, L. J., Knapp, R. A., Stice, M. J., Tunstall, T., Bingham, R. E., Parker, J. M., Longcore, J. E., Moritz, C., Briggs, C. J., and Taylor, J. W. (2007). Population genetics of the frog-killing fungus *Batrachochytrium dendrobatidis*. *Proceedings of the National Academy of Sciences of the United States of America*, 104:13845–13850.

Moss, A. S., Reddy, N. S., Dortaj, I. M., and Francisco, M. J. S. (2008). Chemotaxis of the amphibian pathogen *Batrachochytrium dendrobatidis* and its response to a variety of attractants. *Mycologia*, 100:1–5.

Muletz, C., Meyers, J., Domangue, R., Herrick, J., and Harris, R. (2012). Soil bioaugmentation with amphibian cutaneous bacteria protects amphibian hosts from infection by *Batrachochytrium dendrobatidis*. *Biological Conservation*, 152:119–126.

Muletz-Wolz, C. R., Almario, J. G., Barnett, S. E., DiRenzo, G. V., Martel, A., Pasmans, F., Zamudio, K. R., Toledo, L. F., and Lips, K. R. (2017). Inhibition of fungal pathogens across genotypes and temperatures by amphibian skin bacteria. *Frontiers in Microbiology*, 8:1551.

Myers, J. M., Ramsey, J. P., Blackman, A. L., Nichols, A. E., Minbiole, K. P., and Harris, R. N. (2012). Synergistic inhibition of the lethal fungal pathogen *Batrachochytrium dendrobatidis*: the combined effect of symbiotic bacterial metabolites and antimicrobial peptides of the frog *Rana muscosa*. *Journal of Chemical Ecology*, 38:958–65.

Nicholson, J., Holmes, E., Kinross, J., Burcelin, R., Gibson, G., Jia, W., and Pettersson, S. (2010). Host-gut microbiota metabolic interactions. *Science*, 336:1262–1267.

Nickerson, C., Ott, C., Castro, S., Garcia, V., Molina, T., Briggler, J., Pitt, A., Tavano, J., Byram, J., Barrila, J., and Nickerson, M. (2011). Evaluation of microorganisms cultured from injured and repressed tissue regeneration sites in endangered giant aquatic ozark hellbender salamanders. *PLoS ONE*, 6:e28906.

O'Hanlon, S., Rieux, A., Farrer, R., Rosa, G., Waldman, B., Bataille, A., Kosch, T., Murray, K., Brankovics, B., Fumagalli, M., Martin, M., Wales, N., Alvarado-Rybak, M., Bates, K., Berger, L., Boll, S., Brookes, L., Clare, F., Courtois, E., Cunningham, A., Doherty-Bone, T., Ghosh, P., Gower, D., Hintz, W., Höglund, J., Jenkinson, T., Lin, C., Laurila, A., Loyau, A., Martel, A., Meurling, S., Miaud, C., Minting, P., Pasmans, F., Schmeller, D., Schmidt, B., Shelton, J. G., Skerratt, L., Smith, F., Soto-Azat, C., Spagnoletti, M., Tessa, G., Toledo, L., Valenzuela-Sanchez, A., Verster, R., Voros, J., Webb, R., Wierzbicki, C., Wombwell, E., Zamudio, K., Aanensen, D., James, T., Gilbert, M., Weldon, C., Bosch, J., Balloux, F., Garner, T., and Fisher, M. (2018). Recent asian origin of chytrid fungi causing global amphibian declines. *Science*, 360:621–627.

Ohta, Y., Goetz, W., Hossain, M., Nonanka, M., and Flajnik, M. (2006). Ancestral organization of the mhc revealed in the amphibian *Xenopus*. *Journal of Immunology*, 176:3674–3685.

Oksanen, J., Blanchet, F., Kindt, R., Legendre, P., Minchin, P., O'Hara, R., Simpson, G., Solymos, P., Stevens, M., and Wagner, H. (2016). vegan: community ecology package. *R package version 2.3-4*.

Oliveros, J. (2007). Venny. an interactive tool for comparing lists with venn's diagrams. *http://bioinfogp.cnb.csic.es/tools/venny/index.html*.

Olson, D. H., Aanensen, D. M., Ronnenberg, K. L., Powell, C. I., Walker, S. F., Bielby, J., Garner, T. W. J., Weaver, G., The Bd Mapping Group, and Fisher, M. C. (2013). Mapping the global emergence of *Batrachochytrium dendrobatidis*, the amphibian chytrid fungus. *PLoS ONE*, 8:e56802.

Ottman, N., Smidt, H., de Vos, W. M., and Belzer, C. (2012). The function of our microbiota: who is out there and what do they do? *Frontiers in Cellular and Infection Microbiology*, 2:104.

Ouellet, M., Mikaelian, I., Pauli, B. D., Rodrigue, J., and Green, D. M. (2005). Historical evidence of widespread chytrid infection in north american amphibian populations. *Conservation Biology*, 19:1431–1440.

Owen, O. E., Kalhan, S. C., and Hanson, R. W. (2002). The key role of anaplerosis and cataplerosis for citric acid cycle function. *Journal of Biological Chemistry*, 277:3040930412.

Parris, M. J. and Cornelius, T. O. (2004). Fungal pathogen causes competitive and developmental stress in larval amphibian communities. *Ecology*, 85:3385–3395.

Parsons, H., Ludwig, C., Gunther, U., and Viant, M. (2007). Improved classification accuracy in 1- and 2-dimensional nmr metabolomics data using the variance stabilising generalised logarithm transformation. *BMC Bioinformatics*, 8:234.

Paterson, S., Vogwill, T., Buckling, A., Benmayor, R., Spiers, A. J., Thomson, N. R., Quail, M., Smith, F., Walker, D., Libberton, B., Fenton, A., Hall, N., and Brockhurst, M. A. (2010). Antagonistic coevolution accelerates molecular evolution. *Nature*, 464:275–U154.

Pedersen, H., Gudmundsdottir, V., Nielsen, H., Hyotylainen, T., Nielsen, T., Jensen, B., Forslund, K., Hildebrand, F., Prifti, E., Falony, G., Le Chatelier, E., Levenez, F., Dore, J., Mattila, I., Plichta, D., Poho, P., Hellgren, L., Arumugam, M., Sunagawa, S., Vieira-Silva, S., Jorgensen, T., Holm, J., Trost, K., MetaHIT Consortium, Kristiansen, K., Brix, S., Raes, J., Wang, J., Hansen, T., Bork, P., Brunak, S., Oresic, M., and Ehrlich, S.D.and Pedersen, O. (2016). Human gut microbes impact host serum metabolome and insulin sensitivity. *Nature*, 535:376–381.

Pfennig, K. (2001). Evolution of pathogen virulence: the role of variation in host phenotype. *Proceedings of the Royal Society Biological Sciences*, 268:755–760.

Pham, T. A. and Lawley, T. D. (2014). Emerging insights on intestinal dysbiosis during bacterial infections. *Current Opinion in Microbiology*, 17:67–74.

Piotrowski, J. S., Annis, S. L., and Longcore, J. E. (2004). Physiology of *Batrachochytrium dendrobatidis*, a chytrid pathogen of amphibians. *Mycologia*, 96:9–15.

Piovia-Scott, J., Pope, K., Worth, S. J., Rosenblum, E. B., Poorten, T., Refsnider, J., Rollins-Smith, L. A., Reinert, L. K., Wells, H. L., Rejmanek, D., Lawler, S., and Foley, J. (2015). Correlates of virulence in a frog-killing fungal pathogen: evidence from a california amphibian decline. *The ISME Journal*, 9:1570–1578.

Piovia-Scott, J., Rejmanek, D., Woodhams, D. C., Worth, S. J., Kenny, H., McKenzie, V., Lawler, S. P., and Foley, J. E. (2017). Greater species richness of bacterial skin symbionts better suppresses the amphibian fungal pathogen *Batrachochytrium dendrobatidis*. *Microbial Ecology*, 74:217–226.

Poorten, T. and Rosenblum, E. (2016). Comparative study of host response to chytridiomycosis in a susceptible and a resistant toad species. *Molecular Ecology*, 25:5663–5679.

Pounds, J. A., Bustamante, M. R., Coloma, L. A., Consuegra, J. A., Fogden, M. P. L., Foster, P. N., La Marca, E., Masters, K. L., Merino-Viteri, A., Puschendorf, R., Ron, S. R., Sanchez-Azofeifa, G. A., Still, C. J., and Young, B. E. (2006). Widespread amphibian extinctions from epidemic disease driven by global warming. *Nature*, 439:161–167.

Pruesse, E., Quast, C., Knittel, K., Fuchs, B. M., Ludwig, W., Peplies, J., and Glockner, F. O. (2007). Silva: a comprehensive online resource for quality checked and aligned ribosomal rna sequence data compatible with arb. *Nucleic Acids Research*, 35:7188–96.

R Core Team (2017). *R: A Language and Environment for Statistical Computing*. R Foundation for Statistical Computing, Vienna, Austria.

Rachowicz, L. J., Hero, J. M., Alford, R. A., Taylor, J. W., Morgan, J. A. T., Vredenburg, V. T., Collins, J. P., and Briggs, C. J. (2005). The novel and endemic pathogen hypotheses: Competing explanations for the origin of emerging infectious diseases of wildlife. *Conservation Biology*, 19:1441–1448.

Ramsey, J., Reinert, L., Harper, L., Woodhams, D., and Rollins-Smith, L. (2010). Innate and adaptive immune defenses against a fungus linked to global amphibian declines in the south african clawed frog, *Xenopus laevis*. *Journal of Immunology*, 184.

Rathbone, D. and Bruce, N. (2002). Microbial transformation of alkaloids. *Current Opinion in Microbiology*, 5:274–281.

Reading, C. J. (2007). Linking global warming to amphibian declines through its effects on female body condition and survivorship. *Oecologia*, 151:125–131.

Rebollar, E., Simonetti, S., Shoemaker, W., and Harris, R. (2016a). Direct and indirect horizontal transmission of the antifungal probiotic bacterium *Janthinobacterium lividium* on green frog (*Lithobates clamitans*) tadpoles. *Applied and Environmental Microbiology*, 82:2457–2466.

Rebollar, E. A., Hughey, M. C., Medina, D., Harris, R. N., Ibanez, R., and Belden, L. K. (2016b). Skin bacterial diversity of panamanian frogs is associated with host susceptibility and presence of *Batrachochytrium dendrobatidis*. *The ISME journal*, 10:1682–1695.

Reed, K. D., Ruth, G. R., Meyer, J. A., and Shukla, S. K. (2000). *Chlamydia pneumoniae* infection in a breeding colony of african clawed frogs (*Xenopus tropicalis*). *Emerging Infectious Diseases*, 6:196–199.

Roberts, D. (2016). labdsv: ordination and multivariate analysis for ecology. *R package version 1.8.0*.

Rodriguez, D., Becker, C. G., Pupin, N. C., Haddad, C. F. B., and Zamudio, K. R. (2014). Long-term endemism of two highly divergent lineages of the amphibian-killing fungus in the atlantic forest of brazil. *Molecular Ecology*, 23:774–787.

Rogers, G. B., Keating, D. J., Young, R. L., Wong, M. L., Licinio, J., and Wesselingh, S. (2016). From gut dysbiosis to altered brain function and mental illness: mechanisms and pathways. *Molecular Psychiatry*, 21:738–48.

Rohart, F., Gautier, B., Singh, A., and Le Cao, K. (2017). mixomics: An r package for 'omics feature selection and multiple data integration. *PLoS Computational Biology*, 13:e1005752.

Rollins-Smith, L. and Conlon, J. (2005). Antimicrobial peptide defences against chytridiomycosis, an emerging infectious disease of amphibian populations. *Developmental and Comparative Immunology*, 29:589–598.

Rollins-Smith, L. A., Fites, J., Reinert, L., Shiakolas, A., Umile, T., and Minbiole, K. (2015). Immunomodulatory metabolites released by the frog-killing fungus *Batrachochytrium dendrobatidis*. *Infection and Immunity*, 83:4565–4570.

Rollins-Smith, L. A., Ramsey, J. P., Pask, J. D., Reinert, L. K., and Woodhams, D. C. (2011). Amphibian immune defenses against chytridiomycosis: impacts of changing environments. *Integrative and Comparative Biology*, 51:552–62.

Rollins-Smith, L. A., Ramsey, J. P., Reinert, L., Woodhams, D., Livo, L., and Carey, C. (2009). Immune defences of *Xenopus laevis* against *Batrachochytrium dendrobatidis*. *Frontiers in Bioscience*, 1:68–91.

Rosenblum, E. B., James, T. Y., Zamudio, K. R., Poorten, T. J., Ilut, D., Rodriguez, D., Eastman, J. M., Richards-Hrdlicka, K., Joneson, S., Jenkinson, T. S., Longcore, J. E., Olea, G. P., Toledo, L. F., Arellano, M. L., Medina, E. M., Restrepo, S., Flechas, S. V., Berger, L., Briggs, C. J., and Stajich, J. E. (2013). Complex history of the amphibian-killing chytrid fungus revealed with genome resequencing data. *Proceedings of the National Academy of Sciences of the United States of America*, 110:9385–9390.

Rosenblum, E. B., Poorten, T. J., Settles, M., and Murdoch, G. K. (2012). Only skin deep: shared genetic response to the deadly chytrid fungus in susceptible frog species. *Molecular Ecology*, 21:3110–3120.

Rosenblum, E. B., Poorten, T. J., Settles, M., Murdoch, G. K., Robert, J., Maddox, N., and Eisen, M. (2009). Genome-wide transcriptional response of *Silurana* (*Xenopus*) *tropicalis* to infection with deadly chytrid fungus. *PLoS ONE*, 4:e6494.

Rosenblum, E. B., Stajich, J. E., Maddox, N., and Eisen, M. B. (2008). Global gene expression profiles for life stages of the deadly amphibian pathogen *Batrachochytrium dendrobatidis*. *Proceedings of the National Academy of Sciences of the United States of America*, 105:17034–17039.

Rosenblum, E. B., Voyles, J., Poorten, T., and Stajich, J. E. (2010). The deadly chytrid fungus: A story of an emerging pathogen. *PLoS Pathogens*, 6:e1000550.

Rynkiewicz, E., Pedersen, A., and Fenton, A. (2015). An ecosystem approach to understanding and managing within-host parasite community dynamics. *Trends in Parasitology*, 31:212–221.

Sabino-Pinto, J., Bletz, M. C., Islam, M. M., Shimizu, N., Bhuju, S., Geffers, R., Jarek, M., Kurabayashi, A., and Vences, M. (2016). Composition of the cutaneous bacterial community in japanese amphibians: effects of captivity, host species, and body region. *Microbial Ecology*, 72:460–469.

Saka, H. and Valdiva, R. (2010). Acquisition of nutrients by chlamydiae: unique challenges of living in an intracellular compartment. *Current Opinion in Microbiology*, 13:4–10.

Savage, A. E. and Zamudio, K. R. (2011). Mhc genotypes associate with resistance to a frog-killing fungus. *Proceedings of the National Academy of Sciences of the United States of America*, 108:16705–16710.

Savage, A. E. and Zamudio, K. R. (2016). Adaptive tolerance to a pathogenic fungus drives major histocompatibility complex evolution in natural amphibian populations. *Proceedings of the Royal Society Biological Sciences*, 283:20153115.

Schloegel, L. M., Toledo, L. F., Longcore, J. E., Greenspan, S. E., Vieira, C. A., Lee, M., Zhao, S., Wangen, C., Ferreira, C. M., Hipolito, M., Davies, A. J., Cuomo, C. A., Daszak, P., and James, T. Y. (2012). Novel, panzootic and hybrid genotypes of amphibian chytridiomycosis associated with the bullfrog trade. *Molecular Ecology*, 21:5162–5177.

Schloss, P. D., Gevers, D., and Westcott, S. L. (2011). Reducing the effects of pcr amplification and sequencing artifacts on 16s rrna-based studies. *PLoS ONE*, 6:e27310.

Schloss, P. D., Westcott, S. L., Ryabin, T., Hall, J. R., Hartmann, M., Hollister, E. B., Lesniewski, R. A., Oakley, B. B., Parks, D. H., Robinson, C. J., Sahl, J. W., Stres, B., Thallinger, G. G., Van Horn, D. J., and Weber, C. F. (2009). Introducing mothur: open-source, platform-independent, community-supported software for describing and comparing microbial communities. *Applied and Environmental Microbiology*, 75:7537–41.

Schmid-Hempel, P. and Koella, J. (1994). Variability and its implications for host-parasite interactions. *Parasitology Today*, 10:98–102.

Schmidt, B. R., Bozzuto, C., Lotters, S., and Steinfartz, S. (2017). Dynamics of host populations

affected by the emerging fungal pathogen *Batrachochytrium salamandrivorans*. *Royal Society Open Science*, 4:160801.

Schumacher, U., Adam, E., Hauser, F., Probst, J. C., and Hoffmann, W. (1994). Molecular anatomy of a skin gland - histochemical and biochemical investigations on the mucous glands of *Xenopus laevis*. *Journal of Histochemistry and Cytochemistry*, 42:57–65.

Segata, N., Izard, J., Waldron, L., Gevers, D., Miropolsky, L., Garrett, W., and Huttenhower, C. (2011). Metagenomic biomarker discovery and explanation. *BMC Genome Biology*, 12:R60.

Sender, R., Fuchs, S., and Milo, R. (2016). Are we really vastly outnumbered? revisiting the ratio of bacterial to host cells in humans. *Cell*, 164:337–340.

Servillo, L., Giovane, A., Balestrieri, M., Casale, R., Cautela, D., and Castaldo, D. (2015). *Citrus* genus plants contain n-methylated tryptamine derivatives and their 5-hydroxylated forms. *Journal of Agricultural and Food Chemistry*, 61:5156–5162.

Shannon, P., Markiel, A., Ozier, O., Baliga, N., Wang, J., Ramage, D., Amin, N., Schwikowski, B., and Ideker, T. (2003). Cytoscape: a software environment for integrated models of biomolecular interaction networks. *Genome Research*, 13:2498–504.

Shin, J., Yang, J., Jeon, B., Yoon, Y., Cho, S., Kang, Y., Ryu, D., and Hwang, G. (2011). ^{1}h nmr-based metabolomic profiling in mice infected with *Mycobacterium tuberculosis*. *Journal of Proteome Research*, 10:2238–2247.

Siddiqui, S. and Siddiqui, R. (1931). The alkaloids of *Rauwolfia serpentina*, benth. *Journal of the Indian Chemical Society*, 8:667–678.

Singmann, H., Bolker, B., Westfall, J., and Aust, F. (2017). afex: Analysis of factorial experiments. *R package version 0.18.0*.

Skerrat, L., Berger, L., Speare, R., Cashins, S., McDonald, K., Phillott, A., Hines, H., and Kenyon, N. (2007). Spread of chytridiomycosis has caused the rapid decline and extinction of frogs. *EcoHealth*, 4:125–134.

Smith, K., McCoy, K. D., and Macpherson, A. J. (2007). Use of axenic animals in studying the adaptation of mammals to their commensal intestinal microbiota. *Seminars in Immunology*, 19:59–69.

Smith, P., Howitt, M., Panikov, N., Michaud, M., Gallini, C., Bohlooly-Y, M., Glickman, J., and Garret, W. (2013). The microbial metabolites, short-chain fatty acids, regulate colonic treg cell homeostasis. *Science*, 341:569–573.

Soanes, D., Alam, I., Cornell, M., Wong, H., Hedeler, C., Paton, N., Rattray, M., Hubbard, S., Oliver, S., and Talbot, N. (2008). Comparative genome analysis of filamentous fungi reveals gene family expansions associated with fungal pathogenesis. *PLoS ONE*, 3:e2300.

Solomon, P., Tan, K., and Oliver, R. (2003). The nutrient supply of pathogenic fungi; a fertile field for study. *Molecular Plant Pathology*, 4:203–210.

Speth, C., Rambach, G., Wurzner, R., and Lass-Florl, C. (2008). Complement and fungal pathogens: an update. *Mycoses*, 51:477–496.

Spitzen-van der Sluijs, A., Spikmans, A., Bosman, W., de Zeeuw, M., van der Meij, T., Goverse, E., Kik, M., Pasmans, F., and Martel, A. (2013). Rapid enigmatic decline drives *Salamandra salamandra* to the edge of extinction in the netherlands. *Amphibia-Reptilia*, 34:233–239.

Spry, C., Kirk, K., and Saliba, K. (2008). Coenzyme a biosynthesis: an antimicrobial drug target. *FEMS Microbiology Reviews*, 32:56–106.

Stacy, A., Fleming, D., Lamont, R. J., Rumbaugh, K. P., and Whiteley, M. (2016). A commensal bacterium promotes virulence of an opportunistic pathogen via cross-respiration. *MBio*, 7:e00782–16.

Stuart, S. N., Chanson, J. S., Cox, N. A., Young, B. E., Rodrigues, A. S. L., Fischman, D. L., and Waller, R. W. (2004). Status and trends of amphibian declines and extinctions worldwide. *Science*, 306:1783–1786.

Sumner, L., Amberg, A., Barrett, D., Beale, M., Beger, R., Daykin, C., Fan, T., Fiehn, O., Goodacre, R., Griffin, J., Hankemeier, T., Hardy, N., Harnly, J., Higashi, R., Kopka, J.,

Lane, A., Lindon, J., Marriott, P., Nicholls, A., Reilly, M., Thaden, J., and Viant, M. (2007). Proposed minimum reporting standards for chemical analysis chemical analysis working group (cawg) metabolomics standards initiative (msi). *Metabolomics*, 3:211–221.

Swinton, J., Harwood, J., Grenfell, B. T., and Gilligan, C. A. (1998). Persistence thresholds for phocine distemper virus infection in harbour seal *Phoca vitulina* metapopulations. *Journal of Animal Ecology*, 67:54–68.

Takeuchi, O. and Akira, S. (2010). Pattern recognition receptors and inflammation. *Cell*, 140:805–820.

Talley, B. L., Muletz, C. R., Vredenburg, V. T., Fleischer, R. C., and Lips, K. R. (2015). A century of *Batrachochytrium dendrobatidis* in illinois amphibians (1888-1989). *Biological Conservation*, 182:254–261.

Taylor, J. W. and Berbee, M. L. (2006). Dating divergences in the fungal tree of life: review and new analyses. *Mycologia*, 98:838–849.

Taylor, S. K., Williams, E. S., Thorne, E. T., Mills, K. W., Withers, D. I., and Pier, A. C. (1999). Causes of mortality of the wyoming toad. *Journal of Wildlife Diseases*, 35:49–57.

Tennessen, J., Woodhams, D., Chaurand, P., Reinert, L., Billheimer, D., Shyr, Y., Caprioli, R., Blouin, M., and Rollins-Smith, L. (2009). Variations in the expressed antimicrobial peptide repertoire of northern leopard frog (*Rana pipiens*) populations suggests intraspecific differences in resistance to pathogens. *Developmental and Comparative Immunology*, 33:1247–1257.

Therneau, T. M. (2015). A package for survival analysis in s. *R package version 2.38*.

Tobler, U. and Schmidt, B. (2010). Within- and among-population variation in chytridiomycosis-induced mortality in the toad *Alytes obstetricans*. *PLoS ONE*, 5:e10927.

Turnbaugh, P., Ley, R., Hamady, M., Fraser-Liggett, C., Knight, R., and Gordon, J. I. (2007). The human microbiome project. *Nature*, 449:804–810.

Van Rooij, P., Martel, A., Haesebrouck, F., and Pasmans, F. (2015). Amphibian chytridiomycosis: a review with focus on fungus-host interactions. *Veterinary Research*, 46:137.

Van Valen, L. (1973). A new evolutionary law. *Evolutionary Theory*, 1:1–30.

Venables, W. and Ripley, B. (2002). *Modern Applied Statistics with S*. Springer, New York, fourth edition.

Vences, M., Lyra, M. L., Kueneman, J. G., Bletz, M. C., Archer, H. M., Canitz, J., Handreck, S., Randrianiaina, R. D., Struck, U., Bhuju, S., Jarek, M., Geffers, R., McKenzie, V. J., Tebbe, C. C., Haddad, C. F., and Glos, J. (2016). Gut bacterial communities across tadpole ecomorphs in two diverse tropical anuran faunas. *Die Naturwissenschaften*, 103:25.

Venesky, M. D., Wassersug, R. J., and Parris, M. J. (2010). Fungal pathogen changes the feeding kinematics of larval anurans. *Journal of Parasitology*, 96:552–557.

Villani, G. R., Gallo, G., Scolamiero, E., Salvatore, F., and Ruoppolo, M. (2017). classical organic acidurias: diagnosis and pathogenesis. *Clinical and Experimental Medicine*, 17:305–323.

Vinolo, M., Rodrigues, H., Nachbar, R., and Curi, R. (2011). Regulation of inflammation by short chain fatty acids. *Nutrients*, 3:858–876.

Voyles, J., Young, S., Berger, L., Campbell, C., Voyles, W. F., Dinudom, A., Cook, D., Webb, R., Alford, R. A., Skerratt, L. F., and Speare, R. (2009). Pathogenesis of chytridiomycosis, a cause of catastrophic amphibian declines. *Science*, 326:582–585.

Vredenburg, V. T., Knapp, R. A., Tunstall, T. S., and Briggs, C. J. (2010). Dynamics of an emerging disease drive large-scale amphibian population extinctions. *Proceedings of the National Academy of Sciences of the United States of America*, 107:9689–9694.

Vylkova, S. and Lorenz, M. (2017). Phagosomal neutralization by the fungal pathogen *Candida albicans* induces macrophage pyroptosis. *Infection and Immunity*, 85:e00832–16.

Walke, J., Becker, M., Loftus, S., House, L., Teotonio, T., Minbioloe, K., and Belden, L. (2015a). Community structure and function of amphibian skin microbes: an experiment with bullfrogs exposed to a chytrid fungus. *PLoS ONE*, 10:e0139848.

Walke, J., Harris, R., Reinert, L., Rollins-Smith, L., and Woodhams, D. (2011). Social immunity in amphibians: evidence for vertical transmission of innate defences. *Biotropica*, 43:396–400.

Walke, J. B., Becker, M. H., Hughey, M. C., Swartwout, M. C., Jensen, R. V., and Belden, L. K. (2015b). Most of the dominant members of amphibian skin bacterial communities can be readily cultured. *Applied and Environmental Microbiology*, 81:6589–600.

Walke, J. B., Becker, M. H., Loftus, S. C., House, L. L., Cormier, G., Jensen, R. V., and Belden, L. K. (2014). Amphibian skin may select for rare environmental microbes. *The ISME Journal*, 8:2207–17.

Walke, J. B. and Belden, L. (2016). Harnessing the microbiome to prevent fungal infections: lessons from amphibians. *PLoS Pathogens*, 12:e1005796.

Walker, S. F. (2008). *Geographical patterns in the distribution of Batrachochytrium dendrobatidis and outbreaks of fatal chytridiomycosis in European amphibian populations*. Phd thesis.

Wang, Q., Garrity, G. M., Tiedje, J. M., and Cole, J. R. (2007). Naive bayesian classifier for rapid assignment of rrna sequences into the new bacterial taxonomy. *Applied and Environmental Microbiology*, 73:5261–7.

Warnes, G., Bolker, B., Bonebakker, L., Gentleman, R., Huber, W., Liaw, A., Lumley, T., Maechler, M., Magnusson, A., and Moeller, S. (2009). gplots: Various r programming tools for plotting data. *R package version 2.17.0*, (4).

Waters, C. and Bassler, B. (2005). Quorum sensing: cell-to-cell communication in bacteria. *Annual Review of Cell and Developmental Biology*, 21:319–346.

Weber, R. and Viant, M. (2010). Mi-pack: Increased confidence of metabolite identification in mass spectra by integrating accurate masses and metabolic pathways. *Chemometrics and Intelligent Laboratory Systems*, 104:72–82.

Weldon, C., du Preez, L. H., Hyatt, A. D., Muller, R., and Speare, R. (2004). Origin of the amphibian chytrid fungus. *Emerging Infectious Diseases*, 10:2100–2105.

Weljie, A., Dowlatabadi, R., Miller, B., and Jirik, F. (2007). An inflammatory arthritis-associated metabolite biomarker pattern revealed by 1h nmr spectroscopy. *Journal of Proteome Research*, 6:3456–64.

Wickham, H. (2009). *ggplot2: Elegant Graphics for Data Analysis*. Springer-Verlag, New York.

Woodhams, D., Alford, R., Antwis, R., Archer, H., Becker, M., Belden, L., Bell, S., Bletz, M., Daskin, J., Davis, L., Flechas, S., Lauer, A., Gonzalez, A., Harris, R., Holden, W., Hughey, M., Ibanez, R., Knight, R., Kueneman, J., Rabemananjara, F., Reinert, L., Rollins-Smith, L., Roman-Rodriguez, F., Shaw, S., Walke, J., and McKenzie, V. (2015). Antifungal isolates database of amphibian skin-associated bacteria and function against emerging fungal pathogens. *Ecology*, 96:595.

Woodhams, D., Ardipradja, K., Alford, R., Marantelli, G., Reinert, L., and Rollins-Smith, L. (2007). Resistance to chytridiomycosis varies among amphibian species and is correlated with skin peptide defences. *Animal Conservation*, 10:409–417.

Woodhams, D., Bletz, M., Kueneman, J., and McKenzie, V. (2016). Managing amphibian disease with skin microbiota. *Trends in Microbiology*, 24:161–164.

Woodhams, D., Vredenburg, V., Simon, M., Billheimer, D., Shakhtour, B., Shyr, Y., Briggs, C., Rollins-Smith, L., and Harris, R. (2007b). Symbiotic bacteria contribute to innate immune defenses of the threatened mountain yellow-legged frog, *Rana muscosa*. *Biological Conservation*, 138:390–398.

Woodhams, D. C., Alford, R. A., Briggs, C. J., Johnson, M., and Rollins-Smith, L. A. (2008). Life-history trade-offs influence disease in changing climates: Strategies of an amphibian pathogen. *Ecology*, 89(6):1627–1639.

Woodhams, D. C., Brandt, H., Baumgartner, S., Kielgast, J., Kupfer, E., Tobler, U., Davis, L. R., Schmidt, B. R., Bel, C., Hodel, S., Knight, R., and McKenzie, V. (2014). Interacting

symbionts and immunity in the amphibian skin mucosome predict disease risk and probiotic effectiveness. *PloS ONE*, 9:e104590.

Woodhams, D. C., LaBumbard, B. C., Barnhart, K. L., Becker, M. H., Bletz, M. C., Escobar, L. A., Flechas, S. V., Forman, M. E., Iannetta, A. A., Joyce, M. D., Rabemananjara, F., Gratwicke, B., Vences, M., and Minbiole, K. P. C. (2017). Prodigiosin, violacein, and volatile organic compounds produced by widespread cutaneous bacteria of amphibians can inhibit two *Batrachochytrium* fungal pathogens. *Microbial Ecology*, 75:1049–1062.

Woodhams, D. C., Voyles, J., Lips, K. R., Carey, C., and Rollins-Smith, L. A. (2006). Predicted disease susceptibility in a panamanian amphibian assemblage based on skin peptide defenses. *Journal of Wildlife Diseases*, 42:207–218.

Woods, J. (2003). Knocking on the right door and making a comfortable home: *Histoplasma capsulatum* intracellular pathogenesis. *Current Opinions in Microbiology*, 6:327–331.

Woodworth, B. L., Atkinson, C. T., LaPointe, D. A., Hart, P. J., Spiegel, C. S., Tweed, E. J., Henneman, C., LeBrun, J., Denette, T., DeMots, R., Kozar, K. L., Triglia, D., Lease, D., Gregor, A., Smith, T., and Duffy, D. (2005). Host population persistence in the face of introduced vector-borne diseases: Hawaii amakihi and avian malaria. *Proceedings of the National Academy of Sciences of the United States of America*, 102:1531–1536.

Wyrick, P. B. (2000). Intracellular survival by *Chlamydia*. *Cellular Microbiology*, 2:275–282.

Yap, T. A., Koo, M. S., Ambrose, R. F., Wake, D. B., and Vredenburg, V. T. (2015). Averting a north american biodiversity crisis. *Science*, 349:481–482.

Yu, G. C., Smith, D. K., Zhu, H. C., Guan, Y., and Lam, T. T. Y. (2017). Ggtree: an r package for visualization and annotation of phylogenetic trees with their covariates and other associated data. *Methods in Ecology and Evolution*, 8:28–36.

Yuan, S. Q., Cohen, D. B., Ravel, J., Abdo, Z., and Forney, L. J. (2012). Evaluation of methods for the extraction and purification of dna from the human microbiome. *PloS ONE*, 7:e33865.

Zaneveld, J. R., McMinds, R., and Thurber, R. V. (2017). Stress and stability: applying the anna karenina principle to animal microbiomes. *Nature Microbiology*, 2:17121.

Zelante, T., Iannitti, R., Cunha, C., De Luca, A., Giovannini, G., Pieraccini, G., Zecchi, R., D'Angelo, C., Massi-Benedetti, C., Fallarino, F., Carvalho, A., Puccetti, P., and Romani, L. (2013). Tryptophan catabolites from microbiota engage aryl hydrocarbon receptor and balance mucosal reactivity via interleukin-22. *Immunity*, 39:372–385.

Zhang, J. J., Kobert, K., Flouri, T., and Stamatakis, A. (2014). Pear: a fast and accurate illumina paired-end read merger. *Bioinformatics*, 30:614–620.

Zhao, Y., Jin, Y., Lee, W. H., and Zhang, Y. (2006). Purification of a lysozyme from skin secretions of *Bufo andrewsi*. *Comparative Biochemistry and Physiology C-Toxicology Pharmacology*, 142:46–52.

Zheng, X. W., Levine, D., Shen, J., Gogarten, S. M., Laurie, C., and Weir, B. S. (2012). A high-performance computing toolset for relatedness and principal component analysis of snp data. *Bioinformatics*, 28:3326–3328.

Zuo, T., Wong, S., Pan Cheung, C., Lam, K., Lui, R., Cheung, K., Zhang, F., Tang, W., Ching, J., Wu, J., Chan, P., Sung, J., Yu, J., Chan, F., and Ng, S. (2018). Gut fungal dysbiosis correlates with reduced efficacy of fecal microbiota transplantation in *Clostridium difficile* infection. *Nature Communications*, 9:3663.

.1 Appendix 1: Bacterial indicator OTUs by disease dynamic 2015

Indicator OTU	Taxonomy	Infection	indval	*q* value
Otu000051	Planococcaceae	Enzootic	0.873021699	0.00161
Otu000117	Novosphingobium	Enzootic	0.825401253	0.00161
Otu000150	Actinomycetales	Enzootic	0.781264965	0.00161
Otu000197	Blastococcus	Enzootic	0.775455063	0.00161
Otu000121	Proteobacteria	Enzootic	0.74317053	0.00161
Otu000094	Nocardioidaceae	Enzootic	0.742140577	0.003389474
Otu000038	Burkholderiales	Enzootic	0.734742835	0.003659091
Otu000064	Rhizobiales	Enzootic	0.733387187	0.005278689
Otu000129	Beijerinckiaceae	Enzootic	0.72785104	0.00161
Otu000059	Betaproteobacteria	Enzootic	0.71424298	0.005944615
Otu000362	Rhizobiales	Enzootic	0.7081517	0.00161
Otu000135	Bradyrhizobiaceae	Enzootic	0.682894502	0.015212598
Otu000310	Rhizobiales	Enzootic	0.680807249	0.002385185
Otu000073	Solirubrobacterales	Enzootic	0.653832456	0.00301875
Otu000241	Devosia	Enzootic	0.651676829	0.022717791
Otu000074	Sphingomonadaceae	Enzootic	0.64226749	0.017233803
Otu000776	Acidimicrobiales	Enzootic	0.636455916	0.003864
Otu000068	Alphaproteobacteria	Enzootic	0.632825572	0.009734884
Otu000125	Modestobacter	Enzootic	0.625	0.002385185
Otu000224	Gemmatimonas	Enzootic	0.625	0.00161
Otu000571	Singulisphaera	Enzootic	0.625	0.002385185
Otu000110	Rhizobiales	Enzootic	0.623199658	0.00161
Otu000118	Hymenobacter	Enzootic	0.620118683	0.024341667
Otu000193	Spartobacteria	Enzootic	0.618942864	0.003864
Otu000599	Phenylobacterium	Enzootic	0.61771789	0.003389474
Otu000205	Actinomycetales	Enzootic	0.611243501	0.002385185
Otu000234	unclassified	Enzootic	0.60755814	0.004860377
Otu000133	Actinomycetales	Enzootic	0.607214317	0.005175
Otu000294	Sphingomonas	Enzootic	0.600970246	0.011816514
Otu000402	Geobacter	Enzootic	0.600500494	0.003389474
Otu000314	Conexibacter	Enzootic	0.59375	0.002385185
Otu000748	Acidobacteria	Enzootic	0.59375	0.00161
Otu000311	Chitinophagaceae	Enzootic	0.591951253	0.003659091
Otu000109	Streptococcus	Enzootic	0.587794634	0.020774194
Otu000158	Actinoallomurus	Enzootic	0.587621956	0.00301875
Otu000161	Methylobacterium	Enzootic	0.581172389	0.011618557
Otu000306	Ferruginibacter	Enzootic	0.57863193	0.011304255
Otu000420	Betaproteobacteria	Enzootic	0.578169844	0.003659091
Otu000232	Rhizobiales	Enzootic	0.576906028	0.011816514
Otu000590	Acidobacteria	Enzootic	0.576456311	0.002385185
Otu000143	Methylobacterium	Enzootic	0.573569131	0.041382031
Otu000392	Actinomycetales	Enzootic	0.561425501	0.010375556
Otu000308	Rhizobiales	Enzootic	0.558207131	0.003389474
Otu000196	Rhizobiales	Enzootic	0.551571038	0.003389474
Otu000067	Luteolibacter	Enzootic	0.542659471	0.019489474

Otu000217	Acidobacteria	Enzootic	0.540935546	0.00853494
Otu000450	Acidobacteria	Enzootic	0.539214101	0.005278689
Otu000536	Rhizobiales	Enzootic	0.53865	0.007397297
Otu000305	Rhizobiales	Enzootic	0.53125	0.003659091
Otu000606	Acetobacteraceae	Enzootic	0.53125	0.002385185
Otu000644	Acidobacteria	Enzootic	0.53125	0.003864
Otu000223	Mycobacterium	Enzootic	0.527136559	0.028075862
Otu000346	Acidobacteria	Enzootic	0.516626344	0.017233803
Otu000447	Acetobacteraceae	Enzootic	0.514675357	0.011816514
Otu000226	Conexibacter	Enzootic	0.512084718	0.028213333
Otu000594	Caulobacter	Enzootic	0.511108137	0.010375556
Otu000495	Mucilaginibacter	Enzootic	0.507295092	0.010733333
Otu000240	Acetobacteraceae	Enzootic	0.5	0.005175
Otu000533	Rhizobiales	Enzootic	0.5	0.003389474
Otu000618	Mucilaginibacter	Enzootic	0.5	0.006155882
Otu000854	Armatimonas	Enzootic	0.5	0.003659091
Otu000011	Chryseobacterium	Epizootic	0.928215464	0.00161
Otu000162	Deinococcus	Epizootic	0.884067832	0.00161
Otu000095	Stenotrophomonas	Epizootic	0.83990595	0.00161
Otu000010	Exiguobacterium	Epizootic	0.82918798	0.00161
Otu000024	Brevundimonas	Epizootic	0.812367277	0.003864
Otu000016	Flavobacterium	Epizootic	0.804619447	0.00301875
Otu000237	Shinella	Epizootic	0.757746739	0.00161
Otu000084	Acinetobacter	Epizootic	0.731545094	0.00161
Otu000458	Flavobacterium	Epizootic	0.72018205	0.00161
Otu000014	Rhizobiales	Epizootic	0.687009629	0.041656506
Otu000060	Sphingobacterium	Epizootic	0.685920906	0.005278689
Otu000015	Acinetobacter	Epizootic	0.680382642	0.016347692
Otu000103	Parachlamydia	Epizootic	0.668138607	0.00161
Otu000043	Sphingobacterium	Epizootic	0.658310479	0.003659091
Otu000289	Rhodococcus	Epizootic	0.651255167	0.02568764
Otu000005	Stenotrophomonas	Epizootic	0.637746961	0.041452874
Otu000054	Pseudomonas	Epizootic	0.621148959	0.032627434
Otu000369	Devosia	Epizootic	0.617524932	0.005622222
Otu000113	Xanthomonadaceae	Epizootic	0.613074388	0.041791489
Otu000542	Sphingopyxis	Epizootic	0.586181722	0.00301875
Otu000057	Sphingomonadaceae	Epizootic	0.571846691	0.018526027
Otu000194	Nocardioides	Epizootic	0.555095604	0.022074214
Otu000033	Acinetobacter	Epizootic	0.531902108	0.013305785
Otu000332	Phyllobacterium	Epizootic	0.505011595	0.005622222
Otu000330	Pseudomonas	Epizootic	0.500645233	0.00301875

.2 Appendix 2: Bacterial indicator OTUs by population 2015

Indicator OTU	Taxonomy	Population	indval	*q* value
Otu000110	Rhizobiales	Acherito	0.81312729	0.00410714
Otu000562	Acetobacteraceae	Acherito	0.7985348	0.00410714
Otu000346	Acidobacteria	Acherito	0.79166562	0.03333333
Otu000577	Actinomycetales	Acherito	0.76418787	0.02172222
Otu000919	Alphaproteobacteria	Acherito	0.68916009	0.02719595
Otu000522	Geodermatophilaceae	Acherito	0.68479686	0.0184
Otu001383	Acidobacteria	Acherito	0.67346939	0.02211539
Otu000676	Alphaproteobacteria	Acherito	0.66826215	0.02475694
Otu000825	Actinobacteria	Acherito	0.66734075	0.01848214
Otu000640	Geobacter	Acherito	0.65416286	0.02475694
Otu000161	Methylobacterium	Acherito	0.65358712	0.0184
Otu000241	Devosia	Acherito	0.65226517	0.01369048
Otu001153	Acidobacteria	Acherito	0.64285714	0.02211539
Otu000308	Rhizobiales	Acherito	0.63637008	0.02211539
Otu001311	Actinomycetales	Acherito	0.63265306	0.02908046
Otu000755	Mucilaginibacter	Acherito	0.63137755	0.02967742
Otu000650	Blastococcus	Acherito	0.62961211	0.02908046
Otu000495	Mucilaginibacter	Acherito	0.62811902	0.02211539
Otu000723	Acidobacteria	Acherito	0.61507937	0.02475694
Otu000100	Acidobacteria	Acherito	0.61194284	0.03440029
Otu000638	Acidobacteria	Acherito	0.60084034	0.02967742
Otu000158	Actinoallomurus	Acherito	0.60001132	0.03210417
Otu001027	Actinomycetales	Acherito	0.58874459	0.02908046
Otu000121	unclassified	Acherito	0.58557296	0.00676471
Otu000644	Acidobacteria	Acherito	0.58540373	0.02908046
Otu001736	Caulobacteraceae	Acherito	0.57142857	0.02908046
Otu002749	unclassified	Acherito	0.57142857	0.02211539
Otu000319	Mucilaginibacter	Acherito	0.56774648	0.02211539
Otu000073	Solirubrobacterales	Acherito	0.56337639	0.03440029
Otu001149	Acetobacteraceae	Acherito	0.56231003	0.03182039
Otu001179	Acidobacteria	Acherito	0.55990783	0.02836667
Otu001077	Asticcacaulis	Acherito	0.55966293	0.03214567
Otu000507	Solirubrobacterales	Acherito	0.55429464	0.03210417
Otu000478	Intrasporangiaceae	Acherito	0.54267815	0.04772604
Otu000632	Rhizobiales	Acherito	0.54238293	0.03210417
Otu000196	Rhizobiales	Acherito	0.5333923	0.03440029
Otu000133	Actinomycetales	Acherito	0.52718287	0.03440029
Otu000946	Acidimicrobiales	Acherito	0.52156334	0.03210417
Otu001058	Phenylobacterium	Acherito	0.51875345	0.03214567
Otu001641	Armatimonadetes	Acherito	0.5170068	0.03440029
Otu001756	Acidobacteria	Acherito	0.51428571	0.03210417
Otu000186	Bacteroidetes	Acherito	0.51172708	0.03440029
Otu001208	unclassified	Acherito	0.51020408	0.03322222
Otu000406	Singulisphaera	Acherito	0.50793651	0.03440029
Otu001151	Betaproteobacteria	Acherito	0.50136659	0.03440029

Otu001467	Gammaproteobacteria	Acherito	0.5	0.02967742
Otu001561	Chitinophagaceae	Acherito	0.5	0.03210417
Otu001722	Geothrix	Acherito	0.5	0.03105
Otu001848	Alphaproteobacteria	Acherito	0.5	0.03440029
Otu001938	Caulobacteraceae	Acherito	0.5	0.02908046
Otu001972	Alphaproteobacteria	Acherito	0.5	0.03440029
Otu000016	Flavobacterium	Ansabere	0.76684234	0.00410714
Otu000330	Pseudomonas	Ansabere	0.57042814	0.03440029
Otu000084	Acinetobacter	Ansabere	0.54522162	0.03440029
Otu000002	Comamonadaceae	Ansabere	0.52226478	0.03440029
Otu000162	Deinococcus	Arlet	0.93262294	0.00410714
Otu000095	Stenotrophomonas	Arlet	0.9273617	0.00410714
Otu000010	Exiguobacterium	Arlet	0.83266899	0.01210526
Otu000237	Shinella	Arlet	0.73895059	0.03440029
Otu000043	Sphingobacterium	Arlet	0.69453823	0.03408929
Otu000458	Flavobacterium	Arlet	0.68322395	0.03105
Otu000024	Brevundimonas	Arlet	0.66254904	0.02211539
Otu000103	Parachlamydia	Arlet	0.62685821	0.03210417
Otu000542	Sphingopyxis	Arlet	0.54330213	0.03440029
Otu000301	Pedobacter	Arlet	0.54117299	0.02908046
Otu001794	Paracoccus	Arlet	0.5	0.03105
Otu000340	unclassified	Lhurs	0.87347158	0.00410714
Otu000058	Proteobacteria	Lhurs	0.86729703	0.01829546
Otu000300	Sphingomonadales	Lhurs	0.85933504	0.00410714
Otu001060	unclassified	Lhurs	0.83311195	0.00410714
Otu000483	Lysobacter	Lhurs	0.82894843	0.00410714
Otu000245	Acidimicrobiales	Lhurs	0.81915858	0.00410714
Otu000616	unclassified	Lhurs	0.81711616	0.00676471
Otu000098	Ilumatobacter	Lhurs	0.81437783	0.00410714
Otu000387	Arenimonas	Lhurs	0.80764377	0.00676471
Otu000609	Sphingomonas	Lhurs	0.8075337	0.00410714
Otu000563	Acidimicrobiales	Lhurs	0.79895875	0.00410714
Otu000174	Haliea	Lhurs	0.75992939	0.0184
Otu000785	Solirubrobacterales	Lhurs	0.73763474	0.01848214
Otu000107	unclassified	Lhurs	0.72787141	0.00410714
Otu000307	Actinomycetales	Lhurs	0.72727273	0.01982759
Otu000744	Xanthomonadaceae	Lhurs	0.72727273	0.02172222
Otu001451	Actinobacteria	Lhurs	0.72727273	0.02172222
Otu001460	Rhizobiales	Lhurs	0.72727273	0.02172222
Otu001672	unclassified	Lhurs	0.72727273	0.02172222
Otu001438	unclassified	Lhurs	0.72681126	0.0215625
Otu000356	unclassified	Lhurs	0.72001978	0.02172222
Otu001477	Nocardioides	Lhurs	0.7113325	0.02452206
Otu001443	unclassified	Lhurs	0.71043062	0.02211539
Otu000597	Verrucomicrobiaceae	Lhurs	0.69978132	0.02172222
Otu000521	Rhizobiales	Lhurs	0.68359839	0.03105

Otu000047	Gammaproteobacteria	Lhurs	0.67687983	0.03210417
Otu000805	Xanthomonadaceae	Lhurs	0.66875653	0.01369048
Otu000574	Proteobacteria	Lhurs	0.66611717	0.02211539
Otu000067	Luteolibacter	Lhurs	0.65316803	0.02967742
Otu001697	Terrimonas	Lhurs	0.64646465	0.02211539
Otu000070	Betaproteobacteria	Lhurs	0.6449953	0.02719595
Otu000104	Nocardioides	Lhurs	0.6403193	0.00958333
Otu001360	Gammaproteobacteria	Lhurs	0.64031621	0.02172222
Otu000659	Acidobacteria	Lhurs	0.63778727	0.02908046
Otu001030	Actinobacteria	Lhurs	0.63636364	0.02211539
Otu001933	Actinobacteria	Lhurs	0.63636364	0.01848214
Otu001966	unclassified	Lhurs	0.63636364	0.02211539
Otu003166	Actinobacteria	Lhurs	0.63636364	0.02172222
Otu000934	Actinobacteria	Lhurs	0.63489397	0.02475694
Otu000239	Xanthomonadaceae	Lhurs	0.62657343	0.0215625
Otu001562	Actinobacteria	Lhurs	0.62255693	0.02172222
Otu001171	Nitrospira	Lhurs	0.62056228	0.02172222
Otu000388	unclassified	Lhurs	0.61619073	0.02172222
Otu000416	Acidobacteria	Lhurs	0.60158497	0.02211539
Otu000382	Actinomycetales	Lhurs	0.59725749	0.02211539
Otu000870	Adhaeribacter	Lhurs	0.59000602	0.02211539
Otu000250	Spartobacteria	Lhurs	0.5885654	0.02908046
Otu001753	Acidobacteria	Lhurs	0.58251748	0.02211539
Otu000667	Acidobacteria	Lhurs	0.5756505	0.03333333
Otu000322	Verrucomicrobiaceae	Lhurs	0.56916996	0.03440029
Otu000197	Blastococcus	Lhurs	0.5676105	0.02211539
Otu002517	unclassified	Lhurs	0.56540727	0.02265152
Otu000589	Ilumatobacter	Lhurs	0.55812629	0.03210417
Otu000273	unclassified	Lhurs	0.54545455	0.03440029
Otu000448	Actinomycetales	Lhurs	0.54545455	0.02172222
Otu000818	Acidobacteria	Lhurs	0.54545455	0.02908046
Otu001862	unclassified	Lhurs	0.54545455	0.03182039
Otu002065	Alphaproteobacteria	Lhurs	0.54545455	0.03210417
Otu002199	Actinobacteria	Lhurs	0.54545455	0.03440029
Otu002308	Actinobacteria	Lhurs	0.54545455	0.02211539
Otu002781	unclassified	Lhurs	0.54545455	0.02402985
Otu000057	Sphingomonadaceae	Lhurs	0.5390406	0.03210417
Otu001221	Sphingomonadaceae	Lhurs	0.53601111	0.03105
Otu000450	Acidobacteria	Lhurs	0.53311395	0.03440029
Otu000266	Acidobacteria	Lhurs	0.5319714	0.03440029
Otu000351	Acidobacteria	Lhurs	0.52264086	0.03214567
Otu000285	Pedobacter	Lhurs	0.52155016	0.03210417
Otu000949	unclassified	Lhurs	0.52135816	0.03182039
Otu000064	Rhizobiales	Lhurs	0.51907925	0.03841814
Otu000527	unclassified	Lhurs	0.51193499	0.02211539
Otu000277	Acidimicrobiales	Lhurs	0.50713355	0.03425532

Otu000165	Bacteroidetes	Lhurs	0.50195527	0.03440029
Otu000194	Nocardioides	Lhurs	0.50030285	0.03440029
Otu000268	Sphingomonadaceae	Puits	0.92116126	0.02908046
Otu001003	Chthonomonas	Puits	0.67385445	0.0215625
Otu000395	Sphingomonas	Puits	0.64520767	0.03214567
Otu000068	Alphaproteobacteria	Puits	0.63222002	0.03440029
Otu000567	Chitinophagaceae	Puits	0.60406771	0.03248092
Otu000027	Pedobacter	Puits	0.60160579	0.04271429
Otu000118	Hymenobacter	Puits	0.5881087	0.0365641
Otu000224	Gemmatimonas	Puits	0.57495228	0.03210417
Otu002586	Gemmata	Puits	0.57142857	0.02967742
Otu000754	Conexibacter	Puits	0.5665996	0.03607239
Otu002411	unclassified	Puits	0.55555556	0.02908046
Otu000125	Modestobacter	Puits	0.55137845	0.03440029
Otu000903	unclassified	Puits	0.55102041	0.03322222
Otu001244	Gemmatimonas	Puits	0.54658385	0.03105
Otu001798	Amycolatopsis	Puits	0.54493851	0.02211539
Otu001519	Actinobacteria	Puits	0.54476191	0.03210417
Otu001664	Actinobacteria	Puits	0.53968254	0.03214567
Otu001524	Rhizobiales	Puits	0.53781513	0.03440029
Otu000767	Acidobacteria	Puits	0.53571429	0.03105
Otu000605	Chitinophagaceae	Puits	0.52895211	0.03206731
Otu001738	Acidobacteria	Puits	0.51428571	0.03440029
Otu000611	Gammaproteobacteria	Puits	0.51212938	0.03440029
Otu000469	Spartobacteria	Puits	0.50965251	0.03440029
Otu001739	Acidobacteria	Puits	0.50793651	0.03248092
Otu003055	unclassified	Puits	0.50793651	0.03210417
Otu003506	unclassified	Puits	0.50793651	0.02967742
Otu001094	Gemmatimonas	Puits	0.50691244	0.03440029
Otu000634	Hymenobacter	Puits	0.50666137	0.03440029
Otu002496	Planctomyces	Puits	0.5	0.03440029

.3 Appendix 3: KO terms with LDA score > 2.00

Enzootic differential functional group	**LDA score**	**Epizootic differential function group**	**LDA score**
ABC.SN.A;NitT/TauT family transport system ATP-binding protein	2.21	APOD; apolipoprotein D and lipocalin family protein	2.05
NitT/TauT family transport system permease protein	2.27	TC.FEV.OM; iron complex outer membrane receptor protein	2.70
whiB1_2_3_4; WhiB family transcriptional regulator, redox-sensing transcriptional regulator	2.11		
putative drug exporter of the RND superfamily	2.19		
iron complex transport system substrate-binding protein	2.23		
ABC.PE.A1; peptide/nickel transport system ATP-binding protein	2.00		
ABC.PE.P; peptide/nickel transport system permease protein	2.10		
ABC.SN.S; NitT/TauT family transport system substrate-binding protein	2.24		
prkC, stkP; eukaryotic-like serine/threonine-protein kinase	2.40		

.4 Appendix 4: Summary of *Bd* isolates used for whole genome sequencing

Isolate	Location	Year	Total reads	Reads mapped to JEL423	Mean read length	Sequencing depth	Coverage (%)	Filtered SNPs	Filtered INDELs	Filtered transitions/ transversions
Acherito.1.2_15	Acherito	2015	19320219	17510948	124.4287	45.85	98.25426	59295	7269	4.24
Acherito.3.1_15	Acherito	2015	19016682	17587733	124.3372	46.02	98.2508	58752	7229	4.22
Acherito.4.1_15	Acherito	2015	17358451	16365741	124.3221	42.85	98.25088	58961	7177	4.19
Acherito.5.2_15	Acherito	2015	14818906	13751064	124.3376	35.91	98.24169	58400	7175	4.25
Acherito.c_15	Acherito	2015	17565902	16152969	124.4933	42.25	98.24089	59451	7277	4.24
Acherito.d_15	Acherito	2015	18390712	16870519	124.5462	44.12	98.24546	59918	7289	4.24
ADMALA	Malaga	2012	27524650	25449247	99.45645	53.13	98.44997	50509	6452	4.3
ANS_13No1	Ansabere	2013	44917754	42676404	99.03148	88.49	98.32794	56741	6978	4.29
ANS_13No10	Ansabere	2013	65695345	63418641	97.80449	125.03	98.40129	55394	6599	4.35
ANS_13No12	Ansabere	2013	46553627	44672377	98.86896	92.59	98.33	56334	6829	4.31
ANS_13No4	Ansabere	2013	44712592	42057498	99.07055	87.27	98.32485	57722	7013	4.32
ANS_13No7	Ansabere	2013	40125338	38736388	97.77966	77.63	98.33197	54703	6512	4.34
Ansabere.6.1_15	Ansabere	2015	17876243	16468504	124.2767	43.06	98.25508	58657	7198	4.22
Arlet_13No1	Arlet	2013	34096999	31919421	98.91326	66.24	98.30678	55684	6805	4.32
Arlet_13No2	Arlet	2013	44974936	42135492	98.90642	87.62	98.31885	56554	6892	4.34
Arlet_13No4	Arlet	2013	57091066	54472300	97.87916	110.8	98.35757	55615	6636	4.31
Arlet_13No6	Arlet	2013	65962615	63199569	97.67509	127.84	98.36081	55775	6627	4.32
Arlet_13No8	Arlet	2013	38360209	36512863	99.05865	76.07	98.31484	56531	6883	4.34
Arlet.a_15	Arlet	2015	14686162	13562780	124.364	35.51	98.22778	58011	7159	4.23
Arlet.K_15	Arlet	2015	18149375	16904577	124.3616	44.17	98.24669	58528	7172	4.22
CORN1	Cornwall	2012	28804659	27134395	99.40623	56.54	98.47062	56819	6785	4.44
CORN1B	Cornwall	2012	25273736	23228769	99.46589	48.5	98.43847	57119	6854	4.45
IA_11	Acherito	2011	34512871	32517704	99.00635	66.84	98.31197	56154	6840	4.34
IA_12No1	Acherito	2012	39333849	36881663	99.08777	76.12	98.31788	56225	6810	4.31
IA_12No10	Acherito	2012	38347577	36114008	98.79842	74.46	98.31492	55097	6690	4.32
IA_12No12	Acherito	2012	53717588	51052961	98.73101	104.02	98.35349	56475	6903	4.31
IA_12No3	Acherito	2012	37352155	35157709	98.96685	72.33	98.3152	56047	6835	4.32
IA_12No4	Acherito	2012	48341935	45355584	98.98111	93.47	98.33494	56696	6924	4.3
IA_12No5	Acherito	2012	45714370	43748731	98.72855	87.85	98.35812	55883	6855	4.35
IA_12No8	Acherito	2012	44658328	42471016	98.72919	86.07	98.34968	56121	6883	4.31
IA_12No9	Acherito	2012	58883539	55505860	98.72423	114.25	98.34433	57134	6953	4.28
IA_13No1	Acherito	2013	33782176	31647818	98.95904	65.67	98.31885	57328	6937	4.33
IA_13No12	Acherito	2013	69706609	66034123	98.63422	133.6	98.39651	57172	6841	4.25
IA_13No13_48	Acherito	2013	36184676	33453973	98.94018	69.24	98.32309	56181	6888	4.33
IA_13No13_60	Acherito	2013	47652412	45775278	98.48713	91.35	98.35221	55563	6699	4.37
IA_13No17	Acherito	2013	49299078	46678837	99.05004	96.95	98.32591	53709	6830	4.21
IA_13No6	Acherito	2013	36678691	35084778	99.08121	72.69	98.31466	56137	6871	4.34
IA_13No8	Acherito	2013	35010431	32153654	99.09753	66.09	98.3201	55124	6717	4.34
IA042_Highly_passaged	Acherito	2004	52179230	49750346	98.65392	96.8	98.36262	55163	6734	4.32
IA042_Low_passage	Acherito	2004	42212836	40155271	98.72532	81.03	98.36023	55799	6782	4.34

IA043_cryo	Acherito	2004	57197358	51787562	97.98511	102.28	98.37032	55957	6659	4.33
IA12	Acherito	2012	29991234	27516745	99.4031	57.17	98.31914	54237	6651	4.38
LHURS_11No1	Lhurs	2011	45363031	43089427	99.01004	87.7	98.33664	56376	6776	4.35
LHURS_11No1 1	Lhurs	2011	37389666	34696434	98.97411	71.44	98.32068	56189	6866	4.3
LHURS_11No7	Lhurs	2011	44274635	42419096	99.00445	86.63	98.30984	55259	6703	4.32
LHURS_11No8	Lhurs	2011	30891333	29441101	98.93901	59	98.32083	54709	6673	4.33
Lhurs_13No11	Lhurs	2013	31059479	29637273	99.00147	61.7	98.29957	55563	6787	4.34
Lhurs_13No13	Lhurs	2013	41196510	39294190	98.88586	81.79	98.316	57356	6944	4.32
Lhurs_13No14	Lhurs	2013	36899396	33817672	98.9042	70.01	98.31669	55591	6780	4.29
Lhurs_13No2	Lhurs	2013	45539693	42929004	98.86253	89.06	98.32739	56180	6791	4.31
Lhurs_13No4	Lhurs	2013	63116803	59832617	98.90221	124.56	98.33729	58052	7009	4.31
LHURS8	Lhurs	2011	24712121	22928844	98.0394	47.29	98.24905	55412	6720	4.39
MAL05	Kent	2011	24539566	22803372	99.17093	47.42	98.45053	53192	6558	4.37
MODS27.3	Sardinia	2010	21268430	20771713	97.04827	41.83	98.49348	49379	5952	4.46
MODS28	Sardinia	2010	36714284	35810702	97.14007	72.83	98.51613	50882	6208	4.41
PENNEWT	Penalara	2011	27147515	24828306	99.45558	51.86	98.45052	53936	6601	4.3
PENS-2.4	Penalara	2014	10193531	8417740	125	22.05	98.41073	57516	7168	4.36
PENS-9.2	Penalara	2014	9882878	8443268	125	22.12	98.41268	58008	7192	4.38
PicosAo1	Picos de Europa	2010	28364282	26213326	99.42604	54.52	98.5237	51057	6488	4.36
PNP15150	Lhurs	2015	14039047	12838753	124.3521	33.52	98.26508	58720	7190	4.28
PNP15152	Lhurs	2015	21182557	19406788	124.3029	50.75	98.25309	60077	7327	4.24
PNP15153	Lhurs	2015	19762525	18114495	124.2471	47.36	98.25188	57934	7122	4.23
PNP15156	Lhurs	2015	19002624	17214415	124.2401	45.04	98.25671	59575	7294	4.22
PUITS_11	Puits	2011	42502853	39550846	98.81026	81.12	98.33543	55867	6788	4.32
PUITS_12No3	Puits	2012	43948798	41120065	98.8365	85.02	98.33134	56464	6842	4.31
PUITS_12No4	Puits	2012	50106537	47227462	98.82482	96.86	98.33982	56192	6799	4.32
PUITS_12No5	Puits	2012	48585982	45181308	98.79112	93.74	98.32968	56623	6890	4.31
PUITS_12No7	Puits	2012	44119119	41057695	98.82993	84.55	98.32702	55982	6792	4.32
PUITS_12No8	Puits	2012	48799895	45823290	98.71642	93.49	98.38667	54976	6689	4.31
SFBC014	Cumbria	2010	26437828	25865276	96.94762	52.01	98.43927	54254	6297	4.53
SP10	Sardinia	2010	30377369	28905902	97.14064	56.48	98.52675	47007	6081	4.35
TER_1.1	Maestrazgo	2013	19539780	17928486	124.0832	47.1	98.47481	64411	7507	4.32
TER_3.1	Teruel	2014	16478234	12800235	124.4556	33.44	98.46922	63291	7577	4.32
TER_4.2	Teruel	2014	22364758	20347254	124.2755	53.13	98.47611	65776	7575	4.35
TORO1	Toro	2011	24573588	23293465	99.1146	48.34	98.4659	51334	6474	4.27
UKBEL	Surrey	2012	23451047	21846719	99.36159	45.58	98.46896	59671	7000	4.49
UKBER	Surrey	2012	29917264	28057538	99.40134	58.48	98.49657	60769	7098	4.5
UKMAB	Cumbria	2012	29407628	27365719	99.40606	57	98.45606	56599	6795	4.48
UKSHB	Cumbria	2012	27552036	26111413	99.45199	54.28	98.52456	50164	6414	4.3
UKTVB	Kent	2007	20389635	19276461	124.5551	50.49	98.40343	57925	7023	4.19
VA02	Valencia	2008	17948196	16029601	124.1583	42.01	98.47356	61611	7301	4.31

.5 Appendix 5: Wild versus captive bacterial indicator OTUs for *T. cristatus*

OTU	Taxonomy	Status	indval	*q*-value
Otu033	Micrococcaceae	Captive	0.805055292	0.000341772
Otu050	Arthrobacter	Captive	0.78038181	0.010344828
Otu081	Leucobacter	Captive	0.936342593	0.00012
Otu035	Bacteriovorax	Captive	0.983376212	0.00012
Otu006	Comamonadaceae	Captive	0.774839318	0.00012
Otu089	Herminiimonas	Captive	0.986506747	0.00012
Otu118	Delftia	Captive	0.928675981	0.00012
Otu010	Brevundimonas	Captive	0.814351712	0.00012
Otu026	Rheinheimera	Captive	0.930450302	0.00012
Otu003	Flavobacterium	Captive	0.815462848	0.00012
Otu023	Flavobacteriaceae	Captive	0.851438849	0.004813953
Otu196	Lactococcus	Captive	0.855187638	0.00012
Otu070	Methylophilus	Captive	0.92588165	0.00012
Otu004	Acinetobacter	Captive	0.828529693	0.0005625
Otu005	Cellvibrio	Captive	0.995511187	0.00012
Otu072	Moraxellaceae	Captive	0.857583403	0.001508982
Otu028	Devosia	Captive	0.731738969	0.001508982
Otu034	Rhizobium	Captive	0.715846076	0.000773006
Otu053	Brucellaceae	Captive	0.704814815	0.000773006
Otu092	Shinella	Captive	0.891349481	0.00012
Otu009	Sphingobacterium	Captive	0.796629377	0.000341772
Otu039	Sphingobacteriales	Captive	0.925360652	0.000232258
Otu016	Stenotrophomonas	Captive	0.76317716	0.000773006
Otu060	Acidimicrobiales	Wild	0.997439181	0.00012
Otu110	Ilumatobacter	Wild	0.933333333	0.00012
Otu093	Acidobacteria	Wild	0.998156682	0.00012
Otu145	Acidobacteria	Wild	1	0.00012
Otu129	Acidobacteria	Wild	0.928176796	0.00012
Otu132	Acidobacteria	Wild	1	0.00012
Otu073	Acidobacteria	Wild	1	0.00012
Otu038	Acidobacteria	Wild	1	0.00012
Otu040	Nocardioides	Wild	0.941479401	0.00012
Otu058	Rhodococcus	Wild	0.712482468	0.01512
Otu076	Mycobacterium	Wild	0.993048659	0.00012
Otu085	Nocardioidaceae	Wild	0.973753281	0.00012
Otu086	Pseudonocardia	Wild	0.999158957	0.00012
Otu094	Micromonosporaceae	Wild	1	0.00012
Otu096	Aeromicrobium	Wild	0.939144737	0.00012

OTU	Taxonomy	Status	indval	*q*-value
Otu098	Sanguibacter	Wild	0.896178803	0.00012
Otu131	Intrasporangiaceae	Wild	0.919648094	0.00012
Otu142	Pseudonocardiaceae	Wild	1	0.00012
Otu150	Streptomyces	Wild	1	0.00012
Otu165	Streptomycetaceae	Wild	0.933333333	0.00012
Otu167	Cellulomonas	Wild	1	0.00012
Otu203	Kineosporia	Wild	0.933333333	0.00012
Otu206	Agromyces	Wild	0.919531731	0.00012
Otu220	Nakamurellaceae	Wild	0.866666667	0.00012
Otu222	Marmoricola	Wild	0.933333333	0.00012
Otu233	Sporichthya	Wild	0.8	0.00012
Otu236	Actinoplanes	Wild	0.8	0.00012
Otu246	Kineosporiaceae	Wild	0.8	0.00012
Otu252	Williamsia	Wild	0.866666667	0.00012
Otu259	Blastococcus	Wild	0.8	0.00012
Otu264	Micromonospora	Wild	0.733333333	0.000232258
Otu271	Actinomycetospora	Wild	0.927083333	0.00012
Otu282	Rathayibacter	Wild	0.933333333	0.00012
Otu295	Kribbella	Wild	0.733333333	0.000232258
Otu303	Kineococcus	Wild	0.866666667	0.00012
Otu327	Geodermatophilus	Wild	1	0.00012
Otu347	Humicoccus	Wild	0.933333333	0.00012
Otu189	Geminicoccus	Wild	1	0.00012
Otu155	Pseudoalteromonas	Wild	0.976676385	0.00012
Otu299	Haliea	Wild	0.8	0.00012
Otu133	Armatimonas	Wild	0.8	0.00012
Otu124	Armatimonadetes	Wild	1	0.00012
Otu126	Bacillales	Wild	0.801748634	0.003282353
Otu143	Pasteuria	Wild	1	0.00012
Otu344	Bacillus	Wild	0.859064327	0.00012
Otu078	Ohtaekwangia	Wild	1	0.00012
Otu051	Peredibacter	Wild	0.722222222	0.002556213
Otu083	Oxalobacteraceae	Wild	0.815296015	0.001090909
Otu136	Massilia	Wild	0.834296724	0.00012
Otu151	Polaromonas	Wild	0.896732026	0.00012
Otu178	Burkholderia	Wild	0.927470687	0.00012
Otu181	Herbaspirillum	Wild	0.768758717	0.007179191
Otu197	Duganella	Wild	0.840091414	0.03579661
Otu221	Aquabacterium	Wild	0.784	0.00012

OTU	Taxonomy	Status	indval	*q*-value
Otu256	Naxibacter	Wild	0.85410628	0.00012
Otu071	Caulobacteraceae	Wild	0.86407767	0.00012
Otu103	Phenylobacterium	Wild	0.992084433	0.00012
Otu146	Caulobacter	Wild	0.916335541	0.00012
Otu283	Asticcacaulis	Wild	0.72335958	0.004315789
Otu069	Parachlamydiaceae	Wild	0.99726776	0.00012
Otu139	Chlamydiales	Wild	0.925866667	0.00012
Otu144	Parachlamydia	Wild	1	0.00012
Otu015	Enterobacteriaceae	Wild	0.705133442	0.044292135
Otu061	Yersinia	Wild	0.713217726	0.021375
Otu125	Buttiauxella	Wild	0.797311226	0.001607143
Otu088	Gemmatimonas	Wild	1	0.00012
Otu137	Streptococcus	Wild	0.827956989	0.000987805
Otu048	Legionella	Wild	1	0.00012
Otu095	Aquicella	Wild	0.933333333	0.00012
Otu031	Myxococcales	Wild	1	0.00012
Otu119	Polyangiaceae	Wild	1	0.00012
Otu148	Nannocystaceae	Wild	1	0.00012
Otu154	Chondromyces	Wild	0.933333333	0.00012
Otu043	Halomonas	Wild	0.979444444	0.00012
Otu087	OD1	Wild	0.8	0.00012
Otu082	Opitutus	Wild	1	0.00012
Otu198	Opitutaceae	Wild	0.866666667	0.00012
Otu045	Planctomycetaceae	Wild	0.991803279	0.00012
Otu049	Singulisphaera	Wild	0.993362832	0.00012
Otu121	Planctomyces	Wild	0.928421053	0.00012
Otu135	Gemmata	Wild	0.933333333	0.00012
Otu141	Zavarzinella	Wild	0.866666667	0.00012
Otu002	Pseudomonas	Wild	0.894314074	0.00012
Otu014	Rhizobiales	Wild	0.725316115	0.000341772
Otu056	Methylobacterium	Wild	0.992240041	0.00012
Otu105	Bradyrhizobiaceae	Wild	0.986373166	0.00012
Otu111	Aurantimonas	Wild	0.984435798	0.00012
Otu128	Bosea	Wild	0.832134293	0.000232258
Otu164	Mesorhizobium	Wild	0.992031873	0.00012
Otu205	Microvirga	Wild	0.78	0.00012
Otu213	Hyphomicrobium	Wild	0.733333333	0.000232258
Otu249	Phyllobacterium	Wild	0.856266667	0.00012
Otu274	Bradyrhizobium	Wild	0.996753247	0.00012

OTU	Taxonomy	Status	indval	*q*-value
Otu275	Rhodopseudomonas	Wild	1	0.00012
Otu277	Labrys	Wild	0.866666667	0.00012
Otu191	Amaricoccus	Wild	0.866666667	0.00012
Otu193	Rubellimicrobium	Wild	0.733333333	0.00012
Otu079	Acetobacteraceae	Wild	0.997584541	0.00012
Otu084	Roseomonas	Wild	0.983870968	0.00012
Otu140	Rhodospirillales	Wild	0.933333333	0.00012
Otu225	Acidisoma	Wild	0.733333333	0.00012
Otu296	Skermanella	Wild	0.863480392	0.00012
Otu161	Rickettsia	Wild	1	0.00012
Otu168	Rubrobacter	Wild	0.8	0.00012
Otu059	Solirubrobacterales	Wild	1	0.00012
Otu104	Solirubrobacter	Wild	1	0.00012
Otu113	Conexibacter	Wild	1	0.00012
Otu055	Spartobacteria	Wild	1	0.00012
Otu080	Spartobacteria	Wild	0.990922844	0.00012
Otu018	Chitinophagaceae	Wild	0.996061442	0.00012
Otu030	Sphingobacteriaceae	Wild	0.982032854	0.00012
Otu037	Mucilaginibacter	Wild	0.999727965	0.00012
Otu042	Hymenobacter	Wild	1	0.00012
Otu074	Spirosoma	Wild	1	0.00012
Otu101	Cytophagaceae	Wild	0.995098039	0.00012
Otu107	Ferruginibacter	Wild	1	0.00012
Otu171	Cytophaga	Wild	0.92845953	0.00012
Otu172	Adhaeribacter	Wild	0.8	0.00012
Otu177	Terrimonas	Wild	0.8	0.00012
Otu182	Larkinella	Wild	0.933333333	0.00012
Otu190	Chitinophaga	Wild	1	0.00012
Otu195	Flavitalea	Wild	1	0.00012
Otu212	Sediminibacterium	Wild	0.866666667	0.00012
Otu011	Sphingomonas	Wild	0.990428998	0.00012
Otu027	Sphingomonadaceae	Wild	0.995338831	0.00012
Otu063	Novosphingobium	Wild	0.979725701	0.00012
Otu108	Sphingomonadales	Wild	0.838095238	0.00012
Otu112	Sphingobium	Wild	0.990430622	0.00012
Otu158	Erythrobacteraceae	Wild	1	0.00012
Otu298	Altererythrobacter	Wild	0.8	0.00012
Otu090	Verrucomicrobia	Wild	1	0.00012
Otu001	Unclassified	Wild	0.847361771	0.00012

OTU	Taxonomy	Status	indval	*q*-value
Otu007	Proteobacteria	Wild	0.868037294	0.00012
Otu012	Bacteroidetes	Wild	0.878507555	0.00012
Otu013	Gammaproteobacteria	Wild	0.956131261	0.00012
Otu017	Alphaproteobacteria	Wild	0.979716024	0.00012
Otu025	Betaproteobacteria	Wild	0.864163823	0.00012
Otu036	Actinobacteria	Wild	0.989189189	0.00012
Otu057	Verrucomicrobia	Wild	1	0.00012
Otu062	Deltaproteobacteria	Wild	0.99704142	0.00012
Otu052	Luteolibacter	Wild	0.796347537	0.00012
Otu067	Verrucomicrobiaceae	Wild	0.862116992	0.00012
Otu114	Verrucomicrobium	Wild	1	0.00012
Otu127	Prosthecobacter	Wild	1	0.00012
Otu044	Xanthomonadaceae	Wild	0.85929396	0.00012
Otu116	Pseudoxanthomonas	Wild	0.993490643	0.00012
Otu130	Steroidobacter	Wild	1	0.00012
Otu147	Luteibacter	Wild	1	0.00012
Otu153	Lysobacter	Wild	0.923044619	0.00012
Otu209	Sinobacteraceae	Wild	0.8	0.00012
Otu217	Rhodanobacter	Wild	0.866666667	0.00012
Otu228	Hydrocarboniphaga	Wild	0.733333333	0.00012
Otu243	Arenimonas	Wild	0.933333333	0.00012
Otu330	Dokdonella	Wild	0.733333333	0.00012
Otu336	Xanthomonas	Wild	0.70617284	0.0005625

.6 Appendix 6: Wild versus captive bacterial indicator OTUs for *L. vulgaris*

OTU	Taxonomy	Status	indval	*q*-value
Otu093	Acidobacteria Gp1	wild	1	0.0001913
Otu145	Acidobacteria Gp10	wild	0.86666667	0.0001913
Otu129	Acidobacteria Gp16	wild	0.93333333	0.0001913
Otu132	Acidobacteria Gp3	wild	0.86666667	0.0001913
Otu073	Acidobacteria Gp4	wild	1	0.0001913
Otu038	Acidobacteria Gp6	wild	1	0.0001913
Otu060	Acidimicrobiales	wild	0.99679487	0.0001913
Otu110	Ilumatobacter	wild	0.86666667	0.0001913
Otu020	Actinomycetales	wild	0.89135654	0.0001913
Otu024	Microbacteriaceae	wild	0.85400458	0.0001913
Otu040	Nocardioides	wild	0.97139886	0.0001913
Otu058	Rhodococcus	wild	0.85073867	0.00097778
Otu076	Mycobacterium	wild	0.99210007	0.0001913
Otu077	Corynebacterium	wild	0.72916667	0.00434824
Otu085	Nocardioidaceae	wild	0.98529412	0.0001913
Otu086	Pseudonocardia	wild	0.98637317	0.0001913
Otu094	Micromonosporaceae	wild	0.93135593	0.0001913
Otu096	Aeromicrobium	wild	0.89023162	0.0001913
Otu098	Sanguibacter	wild	0.77507692	0.01413771
Otu131	Intrasporangiaceae	wild	0.9969697	0.0001913
Otu142	Pseudonocardiaceae	wild	1	0.0001913
Otu150	Streptomyces	wild	0.9295082	0.0001913
Otu165	Streptomycetaceae	wild	0.71703704	0.0001913
Otu167	Cellulomonas	wild	0.91014493	0.0001913
Otu203	Kineosporia	wild	1	0.0001913
Otu206	Agromyces	wild	0.75716846	0.01305495
Otu220	Nakamurellaceae	wild	0.99497487	0.0001913
Otu222	Marmoricola	wild	0.72614379	0.00035436
Otu246	Kineosporiaceae	wild	1	0.0001913
Otu247	Clavibacter	wild	0.93333333	0.0001913
Otu252	Williamsia	wild	0.9380531	0.0001913
Otu259	Blastococcus	wild	0.86666667	0.0001913
Otu271	Actinomycetospora	wild	1	0.0001913
Otu282	Rathayibacter	wild	0.8562249	0.0001913
Otu303	Kineococcus	wild	1	0.0001913
Otu316	Nesterenkonia	wild	0.73333333	0.00035436
Otu327	Geodermatophilus	wild	0.994709	0.0001913
Otu347	Humicoccus	wild	0.86666667	0.0001913
Otu050	Arthrobacter	Captive	0.85823443	0.00066835
Otu059	Solirubrobacterales	wild	0.99874844	0.0001913
Otu104	Solirubrobacter	wild	1	0.0001913
Otu113	Conexibacter	wild	0.99772727	0.0001913
Otu207	Patulibacter	wild	0.9529148	0.0001913
Otu036	Actinobacteria	wild	0.98947368	0.0001913
Otu189	Geminicoccus	wild	1	0.0001913

OTU	Taxonomy	Status	indval	*q*-value
Otu093	Acidobacteria Gp1	wild	1	0.0001913
Otu145	Acidobacteria Gp10	wild	0.86666667	0.0001913
Otu129	Acidobacteria Gp16	wild	0.93333333	0.0001913
Otu132	Acidobacteria Gp3	wild	0.86666667	0.0001913
Otu073	Acidobacteria Gp4	wild	1	0.0001913
Otu038	Acidobacteria Gp6	wild	1	0.0001913
Otu060	Acidimicrobiales	wild	0.99679487	0.0001913
Otu110	Ilumatobacter	wild	0.86666667	0.0001913
Otu020	Actinomycetales	wild	0.89135654	0.0001913
Otu024	Microbacteriaceae	wild	0.85400458	0.0001913
Otu040	Nocardioides	wild	0.97139886	0.0001913
Otu058	Rhodococcus	wild	0.85073867	0.00097778
Otu076	Mycobacterium	wild	0.99210007	0.0001913
Otu077	Corynebacterium	wild	0.72916667	0.00434824
Otu085	Nocardioidaceae	wild	0.98529412	0.0001913
Otu086	Pseudonocardia	wild	0.98637317	0.0001913
Otu094	Micromonosporaceae	wild	0.93135593	0.0001913
Otu096	Aeromicrobium	wild	0.89023162	0.0001913
Otu098	Sanguibacter	wild	0.77507692	0.01413771
Otu131	Intrasporangiaceae	wild	0.9969697	0.0001913
Otu142	Pseudonocardiaceae	wild	1	0.0001913
Otu150	Streptomyces	wild	0.9295082	0.0001913
Otu165	Streptomycetaceae	wild	0.71703704	0.0001913
Otu167	Cellulomonas	wild	0.91014493	0.0001913
Otu203	Kineosporia	wild	1	0.0001913
Otu206	Agromyces	wild	0.75716846	0.01305495
Otu220	Nakamurellaceae	wild	0.99497487	0.0001913
Otu222	Marmoricola	wild	0.72614379	0.00035436
Otu246	Kineosporiaceae	wild	1	0.0001913
Otu247	Clavibacter	wild	0.93333333	0.0001913
Otu252	Williamsia	wild	0.9380531	0.0001913
Otu259	Blastococcus	wild	0.86666667	0.0001913
Otu271	Actinomycetospora	wild	1	0.0001913
Otu282	Rathayibacter	wild	0.8562249	0.0001913
Otu303	Kineococcus	wild	1	0.0001913
Otu316	Nesterenkonia	wild	0.73333333	0.00035436
Otu327	Geodermatophilus	wild	0.994709	0.0001913
Otu347	Humicoccus	wild	0.86666667	0.0001913
Otu050	Arthrobacter	Captive	0.85823443	0.00066835
Otu059	Solirubrobacterales	wild	0.99874844	0.0001913
Otu104	Solirubrobacter	wild	1	0.0001913
Otu113	Conexibacter	wild	0.99772727	0.0001913
Otu207	Patulibacter	wild	0.9529148	0.0001913
Otu036	Actinobacteria	wild	0.98947368	0.0001913
Otu189	Geminicoccus	wild	1	0.0001913

Otu118	Delftia	Captive	0.85908017	0.0001913
Otu070	Methylophilus	Captive	0.91956522	0.00035436
Otu293	Chitinibacter	Captive	0.78123953	0.00066835
Otu092	Shinella	Captive	0.8	0.0001913
Otu025	Betaproteobacteria	wild	0.83703704	0.0001913
Otu069	Parachlamydiaceae	wild	1	0.0001913
Otu139	Chlamydiales	wild	0.86666667	0.0001913
Otu144	Parachlamydia	wild	0.72328767	0.00035436
Otu312	Truepera	wild	0.8	0.0001913
Otu051	Peredibacter	wild	0.81257414	0.00051097
Otu169	Vampirovibrio	wild	0.86666667	0.0001913
Otu035	Bacteriovorax	Captive	0.78164467	0.03344
Otu031	Myxococcales	wild	0.99948797	0.0001913
Otu119	Polyangiaceae	wild	1	0.0001913
Otu148	Nannocystaceae	wild	1	0.0001913
Otu154	Chondromyces	wild	0.8	0.0001913
Otu062	Deltaproteobacteria	wild	0.99807692	0.0001913
Otu023	Flavobacteriaceae	wild	0.81863231	0.00314286
Otu163	Cryomorphaceae	wild	0.73333333	0.0001913
Otu003	Flavobacterium	Captive	0.89834855	0.0001913
Otu155	Pseudoalteromonas	wild	0.91732909	0.0001913
Otu026	Rheinheimera	Captive	0.92674884	0.00051097
Otu015	Moraxellaceae	wild	0.83002659	0.00206747
Otu234	Pantoea	wild	0.93238579	0.0001913
Otu048	Legionella	wild	0.992	0.0001913
Otu095	Aquicella	wild	0.86182495	0.0001913
Otu043	Halomonas	wild	0.90287313	0.0001913
Otu002	Pseudomonas	wild	0.79624158	0.0001913
Otu004	Acinetobacter	Captive	0.97139216	0.0001913
Otu005	Cellvibrio	Captive	0.98343897	0.0001913
Otu072	Moraxellaceae	Captive	0.99889625	0.0001913
Otu013	Gammaproteobacteria	wild	0.94387981	0.0001913
Otu044	Xanthomonadaceae	wild	0.81813047	0.0001913
Otu116	Pseudoxanthomonas	wild	0.968	0.0001913
Otu130	Steroidobacter	wild	1	0.0001913
Otu147	Luteibacter	wild	1	0.0001913
Otu153	Lysobacter	wild	0.93333333	0.0001913
Otu209	Sinobacteraceae	wild	1	0.0001913
Otu243	Arenimonas	wild	0.8	0.0001913
Otu336	Xanthomonas	wild	0.8	0.0001913
Otu088	Gemmatimonas	wild	1	0.0001913
Otu087	OD1	wild	0.85932203	0.0001913
Otu082	Opitutus	wild	1	0.0001913
Otu198	Opitutaceae	wild	0.8	0.0001913
Otu045	Planctomycetaceae	wild	0.86666667	0.0001913
Otu049	Singulisphaera	wild	1	0.0001913

Otu135	Gemmata	wild	0.73333333	0.0001913
Otu141	Zavarzinella	wild	0.86666667	0.0001913
Otu055	Spartobacteria	wild	0.99776286	0.0001913
Otu080	Chitinophagaceae	wild	1	0.0001913
Otu008	Pedobacter	wild	0.82114949	0.0001913
Otu018	Chitinophagaceae	wild	0.99418345	0.0001913
Otu030	Sphingobacteriaceae	wild	0.88595094	0.00035436
Otu037	Mucilaginibacter	wild	0.99588868	0.0001913
Otu042	Hymenobacter	wild	0.99969798	0.0001913
Otu074	Spirosoma	wild	0.98669797	0.0001913
Otu101	Cytophagaceae	wild	0.98603352	0.0001913
Otu107	Ferruginibacter	wild	0.99275362	0.0001913
Otu171	Cytophaga	wild	0.83870968	0.0001913
Otu172	Adhaeribacter	wild	0.93333333	0.0001913
Otu182	Larkinella	wild	0.8	0.0001913
Otu190	Chitinophaga	wild	0.86321381	0.0001913
Otu195	Flavitalea	wild	0.86666667	0.0001913
Otu212	Sediminibacterium	wild	0.73333333	0.00035436
Otu223	Fibrella	wild	0.77746479	0.0001913
Otu238	Algoriphagus	wild	0.86666667	0.0001913
Otu009	Sphingobacterium	Captive	0.92558362	0.0001913
Otu001	unclassified	wild	0.8258789	0.0001913
Otu007	Proteobacteria	wild	0.92981919	0.0001913
Otu012	Bacteroidetes	wild	0.72508257	0.0369868
Otu057	Verrucomicrobia	wild	0.99443672	0.0001913
Otu052	Luteolibacter	wild	0.9638286	0.0001913
Otu067	Verrucomicrobiaceae	wild	0.70461539	0.01420435
Otu114	Verrucomicrobium	wild	0.93333333	0.0001913
Otu127	Prosthecobacter	wild	1	0.0001913

.7 Appendix 7: Mean Bsal prevalence (95% CI) and proportion of animals with lesions (%) for *Lissotriton vulgaris* and *Triturus cristatus*

Species	**Day 1**	**Day 7**	**Day 15**	**Day 21**	**Day 28**	**Day 35**	**Day 42**	**Day 49**	**Day 56**
L. vulgaris prevalence (%)	0.0 (0.0, 30.8)	0.0 (0.0, 30.8)	10.0 (0.25, 44.5)	20.0 (2.5, 55.6)	30.0 (6.7, 65.2)	22.2 (2.8, 60.0)	11.1 (0.28, 48.2)	0.0 (0.0, 33.6)	0.0 (0.0, 33.6)
L. vulgaris lesions (%)	0.0	0.0	10.0	30.0	30.0	22.2	22.2	22.2	0.0
T. cristatus prevalence (%)	0.0 (0.0, 30.8)	0.0 (0.0, 30.8)	30.0 (6.7, 65.2)	40 (12.2, 73.8)	60.0 (26.2, 87.8)	60.0 (26.2, 87.8)	50.0 (15.7, 84.3)	42.9 (9.9, 81.6)	28.6 (3.66, 71.0)
T. cristatus lesions (%)	0.0	0.0	0.0	0.0	0.0	20.0	12.5	14.3	14.3

.8 Appendix 8: Results of survival analysis

Variable	Co-efficient	HR (95% CI)	*p*-value
Species	2.74	15.540 (3.96e-5 - 6.10e+6)	0.68
Infection intensity (GE)	0.06	1.067 (1.01 - 1.13)	0.02
Start weight	0.32	1.371 (0.52 - 3.63)	0.53

Whole model $r^2 = 0.516$ $p = 0.02$

.9 Appendix 9: Bacterial indicator OTUs at day 28 based on *Bsal* infection for *L. vulgaris* and *T. cristatus*.

Species	**Group**	**OTU**	**Taxonomy**	**Indicator value**	***q*-value**
L. vulgaris	Control	OTU012	Bacteroidetes	0.980631558	0.0364
L. vulgaris	*Bsal* Positive	OTU0016	*Stenotrophomonas*	0.919563004	0.028
T. cristatus	*Bsal* Positive	OTU0016	*Stenotrophomonas*	0.876889499	0.0363

.10 Appendix 10: Bacterial indicator taxa for each *A. obstetricans* metamorph population, 2016

OTU	Taxonomy	Population	indval	*q* value
Otu001	Unclassified	Acherito	0.500693481	0.000175
Otu008	Proteobacteria	Acherito	0.604026846	0.000175
Otu009	Gammaproteobacteria	Acherito	0.687134503	0.000175
Otu011	Alphaproteobacteria	Acherito	0.675977654	0.000175
Otu015	Chitinophagaceae	Acherito	0.518796992	0.000288235
Otu017	Acinetobacter	Acherito	0.522776716	0.009695745
Otu019	Rhodobacteraceae	Acherito	0.538822879	0.002566667
Otu021	Verrucomicrobia	Acherito	0.635338346	0.000175
Otu031	Deltaproteobacteria	Acherito	0.547619048	0.000408333
Otu037	Aeromonas	Acherito	0.608127921	0.003229545
Otu049	Clostridiales	Acherito	0.608294931	0.000175
Otu095	Exiguobacterium	Acherito	0.503987241	0.008521739
Otu124	Saprospiraceae	Acherito	0.5	0.000175
Otu156	Duganella	Acherito	0.530357143	0.000628205
Otu158	Haliea	Acherito	0.527950311	0.000288235
Otu212	Vogesella	Acherito	0.555690073	0.000175
Otu010	Comamonadaceae	Arlet	0.567155756	0.000175
Otu013	Chryseobacterium	Arlet	0.773250502	0.000175
Otu024	Pedobacter	Arlet	0.52850062	0.021
Otu035	Flavobacterium	Arlet	0.533039648	0.011127083
Otu055	Rhizobium	Arlet	0.524647887	0.000515789
Otu073	Brucellaceae	Arlet	0.516770186	0.001553659
Otu159	Pseudochrobactrum	Arlet	0.690866511	0.000175
Otu166	Brucella	Arlet	0.545454545	0.000175
Otu178	Microbacterium	Arlet	0.586519115	0.000175
Otu192	Parachlamydia	Arlet	0.820668693	0.000175
Otu229	Phyllobacterium	Arlet	0.724687933	0.000175
Otu283	Delftia	Arlet	0.642857143	0.000175
Otu298	Elizabethkingia	Arlet	0.714285714	0.000175
Otu012	Sphingomonas	Lhurs	0.594771242	0.000175
Otu022	Sphingomonadaceae	Lhurs	0.608040201	0.000175
Otu023	Nocardioides	Lhurs	0.65336374	0.000175
Otu039	Hymenobacter	Lhurs	0.524590164	0.000288235
Otu057	Nocardioidaceae	Lhurs	0.678571429	0.000175
Otu086	Solirubrobacter	Lhurs	0.614285714	0.000288235
Otu091	Phycicoccus	Lhurs	0.706382979	0.000175
Otu093	Sphingomonadales	Lhurs	0.758636788	0.000175
Otu094	Pseudonocardia	Lhurs	0.542274052	0.000515789
Otu121	Staphylococcus	Lhurs	0.528677642	0.004573333
Otu127	Streptomyces	Lhurs	0.500736377	0.0011025
Otu138	Adhaeribacter	Lhurs	0.608108108	0.000175

OTU	Taxonomy	Population	indval	*q* value
Otu155	Geodermatophilaceae	Lhurs	0.506493506	0.00262093
Otu164	Phyllobacteriaceae	Lhurs	0.508403361	0.000175
Otu270	Fibrella	Lhurs	0.507936508	0.000408333
Otu288	Kineosporia	Lhurs	0.576923077	0.000175
Otu050	Brevundimonas	Puits	0.605214153	0.000288235
Otu054	Sanguibacter	Puits	0.632674853	0.000175
Otu278	Dietzia	Puits	0.534161491	0.000288235
Otu297	Planomicrobium	Puits	0.571428571	0.000175

.11 Appendix 11: Bacterial indicator taxa based on chytrid disease dynamics 2016

OTU	Taxonomy	Infection	indval	*q* value
Otu012	Sphingomonas	Enzootic	0.91182234	7.00E-04
Otu063	Methylobacterium	Enzootic	0.86883876	7.00E-04
Otu001	Unclassified	Enzootic	0.83622829	7.00E-04
Otu050	Brevundimonas	Enzootic	0.82837615	0.00336
Otu022	Sphingomonadaceae	Enzootic	0.80821319	7.00E-04
Otu039	Hymenobacter	Enzootic	0.7978022	7.00E-04
Otu041	Devosia	Enzootic	0.77205069	0.019659574
Otu008	Proteobacteria	Enzootic	0.76960404	0.0021
Otu060	Bacillales	Enzootic	0.76435935	7.00E-04
Otu015	Chitinophagaceae	Enzootic	0.76302083	7.00E-04
Otu074	Oxalobacteraceae	Enzootic	0.74742268	0.0021
Otu091	Phycicoccus	Enzootic	0.7324263	0.00525
Otu121	Staphylococcus	Enzootic	0.72498493	0.005727273
Otu005	Bacteroidetes	Enzootic	0.72230884	0.034447368
Otu011	Alphaproteobacteria	Enzootic	0.69816327	0.00525
Otu019	Rhodobacteraceae	Enzootic	0.6909464	0.02184
Otu040	Solirubrobacterales	Enzootic	0.68095238	0.003888889
Otu072	Planococcaceae	Enzootic	0.68082923	0.0021
Otu032	Gemmatimonas	Enzootic	0.67953668	0.003340909
Otu009	Gammaproteobacteria	Enzootic	0.67824649	0.02184
Otu045	Acidobacteria Gp4	Enzootic	0.67179926	0.00336
Otu007	Rhizobiales	Enzootic	0.67123288	0.011268293
Otu004	Pseudomonas	Enzootic	0.67047798	0.011268293
Otu036	Acidobacteria Gp3	Enzootic	0.66666667	0.001235294
Otu051	Novosphingobium	Enzootic	0.65469062	0.0049
Otu034	Spartobacteria	Enzootic	0.65174986	0.011268293
Otu053	Intrasporangiaceae	Enzootic	0.63157301	0.006176471
Otu097	Massilia	Enzootic	0.62847713	0.018717391
Otu093	Sphingomonadales	Enzootic	0.62441315	0.009625
Otu047	Conexibacter	Enzootic	0.61018826	0.011268293
Otu026	Acetobacteraceae	Enzootic	0.60892857	0.022817308
Otu048	Xanthomonadaceae	Enzootic	0.60881543	0.028972222
Otu029	Acidobacteria Gp6	Enzootic	0.59990182	0.003634615
Otu090	Methylophilus	Enzootic	0.5952381	0.004706897
Otu057	Nocardioidaceae	Enzootic	0.59356137	0.020125
Otu031	Deltaproteobacteria	Enzootic	0.56101191	0.022647059
Otu103	Marmoricola	Enzootic	0.55168409	0.022981132
Otu028	Myxococcales	Enzootic	0.54896676	0.018717391
Otu123	Terrabacter	Enzootic	0.54793441	0.018717391
Otu065	Corynebacterium	Enzootic	0.52521008	0.030375
Otu021	Verrucomicrobia	Enzootic	0.51719577	0.014895349
Otu043	Acidobacteria Gp1	Enzootic	0.5	0.011268293
Otu013	Chryseobacterium	Epizootic	0.91134879	7.00E-04
Otu192	Parachlamydia	Epizootic	0.85397997	7.00E-04
Otu010	Comamonadaceae	Epizootic	0.8122306	7.00E-04

Otu283	Delftia	Epizootic	0.80136986	7.00E-04
Otu024	Pedobacter	Epizootic	0.77875837	0.0145
Otu035	Flavobacterium	Epizootic	0.77564103	0.004125
Otu229	Phyllobacterium	Epizootic	0.77483935	7.00E-04
Otu055	Rhizobium	Epizootic	0.7595582	0.00336
Otu298	Elizabethkingia	Epizootic	0.71428571	7.00E-04
Otu178	Microbacterium	Epizootic	0.71387755	7.00E-04
Otu159	Pseudochrobactrum	Epizootic	0.70828331	7.00E-04
Otu107	Rhodococcus	Epizootic	0.66714547	0.045559322
Otu167	Leucobacter	Epizootic	0.61781076	0.0069
Otu166	Brucella	Epizootic	0.55555556	0.001235294
Otu073	Brucellaceae	Epizootic	0.55368234	0.003
Otu151	Comamonas	Epizootic	0.54827901	0.041456897

.12 Appendix 12: Fungal indicator taxa for each *A. obstetricans* metamorph population, 2016

Indicator OTU	Taxonomy	Population	indval	*q*-value
OTU288	*Ramularia coleosporii*	Puits	0.78040541	0.0186
OTU394	Unclassified	Puits	0.69746376	0.0186
OTU255	*Aureobasidium pullulans*	Puits	0.59885491	0.0496
OTU260	Dothideomycetes	Acherito	0.58879651	0.0465
OTU333	*Batrachochytrium* sp.	Arlet	0.64615385	0.0465
OTU044	*Phoma* sp.	Arlet	0.57210149	0.052

.13 Appendix 13: Fungal indicator taxa based on chytrid disease dynamics 2016

Indicator OTU	**Taxonomy**	**Infection**	**indval**	***q*-value**
OTU044	*Phoma* sp.	Epizootic	0.65384615	0.0186
OTU333	*Batrachochytrium* sp.	Epizootic	0.68181818	0.0186

.14 Appendix 14: Top metabolite biomarkers of enzootic and epizootic *A. obstetricans* populations

m/z	Intensity	RT (min)	VIP	Putative Annotation	Kegg ID	Possible Pathway	FC Arlet	FC Lhurs	FC Puits
144.0461	25596657	4.8647	2.956	8-hydroxyquinoline	C19434	NA	19.403	1.596	6.799
111.0204	25588835	0.2366	3.313	Uracil	C00106	Pyrimidine metabolism	11.881	0.369	3.556
125.0361	40982403	0.3224	2.432	Thymine	C00178	Pyrimidine metabolism	10.338	1.095	2.801
472.8283	5752983	1.1091	2.064	NA	NA	NA	9.076	1.423	2.364
476.8224	3743041	13.5518	2.001	NA	NA	NA	8.728	1.436	2.260
654.4594	43394255	12.1800	3.294	NA	NA	NA	8.169	0.655	0.685
137.0363	29777557	9.3888	2.312	urocanate	C00785	Amino acids and metabolites	7.549	0.720	2.777
135.0319	69945302	0.261939	2.408	Hypoxanthine	C00262	Purine metabolism	7.359455	0.646654	5.427057
267.0748	49538404	18.8734	2.126	Inosine	C00294	Purine metabolism	7.173	0.459	2.158
402.2018	44818069	6.9094	2.347	NA	NA	NA	6.485	0.342	0.824
207.0134	752760668	7.4102	4.504	1-Naphthalenesulfonic acid	C16201	Napthalene degradation	6.058	0.738	0.136
151.0268	96296765	0.8617	3.061	Xanthine	C00385	Alkaloid Biosynthesis	5.959	0.772	8.510
192.0677	1841398123	7.3775	2.673	Indolin-2-one	C12312	Biosynthesis of secondary	5.953	2.108	4.849
178.0378	118592644	3.5404	2.897	Isoxanthopterin	C03975	NA	5.946	0.982	5.149
150.0566	10660915	0.2352	3.908	(E)-4-	C04350	Biosynthesis of secondary	5.938	1.606	38.476
209.0088	27016375	7.2187	2.081	NA	NA	NA	5.663	0.727	1.484
148.0774	88685124	18.4460	2.177	D-Cathinone	C08301	Amino acid metabolism	5.027	1.661	3.796
353.2351	9036963	11.6438	2.396	(9Z)-(13S)-12,13-	C04594	NA	4.323	0.411	0.858
302.8305	22397736	6.1532	2.098	NA	NA	NA	3.721	0.539	0.780
304.8285	37316758	1.6977	2.101	NA	NA	NA	3.713	0.534	0.787
146.0466	8130439	0.8888	2.235	2-Oxo-4-hydroxy-5-aminovalerate	C05941	Amino acid metabolism	3.616	0.377	0.825
258.1472	28461695	0.2774	2.208	NA	NA	NA	3.494	0.515	0.822
282.0857	46923067	8.6293	2.077	Gaunosine	C00387	Purine metabolism	3.373	0.376	2.587
581.3699	17560128	10.3106	2.057	NA	NA	NA	2.851	0.570	0.435
287.0901	35732348	1.2086	2.554	Deoxyuridine	C00526	Pyrimidine metabolism	2.530	0.322	5.789

m/z	Intensity	RT (min)	VIP	Putative Annotation	Kegg ID	Possible Pathway	FC Arlet	FC Lhurs	FC Puits
160.0412	9941546	1.5000	2.513	4,6-Dihydroxyquinoline	C05639	Amino acids and metabolites	2.473	0.458	2.798
167.0219	374127647	18.3771	2.948	Urate	C00366	Purine metabolism	2.423	3.159	14.211
178.0518	405997366	6.6888	2.457	N-Acetylanthranilate	C06332	Alkaloid Biosynthesis	2.154	1.368	5.980
332.1678	10493313	0.8322	2.008	(alphaS,betaS)-alpha-Ethyl-alpha-(4-	C15458	NA	2.038	0.504	0.469
134.0479	39066543	1.0833	2.099	Adenine	C00147	Purine metabolism	1.954	0.281	1.236
433.1303	10896333	3.9371	2.241	NA	NA	NA	1.858	1.378	0.332
218.1045	59524752	8.0365	2.575	Pantothenate	C00864	Amino acid metabolism	1.791	0.773	3.804
130.0878	1969908	1.0303	2.004	L-Leucine	C00123	Amino acid metabolism	1.564	0.233	0.468
298.1578	78766058	0.2621	2.355	Anatalline	C12454	Alkaloid Biosynthesis	1.545	0.875	0.231
501.1177	5213841	#N/A	2.158	NA	NA	NA	1.531	1.440	0.310
312.0969	15540167	0.2215	2.247	Neopterin	C05926	Folate biosythesis	1.487	0.273	1.474
149.0251	53419051	1.8939	2.288	2-Carboxybenzaldehyde	C03057	Microbial Metabolism	1.475	0.880	0.229
366.1460	7132475	5.3188	2.313	Pefurazoate	C18480	NA	1.467	1.055	0.230
237.1507	23664765	0.8063	2.505	4-n-Hexylphenol	C14465	NA	1.276	0.888	6.233
252.1334	7663211	2.4908	2.113	NA	NA	NA	1.211	0.752	4.065
168.0251	15127806	10.8312	2.513	2-Amino-4-oxopentanoic acid	C03341	Amino acid metabolism	1.137	0.895	2.666
169.0878	4002204	0.3216	3.516	Furfural diethyl acetal	C14280	NA	1.084	0.383	0.075
251.1302	55771950	7.7975	2.423	Thymyl acetate	C09909	NA	1.062	0.704	4.646
194.0330	46198074	9.0964	2.636	NA	NA	NA	1.012	0.493	2.245
297.1544	557824662	10.6297	2.456	NA	NA	NA	0.955	0.515	0.115
386.1227	14485970	5.0961	2.271	NA	NA	NA	0.851	5.305	1.108
238.1541	3062412	7.0250	2.146	NA	NA	NA	0.822	0.724	3.401
515.1253	17811488	8.9961	2.297	NA	NA	NA	0.800	3.555	3.093
266.9476	5147020	10.4543	2.341	NA	NA	NA	0.706	1.220	3.466
335.0516	50413347	8.5795	3.547	Afrormosin	C!0199	NA	0.672	2.254	11.649
229.1457	143381424	18.3771	2.139	Dodecanedioic acid	C02678	NA	0.653	0.744	3.314
230.1488	17702655	10.4921	2.126	NA	NA	NA	0.650	0.779	3.499

m/z	Intensity	RT (min)	VIP	Putative Annotation	Kegg ID	Possible Pathway	FC Arlet	FC Lhurs	FC Puits
209.0864	1735946102	10.1802	2.599	N-methyltryptamine	C06213	Amino acid metabolism	0.567	0.423	2.324
175.0983	42625272	9.9454	2.229	Hexanoic acid	C01585	NA	0.520	0.219	0.140
188.1017	39191744	0.2900	2.156	NA	NA	NA	0.512	0.182	0.181
187.0986	401526106	10.0734	2.093	Azelaic acid	C08261	Pyrimidine metabolism	0.511	0.189	0.188
311.2240	12357024	10.6416	2.278	9,10-12,13-	C14836	Linoleic acid metabolism	0.444	0.202	0.132
125.0977	31612326	0.2352	2.43	Trans-2-octenal	C21138	Biosynthesis of antibiotics	0.425	0.141	0.144
126.1010	2680741	7.4683	2.261	NA	NA	NA	0.420	0.131	0.129
159.1034	33449906	5.1394	2.13	3-Hydroxyoctanoate	C16651	cAMP signalling pathway	0.420	0.172	0.217
417.2153	15287484	7.0804	2.09	NA	NA	NA	0.362	0.739	0.154
117.0561	21446008	7.1321	2.592	3-hydroxyisovalerate	C20827	Amino acid metabolism	0.351	1.113	3.345
363.1678	15475105	5.5080	2.789	Ajmaline	C06542	Alkaloid Biosynthesis	0.292	0.465	0.061
206.0330	14261667	0.2352	2.072	NA	NA	NA	0.283	0.833	1.833
213.5149	19903974	0.2351	2.718	NA	NA	NA	0.233	0.560	0.063
237.0416	4386738	12.0743	2.117	Esculetin	C09263	Biosynthesis of phenylpropanoids	0.222	0.188	0.204
213.0129	84246306	9.7239	2.376	NA	NA	NA	0.202	0.548	0.092
173.0464	29510090	4.9105	2.327	(2S)-2-Isopropyl-3-	C04236	Amino acid metabolism	0.201	0.299	0.098
146.0547	4782251	18.8523	2.21	NA	NA	NA	0.174	0.163	0.226
127.0405	7984097	1.4159	2.028	(4E)-2-Oxohexenoic acid	C06761	NA	0.169	0.191	0.226
261.1354	150635863	0.9741	3.724	Sebacic acid	C08277	NA	0.152	0.042	0.068
221.0465	6759998	18.7876	2.256	2-Hydroxy-4-	C14107	Microbial Metabolism	0.136	0.151	0.123
385.1887	25280956	10.4345	2.372	Fortimicin B	C17709	Biosynthesis of antibiotics	0.130	0.549	0.092
373.1892	21177963	8.4994	2.064	NA	NA	NA	0.110	0.480	0.131
133.0512	6575877	5.1650	2.218	Propanoate	C00163	Microbial Metabolism	0.099	0.253	0.067
445.2110	10461508	0.8320	2.119	NA	NA	NA	0.092	0.393	0.277
315.1827	44140581	1.8434	2.067	NA	NA	NA	0.087	0.497	0.155
257.1409	168486545	7.2746	2.459	NA	NA	NA	0.085	0.496	0.121
259.1562	39690782	10.5900	2.017	NA	NA	NA	0.084	0.431	0.193
165.0564	8329760	18.8272	2.312	3-(2-	C01198	Amino acids and metabolites	0.080	0.171	0.145
213.0779	46384202	7.4808	2.433	Vanillyl alcohol	C06317	Alkaloid Biosynthesis	0.079	0.181	0.060
261.9791	16825762	5.9297	2.445	NA	NA	NA	0.076	0.623	0.317
261.9791	16825762	5.9297	2.133	NA	NA	NA	0.076	0.623	0.317
303.9900	11019117	12.5420	2.511	NA	NA	NA	0.061	0.381	0.065
117.0562	59185347	8.5490	2.24	3-Hydroxyisovalerate	C20827	Amino acid metabolism	0.058	0.455	0.197
245.1041	120039053	18.6673	4.012	cis-2-Carboxycyclohexyl-	C14112	Microbial Metabolism	0.007	0.195	0.021

.15 Appendix 15: Table of bacterial-metabolite correlations

OTU	Taxonomy	m/z	Metabolite ID	Cor	p.adj	Kegg
Otu283	Delftia	111.0204	Uracil	0.699	5.4E-05	C00106
Otu013	Chryseobacterium	111.0204	Uracil	0.625	3.1E-04	C00106
Otu159	Pseudoochrobactrum	111.0204	Uracil	0.600	5.4E-04	C00106
Otu010	Comamonadaceae	130.0878	L-Leucine	0.655	1.6E-04	C00123
Otu283	Delftia	125.0361	Thymine	0.638	2.3E-04	C00178
Otu013	Chryseobacterium	125.0361	Thymine	0.616	3.6E-04	C00178
Otu159	Pseudoochrobactrum	125.0361	Thymine	0.614	3.9E-04	C00178
Otu283	Delftia	135.0319	Hypoxanthine	0.635	2.4E-04	C00262
Otu001	Unclassified	159.0306	2-Oxoadipate	0.615	3.8E-04	C00322
Otu159	Pseudoochrobactrum	351.2193	Prostaglandin E2	0.634	2.4E-04	C00584
Otu192	Parachlamydia	351.2193	Prostaglandin E2	0.610	4.1E-04	C00584
Otu001	Unclassified	113.0249	2-Hydroxy-2,4-pentadienoate	0.633	2.5E-04	C00596
Otu010	Comamonadaceae	151.0407	4-Hydroxyphenylacetate	0.666	1.1E-04	C00642
Otu192	Parachlamydia	151.0407	4-Hydroxyphenylacetate	0.629	2.8E-04	C00642
Otu283	Delftia	137.0363	Urocanate	0.656	1.5E-04	C00785
Otu021	Verrucomicrobia	103.0408	(R)-3-hydroxybutanoate	0.668	1.0E-04	C01089
Otu008	Proteobacteria	103.0408	(R)-3-hydroxybutanoate	0.624	3.1E-04	C01089
Otu001	Unclassified	103.0408	(R)-3-hydroxybutanoate	0.619	3.5E-04	C01089
Otu043	Acidobacteria	165.0929	4-Trimethylammoniobutanal	0.629	2.8E-04	C01149
Otu001	Unclassified	157.1241	['Nonanoic acid']	0.654	1.6E-04	C01601
Otu009	Gammaproteobacteria	157.1241	['Nonanoic acid']	0.611	4.1E-04	C01602
Otu021	Verrucomicrobia	344.1448	Paromamine	0.618	3.5E-04	C01743
Otu015	Chitinophagaceae	169.1606	2-Undecanone	0.681	6.8E-05	C01875
Otu001	Unclassified	169.1606	2-Undecanone	0.668	1.0E-04	C01875
Otu283	Delftia	164.0724	Phenlyalanine	0.679	7.2E-05	C02057
Otu022	Sphingomonadaceae	200.9873	4-Sulfobenzoate	0.637	2.3E-04	C02236
Otu192	Parachlamydia	328.0473	2',3-Cyclic AMP	0.636	2.3E-04	C02353
Otu283	Delftia	328.0473	2',3-Cyclic AMP	0.625	3.1E-04	C02354
Otu001	Unclassified	213.1508	3-Oxododecanoic acid	0.618	3.5E-04	C02367
Otu001	Unclassified	273.1719	3-Oxododecanoic acid	0.611	4.1E-04	C02367
Otu036	Acidobacteria	273.1719	3-Oxododecanoic acid	0.602	5.1E-04	C02367
Otu158	Haliea	215.1298	Nonane-4,6-dione	0.635	2.4E-04	C02445
Otu001	Unclassified	215.1298	Nonane-4,6-dione	0.601	5.4E-04	C02445
Otu001	Unclassified	229.1458	Dodecanedioic acid	0.600	5.4E-04	C02678
Otu013	Chryseobacterium	149.0250	2-Carboxybenzaldehyde	0.640	2.2E-04	C03057
Otu283	Delftia	201.0237	S-Methyl-L-methionine	0.613	3.9E-04	C03172
Otu013	Chryseobacterium	201.0237	S-Methyl-L-methionine	0.600	5.4E-04	C03172

OTU	Taxonomy	m/z	Metabolite ID	Cor	p.adj	Kegg
Otu192	Parachlamydia	353.2351	(9Z)-(13S)-12,13-Epoxyoctadeca-9,11-dienoic acid	0.622	3.2E-04	C04594
Otu159	Pseudoochrobactrum	353.2351	(9Z)-(13S)-12,13-Epoxyoctadeca-9,11-dienoic acid	0.617	3.6E-04	C04594
Otu283	Delftia	353.2351	(9Z)-(13S)-12,13-Epoxyoctadeca-9,11-dienoic acid	0.615	3.8E-04	C04594
Otu158	Haliea	331.1777	(2S,3S)-2-Hydroxytridecane-1,2,3-tricarboxylate	0.612	4.1E-04	C04655
Otu298	Elizabethkingia	230.0413	Phenylacetylglycine	0.603	4.9E-04	C05598
Otu054	Sanguibacter	308.0102	Pelargonidin	0.640	2.2E-04	C05904
Otu041	Deovsia	308.0102	Pelargonidin	0.603	4.9E-04	C05904
Otu283	Delftia	146.0466	2-Oxo-4-hydroxy-5-aminovalerate	0.616	3.6E-04	C05941
Otu283	Delftia	167.0359	2,6-Dihydroxyphenylacetate	0.624	3.1E-04	C06207
Otu057	Nocardioidaceae	299.0139	Galactitol 1-phosphate	0.625	3.1E-04	C06311
Otu158	Haliea	213.0779	Vanillyl alcohol	0.636	2.3E-04	C06317
Otu001	Unclassified	401.2567	Erythronolide B	0.607	4.5E-04	C06635
Otu158	Haliea	229.0727	1,2-Dihydroxy-6-methylcyclohexa-3,5-dienecarboxylate	0.605	4.8E-04	C06731
Otu001	Unclassified	157.0513	Betaine aldehyde hydrate	0.620	3.4E-04	C07345
Otu001	Unclassified	201.1143	Sebacic Acid	0.604	4.9E-04	C08277
Otu022	Sphingomonadaceae	215.1662	12-Hydroxydodecanoic acid	0.628	2.9E-04	C08317
Otu093	Sphingomonadales	215.1662	12-Hydroxydodecanoic acid	0.624	3.1E-04	C08317
Otu158	Haliea	513.2728	Rhodojaponin IV	0.626	3.0E-04	C09180
Otu158	Haliea	367.1783	Inulicin	0.605	4.7E-04	C09483
Otu001	Unclassified	367.1783	Inulicin	0.604	4.9E-04	C09483
Otu001	Unclassified	397.1523	1-Peroxyferolide	0.610	4.3E-04	C09526
Otu022	Sphingomonadaceae	479.1589	Glycyphyllin	0.675	8.4E-05	C09754
Otu158	Haliea	255.1615	(1S,2R,4S)-(-)-Bornyl acetate	0.613	3.9E-04	C09837
Otu283	Delftia	232.0603	Enicoflavine	0.612	4.0E-04	C09946
Otu283	Delftia	182.0468	Picolinic acid	0.689	6.8E-05	C10164
Otu074	Oxalobacteraceae	431.1375	Sinensetin	0.618	3.5E-04	C10186
Otu158	Haliea	441.1795	Lusitanicoside	0.602	5.1E-04	C10474
Otu192	Parachlamydia	233.0446	Danielone	0.618	3.5E-04	C10674

OTU	Taxonomy	m/z	Metabolite ID	Cor	p.adj	Kegg
Otu298	Elizabethkingia	285.0089	Tryptanthrine	0.608	4.5E-04	C10742
Otu001	Unclassified	439.2000	10-Deacetyl-2-debenzoylbaccatin III	0.607	4.6E-04	C11899
Otu001	Unclassified	355.2143	10-Deoxymethynolide	0.621	3.3E-04	C1193
Otu001	Unclassified	345.1574	Tetraphyllicine	0.643	2.1E-04	C12075
Otu022	Sphingomonadaceae	345.1574	Tetraphyllicine	0.606	4.7E-04	C12075
Otu057	Nocardioidaceae	257.0777	1,2-Dimethoxy-4-[2-(2-propenyloxy)ethenyl]-benzene	0.681	6.8E-05	C12263
Otu010	Comamonadaceae	163.0409	trans-3-Hydroxycinnamate	0.649	1.8E-04	C12621
Otu192	Parachlamydia	163.0409	trans-3-Hydroxycinnamate	0.641	2.1E-04	C12621
Otu159	Pseudoochrobactrum	163.0409	trans-3-Hydroxycinnamate	0.622	3.2E-04	C12621
Otu001	Unclassified	243.1611	Undecylenic acid	0.607	4.6E-04	C13910
Otu001	Unclassified	245.1041	cis-2-Carboxycyclohexyl-acetic acid	0.627	2.9E-04	C14112
Otu158	Haliea	181.1243	Decahydro-2-naphthoic acid	0.623	3.2E-04	C14113
Otu001	Unclassified	241.1457	Decahydro-2-naphthoic acid	0.652	1.7E-04	C14113
Otu057	Nocardioidaceae	272.9603	1,3-Benzenedisulfonamide	0.628	2.9E-04	C14182
Otu001	Unclassified	295.1563	4-Heptyloxybenzoic acid	0.656	1.5E-04	C14274
Otu158	Haliea	295.1563	4-Heptyloxybenzoic acid	0.620	3.4E-04	C14274
Otu001	Unclassified	461.2054	3beta-Hydroxy-16-phosphonopregn-5-en-20-one monoethyl ester	0.606	4.7E-04	C15173
Otu192	Parachlamydia	207.0134	1-Naphthalenesulfonic acid	0.680	6.8E-05	C16201
Otu159	Pseudoochrobactrum	207.0134	1-Naphthalenesulfonic acid	0.615	3.8E-04	C16201
Otu298	Elizabethkingia	207.0134	1-Naphthalenesulfonic acid	0.605	4.8E-04	C16201
Otu039	Hymenobacter	207.1037	1-Naphthalenesulfonic acid	0.607	4.6E-04	C16201
Otu001	Unclassified	271.1564	12-Oxo-9(Z)-dodecenoic acid	0.632	2.6E-04	C16311
Otu158	Haliea	271.1564	12-Oxo-9(Z)-dodecenoic acid	0.624	3.1E-04	C16311
Otu158	Haliea	211.1351	12-Oxo-9(Z)-dodecenoic acid	0.626	3.0E-04	C16311

OTU	Taxonomy	m/z	Metabolite ID	Cor	p.adj	Kegg
Otu158	Haliea	197.1194	3,6-Nonadienal	0.642	2.1E-04	C16323
Otu158	Haliea	343.2142	(10S)-Juvenile hormone III diol	0.665	1.1E-04	C16505
Otu158	Haliea	343.2142	(10S)-Juvenile hormone III diol	0.632	2.6E-04	C16505
Otu022	Sphingomonadaceae	345.1214	Gastrodin	0.618	3.5E-04	C16964
Otu015	Chitinophagaceae	345.1214	Gastrodin	0.617	3.6E-04	C16964
Otu057	Nocardioidaceae	477.1434	Liquiritin	0.631	2.7E-04	C16989
Otu013	Chryseobacterium	273.2084	Tridecanoic acid	0.635	2.3E-04	C17076
Otu283	Delftia	273.2084	Tridecanoic acid	0.604	4.9E-04	C17076
Otu158	Haliea	441.2152	Cinncassiol A	0.629	2.8E-04	C17641
Otu001	Unclassified	441.2152	Cinncassiol A	0.616	3.6E-04	C17641
Otu057	Nocardioidaceae	541.2739	Gentamicin X2	0.630	2.8E-04	C17702
Otu158	Haliea	441.2523	Sarcostin	0.636	2.3E-04	C177770
Otu057	Nocardioidaceae	476.1884	5-Ribosylparomamine	0.616	3.6E-04	C18002
Otu283	Delftia	210.0123	Tricyclazole	0.673	8.4E-05	C18492
Otu298	Elizabethkingia	210.0123	Tricyclazole	0.619	3.4E-04	C18492
Otu192	Parachlamydia	210.0123	Tricyclazole	0.610	4.1E-04	C18492
Otu013	Chryseobacterium	210.0123	Tricyclazole	0.606	4.7E-04	C18492
Otu010	Comamonadaceae	210.0123	Tricyclazole	0.605	4.7E-04	C18492
Otu001	Unclassified	285.1356	Butopyronoxyl	0.608	4.5E-04	C19142
Otu057	Nocardioidaceae	250.9659	Niridazole	0.604	4.9E-04	C19268
Otu283	Delftia	144.0461	8-Hydroxyquinoline	0.656	1.5E-04	C19434
Otu013	Chryseobacterium	144.0461	8-Hydroxyquinoline	0.636	2.3E-04	C19434
Otu158	Haliea	357.1574	Neoilludin A	0.609	4.3E-04	C19956
Otu091	Phycicoccus	285.1283	1-Deoxy-11beta-hydroxypentalenate	0.604	4.9E-04	C20403
Otu001	Unclassified	117.0561	3-Hydroxyisovalerate	0.667	1.0E-04	C20827
Otu019	Rhodobacteraceae	117.0561	3-Hydroxyisovalerate	0.611	4.1E-04	C20827
Otu008	Proteobacteria	117.0561	3-Hydroxyisovalerate	0.601	5.3E-04	C20827
Otu158	Haliea	341.1259	4-Oxonebramine	0.603	4.9E-04	C21258
Otu178	Microbacterium	126.0394	Unknown	0.635	2.3E-04	NA
Otu283	Delftia	176.0362	Unknown	0.618	3.5E-04	NA
Otu159	Pseudoochrobactrum	176.0362	Unknown	0.606	4.7E-04	NA
Otu192	Parachlamydia	208.0164	Unknown	0.644	2.1E-04	NA
Otu159	Pseudoochrobactrum	208.0164	Unknown	0.604	4.9E-04	NA
Otu192	Parachlamydia	209.0088	Unknown	0.629	2.8E-04	NA
Otu298	Elizabethkingia	209.0088	Unknown	0.601	5.4E-04	NA
Otu298	Elizabethkingia	210.9505	Unknown	0.615	3.8E-04	NA
Otu039	Hymenobacter	215.0031	Unknown	0.653	1.6E-04	NA
Otu192	Parachlamydia	219.1070	Unknown	0.617	3.6E-04	NA
Otu192	Parachlamydia	224.1150	Unknown	0.613	3.9E-04	NA
Otu283	Delftia	224.1150	Unknown	0.600	5.4E-04	NA
Otu192	Parachlamydia	224.9199	Unknown	0.643	2.1E-04	NA
Otu159	Pseudoochrobactrum	224.9199	Unknown	0.616	3.7E-04	NA

OTU	Taxonomy	m/z	Metabolite ID	Cor	p.adj	Kegg
Otu298	Elizabethkingia	224.9199	Unknown	0.607	4.6E-04	NA
Otu192	Parachlamydia	225.9231	Unknown	0.642	2.1E-04	NA
Otu298	Elizabethkingia	225.9231	Unknown	0.607	4.6E-04	NA
Otu159	Pseudoochrobactrum	225.9231	Unknown	0.605	4.7E-04	NA
Otu192	Parachlamydia	226.9166	Unknown	0.644	2.1E-04	NA
Otu298	Elizabethkingia	226.9166	Unknown	0.607	4.6E-04	NA
Otu159	Pseudoochrobactrum	226.9166	Unknown	0.605	4.7E-04	NA
Otu298	Elizabethkingia	227.1414	Unknown	0.628	2.9E-04	NA
Otu159	Pseudoochrobactrum	227.1414	Unknown	0.609	4.3E-04	NA
Otu192	Parachlamydia	227.9198	Unknown	0.664	1.2E-04	NA
Otu159	Pseudoochrobactrum	227.9198	Unknown	0.634	2.4E-04	NA
Otu298	Elizabethkingia	227.9198	Unknown	0.623	3.2E-04	NA
Otu192	Parachlamydia	228.9132	Unknown	0.641	2.1E-04	NA
Otu298	Elizabethkingia	228.9132	Unknown	0.607	4.6E-04	NA
Otu159	Pseudoochrobactrum	228.9132	Unknown	0.605	4.7E-04	NA
Otu192	Parachlamydia	229.9165	Unknown	0.636	2.3E-04	NA
Otu159	Pseudoochrobactrum	229.9165	Unknown	0.613	3.9E-04	NA
Otu298	Elizabethkingia	229.9165	Unknown	0.607	4.6E-04	NA
Otu192	Parachlamydia	230.9089	Unknown	0.646	2.0E-04	NA
Otu159	Pseudoochrobactrum	230.9089	Unknown	0.619	3.5E-04	NA
Otu298	Elizabethkingia	230.9089	Unknown	0.610	4.3E-04	NA
Otu192	Parachlamydia	230.9982	Unknown	0.650	1.7E-04	NA
Otu192	Parachlamydia	258.8806	Unknown	0.664	1.2E-04	NA
Otu159	Pseudoochrobactrum	258.8806	Unknown	0.622	3.2E-04	NA
Otu192	Parachlamydia	260.8778	Unknown	0.662	1.2E-04	NA
Otu159	Pseudoochrobactrum	260.8778	Unknown	0.617	3.6E-04	NA
Otu192	Parachlamydia	262.8747	Unknown	0.654	1.6E-04	NA
Otu283	Delftia	262.8747	Unknown	0.628	2.9E-04	NA
Otu159	Pseudoochrobactrum	262.8747	Unknown	0.617	3.6E-04	NA
Otu192	Parachlamydia	263.1876	Unknown	0.683	6.8E-05	NA
Otu298	Elizabethkingia	284.9413	Unknown	0.601	5.3E-04	NA
Otu192	Parachlamydia	296.9007	Unknown	0.600	5.4E-04	NA
Otu192	Parachlamydia	302.8305	Unknown	0.673	8.4E-05	NA
Otu159	Pseudoochrobactrum	302.8305	Unknown	0.627	2.9E-04	NA
Otu298	Elizabethkingia	302.8305	Unknown	0.600	5.4E-04	NA
Otu192	Parachlamydia	303.8341	Unknown	0.656	1.5E-04	NA
Otu159	Pseudoochrobactrum	303.8341	Unknown	0.622	3.2E-04	NA
Otu298	Elizabethkingia	303.8341	Unknown	0.600	5.4E-04	NA
Otu192	Parachlamydia	304.8284	Unknown	0.673	8.4E-05	NA
Otu159	Pseudoochrobactrum	304.8284	Unknown	0.627	2.9E-04	NA
Otu298	Elizabethkingia	304.8284	Unknown	0.600	5.4E-04	NA
Otu192	Parachlamydia	305.8318	Unknown	0.673	8.4E-05	NA
Otu159	Pseudoochrobactrum	305.8318	Unknown	0.627	2.9E-04	NA
Otu283	Delftia	305.8318	Unknown	0.625	3.1E-04	NA
Otu298	Elizabethkingia	305.8318	Unknown	0.605	4.7E-04	NA

OTU	Taxonomy	m/z	Metabolite ID	Cor	p.adj	Kegg
Otu192	Parachlamydia	306.8256	Unknown	0.661	1.3E-04	NA
Otu159	Pseudoochrobactrum	306.8256	Unknown	0.619	3.5E-04	NA
Otu298	Elizabethkingia	306.8256	Unknown	0.611	4.1E-04	NA
Otu192	Parachlamydia	307.8290	Unknown	0.613	3.9E-04	NA
Otu192	Parachlamydia	308.8225	Unknown	0.676	8.4E-05	NA
Otu159	Pseudoochrobactrum	308.8225	Unknown	0.625	3.1E-04	NA
Otu298	Elizabethkingia	308.8225	Unknown	0.603	5.1E-04	NA
Otu159	Pseudoochrobactrum	384.0761	Unknown	0.641	2.1E-04	NA
Otu298	Elizabethkingia	384.0761	Unknown	0.622	3.2E-04	NA
Otu192	Parachlamydia	401.8691	Unknown	0.620	3.4E-04	NA
Otu192	Parachlamydia	472.8283	Unknown	0.616	3.6E-04	NA
Otu298	Elizabethkingia	472.8283	Unknown	0.604	4.9E-04	NA
Otu298	Elizabethkingia	473.8319	Unknown	0.621	3.3E-04	NA
Otu192	Parachlamydia	542.8134	Unknown	0.651	1.7E-04	NA
Otu001	Unclassified	118.0595	Unknown	0.621	3.3E-04	NA
Otu008	Proteobacteria	118.0595	Unknown	0.603	4.9E-04	NA
Otu001	Unclassified	202.1175	Unknown	0.608	4.5E-04	NA
Otu021	Verrucomicrobia	206.1123	Unknown	0.652	1.7E-04	NA
Otu008	Proteobacteria	206.1123	Unknown	0.650	1.7E-04	NA
Otu015	Chitinophagaceae	206.1123	Unknown	0.629	2.8E-04	NA
Otu001	Unclassified	214.1542	Unknown	0.614	3.9E-04	NA
Otu022	Sphingomonadaceae	215.0031	Unknown	0.618	3.5E-04	NA
Otu001	Unclassified	215.0031	Unknown	0.613	3.9E-04	NA
Otu158	Haliea	216.1332	Unknown	0.614	3.9E-04	NA
Otu001	Unclassified	216.1332	Unknown	0.610	4.2E-04	NA
Otu001	Unclassified	230.1490	Unknown	0.601	5.4E-04	NA
Otu057	Nocardioidaceae	237.9384	Unknown	0.614	3.9E-04	NA
Otu001	Unclassified	244.1646	Unknown	0.604	4.9E-04	NA
Otu021	Verrucomicrobia	247.9635	Unknown	0.627	2.9E-04	NA
Otu001	Unclassified	247.9635	Unknown	0.620	3.4E-04	NA
Otu001	Unclassified	259.1562	Unknown	0.636	2.3E-04	NA
Otu022	Sphingomonadaceae	261.9791	Unknown	0.624	3.1E-04	NA
Otu057	Nocardioidaceae	264.9358	Unknown	0.628	2.9E-04	NA
Otu057	Nocardioidaceae	265.9520	Unknown	0.601	5.4E-04	NA
Otu057	Nocardioidaceae	271.9253	Unknown	0.618	3.5E-04	NA
Otu021	Verrucomicrobia	274.1756	Unknown	0.620	3.4E-04	NA
Otu001	Unclassified	276.8260	Unknown	0.601	5.3E-04	NA
Otu001	Unclassified	285.1721	Unknown	0.654	1.6E-04	NA
Otu158	Haliea	288.1912	Unknown	0.618	3.5E-04	NA
Otu057	Nocardioidaceae	304.9156	Unknown	0.684	6.8E-05	NA
Otu057	Nocardioidaceae	307.9124	Unknown	0.659	1.4E-04	NA
Otu057	Nocardioidaceae	309.9116	Unknown	0.681	6.8E-05	NA
Otu001	Unclassified	315.1827	Unknown	0.639	2.2E-04	NA
Otu001	Unclassified	316.1865	Unknown	0.630	2.8E-04	NA
Otu057	Nocardioidaceae	322.8883	Unknown	0.635	2.4E-04	NA

OTU	Taxonomy	m/z	Metabolite ID	Cor	p.adj	Kegg
Otu057	Nocardioidaceae	333.8999	Unknown	0.685	6.8E-05	NA
Otu021	Verrucomicrobia	346.1244	Unknown	0.631	2.7E-04	NA
Otu015	Chitinophagaceae	346.1244	Unknown	0.623	3.2E-04	NA
Otu057	Nocardioidaceae	346.1736	Unknown	0.618	3.5E-04	NA
Otu057	Nocardioidaceae	355.0217	Unknown	0.640	2.2E-04	NA
Otu057	Nocardioidaceae	358.9223	Unknown	0.638	2.2E-04	NA
Otu057	Nocardioidaceae	367.2665	Unknown	0.622	3.2E-04	NA
Otu057	Nocardioidaceae	368.2699	Unknown	0.631	2.7E-04	NA
Otu001	Unclassified	395.1738	Unknown	0.614	3.9E-04	NA
Otu057	Nocardioidaceae	401.9281	Unknown	0.621	3.3E-04	NA
Otu057	Nocardioidaceae	408.8750	Unknown	0.637	2.3E-04	NA
Otu057	Nocardioidaceae	408.9357	Unknown	0.626	3.0E-04	NA
Otu158	Haliea	428.2403	Unknown	0.609	4.3E-04	NA
Otu057	Nocardioidaceae	428.9643	Unknown	0.611	4.1E-04	NA
Otu057	Nocardioidaceae	432.1403	Unknown	0.635	2.4E-04	NA
Otu001	Unclassified	434.2143	Unknown	0.634	2.4E-04	NA
Otu001	Unclassified	445.2110	Unknown	0.622	3.2E-04	NA
Otu057	Nocardioidaceae	454.9303	Unknown	0.640	2.2E-04	NA
Otu158	Haliea	455.1955	Unknown	0.608	4.4E-04	NA
Otu001	Unclassified	455.1955	Unknown	0.607	4.5E-04	NA
Otu057	Nocardioidaceae	455.9324	Unknown	0.635	2.3E-04	NA
Otu057	Nocardioidaceae	457.7857	Unknown	0.636	2.3E-04	NA
Otu057	Nocardioidaceae	474.4064	Unknown	0.608	4.5E-04	NA
Otu001	Unclassified	475.2217	Unknown	0.613	3.9E-04	NA
Otu057	Nocardioidaceae	486.8849	Unknown	0.636	2.3E-04	NA
Otu057	Nocardioidaceae	503.8657	Unknown	0.648	1.9E-04	NA
Otu057	Nocardioidaceae	515.1253	Unknown	0.657	1.5E-04	NA
Otu057	Nocardioidaceae	516.1279	Unknown	0.614	3.9E-04	NA
Otu091	Phycicoccus	530.2850	Unknown	0.686	6.8E-05	NA
Otu022	Sphingomonadaceae	530.2850	Unknown	0.653	1.6E-04	NA
Otu012	Sphingomonas	530.2850	Unknown	0.630	2.8E-04	NA
Otu057	Nocardioidaceae	530.2850	Unknown	0.615	3.7E-04	NA
Otu057	Nocardioidaceae	531.8873	Unknown	0.624	3.1E-04	NA
Otu057	Nocardioidaceae	531.8873	Unknown	0.641	2.1E-04	NA
Otu057	Nocardioidaceae	537.9040	Unknown	0.604	4.9E-04	NA
Otu057	Nocardioidaceae	574.3602	Unknown	0.605	4.8E-04	NA
Otu057	Nocardioidaceae	590.9064	Unknown	0.632	2.6E-04	NA
Otu057	Nocardioidaceae	597.0014	Unknown	0.653	1.6E-04	NA
Otu057	Nocardioidaceae	610.5641	Unknown	0.651	1.7E-04	NA
Otu057	Nocardioidaceae	615.8403	Unknown	0.669	1.0E-04	NA
Otu057	Nocardioidaceae	642.8318	Unknown	0.618	3.5E-04	NA
Otu057	Nocardioidaceae	654.8115	Unknown	0.601	5.3E-04	NA
Otu057	Nocardioidaceae	659.8293	Unknown	0.652	1.6E-04	NA
Otu057	Nocardioidaceae	674.8067	Unknown	0.628	2.9E-04	NA
Otu057	Nocardioidaceae	699.3384	Unknown	0.608	4.5E-04	NA

OTU	Taxonomy	m/z	Metabolite ID	Cor	p.adj	Kegg
Otu057	Nocardioidaceae	705.8149	Unknown	0.643	2.1E-04	NA
Otu057	Nocardioidaceae	708.8272	Unknown	0.644	2.1E-04	NA
Otu057	Nocardioidaceae	714.8128	Unknown	0.611	4.1E-04	NA
Otu057	Nocardioidaceae	742.7928	Unknown	0.609	4.3E-04	NA
Otu057	Nocardioidaceae	789.7880	Unknown	0.624	3.1E-04	NA
Otu057	Nocardioidaceae	795.9995	Unknown	0.643	2.1E-04	NA
Otu057	Nocardioidaceae	806.8004	Unknown	0.719	1.5E-05	NA
Otu057	Nocardioidaceae	819.8350	Unknown	0.643	2.1E-04	NA
Otu057	Nocardioidaceae	888.8301	Unknown	0.692	6.7E-05	NA

.16 Appendix 16: Articles published from chapters in this thesis

nature COMMUNICATIONS

ARTICLE

DOI: 10.1038/s41467-018-02967-w OPEN

Amphibian chytridiomycosis outbreak dynamics are linked with host skin bacterial community structure

Kieran A. Bates[1,2], Frances C. Clare[2], Simon O'Hanlon[1], Jaime Bosch[3], Lola Brookes[2], Kevin Hopkins[2], Emilia J. McLaughlin[2], Olivia Daniel[1], Trenton W. J. Garner[2], Matthew C. Fisher[1] & Xavier A. Harrison[2]

Host-associated microbes are vital for combatting infections and maintaining health. In amphibians, certain skin-associated bacteria inhibit the fungal pathogen *Batrachochytrium dendrobatidis* (*Bd*), yet our understanding of host microbial ecology and its role in disease outbreaks is limited. We sampled skin-associated bacteria and *Bd* from Pyrenean midwife toad populations exhibiting enzootic or epizootic disease dynamics. We demonstrate that bacterial communities differ between life stages with few shared taxa, indicative of restructuring at metamorphosis. We detected a significant effect of infection history on metamorph skin microbiota, with reduced bacterial diversity in epizootic populations and differences in community structure and predicted function. Genome sequencing of *Bd* isolates supports a single introduction to the Pyrenees and reveals no association between pathogen genetics and epidemiological trends. Our findings provide an ecologically relevant insight into the microbial ecology of amphibian skin and highlight the relative importance of host microbiota and pathogen genetics in predicting disease outcome.

[1] Department of Infectious Disease Epidemiology, Imperial College London, London W2 1PG, UK. [2] Institute of Zoology, Zoological Society of London, Regent's Park, London NW1 4RY, UK. [3] Museo Nacional de Ciencias Naturales, CSIC, Jose Gutierrez Abascal 2, 28006 Madrid, Spain. Correspondence and requests for materials should be addressed to K.A.B. (email: k.bates14@imperial.ac.uk) or to X.A.H. (email: xavier.harrison@ioz.ac.uk)

The communities of bacteria resident on multicellular organisms are of significant importance to host health[1]. In addition to their involvement in essential host physiological processes[2–5], bacterial interactions with invading pathogens are key in defining disease outcome[6]. Commensal bacteria may confer protection against pathogens through limiting pathogen adhesion to host cells[7], resource competition[8], interacting with the host immune system[9], or production of antimicrobial compounds[10]. Conversely, some commensal bacteria interact synergistically with pathogens exacerbating infection[11]. At a community level, disruption of the microbiome (a process termed dysbiosis) can negatively impact host health bringing about pathophysiological changes and in some instances facilitating infection by opportunistic pathogens[12].

The emerging infectious disease, chytridiomycosis caused by the fungal pathogen *Batrachochytrium dendrobatidis* (*Bd*) is known to affect over 500 amphibian species worldwide[13]. *Bd* infects keratinised skin of post-metamorphic anurans where it disrupts osmoregulation leading to cardiac abnormalities and in some cases death[14]. Larval anurans exhibit little *Bd*-induced pathology since the skin is deficient of keratin and infection is restricted to the mouthparts[15]. Prior studies have gained insight into the drivers of *Bd* infection dynamics by examining host and pathogen biology in addition to environmental effects on disease outcome[16–18]. Recently attention has shifted to include the role of skin-associated bacteria in infection based on findings that certain taxa inhibit *Bd*[19,20]. Other studies have shown associations between bacterial communities and infection in the field[21–24]; however, research has largely focused on within-population infection dynamics and on species solely from the Americas. With the exception of an amphibian study system in the Western United States[21,24], most studies to date are based on short-term surveillance programmes and therefore lack vital information such as time of initial *Bd* emergence. In addition, while previous studies have demonstrated that pathogen genetics can underpin *Bd* virulence[17] and disease dynamics in the field[25], the relative importance of the microbiome and pathogen genetics have not been simultaneously investigated in the wild. Therefore, it remains to be established whether pathogen genetics and microbiome covary and the extent to which they are associated with disease dynamics. Consequently prior studies have been limited in their ability to examine the relationships between host bacterial communities and disease dynamics in complex ecosystems.

In this study, we use 16s metabarcoding to disentangle the relationship between skin bacterial community structure, life stage and *Bd* infection in wild common midwife toads (*Alytes obstetricans*). We also use whole genome sequencing to investigate the spatial and temporal genetic structure of *Bd* isolates from host populations exhibiting distinct disease dynamics. Our work focuses on a long-term study system in the Pyrenees of France and Spain in which infection has been monitored continuously for over 10 years[26,27]. While *A. obstetricans* is native throughout Europe, it has shown catastrophic declines in the Pyrenees with several populations undergoing mass mortality events[26–28]. In recent years however, certain populations have shown signs of tolerance to infection and an associated resurgence in abundance consistent with the establishment of enzootic disease dynamics. Conversely, other populations infected at approximately the same time remain in decline and show high susceptibility to *Bd* indicative of epizootic dynamics.

Our results demonstrate that *Bd* in the Pyrenees arose from a single introduction and isolates from enzootic and epizootic populations are not genetically distinct. Significant differences were however found in the skin microbiome of amphibians, with life stage, population and *Bd* infection dynamics exhibiting a strong association with bacterial community structure. We further show that the predicted function of metamorph skin bacterial communities differs based on disease dynamics. We identify a conserved set of bacterial taxa associated with different disease states that may represent a dysbiosis contributing to epizootic dynamics, or selection of protective symbionts leading to an enzootic disease state. Our findings show that among populations with little spatial separation, bacterial community structure but not pathogen genetics is associated with divergent disease outcomes.

Results

Host skin microbiota differs by life stage and population. We collected midwife toad larvae and metamorphs in August 2015 from five populations in the Pyrenees mountains of France and Spain (Table 1). Each population has been part of a long-term study in which population abundance and infection have been monitored (Supplementary Table 1, Supplementary Fig. 1).

We quantified the bacterial communities of amphibian skin and environmental samples by sequencing the V4 region of the 16s rRNA gene. To determine the importance of life stage and the environment in shaping the amphibian microbiome, we first calculated the proportion of bacterial operational taxonomic units (OTUs) common to different samples. We detected a total of 11,112 OTUs, of which 17.3% were shared by larvae and metamorphs, 10.8% were shared by larvae and the environment, 10.1% were shared by metamorphs and the environment, and 7.8% were common to all sample types (Fig. 1a). Similar results were obtained when analysing populations on an individual basis (Supplementary Table 2). In larvae and metamorphs, over 98% of OTUs had a relative abundance of less than 1% in the environment.

To assess differences in bacterial community structure between amphibian life stages and the environment, we calculated alpha and beta diversity metrics. Shannon diversity differed only among samples from Acherito (ANOVA $F_{(3,30)} = 6.462$, $P = 0.002$) in which sediment had a significantly lower value relative to larvae, metamorphs and lake water (Tukey's test: sediment-larva $P = 0.001$; sediment-metamorph $P = 0.002$; sediment-water $P = 0.04$, Fig.1b, Supplementary Fig. 2). Both life stage and population were associated with variation in beta diversity of

Table 1 Sample summary of each lake

Population	Larvae	Metamorphs	Environmental samples	Elevation (m)	*Bd* first detected	*Bd* infection status
Acherito	16	14	Water sediment	1869	2004	Enzootic
Lhurs	15	11	Water sediment	1691	2009	Enzootic
Puits d'Arious	17	7	Water sediment	1867	2006	Enzootic
Ansabere	15	3	Water sediment	1859	2005	Epizootic
Arlet	0	16	Water sediment	1986	2005	Epizootic

$N = 2$ environmental samples each for water and sediment at each population

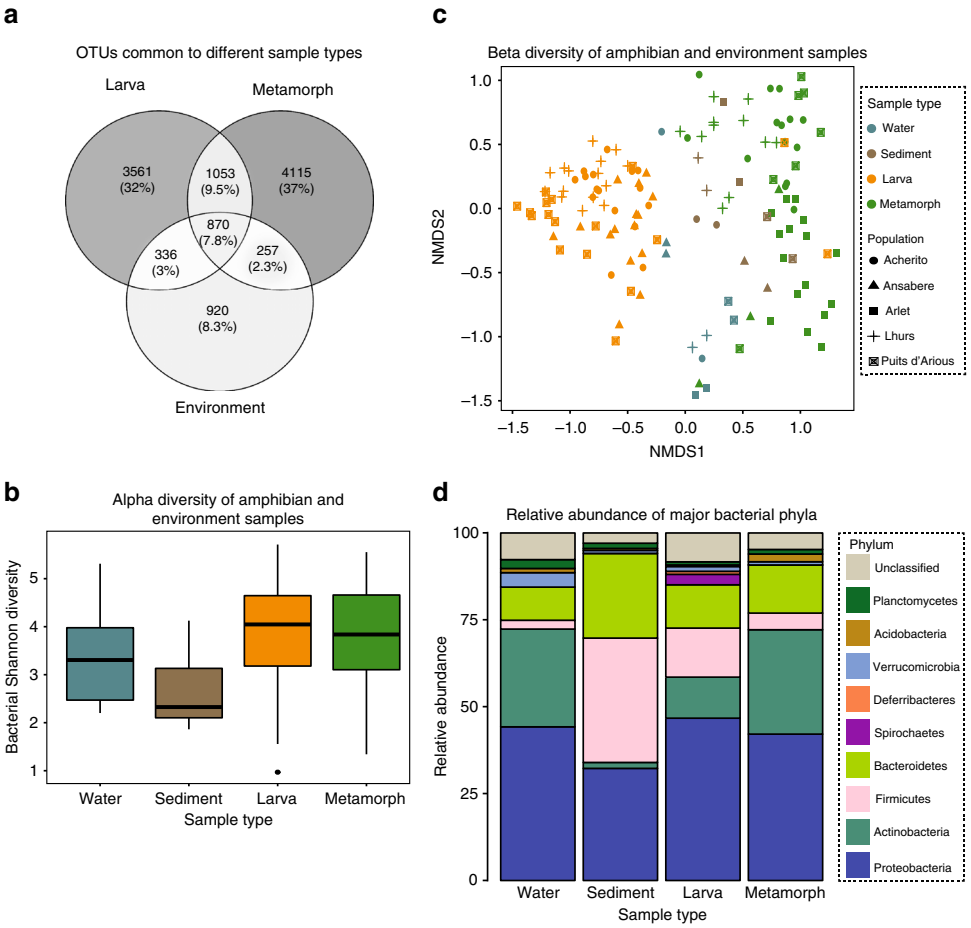


Fig. 1 Bacterial communities of *Alytes obstetricans* skin across life stages and in environmental samples. **a** OTUs common among life stages and environmental samples. **b** Shannon diversity by sample type (boxes represent 25 and 75 percentile, the horizontal line is the median, whiskers are maximum and minimum values). **c** NMDS plot of bacterial communities based on life stage, environmental samples and population. **d** Stacked bar chart of the ten most abundant phyla for lake water, sediment, larvae and metamorphs. Sample sizes were: $n = 63$ (larvae); $n = 51$ (metamorphs); $n = 20$ (environment)

amphibian skin (Life Stage: PERMANOVA Pseudo-$F_{(1,112)} = 19.821$, $P = 0.001$; Population: PERMANOVA Pseudo-$F_{(4,109)} = 6.6086$, $P = 0.001$; Fig. 1c). There was a significant difference in beta diversity of environmental samples compared to larvae and metamorphs (Larva-Environment: PERMANOVA $F_{(1,81)} = 12.372$, $P = 0.001$; Metamorph-Environment: PERMANOVA $F_{(1,69)} = 6.0735$, $P = 0.001$; Supplementary Table 3).

The composition of bacterial communities also differed between amphibian life stages and the environment. Larvae had a higher relative abundance of Firmicutes and Spirochaetes compared to metamorphs, while metamorphs were enriched for Actinobacteria and Acidobacteria. Of the environmental samples, water had a higher relative abundance of Verrucomicrobia compared to sediment and amphibian skin, while sediment exhibited the highest relative abundance of Firmicutes and Bacteroidetes of any sample type (Fig. 1d, Supplementary Fig. 3).

Microbiota differ by metamorph population and disease state. The infection history of each Pyrenean population is well documented with estimates of *Bd* emergence for each locality. Populations have shown different responses to infection over time with Arlet and Ansabere exhibiting epizootic disease dynamics based on continued declining larval population abundance coinciding with *Bd* infection. Meanwhile, though Lhurs, Acherito and Puits d'Arious displayed *Bd*-associated decline in the initial years from when *Bd* was first detected, all have recently shown the hallmarks of enzootic infection characterised by stable larval population abundance in the presence of sustained *Bd* infection (Fig. 2, Supplementary Table 1, Supplementary Fig. 1). Analysis of the relationship between *Bd* infection dynamics and bacterial community structure was performed for metamorphs only since we were not able to collect larvae from one epizootic population (Arlet). *Bd*-associated mortality occurs during or after metamorphosis; so we consider the bacterial communities of metamorph skin to be most informative in terms of response to infection.

Enzootic populations exhibited lower *Bd* prevalence and significantly reduced infection intensity compared to epizootic populations (Chi-sq = 59.855, df = 4, $P < 0.0001$, Fig. 2, Supplementary Table 4). Bacterial Shannon diversity was reduced in epizootic populations compared to enzootic populations (ANOVA $F_{(4,46)} = 6.837$, $P = 0.0002$; Tukey's tests: Ansabere–Acherito, $P = 0.008$; Ansabere–Lhurs, $P = 0.05$; Ansabere–Puits d'Arious $P = 0.06$; Arlet–Acherito, $P = 0.001$; Arlet–Lhurs, $P = 0.04$; Arlet–Puits d'Arious, $P = 0.08$; Fig. 3a). Beta diversity of host skin bacterial communities based on Bray–Curtis distances differed according to both population (PERMANOVA Pseudo-$F_{(4,46)} = 3.175$, $P = 0.001$) and infection dynamic (PERMANOVA Pseudo-$F_{(1,49)} = 4.5125$, $P = 0.001$, Fig. 3b).

Bacterial community composition differed in enzootic and epizootic populations (Fig. 3c). Enzootic populations had a higher

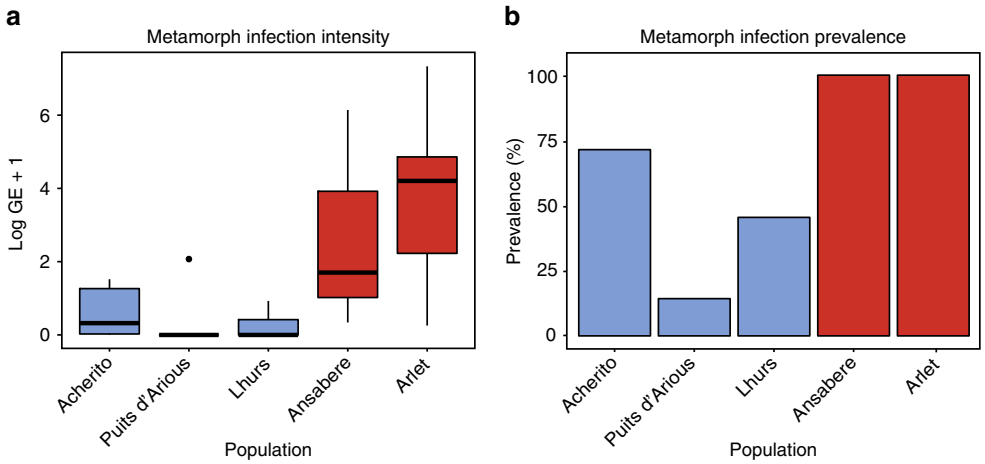


Fig. 2 *Bd* infection profiles of *Alytes obstetricans* metamorph populations. **a** Boxplot of *Bd* infection intensity in metamorphs sampled in 2015 showing reduced infection intensity in enzootic populations (Chi-sq = 59.855, $P < 0.0001$). Boxes represent 25 and 75 percentile, the horizontal line is the median and whiskers are maximum and minimum values of infection intensity. **b** Bar chart of *Bd* infection prevalence in metamorphs. Enzootic populations are coloured in blue, epizootic populations are coloured in red. Sample sizes were: Enzootic = 32 (Acherito = 14, Lhurs = 11, Puits d'Arious = 7); Epizootic = 19 (Arlet = 16, Ansabere = 3)

relative abundance of OTUs from the phyla Acidobacteria, Verrucomicrobia and Planctomycetes, while epizootic populations had higher relative abundance of Bacteroidetes. Arlet, which has shown the highest mortality rate of any lake, featured an increased relative abundance of Chlamydiae, a phylum whose members include obligate intracellular pathogens[29]. The differences in bacterial community structure and composition between enzootic and epizootic populations are not an artefact of spatial non-independence given the lack of clustering of sites displaying similar disease dynamics (Fig. 3d)

We performed indicator analysis to identify bacterial taxa driving the differences in beta diversity based on both disease dynamic and population. We identified 61 indicator OTUs that were associated with enzootic dynamics and 25 OTUs associated with epizootic dynamics (Fig. 4, Supplementary Data 1). Indicator OTUs from enzootic sites spanned nine phyla and 16 classes with the orders Actinomycetales and Rhizobiales accounting for the majority of taxa. Conversely OTUs from epizootic populations represented a less diverse array of lineages with six phyla and nine classes of which Pseudomonadales and Flavobacteriales were the most abundant orders.

A range of OTUs contributed to differences in bacterial community structure between individual populations (Supplementary Data 2). Lhurs, Acherito and Puits d'Arious were characterised by 73, 51 and 29 OTUs respectively, while Arlet and Ansabere had a total of 11 and four indicator OTUs.

Predicted function differs by population and disease state. The predicted function of bacterial communities supported the patterns shown by bacterial taxonomic composition with significant differences based on both disease dynamic (PERMANOVA Pseudo-$F_{(1,49)} = 7.1993$, $P = 0.001$) and population (PERMANOVA Pseudo-$F_{(4,46)} = 2.9201$, $P = 0.005$, Supplementary Fig. 4). In addition, 11 functional features were found to be significantly differentially abundant between enzootic and epizootic populations (LEfSe LDA > 2). Nine functional features were more abundant in enzootic populations and two were more abundant in epizootic populations (Supplementary Table 5). Differential functional features in both enzootic and epizootic populations were largely associated with mineral and ion transport (Supplementary Table 5).

***Bd* genomic analysis**. Whole genome sequencing was performed on 81 *Bd* isolates collected between 2004 and 2015 (Supplementary Data 3). Phylogenetic analysis with the inclusion of *Bd* isolates collected from other European localities gave 100% bootstrap support for a single introduction of *Bd* into the Pyrenees (Fig. 5a). A principle component analysis (PCA) of identified single nucleotide polymorphisms (SNPs) revealed little temporal or spatial genetic structure among populations in the pathogen (Fig. 5b, c, Supplementary Fig. 5)

Discussion

Our understanding of the microbial ecology of amphibian skin is rapidly increasing[21–23,30,31]. However, examining the dynamics of bacterial communities across wild populations exhibiting enzootic and epizootic disease states remains an important and understudied area[21,24]. In addition, our knowledge of how bacterial communities of amphibian skin differ between developmental stages is based on a limited number of studies[22,31,32]. In this study we address these gaps in our knowledge by characterising the skin-associated bacterial communities of amphibians from different life stages and metamorph populations displaying enzootic or epizootic disease dynamics. In addition, for the first time we investigate the relationship between *Bd* genetics and the microbiome in disease outcome by sequencing *Bd* isolates from each population. We demonstrate that host population, infection dynamics and life stage are all significant factors in shaping amphibian skin bacterial communities, with population accounting for the greatest amount of variation. While there was a clear microbiome signature corresponding to disease outcome, an association between disease state and pathogen genetics was not evident.

The bacterial community structure of amphibian skin differed significantly based on both life stage and population, accounting for 15 and 20% of variation respectively. Despite the strong effect of population, few OTUs were shared between amphibian skin and the environment, and those that were had a low relative abundance in the environment. The small proportion of OTUs shared between the host and its surrounding environment, coupled with the low abundance of environmental OTUs has been found in similar studies[30] and may be indicative of selection occurring on the skin for rare environmental bacterial species[33].

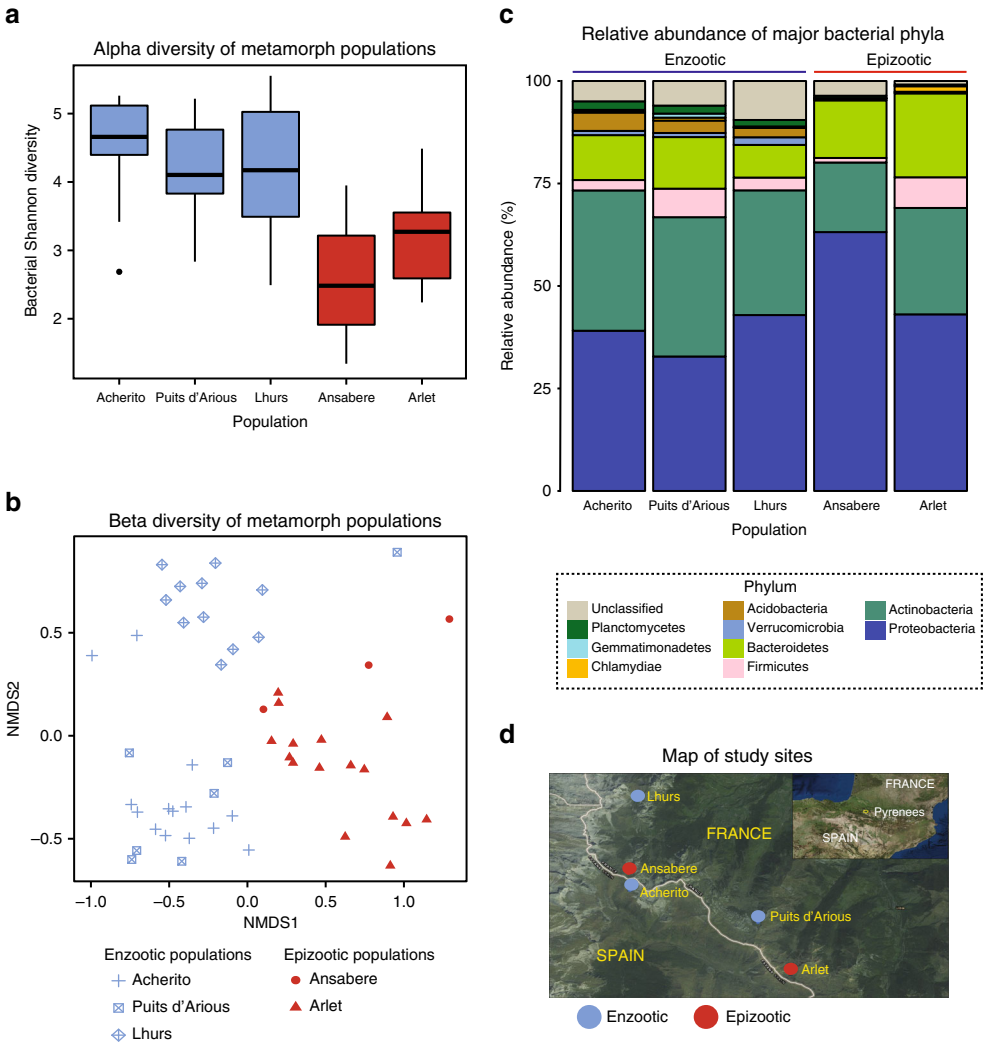


Fig. 3 Bacterial community profiles of *Alytes obstetricans* metamorph skin from enzootic and epizootic populations. **a** Shannon diversity of metamorph populations. Epizootic populations are in red and enzootic populations are blue. Boxes represent 25 and 75 percentile; the horizontal line is the median and whiskers are maximum and minimum values. **b** NMDS plot based on Bray–Curtis distances displaying beta diversity of enzootic and epizootic populations. **c** Stacked bar chart of abundant bacterial phyla for each metamorph population. **d** Map showing location of enzootic and epizootic populations. Map generated using ArcGIS version 10.0 (http://www.esri.com/software/arcgis) with the World Imagery Basemap. Source: Esri, DigitalGlobe, GeoEye, Earthstar, Geographics, CNES/Airbus DS, USDA, USGS, AeroGRID, IGN, the GIS User Community. Sample sizes were: Enzootic = 32 (Acherito = 14, Lhurs = 11, Puits d'Arious = 7); Epizootic = 19 (Arlet = 16, Ansabere = 3)

This finding is surprising given the strong effect that host population was found to have on bacterial community structure, and existing evidence from other studies suggesting environmental reservoirs are important in shaping the vertebrate microbiome[20,34,35]. Our results may therefore reflect that host OTUs also present in the environment may be at sub-detectable levels.

Larvae and metamorphs were dominated by the phylum Proteobacteria of which an OTU belonging to the family Comamonadaceae was most abundant. Comamonadaceae have also been identified as the most common taxonomic group in other studies of North American amphibian species[22,36], suggesting some members of the core skin microbiota may be conserved across continents as has previously been shown for constituents of the tadpole gut microbiome[37]. Unlike prior studies[22,31], we found no significant difference in alpha diversity of metamorph and larval amphibians. There was however clear evidence for restructuring of skin-associated bacterial communities during metamorphosis. Specifically, there was a significant difference in beta diversity of metamorphs and larvae and only a small proportion (17.3%) of OTUs were shared between life stages. This restructuring of the skin bacterial community is probably due to a combination of factors including the shift from a wholly aquatic to terrestrial environment and the extensive physiological changes that the skin undergoes during metamorphosis. Of particular importance is likely to be the heavily expanded repertoire of skin secretions produced post-metamorphosis that transforms the skin into a very different niche for bacteria[38].

Our findings show that while there was no distinction in pathogen genetic structure across enzootic and epizootic populations, there were clear differences in community structure and predicted function of bacteria on metamorph skin based on population and disease dynamic. Importantly, differences in bacterial community structure also reflect variation in bacterial predicted function. This finding is not indicative of functional redundancy among disparate bacterial communities and supports an active role of bacteria in host defence. Alpha diversity was significantly lower in epizootic populations compared to those

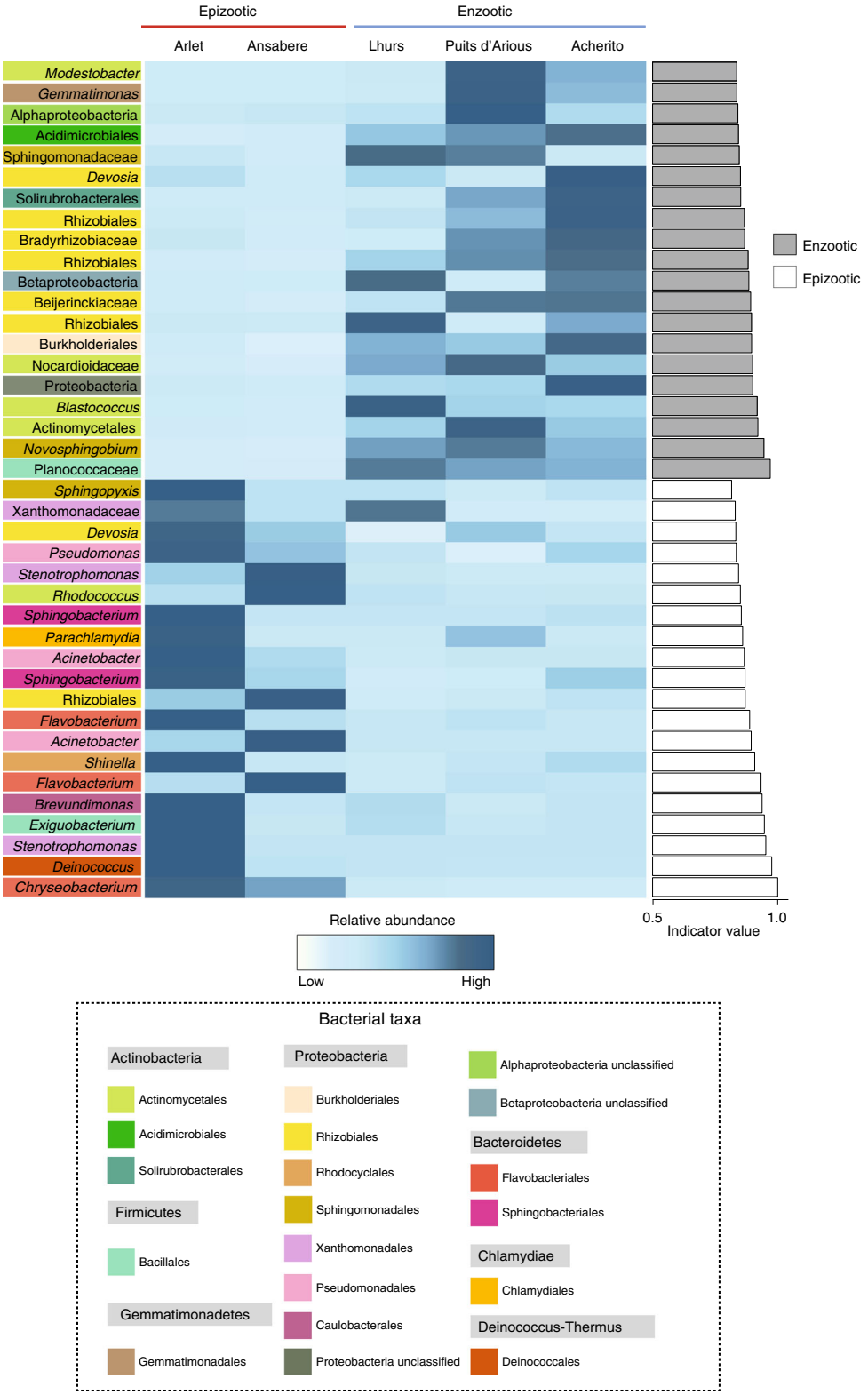


Fig. 4 Heatmap displaying the normalised relative abundance of the top 20 bacterial OTUs from enzootic and epizootic populations identified from indicator analysis. Sample sizes were: Enzootic = 32 (Acherito = 14, Lhurs = 11, Puits d'Arious = 7); Epizootic = 19 (Arlet = 16, Ansabere = 3)

presenting enzootic dynamics. This finding corroborates that of other studies[39] and may indicate that high alpha diversity offers enhanced protection, for example through production of a larger arsenal of antifungal metabolites or by competing for resources more effectively than the invading *Bd*. High *Bd* infection intensity in epizootic populations also results in increased skin sloughing which has been shown to decrease resident bacterial community diversity[40]. Further, epizootic populations may experience a more severe inflammatory response to *Bd* and impaired immune function[41] that promotes dysbiosis. This in turn can lead to enrichment of bacteria that exploit weakened host defences and consequently outcompete beneficial symbionts leading to

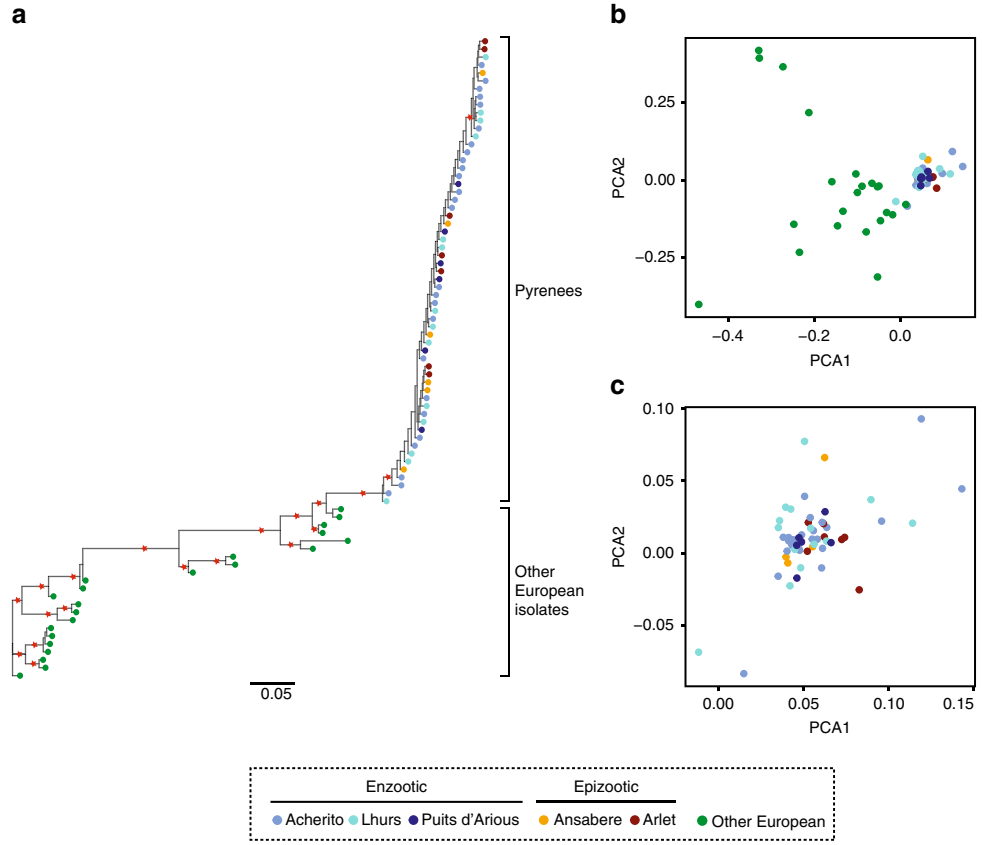


Fig. 5 *Bd* genetics across space and time in the Pyrenees. **a** Phylogeny of *Bd* isolates collected from the Pyrenees and other European localities. Red stars indicate bootstrap values of 100. **b** PCA plot of identified SNPs from *Bd* isolates from all localities. **c** PCA plot of identified *Bd* SNPs from Pyrenean lakes only. Sample sizes were: $n = 6$ (Ansabere); $n = 7$ (Arlet); $n = 26$ (Acherito); $n = 14$ (Lhurs); $n = 6$ (Puits d'Arious), $n = 22$ (other European isolates)

dominance of a small number of opportunistic pathogenic bacterial species[42].

Indicator analysis based on population identified key taxa driving differences in beta diversity and revealed OTUs of potential importance to population-specific disease dynamics. Of particular interest is the indicator OTU profile of Lhurs, where metamorphs carried a high abundance of an OTU belonging to the *Lysobacter* genus (Supplementary Fig. 6). *Lysobacter* is inhibitory to several fungal pathogens including *Bd*[43] and anti-*Bd* functional traits have been identified for this genus. Genomic studies reveal that *Lysobacter* possesses strong chitinase functionality[44] that may make it efficient at breaking down the chitin rich cell wall of *Bd* zoosporangia. Further, one study showed that *Lysobacter gummosus* produced the metabolite 2,4-diacetylphloroglucinol (2,4-DAPG) which is strongly inhibitory to *Bd*[10]. Since Lhurs was the most recently infected population, it is unlikely to have fixed host-associated genes for resistance faster than previously infected populations that remain susceptible. Therefore, one possibility is that tolerance to *Bd* may have arisen through selection of beneficial bacteria such as *Lysobacter*. This biotic shift has the potential to occur over a relatively short temporal scale given the rapid generation time of bacteria, which can subsequently become established members of the skin bacterial community and confer protective benefits to the host.

Arlet also revealed an interesting indicator OTU profile with high abundance of an OTU belonging to the *Parachlamydia* genus (Supplementary Fig. 7a). The Chlamydiae comprise obligate intracellular pathogens that infect mucosal epithelial cells[29]. Prior studies show that co-infection with Chlamydiae and *Bd* can result in mortality and epizootic dynamics[45]. Arlet experienced a severe population decline coinciding with *Bd* emergence[18,27] and despite being infected longer than two enzootic populations (Lhurs and Puits d'Arious) has shown no signs of recovery. Analysis of Chlamydiae across all populations shows a higher relative abundance in metamorphs than either larvae or environmental samples indicating either colonisation or proliferation at metamorphosis (Supplementary Fig. 7b). If Chlamydiae are found to induce pathology in Arlet metamorphs, then identifying whether this phylum is potentially associated with secondary infection or acting synergistically to promote *Bd* growth will be of paramount importance.

Indicator analysis based on infection dynamic identified a wide range of bacterial groups. The OTU with the highest indicator value for enzootic populations belonged to the family Planococcaceae of which several taxa are known to possess strong inhibitory capabilities against multiple pathogenic fungi including *Bd*[43,46]. Members of the Actinomycetales and Rhizobiales represented the most abundant indicator OTUs in enzootic populations. These orders are common constituents of soil[47] and have previously been documented for their anti-*Bd* activity in vitro[43]. Actinomycetales in particular are likely to be important candidates contributing to *Bd* resistance with prior studies identifying associations between members of this order and *Bd* tolerance in the wild[21,23]. The Actinomycetales are also functionally important producing an estimated 53% of bioactive microbial metabolites of known antibiotic capability[48].

Among epizootic populations, members of the Moraxellaceae, and Flavobacteriaceae were highly represented indicator OTUs that have all been associated with high *Bd* loads in prior studies[21,23,49]. All indicator OTUs assigned to the family

Moraxellaceae belonged to the *Acinetobacter* genus. Isolates of *Acinetobacter* taken from multiple amphibian species (including *A. obstetricans*) have shown a great deal of functional diversity, including both *Bd* enhancement and inhibition[43]. These results extend to in vivo studies of which one field study found *Acinetobacter* to be enriched in non-susceptible populations[23], while a controlled experiment showed members of the Moraxellaceae to be strongly associated with *Bd*-induced mortality[49]. Flavobacteriaceae are also often positively correlated with *Bd* load in wild amphibian populations[21] and in some cases enhance *Bd* growth in co-culture[43].

Overall, our findings reveal that while individual populations may be characterised by unique OTUs that likely reflect the ecology of each habitat, there exists a subset of bacterial taxa that are conserved across populations depending on disease state. This may indicate the existence of common selection pressures linked with disease dynamics across sites that are associated with enhanced success of certain taxa. Such selection pressures are likely to be complex and mediated by the host, microbe–microbe interactions and the environment[50].

One possibility is that the pathogen itself may contribute to shaping the skin bacterial community of amphibians from each population. While *Bd* from epizootic and enzootic populations lacked marked differences in genetic structure, it remains possible that there is among-population heterogeneity in the way that bacterial taxa could respond to *Bd* genotypes[51]. Differences in bacterial communities among populations exhibiting contrasting infection dynamics may also be mediated by host factors such as the composition and volume of skin secretions that may be linked to proliferation of certain bacteria[52]. If co-evolution of the host with protective symbionts has occurred, this may not only lead to tolerance of infection through direct inhibition of *Bd* but may also culminate in reduced pathogen virulence[53]. Such a scenario may provide an elegant explanation for the dynamics of the Pyrenees system whereby *Bd* persists in enzootic populations without causing pathology to the host. Ultimately, identifying the selection pressures acting on amphibian-associated bacteria, whether mediated by the host, pathogen or environment will be insightful in furthering our knowledge of microbial ecology of disease dynamics in nature. While a great body of work has focussed on in vitro studies identifying single bacterial isolates that are inhibitory to *Bd*, our findings highlight that differences in epizootic and enzootic populations are likely driven by communities of bacteria. This may be particularly important since many constituents of a bacterial community may not directly inhibit or promote *Bd* growth but instead may produce metabolic by-products that interact with *Bd*[54]. In addition, our current knowledge of bacterial phenotypic plasticity, which can be affected by factors such as community structure and other biotic and abiotic conditions[55] reinforces the necessity to shift attention from single bacterial studies to those that take into account entire communities.

Amphibians globally are facing an extinction crisis and emerging infectious diseases are a major contributor to their decline. Understanding the role of host-associated bacteria in infection will greatly enhance our knowledge of the drivers underpinning heterogeneity in disease dynamics across space and time. By demonstrating significant associations between host skin bacterial communities, life stage and infection dynamics, this study develops an insight into the microbial ecology of amphibian skin in its natural setting. In addition, the lack of association between pathogen genetics and disease outcome suggests that the microbiome may play a more important role in infection than previously expected. In this Pyrenean montane system, we identify a conserved assemblage of bacterial taxa associated with disease state, many of which have previously been identified for their positive or negative impact on *Bd*. Despite the convincing patterns in bacterial community structure and predicted function based on disease state, our findings lack direct functional evidence to support the hypothesis that putatively beneficial or detrimental bacteria are associated with clinically relevant effects on disease outcome. In addition, other potentially important microbial groups such as Fungi were not examined in this study. Future studies should therefore seek to survey a broader range of microbial kingdoms. There is a need to move beyond functional prediction based on 16S marker genes and instead capture direct functional information, for example through metabolomics to uncover associations between microbial community structure and function in disease ecology.

Methods

Ethics statement. Research was performed under licence from the Parc National des Pyrenees and the Instituto Aragonés de Gestión Ambiental.

Sample collection. Recently metamorphosed and larval *A. obstetricans* were captured and rinsed with sterile water to remove transient bacteria on the skin[56]. Using single sterile swabs, we sampled the skin microbiome by swabbing the body of tadpoles and metamorphs ten times, additionally swabbing the fore- and hindlimbs of metamorphs five times. To sample for *Bd* in metamorphs, we swabbed the pelvic patch and ventral surface of the hind limbs ten times. A fresh pair of sterile latex gloves was worn for each animal to avoid cross contamination of *Bd* or bacteria. Environmental water samples were collected following previously published methods[31]. For water samples a sterile swab was moved through lake water for 30 s at a depth of approximately 30 cm. Sediment samples were collected at the same location as water samples by embedding the swab into sediment for 30 s. All swabs were immediately stored on ice before being transferred to a freezer. MW100 rayon tipped dry swabs (MWE Medical Wire, Corsham, UK) were used for *Bd* and bacterial sampling. Characterisation of disease dynamics for each *A. obstetricans* population was done through long-term ecological monitoring (see Supplementary Note 1 for further details).

DNA extraction and sample processing. Genomic DNA was extracted from microbiome swabs using the DNeasy Blood and Tissue kit (Qiagen, Venlo, the Netherlands) according to the manufacturer's instructions. A pre-treatment with mutanolysin was included to enhance recovery of bacterial DNA[57]. DNA extracted from swabs was used to amplify the V4 region of the 16S rRNA gene using custom barcoded primers and PCR conditions adapted from a prior study[58]. PCR conditions consisted of a denaturing step of 95 °C for 15 min, followed by 28 cycles of 95 °C for 20 s, 50 °C for 60 s, 72 °C for 60 s and a final extension step of 72 °C for 10 min. Each PCR including a negative water control was performed in triplicate. Amplicons were visualised on a 2% agarose gel and pooled yielding a final per sample volume of 24 µl. Pooled amplicon DNA was purified using an Ampure XP PCR purification kit (Beckman Coulter, California, USA). Following purification, 1 µl of each combined sample was pooled into a preliminary library and the concentration was determined using Qubit fluorometric quantification (Life Technologies, California, USA). Amplicon quality and incidence of primer dimer was assessed using an Agilent 2200 TapeStation system (Agilent Technologies, California, USA). A titration run of 300 sequencing cycles was performed on an MiSeq instrument (Illumina, California, USA) to quantify the number of reads yielded per sample from the preliminary library. An equimolar concentration of each sample was then pooled into a final composite library based on the index representation from the titration run and subsequently sequenced on a 500 cycle MiSeq run with a 250 bp paired-end strategy. Genomic DNA from *Bd* swabs was extracted using a bead-beating protocol[59]. DNA extractions were diluted 1/10 before undergoing qPCR amplification with each sample run in duplicate[59] and with *Bd* standards of 100, 10, 1 and 0.1 zoospore genomic equivalents (GE). Samples with greater than 0.1 GE were considered positive for *Bd*.

Sequence analysis. Sequences were processed using MOTHUR[60] following a previously described method[58]. Paired-end reads were split by sample and assembled into contigs. Sequences were quality filtered by removing ambiguous base calls, removing homopolymer regions longer than 8 bp, and trimming reads longer than 275 bp. Duplicate sequences were merged and aligned with 16S reference sequences from the SILVA small-subunit rRNA sequence database[61]. A pre-clustering step grouped sequences differing by a maximum of 2 bp. Chimeric sequences were removed using UCHIME[62] as implemented in MOTHUR. 16S rRNA gene sequences were clustered into groups according to their taxonomy at the level of Order and assigned OTUs at a 3% dissimilarity level. Sequences were taxonomically classified with an 80% bootstrap confidence threshold using a naïve Bayesian classifier with a training set (version 9) made available through the Ribosomal Database Project (http://rdp.cme.msu.edu)[63]. Sequences derived from chloroplasts, mitochondria, archaea, eukaryotes or unknown reads were

eliminated. The number of sequences per sample ranged from 3345 to 252,910. To mitigate the effects of uneven sampling[64], all samples were rarefied to 3345 sequences corresponding to the size of the lowest read sample. Rarefying at a higher threshold of 10,000 sequences led to some samples being discarded but had minimal impact on results for alpha and beta diversity. Downstream analysis of OTUs was carried out using the package Phyloseq[65] in R[66] version 3.4.1.

Infection analysis. All statistical analyses were carried out using R[66] version 3.4.1. Analysis of infection intensity followed previously published methods[18]. Genomic equivalents were rounded to whole numbers and treated as count data. A negative binomial regression model (function 'glm.nb', package MASS[67]) was used to establish if infection intensity differed between populations. A likelihood ratio test was used to assess significance of population in the model. Tukey post-hoc testing (function 'glht', package multcomp[68]) was performed to identify populations that had significantly different infection intensities. Genomic equivalents data were visualised using boxplots and log+1 transformed for presentation purposes. Prevalence data was displayed using barplots.

Bacterial communities across space and life history stage. To determine the relationship between life stage, environmental bacteria and host bacterial communities, we calculated the proportion of shared and unique OTUs between host and environmental samples and between developmental stages. Water and sediment samples were combined into a single factor called 'Environment' for computing shared OTUs since we were interested in how the environment regardless of specific sample type shaped the host-associated bacterial community. Shared OTUs between groups of interest were visualised using Venn diagrams generated using the program Venny[69].

Shannon diversity was calculated for each life stage and environment samples. We used ANOVA to compare Shannon diversity of different samples and Tukey's test to identify which groups differed significantly. A Bray–Curtis distance matrix was used to calculate beta diversity of samples and visualised using a non-metric multidimensional scaling (NMDS) plot. The relative contribution of life stage and population in structuring the microbiome was assessed using permutational multivariate analysis of variance (PERMANOVA)[70] using the adonis function in the Vegan[71] package in R. PERMANOVA was also carried out to compare community structure of larvae and metamorphs with environmental samples. Analysis was performed for combined populations to isolate the effect of site as well as for individual populations to compare between site effects.

Microbiota in epizootic and enzootic metamorph populations. To determine the extent to which metamorph skin bacterial communities differed between populations, Shannon diversity was calculated and ANOVA was used to determine significant differences between groups. A post-hoc Tukey's test was carried out to identify populations that differed significantly.

Beta diversity of populations was calculated using a Bray–Curtis distance matrix and visualised using NMDS plots. PERMANOVA was carried out to determine the relative effects of disease dynamic and population in shaping bacterial communities. Indicator analysis[72] was performed using the labdsv package[73] in R to identify OTUs that best explained differences between populations and disease states. Indicator analysis calculates the product of an OTU's frequency and relative abundance in predefined groups. An indicator value of 1 represents the presence of an OTU in one group but not others, while an indicator value of zero is indicative of an OTU evenly distributed across all groups. Multiple comparisons were taken into account using the false discovery rate procedure[74]. OTUs with an indicator value >0.5 and q-value < 0.05 were considered informative. A heatmap displaying the relative abundance of the top 20 OTUs for enzootic and epizootic populations was generated using the function heatmap.2 in the gplots[75] package in R.

To examine whether function of bacterial communities from enzootic and epizootic metamorph populations differed, gene prediction was performed using Piphillin[76]. A sequence identity cut-off of 97% was used and sequences were assigned putative function using the KEGG reference database (May 2017 release). Beta diversity of KEGG orthology (KO) abundances was calculated using the Bray–Curtis metric. Comparison of functional profiles of each population was performed using NMDS ordination and PERMANOVA in the R packages Phyloseq[65] and Vegan[71]. Differentially abundant features between enzootic and epizootic populations were determined using linear discriminant analysis (LDA) effect size (LEfSe)[77]. Classes were defined as enzootic or epizootic with population as a subclass and an LDA score of ≥2.0 was used as a cut-off.

***Bd* isolation and genome sequencing**. *Bd* was isolated from *A. obstetricans* toe clips taken from each population between 2004 and 2015. A summary of the isolates used is shown in Supplementary Data 3. Isolates were grown in 50 ml Nalgene Nunc™ tissue culture-treated flasks (Thermo Fisher Scientific, Massachusetts, USA) for 10–14 days at 18–20 °C. DNA extraction was performed using the MasterPure™ Yeast DNA Purification Kit (Epicentre, Wisconsin, USA) or Qiagen Genomic Tips 20/G and DNeasy Blood and Tissue Kits (Qiagen, Venlo, Netherlands). DNA extractions were quantified using a Tapestation 2200 (Agilent Technologies, California, United States) and Quibt 2.0 fluorometer (Thermo Fisher Scientific, Massachusetts, USA). We prepared DNA samples for sequencing on an Illumina HiSeq 2000 (Illumina, California, USA).

Raw sequencing reads were first cleaned of adapter sequences and quality trimmed using cutadapt v1.10[78]. Reads were mapped to the JEL423 reference genome (GenBank assembly accecssion: GCA_000149865.1) using Burrows–Wheeler Aligner (BWA-mem) v0.7.8[79]. Resulting sequence alignment/map (SAM) files were processed using SAMtools v1.3.1[80] using the 'fixmate' and 'sort' programs to ready the files for variant discovery. Variant discovery was done using freebayes version dbb6160[81]. In the first step, sorted BAM files for each of the isolates in the study were independently called to find variant positions. The set of all variable positions identified across all samples were merged into a single variant call format (VCF) file. In the second step, genotype calls were independently made for each isolate, at each of the positions identified in the first step to produce a squared-off call set (each sample VCF has genotype calls at the same loci, including homozygous reference calls, and explicitly identifying positions without sequencing read coverage). The sample VCF files were processed by vcflib[82] to break complex variants into allelic primitives and then to normalise short insertion and deletion sequences (indels). VCFs were then quality filtered with bcftools version 1.3.1[80]. Sites with homozygous reference genotypes covered by four reads, or sites not covered by any reads were set to missing. Subsequently, putative non-reference genotype calls were set to homozygous reference if they failed any of the following filters: there was not enough evidence to support a variant genotype call; an alternate allele is in the called genotype without supporting reads ('AC > 0 && NUMALT = = 0). The phred-scaled quality score is less than 5 when there are any reads covering the position (%QUAL < 5 && DP > 0); any called allele is not supported by at least two reads (AF[*] < = 0.5 && DP < 4); alternate alleles are supported by only low-quality reads (AF[*] < = 0.5 && DP < 13 && %QUAL < 10)| (AF[*] > 0.5 && DP < 4 && %QUAL < 50); the quality, scaled by depth of supporting reads is less than a threshold (%QUAL / AO < 10); a called allele does not appear on both forward and reverse strands (SAF = = 0 | SAR = = 0); alleles are only supported by reads entirely placed right or left of the query variant (RPR = 0 | RPL = 0). The individual filtered VCF files were merged into a single multi-sample VCF using vcfstreamsort[82] to ensure sorting of out of order variants resulting from breaking complex variants in individual files into their simplest allelic representation. A phylogeny of the *Bd* isolates used in this study was visualised using ggtree[83].

Principle component analysis was carried out using bi-allelic SNP positions using the package *SNPrelate* v1.10.2[84] in R version 3.4.1. SNPs in high linkage disequilibrium (LD) were pruned using a threshold of approximately half the maximum value of LD in *Bd*GPL (an LD50 of 0.125). A subset of 771 from 50,561 SNPs were used in the PCA analysis. PCA data was plotted using ggplot2[85].

Data availability. Sequence data have been deposited on the BioProject database under accession codes PRJNA421328 and PRJNA413876. All other data are available upon request from the authors.

Received: 17 April 2017 Accepted: 10 January 2018
Published online: 15 February 2018

References

1. Ottman, N., Smidt, H., de Vos, W. M. & Belzer, C. The function of our microbiota: who is out there and what do they do? *Front. Cell. Infect. Microbiol.* **2**, 104 (2012).
2. Shin, S. C. et al. *Drosophila* microbiome modulates host developmental and metabolic homeostasis via insulin signaling. *Science* **334**, 670–674 (2011).
3. Honda, K. & Littman, D. R. The microbiome in infectious disease and inflammation. *Annu. Rev. Immunol.* **30**, 759–795 (2012).
4. Rogers, G. B. et al. From gut dysbiosis to altered brain function and mental illness: mechanisms and pathways. *Mol. Psychiatry* **21**, 738–748 (2016).
5. Smith, K., McCoy, K. D. & Macpherson, A. J. Use of axenic animals in studying the adaptation of mammals to their commensal intestinal microbiota. *Semin. Immunol.* **19**, 59–69 (2007).
6. Hooper, L. V., Littman, D. R. & Macpherson, A. J. Interactions between the microbiota and the immune system. *Science* **336**, 1268–1273 (2012).
7. Buffie, C. G. & Pamer, E. G. Microbiota-mediated colonization resistance against intestinal pathogens. *Nat. Rev. Immunol.* **13**, 790–801 (2013).
8. Kamada, N. et al. Regulated virulence controls the ability of a pathogen to compete with the gut microbiota. *Science* **336**, 1325–1329 (2012).
9. Gensollen, T., Iyer, S. S., Kasper, D. L. & Blumberg, R. S. How colonization by microbiota in early life shapes the immune system. *Science* **352**, 539–544 (2016).
10. Brucker, R. M. et al. The identification of 2,4-diacetylphloroglucinol as an antifungal metabolite produced by cutaneous bacteria of the salamander *Plethodon cinereus*. *J. Chem. Ecol.* **34**, 39–43 (2008).

11. Stacy, A., Fleming, D., Lamont, R. J., Rumbaugh, K. P. & Whiteley, M. A commensal bacterium promotes virulence of an opportunistic pathogen via cross-respiration. *mBio* **7**, e00782-16 (2016).
12. Croswell, A., Amir, E., Teggatz, P., Barman, M. & Salzman, N. H. Prolonged impact of antibiotics on intestinal microbial ecology and susceptibility to enteric *Salmonella* infection. *Infect. Immun.* **77**, 2741–2753 (2009).
13. Olson, D. H. et al. Mapping the global emergence of *Batrachochytrium dendrobatidis*, the amphibian chytrid fungus. *PLoS ONE* **8**, e56802 (2013).
14. Voyles, J. et al. Pathogenesis of chytridiomycosis, a cause of catastrophic amphibian declines. *Science* **326**, 582–585 (2009).
15. Berger, L. et al. Chytridiomycosis causes amphibian mortality associated with population declines in the rain forests of Australia and Central America. *Proc. Natl Acad. Sci. USA* **95**, 9031–9036 (1998).
16. Savage, A. E. & Zamudio, K. R. MHC genotypes associate with resistance to a frog-killing fungus. *Proc. Natl Acad. Sci. USA* **108**, 16705–16710 (2011).
17. Farrer, R. A. et al. Multiple emergences of genetically diverse amphibian-infecting chytrids include a globalized hypervirulent recombinant lineage. *Proc. Natl Acad. Sci. USA* **108**, 18732–18736 (2011).
18. Clare, F. C. et al. Climate forcing of an emerging pathogenic fungus across a montane multi-host community. *Philos. Trans. R. Soc. B* **371**, 20150454 (2016).
19. Woodhams, D. C. et al. Symbiotic bacteria contribute to innate immune defenses of the threatened mountain yellow-legged frog, *Rana muscosa*. *Biol. Conserv.* **138**, 390–398 (2007).
20. Kueneman, J. G. et al. Probiotic treatment restores protection against lethal fungal infection lost during amphibian captivity. *Proc. R. Soc. B* **283**, 20161553 (2016).
21. Jani, A. J. & Briggs, C. J. The pathogen *Batrachochytrium dendrobatidis* disturbs the frog skin microbiome during a natural epidemic and experimental infection. *Proc. Natl Acad. Sci. USA* **111**, E5049–E5058 (2014).
22. Kueneman, J. G. et al. Inhibitory bacteria reduce fungi on early life stages of endangered Colorado boreal toads (*Anaxyrus boreas*). *ISME J.* **10**, 934–944 (2016).
23. Rebollar, E. A. et al. Skin bacterial diversity of Panamanian frogs is associated with host susceptibility and presence of *Batrachochytrium dendrobatidis*. *ISME J.* **10**, 1682–1695 (2016).
24. Jani, A. J., Knapp, R. A. & Briggs, C. J. Epidemic and endemic pathogen dynamics correspond to distinct host population microbiomes at a landscape scale. *Proc. R. Soc. B* **284**, 20170944 (2017).
25. Piovia-Scott, J. et al. Correlates of virulence in a frog-killing fungal pathogen: evidence from a California amphibian decline. *ISME J.* **9**, 1570–1578 (2015).
26. Walker, S. F. *Geographical patterns in the distribution of Batrachochytrium dendrobatidis and outbreaks of fatal chytridiomycosis in European amphibian populations*. PhD thesis, Imperial College London (2008).
27. Clare, F. C. *Quantifying the impact of infection by Batrachochytrium dendrobatidis on montane populations of Alytes obstetricans*. PhD thesis, Imperial College London (2014).
28. Bosch, J., Martinez-Solano, I. & Garcia-Paris, M. Evidence of a chytrid fungus infection involved in the decline of the common midwife toad (*Alytes obstetricans*) in protected areas of central Spain. *Biol. Conserv.* **97**, 331–337 (2001).
29. Wyrick, P. B. Intracellular survival by *Chlamydia*. *Cell. Microbiol.* **2**, 275–282 (2000).
30. Walke, J. B. et al. Amphibian skin may select for rare environmental microbes. *ISME J.* **8**, 2207–2217 (2014).
31. Kueneman, J. G. et al. The amphibian skin-associated microbiome across species, space and life history stages. *Mol. Ecol.* **23**, 1238–1250 (2014).
32. Knutie, S. A., Wilkinson, C. L., Kohl, K. D. & Rohr, J. R. Early-life disruption of amphibian microbiota decreases later-life resistance to parasites. *Nat. Commun.* **8**, 86 (2017).
33. Loudon, A. H. et al. Vertebrate hosts as islands: dynamics of selection, immigration, loss, persistence, and potential function of bacteria on salamander skin. *Front. Microbiol.* **7**, 333 (2016).
34. Lax, S. et al. Longitudinal analysis of microbial interaction between humans and the indoor environment. *Science* **345**, 1048–1052 (2014).
35. Hyde, E. R. et al. The oral and skin microbiomes of captive komodo dragons are significantly shared with their habitat. *mSystems* **1**, e00046-16 (2016).
36. McKenzie, V. J., Bowers, R. M., Fierer, N., Knight, R. & Lauber, C. L. Co-habiting amphibian species harbor unique skin bacterial communities in wild populations. *ISME J.* **6**, 588–596 (2012).
37. Vences, M. et al. Gut bacterial communities across tadpole ecomorphs in two diverse tropical anuran faunas. *Sci. Nat.* **103**, 25 (2016).
38. Rollins-Smith, L. A., Ramsey, J. P., Pask, J. D., Reinert, L. K. & Woodhams, D. C. Amphibian immune defenses against chytridiomycosis: impacts of changing environments. *Integr. Comp. Biol.* **51**, 552–562 (2011).
39. Longo, A. V., Savage, A. E., Hewson, I. & Zamudio, K. R. Seasonal and ontogenetic variation of skin microbial communities and relationships to natural disease dynamics in declining amphibians. *R. Soc. Open Sci.* **2**, 140377 (2015).
40. Meyer, E. A., Cramp, R. L., Bernal, M. H. & Franklin, C. E. Changes in cutaneous microbial abundance with sloughing: possible implications for infection and disease in amphibians. *Dis. Aquat. Org.* **101**, 235–242 (2012).
41. Fites, J. S. et al. The invasive chytrid fungus of amphibians paralyzes lymphocyte responses. *Science* **342**, 366–369 (2013).
42. Pham, T. A. & Lawley, T. D. Emerging insights on intestinal dysbiosis during bacterial infections. *Curr. Opin. Microbiol.* **17**, 67–74 (2014).
43. Woodhams, D. C. et al. Antifungal isolates database of amphibian skin-associated bacteria and function against emerging fungal pathogens. *Ecology* **96**, 595 (2015).
44. de Bruijn, I. et al. Comparative genomics and metabolic profiling of the genus *Lysobacter*. *BMC Genomics* **16**, 991 (2015).
45. Reed, K. D., Ruth, G. R., Meyer, J. A. & Shukla, S. K. *Chlamydia pneumoniae* infection in a breeding colony of African clawed frogs (*Xenopus tropicalis*). *Emerg. Infect. Dis.* **6**, 196–199 (2000).
46. Chen, L. et al. Phylogenetic analysis and screening of antimicrobial and cytotoxic activities of moderately halophilic bacteria isolated from the Weihai Solar Saltern (China). *World J. Microbiol. Biotechnol.* **26**, 879–888 (2009).
47. Janssen, P. H. Identifying the dominant soil bacterial taxa in libraries of 16S rRNA and 16S rRNA genes. *Appl. Environ. Microbiol.* **72**, 1719–1728 (2006).
48. Bérdy, J. Bioactive microbial metabolites—a personal view. *J. Antibiot.* **58**, 1–26 (2005).
49. Becker, M. H. et al. Composition of symbiotic bacteria predicts survival in Panamanian golden frogs infected with a lethal fungus. *Proc. R. Soc. B* **282**, 20142881 (2015).
50. Foster, K. R., Schluter, J., Coyte, K. Z. & Rakoff-Nahoum, S. The evolution of the host microbiome as an ecosystem on a leash. *Nature* **548**, 43–51 (2017).
51. Antwis, R. E., Preziosi, R. F., Harrison, X. A. & Garner, T. W. Amphibian symbiotic bacteria do not show a universal ability to inhibit growth of the global panzootic lineage of *Batrachochytrium dendrobatidis*. *Appl. Environ. Microbiol.* **81**, 3706–3711 (2015).
52. Grice, E. A. & Segre, J. A. The skin microbiome. *Nat. Rev. Microbiol.* **9**, 244–253 (2011).
53. Ford, S. A., Kao, D., Williams, D. & King, K. C. Microbe-mediated host defence drives the evolution of reduced pathogen virulence. *Nat. Commun.* **7**, 13430 (2016).
54. Loudon, A. H. et al. Interactions between amphibians' symbiotic bacteria cause the production of emergent anti-fungal metabolites. *Front. Microbiol.* **5**, 441 (2014).
55. Gray, M. J., Freitag, N. E. & Boor, K. J. How the bacterial pathogen *Listeria monocytogenes* mediates the switch from environmental Dr. Jekyll to pathogenic Mr. Hyde. *Infect. Immun.* **74**, 2505–2512 (2006).
56. Culp, C. E., Falkinham, J. O. & Belden, L. K. Identification of the natural bacterial microflora on the skin of eastern newts, bullfrog tadpoles and redback salamanders. *Herpetologica* **63**, 66–71 (2007).
57. Yuan, S. Q., Cohen, D. B., Ravel, J., Abdo, Z. & Forney, L. J. Evaluation of methods for the extraction and purification of DNA from the human microbiome. *PLoS ONE* **7**, e33865 (2012).
58. Kozich, J. J., Westcott, S. L., Baxter, N. T., Highlander, S. K. & Schloss, P. D. Development of a dual-index sequencing strategy and curation pipeline for analyzing amplicon sequence data on the MiSeq Illumina sequencing platform. *Appl. Environ. Microbiol.* **79**, 5112–5120 (2013).
59. Boyle, D. G., Boyle, D. B., Olsen, V., Morgan, J. A. T. & Hyatt, A. D. Rapid quantitative detection of chytridiomycosis (*Batrachochytrium dendrobatidis*) in amphibian samples using real-time Taqman PCR assay. *Dis. Aquat. Org.* **60**, 141–148 (2004).
60. Schloss, P. D. et al. Introducing mothur: open-source, platform-independent, community-supported software for describing and comparing microbial communities. *Appl. Environ. Microbiol.* **75**, 7537–7541 (2009).
61. Pruesse, E. et al SILVA: a comprehensive online resource for quality checked and aligned ribosomal RNA sequence data compatible with ARB. *Nucleic Acids Res.* **35**, 7188–7196 (2007).
62. Edgar, R. C., Haas, B. J., Clemente, J. C., Quince, C. & Knight, R. UCHIME improves sensitivity and speed of chimera detection. *Bioinformatics* **27**, 2194–2200 (2011).
63. Wang, Q., Garrity, G. M., Tiedje, J. M. & Cole, J. R. Naive Bayesian classifier for rapid assignment of rRNA sequences into the new bacterial taxonomy. *Appl. Environ. Microbiol.* **73**, 5261–5267 (2007).
64. Schloss, P. D., Gevers, D. & Westcott, S. L. Reducing the effects of PCR amplification and sequencing artifacts on 16S rRNA-based studies. *PLoS ONE* **6**, e27310 (2011).
65. McMurdie, P. J. & Holmes, S. phyloseq: an R package for reproducible interactive analysis and graphics of microbiome census data. *PLoS ONE* **8**, e61217 (2013).
66. R Development Core Team. R: A Language and Environment for Statistical Computing. R Foundation for Statistical Computing. http://www.R-project.org (2017).

67. Venables W. N. & Ripley B. D. *Modern Applied Statistics with S.* (Springer, New York, 2002).
68. Hothorn, T., Bretz, F. & Westfall, P. Simultaneous inference in general parametric models. *Biom. J.* **50**, 346–363 (2008).
69. Oliveros, J.C. Venny. An interactive tool for comparing lists with Venn's diagrams. http://bioinfogp.cnb.csic.es/tools/venny/index.html (2007).
70. Anderson, M. J. A new method for non-parametric multivariate analysis of variance. *Austral. Ecol.* **26**, 32–46 (2001).
71. Oksanen, J. et al. Vegan: Community Ecology Package. R package version 2.3.4 (2016).
72. Dufrene, M. & Legendre, P. Species assemblages and indicator species: the need for a flexible asymmetrical approach. *Ecol. Monogr.* **67**, 345–366 (1997).
73. Roberts, D. W. labdsv: ordination and multivariate analysis for ecology. R package version 1.8.0 (2016).
74. Benjamini, Y. & Hochberg, Y. Controlling the false discovery rate: a practical and powerful approach to multiple testing. *J. R. Stat. Soc. B.* **57**, 289–300 (1995).
75. Warnes, G. R. et al. gplots: various R programming tools for plotting data. R package version 2.17.0 (2009).
76. Iwai, S. et al. Piphillin: improved prediction of metagenomic content by direct inference from human microbiomes. *PLoS ONE* **11**, e0166104 (2016).
77. Segata, N. et al. Metagenomic biomarker discovery and explanation. *Genome Biol.* **12**, R60 (2011).
78. Martin, M. Cutadapt removes adapter sequences from high-throughput sequencing reads. *EMBnet J.* **17**, 10–12 (2011).
79. Li, H. & Durbin, R. Fast and accurate short read alignment with Burrows –Wheeler transform. *Bioinformatics* **25**, 1754–1760 (2009).
80. Li, H. et al. The sequence alignment/map format and SAMtools. *Bioinformatics* **25**, 2078–2079 (2009).
81. Garrison, E. & Marth, G. Haplotype-based variant detection from short-read sequencing. Preprint at https://arxiv.org/abs/1207.3907 (2012).
82. Garrison, E. vcflib: A C++ library for parsing and manipulating VCF files, https://github.com/vcflib/vcflib (accessed July 21 2015) (2012).
83. Yu, G. C., Smith, D. K., Zhu, H. C., Guan, Y. & Lam, T. T. Y. GGTREE: an R package for visualization and annotation of phylogenetic trees with their covariates and other associated data. *Methods Ecol. Evol.* **8**, 28–36 (2017).
84. Zheng, X. et al. A high-performance computing toolset for relatedness and principal component analysis of SNP data. *Bioinformatics* **28**, 3326–3328 (2012).
85. Wickham H. *ggplot2: Elegant Graphics for Data Analysis* (Springer-Verlag, New York, 2009).

Acknowledgements

Dirk Schmeller and Adeline Loyau were invaluable in their support and organisation of permits. Jennifer Shelton, Nick Grassly and Maryam Grassly provided dedicated field support. We thank the community of Lescun and Parc National de Pyrenees for continued support. K.A.B. was funded by a CASE studentship from NERC; M.C.F. and T.W. J.G. were funded by the NERC award NE/E006701/1 and the Biodiversa project RACE: Risk Assessment of Chytridiomycosis to European Amphibian Biodiversity.

Author contributions

K.A.B., J.B., F.C.C., O.D. and M.C.F. collected the data. K.A.B., K.H., F.C.C., E.J.M., S.O., L.B. and X.A.H. analysed the data. K.A.B., M.C.F., T.W.J.G. and X.A.H. wrote the paper.

Additional information

Supplementary Information accompanies this paper at https://doi.org/10.1038/s41467-018-02967-w.

Competing interests: The authors declare no competing financial interests.

Reprints and permission information is available online at http://npg.nature.com/reprintsandpermissions/

Publisher's note: Springer Nature remains neutral with regard to jurisdictional claims in published maps and institutional affiliations.

Open Access This article is licensed under a Creative Commons Attribution 4.0 International License, which permits use, sharing, adaptation, distribution and reproduction in any medium or format, as long as you give appropriate credit to the original author(s) and the source, provide a link to the Creative Commons license, and indicate if changes were made. The images or other third party material in this article are included in the article's Creative Commons license, unless indicated otherwise in a credit line to the material. If material is not included in the article's Creative Commons license and your intended use is not permitted by statutory regulation or exceeds the permitted use, you will need to obtain permission directly from the copyright holder. To view a copy of this license, visit http://creativecommons.org/licenses/by/4.0/.

© The Author(s) 2018